LEABHARLANN CHOLÁISTE NA TRÍONÓIDE, BAILE ÁTHA CLIATH | TRINITY COLLEGE LIBRARY DUBLIN
Ollscoil Átha Cliath | The University of Dublin

Terms and Conditions of Use of Digitised Theses from Trinity College Library Dublin

Copyright statement

All material supplied by Trinity College Library is protected by copyright (under the Copyright and Related Rights Act, 2000 as amended) and other relevant Intellectual Property Rights. By accessing and using a Digitised Thesis from Trinity College Library you acknowledge that all Intellectual Property Rights in any Works supplied are the sole and exclusive property of the copyright and/or other IPR holder. Specific copyright holders may not be explicitly identified. Use of materials from other sources within a thesis should not be construed as a claim over them.

A non-exclusive, non-transferable licence is hereby granted to those using or reproducing, in whole or in part, the material for valid purposes, providing the copyright owners are acknowledged using the normal conventions. Where specific permission to use material is required, this is identified and such permission must be sought from the copyright holder or agency cited.

Liability statement

By using a Digitised Thesis, I accept that Trinity College Dublin bears no legal responsibility for the accuracy, legality or comprehensiveness of materials contained within the thesis, and that Trinity College Dublin accepts no liability for indirect, consequential, or incidental, damages or losses arising from use of the thesis for whatever reason. Information located in a thesis may be subject to specific use constraints, details of which may not be explicitly described. It is the responsibility of potential and actual users to be aware of such constraints and to abide by them. By making use of material from a digitised thesis, you accept these copyright and disclaimer provisions. Where it is brought to the attention of Trinity College Library that there may be a breach of copyright or other restraint, it is the policy to withdraw or take down access to a thesis while the issue is being resolved.

Access Agreement

By using a Digitised Thesis from Trinity College Library you are bound by the following Terms & Conditions. Please read them carefully.

I have read and I understand the following statement: All material supplied via a Digitised Thesis from Trinity College Library is protected by copyright and other intellectual property rights, and duplication or sale of all or part of any of a thesis is not permitted, except that material may be duplicated by you for your research use or for educational purposes in electronic or print form providing the copyright owners are acknowledged using the normal conventions. You must obtain permission for any other use. Electronic or print copies may not be offered, whether for sale or otherwise to anyone. This copy has been supplied on the understanding that it is copyright material and that no quotation from the thesis may be published without proper acknowledgement.

Bound By:
THE
THESIS CENTRE
65 Camden St. Lwr.,
Dublin 2. Ph: 475 3616
www.thesiscentre.com

TRINITY COLLEGE DUBLIN
23 SEP 2015
ACADEMIC REGISTRY

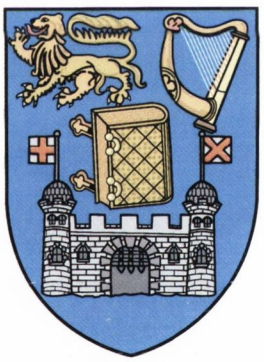
PhD in Genetics &
Microbiology

THE INTERPLAY BETWEEN CELL DEATH AND INFLAMMATION

Thesis submitted to Trinity College Dublin
for the degree of Doctor of Philosophy

Conor Maurice Henry

May 2015



PhD thesis supervisor: Professor Seamus J. Martin
Molecular Cell Biology Laboratory
Department of Genetics
University of Dublin
Trinity College

TRINITY COLLEGE
0 6 OCT 2015
LIBRARY DUBLIN

Thesis 10896

DECLARATION

I certify that this thesis, submitted to Trinity College Dublin for the degree of Doctor of Philosophy, has not been submitted as an exercise for a degree at this or any other university. I certify that the work presented here is entirely my own, except where otherwise acknowledged. This thesis may be made available for consultation within the university library and may be copied or lent to other libraries upon request.



Conor Maurice Henry
May 2015

ACKNOWLEDGEMENTS

Distinct from previous types of structured learning, a PhD is not entirely unstructured, by does require skills learned, not simple from doing, but more importantly, learning from observing those that do this expertly.

I would like to express my gratitude to my supervisor, Professor Seamus Martin, for his invaluable expertise, guidance and for granting me numerous opportunities to develop as a scientist, and for instilling in me a method of pursuing scientific questions with passion, skill and with the utmost integrity.

To all members of the lab, past and present, I thank them for all their help and support. I have had the luck to work with some great and highly motivated people. Because of the collaborative role they played in the research reported here I acknowledge the following people by name, Dr. Sean Cullen, Graeme Sullivan, Dr. Conor Kearney, Laura Williams, Dr. Richie Carroll, Dr. Emilie Hollville, Dani Clancy, Dr. Inna Afonina and Dr. Susan Logue.

Lastly, to Laura, without whose never-failing encouragement and sympathy has emboldened me to succeed in this pursuit, and who, having been a witness to this episode of my life, can testify to how utterly calm and collected I've been, especially in the past few months.....right? You're a top bird!

Conor
May 2015

LIST OF FIGURES

CHAPTER I

Figure 1.1 Tissue damage and infection are potent inducers of acute inflammation

Figure 1.2 Major pathways of apoptosis

Figure 1.3 Different modes of cell death elicit distinct immune responses

Figure 1.4 Apoptotic cells release multiple signals to facilitate their removal

Figure 1.5 Death receptors may promote cancer through inflammatory signalling

Figure 1.6 Members of the human IL-1 family of cytokines

Figure 1.7 Current model of IL-1 signalling

Figure 1.8 Cytokine network in psoriasis

CHAPTER III

Figure 3.1 TRAIL stimulation induces apoptosis as well as multiple pro-inflammatory cytokines

Figure 3.2 Pro-inflammatory cytokines and chemokines are produced by cells with clear features of apoptosis

Figure 3.3 TRAIL stimulation induces the secretion of a diverse array of pro-inflammatory cytokines

Figure 3.4 TRAIL production of pro-inflammatory cytokines is caspase-independent

Figure 3.5 TRAIL receptor engagement in multiple cell types promotes the secretion of cytokines and chemokines

Figure 3.6 TRAIL-induced death and cytokines are not dependent on TNF autocrine signalling

Figure 3.7 IAP antagonist BV6 modulates TRAIL-induced cytokine and chemokines

Figure 3.8 TRAIL receptor engagement activates multiple inflammatory signalling pathways

Figure 3.9 RIPK1 is required for optimal TRAIL-induced cytokines and chemokines

Figure 3.10 NF-kappa B and p38 are required for TRAIL and Fas-induced cytokine and chemokine production

Figure 3.11 DISC adaptors caspase-8, FADD and RIPK1 are sufficient to drive cytokine and chemokine production

Figure 3.12 Caspase-8 and FADD are critical for TRAIL/Fas-induced cytokine and chemokine production

Figure 3.13 Caspase-8 and FADD modulate cytokine and chemokine production

Figure 3.14 Caspase-8 knockdown attenuates cytokine and chemokine production in the absence of death

Figure 3.15 TRAIL/Fas-induced chemokines in HT-29 cells are independent of RIP kinases

Figure 3.16 TRAIL-induced apoptosis elicits chemotaxis of THP-1 monocytes

Figure 3.17 TRAIL-induced chemotaxis is ATP-independent

Figure 3.18 Depletion of specific cytokines and chemokines from apoptotic supernatants

Figure 3.19 TRAIL-induced chemotaxis is dependent on the chemokines IL-8 and MCP-1

Figure 3.20 MCP-1 release from apoptotic cells promotes chemotaxis of THP-1 monocytes

CHAPTER IV

Figure 4.1 Recombinant IL-36 and DEVD-modified IL-36 expression and purification from bacteria

Figure 4.2 DEVD-modified IL-36 proteins are cleaved by caspase-3

Figure 4.3 Establishment of HeLA^{IL-36R} cell lines

Figure 4.4 Proteolytic processing of DEVD-modified IL-36 proteins releases their biological activity

Figure 4.5 HaCat keratinocytes respond to DEVD-modified IL-36 cytokines

Figure 4.6 Neutrophil-derived proteases activate IL-36 cytokines

Figure 4.7 Inhibitor screen of IL-36 activation using neutrophil degranulates

Figure 4.8 Identification of IL-36-activating proteases

Figure 4.9 Selective depletion of neutrophil degranulates with biotin-FLF-CMK peptide specifically attenuates IL-36β activation

Figure 4.10 Inhibitors of neutrophil proteases attenuate IL-36 activation

Figure 4.11 Design of peptide inhibitors

Figure 4.12 Screen of novel cathepsin-G targeted peptide inhibitors with IL-36α

Figure 4.13 Screen of novel cathepsin-G targeted peptide inhibitors with IL-36β

Figure 4.14 Novel cathepsin-G targeted peptide inhibitors do not block neutrophil degranulate activation of IL-36γ

Figure 4.15 Screen of novel elastase targeted peptide inhibitors with IL-36γ

Figure 4.16 Novel elastase targeted peptide inhibitors do not block neutrophil degranulate activation of IL-36β

Figure 4.17 Mixing of cathepsin-G and elastase targeted peptides block IL-36 activation by neutrophil degranulates

Figure 4.18 IL-36 receptor antagonist attenuates IL-36 signalling

Figure 4.19 IL-36β is cleaved by cathepsin-G after arginine 5

Figure 4.20 IL-36β is activated by cathepsin-G after arginine 5

Figure 4.21 IL-36β is activated by neutrophil degranulates after arginine 5

Figure 4.22 IL-36γ is cleaved by elastase after valine 15

Figure 4.23 IL-36γ is activated by elastase after valine 15

Figure 4.24 IL-36γ is activated by neutrophil degranulates after valine 15

CHAPTER V

Figure 5.1 IL-36 cytokines are biologically active on HaCat keratinocytes

Figure 5.2 IL-36 cytokines are biologically active on primary keratinocytes

Figure 5.3 IL-36-induced gene expression array heat maps

Figure 5.4 TNF-induced gene expression array heat map

Figure 5.5 IL-36 and TNF induce distinct gene expression profiles with a subset of overlapping genes

Figure 5.6 IL-36 and TNF display distinct pro-inflammatory gene profiles

Figure 5.7 Primary keratinocytes upregulate multiple pro-inflammatory genes at both the RNA and protein level

Figure 5.8 IL-17C promotes cytokine production from primary keratinocytes

Figure 5.9 IL-36 does not modulate HaCat proliferation in nomenclature

Figure 5.10 IL-36 does not modulate primary keratinocyte proliferation in monoculture

Figure 5.11 Morphological features of calcium-induced differentiation of primary keratinocytes

Figure 5.12 Calcium-induced differentiation of primary keratinocytes is not modulated by IL-36 in monoculture

Figure 5.13 IL-36 does not modulate primary keratinocyte proliferation in the presence of calcium

Figure 5.14 Activated IL-36 promotes impaired differentiation in a 3D organotypic skin model

Figure 5.15 Mouse IL-36β is cleaved by neutrophil proteases

Figure 5.16 Mouse IL-36β is not activated by neutrophil proteases

Figure 5.17 Validation of rabbit polyclonal antibodies raised against IL-36 proteins

Figure 5.18 IL-36 stimulates upregulation of IL-1 family cytokines in primary keratinocytes in a dose and time-dependent manner

Figure 5.19 IL-36 stimulates upregulation of IL-1 family cytokines in HaCat in a dose and time-dependent manner

Figure 5.20 Expression of IL-36 proteins during calcium-induced differentiation of primary keratinocytes

Figure 5.21 IL-36 is released during necrosis of primary keratinocytes

Figure 5.22 Endogenous IL-1 cytokines are cleaved by neutrophil proteases

Figure 5.23 Endogenous IL-36γ is cleaved by elastase and neutrophil degranulates

Figure 5.24 IL-36 cytokines are cleaved by neutrophil proteases in 293T lysates

Figure 5.25 IL-36 cytokines are activated by neutrophil proteases in 293T lysates

Figure 5.26 IL-36γ is highly expressed in biopsy samples from patients with plaque psoriasis

CHAPTER VI

Figure 6.1 Model of IL-36 activation

ABBREVIATIONS

AAPV-AMC	Alaline- Alaline-7-Amino-4-methylcoumarin
AFC	7-amino-4-trifluoromethyl coumarin
AMC	7-Amino-4-methylcoumarin
APAF	Apoptotic protease activating factor
BSA	Bovine serum albumin
biotin-VAD-FMK	biotin-Valine-alaline-Aspartic acid- fluoromethylketone-FMK
biotin-FLF-CMK	biotin-Phenlyalaline-Leucine-Phenlyalaline chloromethylketone
CAD	Caspase-activated DNase
CARD	Caspase activation and recruitment domain
CASPASE	Cysteinyl aspartate-specific protease
CATG I 1	Cathepsin G inhibitor 1
CD95L	Cluster of differentiation 95 ligand
CEB	Cell extract buffer
CFE	Cell-free extract
CHAPS	3-Cholamidopropyldimethylammonio-1-propanesulfonate
CHX	Cyclohexamide
CMK	Chloromehtlketone
CTL	Cytotoxic lymphocyte
Cyt c	Cytochrome c
dATP	Deoxyadenosine triphosphate
ddH_2O	Double distilled H_2O
DAMP	Danger-associated Molecular pattern
DED	Death effector domain
DEVD	Aspartic acid-glutamic acid-valine-aspartic acid
DISC	Death-inducing signalling complex
DMEM	Dulbecco's modified eagle medium
DMSO	Dimethyl sulphoxide
DNA	Deoxyribonucleic acid
DTT	Dithiothreitol
EDTA	Ethylenediaminetetraacetic acid
ER	Endoplasmic reticulum
FACS	Fluorescence-activated cell sorter
FADD	Fas-associated protein with death domain
FasL	Fas ligand
FCS	Fetal calf serum
FITC	Fluorescein isothiocyanate
FL-	Full length
FMK	Fluoreomethylketone
HEK	Human embryonic kidney
HEPES	N-(2-hydroxyethyl) piperazine-N'-(2-ethanesulphonic acid)
Ig	Immunoglobulin
IPTG	Isopropylthio-β-D-galactoside

kDa	kilodaltons
IL	Interleukin
IP	Intraperitioneal
MOMP	Mitochondrial Outer Membrane Permebilization
NE I IV	Neutrophil elastase Inhibitor IV
NF-κB	nuclear factor kappa-light-chain-enhancer of activated B cell
NP40	Nonidet P40
Oligo	Oligonucleotide
PAGE	Polyacrylamide gel electrophoresis
PAMP	Pathogen-Associated Molecular pattern
PBS	Phosphate-buffered saline
PCR	Polymerase chain reaction
PIPES	Piperazine-N-N'-bis(2-ethanesulphonic acid)
PMA	Phorbal 12-myristate 13-acetate
PMSF	Phenylmethylsulphonylfluoride
PRB	Protease reaction buffer
PS	Phosphatidylserine
RNAi	RNA interference
RPMI	Roswell Park Memorial Institute
SDS	Sodium dodecyl sulphate
siRNA	Small interfering RNA
TAE	Tris acetate EDTA
TE	Tris EDTA
TLR	Toll-like receptor
TNF	Tumour necrosis factor
TNFR	Tumour necrosis factor receptor
TPCK	*N*-tosyl-l-phenylalanine chloromethyl ketone
TRADD	TNFR-1-associated death domain protein
TRAIL	Tumour necrosis factor-related apoptosis-inducing ligand
TRAIL-R	Tumour necrosis factor-related apoptosis-inducing ligand receptor
WT	Wild-type
WEHD	Tryptophan-Glumatic acid-Hisatine-Aspartic acid
YVAD	Tyrosine-valine-alanine-aspartic acid
z-VAD-fmk	Benzylocarbonyl-Val-Ala-Asp-(OMe) fluoromethylketone

SUMMARY

The connection between cell death and inflammation is an ancient one, first documented in the first century AD by the roman physician Galen. Cell death, as a consequence of tissue injury or infection, is a potent and universal stimulator of inflammation. This work sought to investigate two major aspects of how dying cells under different contexts might interact with the immune system. First, we investigated a role of the pro-apoptotic molecule TRAIL, as an inducer of inflammatory signalling, and explored the implications for the immune system in deciphering this mode of cell death. Second, we discovered the proteases responsible for the proteolysis and activation of IL-36 cytokines; members of the IL-1 cytokine family which represent key endogenous danger signals that alert the immune system in the event of necrotic cell death.

The work described in chapter 3 of this thesis sought to test the hypothesis that TRAIL is a pro-inflammatory cytokine. We demonstrated that TRAIL-receptor stimulation induced the production of several pro-inflammatory cytokines and chemokines, a subset of which could trigger chemotaxis of phagocytic cells towards the source of these factors. The production of conventional chemotatic factors such as IL-8 and MCP-1 suggested that perhaps TRAIL signalling was capable of recruiting cells of the immune system such as neutrophils and macrophages, which in the context of TRAIL induced apoptosis might facilitate removal of apoptotic cells by these phagocytic cell types. We confirmed through a series of experiments that apoptotic supernatants from TRAIL stimulated cells contain a chemotatic potential. Immunodepletion of specific chemokines and cytokines demonstrated that this chemotaxis was mediated by IL-8, in the context of neutrophil recruitment and MCP-1 in the context of monocyte recruitment. The data presented in this chapter suggests that not all apoptotic cell death may be immunologically silent and certain stimuli, such as TRAIL receptor engagement, can actively engage the immune system through

the secretion of conventional cytokines and chemokines from apoptotic cells.

The work described in chapter 4 sought to test the hypothesis that IL-36 cytokines may be activated by neutrophil serine proteases. Purified neutrophil enzymes or human neutrophil degranulates were used to explore the activation of IL-36 cytokines using enzyme-linked immunosorbent assay (ELISA) to measure cytokines induced by biologically active IL-36 cytokines. This was followed by mapping of the cathepsin-G and elastase cleavage sites within IL-36β and IL-36γ using Edman degradation sequencing followed by site-directed mutagenesis to confirm these amino acids as the proposed cleavage sites. We developed a novel strategy to design peptide inhibitors that were based on preferred amino acid sequences for elastase and cathepsin-G enzymes. Candidate peptides were tested using a cell culture-based bioassay. Through this approach we identified a number of novel inhibitory peptides of elastase and cathepsin-G.

Finally, chapter 5 investigated a number of potential biological implications for activated IL-36. To capture a more global perspective on IL-36-induced genes we performed gene expression array analysis of primary keratinocytes. Of particular interest was a strong pro-inflammatory signature induced by activated IL-36 in primary keratinocytes that was sufficient to drive the production of a number of important pro-inflammatory cytokines, many of which are highly elevated in psoriatic lesional skin. This gene expression dataset was further validated by real-time PCR and ELISA experiments. We also investigated the potential of IL-36 to regulate the proliferation and differentiation of primary keratinocytes, a cell type that displays a hyperproliferative phenotype in psoriasis. Furthermore, we explored the effects of active IL-36β in a three-dimensional organotypic skin model and found that active IL-36β was sufficient to perturb skin proliferation and differentiation, producing features resembling psoriasis such as a significant thickening of the epidermal layer.

TABLE OF CONTENT

DECLARATION

ACKNOWLEDGEMENTS

LIST OF FIGURES

ABBREVIATIONS

THESIS SUMMARY

CHAPTER 1 - Literature Review

1.1 INTRODUCTION 1

1.2 INFLAMMATION 2

1.2.1 THE ROLE OF INFLAMMATION 2

1.2.2 CELL DEATH AND INFLAMMATION 3

1.3 DIFFERENT MODES OF CELL DEATH 5

1.3.1 APOPTOSIS AND NECROSIS 5

1.3.2 PATHWAYS OF APOPTOSIS 6

The Extrinsic pathway 7

Granzyme B pathway 8

The Intrinsic pathway 8

1.4 CASPASES AS MODULATORS OF INFLAMMATION 9

1.4.1 DEATH BY A THOUSAND CUTS 9

1.4.2 ADVERTISING A CELL FOR REMOVAL 10

1.4.3 APOPTOTIC CASPASES MEDIATE THE INACTIVATION OF DANGER SIGNALS 12

1.5 ALTERNATIVE ENDPOINTS TO DEATH RECEPTOR SIGNALLING 14

1.5.1 TRAIL AND FAS ARE IMMUNOSTIMULATORY MOLECULES 14

1.5.2 A PARADOXICAL ROLE FOR DEATH RECEPTORS IN TUMORIGENESIS 16

1.5.3 INFLAMMATION AND TUMORIGENESIS 17

1.6 INTERLEUKIN-1 FAMILY 19

1.6.1 OVERVIEW OF IL-1 MEMBERS 20

1.6.2 IL-1 SIGNALLING PATHWAY 20

1.6.3 IL-1 CYTOKINES 21

IL-1α/β 22

IL-36 cytokines 24

IL-1 cytokines and inflammatory diseases 24

IL-36 cytokines and psoriasis 26

1.6.4 PROTEOLYSIS OF IL-1 CYTOKINES BY IMMUNE-RELATED PROTEASES AS A GENERAL MECHANISM TO MODULATE THEIR BIOLOGICAL ACTIVITY 28

1.7 THESIS AIMS 29

CHAPTER 2 - Materials and Methods

2.1. REAGENTS 31
2.1.1 Recombinant protein, ELISA kits and chemicals 31
2.1.2 Antibodies 31
2.1.3 Synthetic polypeptide synthesis 31

2.2 RECOMBINANT PROTEINS 32
2.2.1 Expression and purification of recombinant proteins in Escherichia coli 32
2.2.2 LPS depletion 32
2.2.3 In vitro transcription/translation 33

2.3 PROTEIN DETECTION 33
2.3.1 SDS-PAGE electophoresis 33
2.3.2 Tricine gels 33
2.3.3 Western immunoblotting 34
2.3.4 Protease Activity Assays 35

2.4 CELL-BASED ASSAYS 35
2.4.1 Cell culture 35
2.4.2 Generation of HeLa cell lines 35
2.4.3 Bioactivity assay 36
2.4.4 RNA interference 36
2.4.5 ELISA 37
2.4.6 Human cytokine and angiogenesis Arrays 37
2.4.7 Intracellular cytokine staining 38

2.5 NEUTROPHIL DEGRANULATE PREPARATIONS 38
2.5.1 Purification of primary cell populations and preparation of degranulates 38

2.6 CHEMOTAXIS ASSAYS 39
2.6.1 Detection/Inhibition of ATP in apoptotic supernatants 39

2.7 CELL DEATH ASSAYS 39
2.7.1 Annexin V/propidium iodide staining 39
2.7.2 Morphological apoptosis assays 40

2.8 SITE-DIRECTED MUTAGENESIS 40

2.9 GENERATION AND IMMUNHISTOCHEMICAL ANALYSES OF ORGANOTYPIC SKIN EQUIVALENTS. 40

2.10 PSORIATIC PATIENT SAMPLES 41

2.11 GENE EXPRESSION ANALYSIS 42
2.11.1 Gene expression microarray 42
2.11.2 RNA analysis by Real-Time PCR (RT-PCR) 42
2.11.3 Primers for RT-PCR 42

CHAPTER 3 - TRAIL promotes pro-inflammatory cytokine and chemokine production

3.1 INTRODUCTION 44

3.2 RESULTS 46

3.2.1 TRAIL-R ENGAGEMENT INDUCES PRODUCTION OF MULTIPLE CYTOKINES AND CHEMOKINES 47

3.2.2 PRO-INFLAMMATORY CYTOKINES AND CHEMOKINES ARE PRODUCED BY CELLS WITH CLEAR FEATURES OF APOPTOSIS 47

3.2.3 TRAIL-INDUCED PRODUCTION OF PRO-INFLAMMATORY CYTOKINES IS CELL DEATH AND CASPASE-INDEPENDENT 47

3.2.4 TRAIL-INDUCED CHEMOKINE PRODUCTION CAN BE INHIBITED THROUGH ANTAGONISM OF IAPS 48

3.2.5 RIPK1 AND MULTIPLE KINASE PATHWAYS REGULATE TRAIL-INDUCED CYTOKINES 49

3.2.6 COMPONENTS OF THE DISC DIFFERENTIALLY MODULATE CYTOKINE PRODUCTION 50

3.2.7 CASPASE-8 IS CRITICAL FOR TRAIL/FAS-INDUCED CYTOKINES AND IS INDEPENDENT OF ITS ROLE IN MEDIATING APOPTOSIS 50

3.2.8 CASPASE-8/FADD/CFLIP ARE THE KEY PROTEINS THAT MODULATE TRAIL- AND FAS-INDUCED CYTOKINES 51

3.2.9 RIPK1 MODULATION OF TRAIL/FAS-INDUCED CYTOKINES 51

3.2.10 SUPERNATANTS FROM TRAIL-STIMULATED CELLS PROMOTE PHAGOCYTE CHEMOTAXIS 52

3.2.10 TRAIL-INDUCED MCP-1 AND IL-8 SERVE AS 'FIND ME' SIGNALS FOR APOPTOTIC CELLS 53

3.3 DISCUSSION 55

3.3.1 TRAIL IS A PRO-INFLAMMATORY MOLECULE 55

3.3.2 TRAIL-INDUCED CHEMOKINES AS POTENTIAL 'FIND-ME' SIGNALS FOR APOPTOTIC CELLS 55

3.3.3 KEY COMPONENTS OF THE TRAIL INFLAMMATORY SIGNALLING COMPLEX 57

3.3.4 IMPLICATIONS OF TRAIL-INDUCED CYTOKINES AND CHEMOKINES 59

CHAPTER 4 - Identification and characterization of IL-36 activating enzymes

4.1 INTRODUCTION 62

4.2 RESULTS 63

4.2.1 PRODUCTION OF RECOMBINANT INTERLEUKIN-36 LIGANDS 64

4.2.2 PRODUCTION OF ARTIFICALLY TRUNCATED INTERLEUKIN-36 LIGANDS: ACTIVATION UPON CASPASE-3 PROTEOLYSIS 64

4.2.3 ESTABLISHMENT OF AN IL-36 BIOACTIVITY ASSAY WITH TRUNCATED IL-36 LIGANDS 64

4.2.4 PROTEOLYTIC PROCESSING OF DEVD-MODIFIED IL-36 CONFERS BIOLOGICAL ACTIVITY 65

4.2.5 NEUTROPHIL-DERIVED PROTEASES ACTIVATE IL-36 CYTOKINES 65

4.2.6 IDENTIFICATION OF IL-36-ACTIVATING PROTEASES 66

4.2.7 PURIFIED CATHEPSIN-G AND ELASTASE ACTIVATE IL-36 CYTOKINES 66

4.2.8 Depletion of IL-36 processing activity using a biotin-FLF-CMK peptide 67
4.2.9 Design and functional validation of novel neutrophil protease inhibitors . 67
4.2.10 IL-36 receptor antagonist attenuates IL-36-induced cytokines 68
4.2.11 Mapping of cathepsin-G and elastase cleavage sites in IL-36 cytokines 69

4.3 DISCUSSION 70
4.3.1 IL-36 cytokines are activated by neutrophil proteases 70
4.3.2 Effects of proteolysis on IL-36 signalling 70
4.3.2 Neutrophils as critical drivers of inflammation 72
4.3.4 Targeting neutrophil protease activity using peptide inhibitors 73
4.3.5 Sequence mapping of neutrophil cleavage sites witin IL-36 75

CHAPTER 5 - Exploring the functional role of IL-36

5.1 INTRODUCTION 77

5.2 RESULTS 78
5.2.1 Activated IL-36 promotes robust cytokine production by keratinocytes 78
5.2.2 IL-36 and TNF drive distinct inflammatory gene signatures in primary keratinocytes 78
5.2.3 Validation of genome wide gene array data 79
5.2.4 Activated IL-36 does not modulate keratinocyte proliferation 79
5.2.5 Calcium-induced proliferative arrest and differentiation of keratinocyte monolayer is not modulated by IL-36 80
5.2.6 Activated IL-36 perturbs proliferation and differentiation in a three-dimentional (3D) skin model 80
5.2.7 Human IL-36 is does not activate the mouse IL-36R 81
5.2.8 Mouse IL-36B is cleaved but not activated by neutrophil proteases 82
5.2.9 Endogenous IL-36 cytokines are induced by IL-36 and TLR signalling 82
5.2.10 Calcium-induced differentiation upregulates endogenous IL-36 expression 83
5.2.11 IL-1 cytokines are released during necrotic cell death 83
5.2.12 Endogenous IL-36γ is cleaved by neutrophil proteases 84
5.2.13 Overexpressed IL-36 is cleaved and activated by neutrophil proteases 84
5.2.14 IL-36γ is greatly elevated within lesional skin from psoriasis patients 85

5.3 DISCUSSION 86
5.3.1 Proteolytic processing of IL-36 drives a potent inflammatory response in primary keratinocytes 86
5.3.2 The apicial cytokines IL-36 and TNF promote overlapping yet distinct inflammatory profiles 88
5.3.3 Active IL-36 perturbs normal epidermal proliferation and differentiation . 89
5.3.4 IL-1 cytokines are released during necrosis 90

CHAPTER 6 - General Discussion

6.1 INTRODUCTION 93

6.2 DEATH RECEPTOR-INDUCED APOPTOSIS AND ITS IMMUNOLOGICAL CONSEQUENCES 94
6.3 NON-APOPTOTIC OUTCOMES OF TRAIL SIGNALLING 96
6.4 PROTEOLYSIS OF IL-36 CYTOKINES 97
6.5 ROLE OF NEUTROPHILS AND IL-36 IN INFLAMMATORY SKIN CONDITIONS AND THE POTENTIAL FOR THERAPEUTIC INTERVENTION 100
6.6 CONCLUSION 102

REFERENCES

APPENDIX I

APPENDIX II

Chapter 1

Literature Review

1.1 Introduction

The molecules of interest in this thesis are cytokines, proteins that are released into the extracellular space by one cell, to communicate a messege to another cell. Cytokines are produced by a broad range of cell types including immune cells, such as neutrophils, macrophages and T-cells, as well as non-immune cells, such as cells of the endothelium, epithelium and stroma. Cytokines are the principal messengers of the immune system, a complex network of specialized cell types and organs that work in unison to protect the host from external and internal insults. The name 'cytokine', in fact represents a broad category of many different types of proteins, each with their own particular characteristics, but what they all have is common is the ability to communicate a message. This thesis will focus upon two diverse families of cytokine, and what unites them, namely cell death.

The first cytokine that we will encounter can communicate two different messages. The first is a message that instructs a cell to undergo apoptosis, a programmed form of cell death. The second message it conveys is to make and release pro-inflammatory molecules. It is called TNF-related apoptosis inducing ligand (TRAIL) and is a member of the Tumor necrosis factor (TNF) family of cytokines.

The second cytokine family we will encounter is the Interleukin-1 (IL-1) family, in particular the IL-36 members of this family. These cytokines are normally sequestered within live cells. When a cell is subject to sudden injury such as a burn or laceration, it dies rapidly by a form of cell death called necrosis. IL-1 family cytokines are released from cells during necrotic cell death, and communicate a message to the immune system that alerts it to potential danger.

This chapter will describe the nature of these two different families of cytokines, their mechanisms of action, the roles they play in different forms of cell death, and the effects these different forms of cell death have on the immune system.

1.2 Inflammation

1.2.1 The role of inflammation

Inflammation is an adaptive response that evolved to counteract noxious stimuli such as infection or tissue damage, and serves to return the affected tissue to homeostasis (Medzhitov, 2008). The four cardinal signs of inflammation include *rubor* (redness), *tumor* (swelling), *calor* (heat) and *dulor* (pain), and were first defined by Celsus over 2000 years ago. Even though Galen made the link between tissue injury and inflammation in the first century AD, the molecular and cellular events of the acute inflammatory response have been best characterized for infection. More recently, tissue injury, and the associated cell death, has been characterized as the other major route to inflammation (Matzinger, 1994). Of course, infection and tissue damage are not distinct and unrelated instigators of inflammation, but often occur in tandem and/or as a result of one another, such as in extensive tissue damage associated with the bacterial syndrome, necrotizing fasciitis. Therefore, it is entirely appropriate that the immune system has adapted to respond to tissue damage, as this not only requires tissue repair but also safeguards against the threat of infection.

In the event of infection, or after tissue injury, there is rapid vasodilation of the surrounding blood vessels and influx of plasma factors such as complement and IgG antibodies as well as leukocytes, which are mainly comprised of neutrophils. This initial reponse is orchestrated by tissue resident macrophages and mast cells that have responded to pathogens through recognition by innate immune receptors such as the Toll-like receptors (TLRs) or by recognition of tissue damage through necrotic release of host derived factors or 'danger signals' such as Interleukin-1 family cytokines (IL-1, IL-36, IL-33) (**Fig. 1.1**). Activated macrophages and mast cells produce a huge variety of inflammatory mediators including cytokines (TNF, IL-1, IL-6), chemokines (IL-8, CCL20, CXCL1), eicosanoids (leukotrienes and prostaglandins), and vasoactive amines (histamine, serotonin), which coordinate to promote blood vessel dilation and permeability, and are responsible for the characteristic redness, swelling and

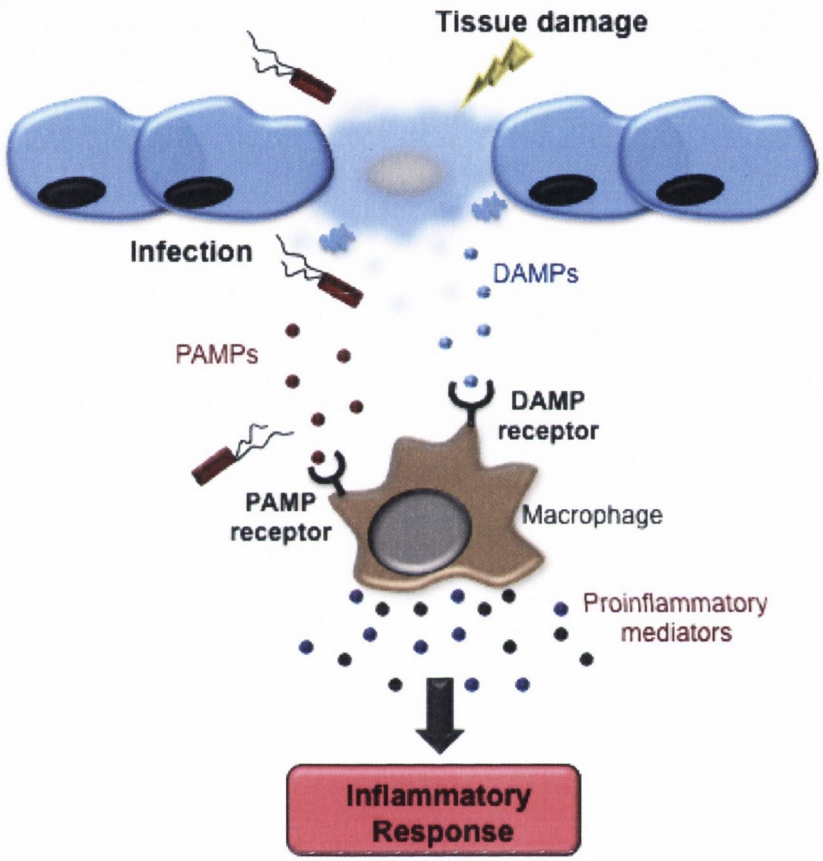


Figure 1.1 Tissue damage and infection are potent inducers of acute inflammation
Necrotic cell death, as a result of tissue injury, results in an inflammatory response through the release of danger-associated molecular patterns (DAMPs). Opportunistic pathogens may also infect damaged tissue and alert the immune system through the recognition of Pathogen-associated molecular patterns (PAMPs) by Pathogen recognition receptors (PRRs) expressed on immune cells. This family of PRRs include the Toll-like receptors (TLRs) and NOD-like receptors (NLRs).

pain. Furthermore, the now permeable blood vessels allow for the infiltration of neutrophils and plasma factors into the infected site. Upon arrival at the site of infection, neutrophils become further activated, either through contact with pathogens and/or by cytokines secreted by resident cells. Activated neutrophils ingest and attempt to destroy the pathogens by utilizing an extensive library of toxic agents including proteases (cathepin-G, elastase, proteinase-3), reactive oxygen species (ROS), and antimicrobial peptides (defensins). In the wake of neutrophil activation, collateral damage to surrounding tissue is unavoidable but represents a short-term cost accrued for the long-term benefit of the organism. Genetic diseases that impair neutrophil function have an extremely low prevalence in human populations, and underscore the importance of these cells in host defence. Nonetheless, rare genetic conditions such as Papillon-Lefevre syndrome, resign these patients to repeated infections, high morbidity and increased mortality as a result of impaired function of neutrophil granule proteases (Bardoel et al., 2014).

In the wake of a successful acute inflammatory response, there is a resolution and repair phase – a return to homeostasis (Serhan & Savill, 2005; Medzhitov, 2008). Activated neutrophils in inflamed tissue undergo apoptotic cell death and are engulfed by macrophages. Further recruitment of neutrophils is actively blocked through macrophage secretion of lipoxins that in turn can further stimulate macrophages to ingest and clear apoptotic neutrophils. Engulfment of dying neutrophils by macrophages mediates the switch from secretion of inflammatory to anti-inflammatory mediators (IL-10, lipoxins, resolvins, TGF-β), and rewiring of macrophages to a 'wound healing' or M2 phenotype, which orchestrate tissue repair and the return to normal tissue homeostasis (Serhan & Savill, 2005)

1.2.2 Cell death and inflammation

The connection between tissue injury and inflammation is an ancient one, first documented by the roman physician Galen, who linked tissue injury to inflammation from tending to the wounds of gladiators. It was over a millennium

later that infection was discovered as the other major initiator of inflammation, in part awaiting the discovery of the germ theory of disease (Wallach et al., 2014). It is now well established that cell death, as a consequence of tissue injury or infection, is a potent and universal stimulator of inflammation, however the mechanisms through which this occurs are only now being illuminated (Kono & Rock, 2008). The nature of how a cell dies is of paramount importance and our immune system responds to different forms of cell death with very different outcomes.

Necrotic cell death is typically associated with tissue damage, and so the outcome of necrotic cell recognition by the immune system is an inflammatory one (Kono & Rock, 2011). In stark contrast, billions of cells die each day by programmed cell death or apoptosis, yet this form of cell death does not elicit an overt inflammatory response. Because of the scale of apoptosis *in vivo*, a failure to discriminate between apoptosis and necrosis would result in inappropriate immune activation, breakdown of tolerance and autoimmunity. Furthermore, apoptotic cells may actively elicit anti-inflammatory responses from macrophages, promote cell proliferation of neighbouring cells and tissue repair responses, to replace those cells that have died (Martin et al., 2012). However, apoptosis may not always be anti-inflammatory, as certain pro-apoptotic stimuli such as members of the TNF family (e.g. TRAIL, Fas) may be inherently pro-inflammatory, and so override anti-inflammatory responses (Bossaller et al., 2012; Cullen et al., 2013). Nonetheless, qualitative and quantitative differences between necrosis and apoptosis exist and they underlie how the immune system should decipher these different modes of cell death to take the appropriate action.

Necrosis can occur for a multitude of reasons including burns, lacerations, compression injuries, or as a result of pathogens (Rock et al., 2011). Necrotic cells are through to elicit their inflammatory effects through the release of endogenous danger signals or danger-associated molecular patterns (DAMPs). Of note, Polly Matzinger predicted the existence of DAMPs in her seminal 1994 paper that hypothesized that only in the context of danger (tissue injury) does the immune system mount a robust response to a particular noxious insult (e.g.

pathogens, adjuvant) (Matzinger, 1994). Over the past decade a large number of potential DAMPs have been discovered with some representing classical pro-inflammatory cytokines such IL-1 family members (IL-1, IL-33), while other reported DAMPs include uric acid crystals, ATP, HMGB1 and genomic DNA (Rock et al., 2011; Martin et al., 2012). In particular, IL-1 family members (IL1α, IL-33, IL-36) are excellent candidates as DAMPs insofar as they represent highly pro-inflammatory molecules that are capable of mediating a robust immune response. These cytokines are highly expressed in barrier tissue (e.g. skin, airway epithelial) and so are ideally placed for release upon injury. Furthermore, these cytokines lack a secretory signal and are only released during necrosis. In addition, a number of studies have implicated IL-1α as the dominant inflammatory component of the immune response associated with sterile injury (Chen et al., 2007; Eigenbrod et al., 2008, Rock et al., 2011). Interestingly, recent studies have demonstrated that certain DAMPs are inactivated or sequestered during apoptosis, suggesting a mechanism to disarm dying cells of these other potent immunostimulatory molecules (Martin et al., 2012; Luthi et al., 2009; Kazama et al., 2008; Cohen et al., 2010; Marichal et al., 2011).

While recognition of a wide variety of pathogen components by innate immune receptors such as the TLRs is vital to mounting an innate immune response, the release of DAMPs during necrotic cell death that may precede or occur because of infection, act as a additional line of defence against infectious agents. Furthermore, in the context of sterile injury, where DAMPs (e.g. IL-1α) act as the major inducers of inflammation, they also promote the subsequent repair of damaged tissue (Kono & Rock, 2008).

1.3 Different modes of cell death

1.3.1 Apoptosis and necrosis

We turn over approximately 1 million cells per second as part of normal tissue homeostasis (Ravichandran et al., 2011). This remarkable feat of waste

management is primarily mediated by apoptosis, a mode of cell death that is critical for the disposal of superfluous or aberrant cells during development, for removal of autoreactive T-cells in the thymus, and also of aged, transformed, infected and injured cells (Kerr et al., 1972; Jacobson et al., 1997; Taylor et al., 2008). Apoptosis is the biological counterweight to mitosis in regulating cell numbers in multicellular organisms. Just like mitosis, apoptosis is under tight molecular control orchestrated by a dedicated set of enzymes and their regulators (Taylor et al., 2008). Members of a family of cysteine proteases, the caspases, become activated during apoptosis and coordinate the events that take place to ensure swift recognition and removal of apoptotic cells by phagocytes (Taylor et al., 2008; Martin et al., 2012). Although a clear understanding of the biological significance of most caspase-dependent cleavage events has yet to be achieved, the major endpoint is the presentation of apoptotic cells and apoptotic bodies to resident phagocytes responsible for cleaning up the cellular debris. This event is remarkable when one considers that phagocytes are typically engaged in the business of recognizing and eating foreign 'non-self' antigens, yet in the context of apoptosis, the dying cell is designated for removal despite being part of 'self' only moments earlier. For reasons that will be discussed below, apoptotic cells are recognised as being different from their viable counterparts as well as cells that die by necrosis. Necrotic cell death is characterized by rapid swelling followed by cell rupture, causing the release of cellular contents into the extracellular space. How the immune system responds to apoptotic versus necrotic cells is fundamentally different (reviewed in Birge & Ucker, 2008). Whereas necrotic cell death is characterized by the release of self-derived danger signals and an acute inflammation response, apoptosis is thought to be largely 'silent' or even actively anti-inflammatory (Kono & Rock, 2008, Medzhitov, 2008; Martin et al., 2012)

1.3.2 Pathways of apoptosis

The fate of individual cells in a multicellular organism is carefully controlled to ensure that unsolicited population expansions or contractions do not occur. It is

now understood that cell death, just like cell division, is a highly regulated by a genetically programmed process.

There are three major routes leading to apoptotic cell death. These have been termed the extrinsic, intrinsic and granzyme B pathways (**Fig. 1.2**). Common to all these pathways is activation or introduction of an apical protease (i.e. caspase 8 or granzyme B) as the first step in initiating the caspase activation cascade (Taylor et al., 2008). The range of substrates cleaved by these initiators is relatively narrow, but importantly includes the executioner caspases that, upon activation, can go on to mediate hundreds of proteolytic events within the cell (Martin & Green, 1995). In this way the caspase cascade is amplified from tightly regulated events occurring at a specific location in the cell (i.e. the plasma membrane or mitochondria), to a cell-wide proteolytic demolition which impacts on all aspects of cellular physiology, resulting in the demise of the cell.

The Extrinsic pathway

The extrinsic pathway is so called because the signal for a cell to kill itself is delivered by another cell, typically a cytotoxic T-lymphocyte (CTL), through extracellular signaling in the form of death receptor engagement (**Figure 1.2)**. The binding of receptors such as TRAIL receptors (DR4/DR5) or Fas receptor (CD95/APO-1) expressed on the target cell, to corresponding ligands expressed on cytotoxic cells, leads to the assembly of a caspase activation platform known as the death-induced signaling complex (DISC). This complex is composed of adapters such as FADD as well as the initiator enzyme caspase-8 and in some circumstances caspase-10, however there is conflicting evidence as to whether caspase-10 is capable of initiating apoptosis in the absence of caspase-8 at the DISC. (Wiley et al., 1995; Schneider et al., 1997; Sprick et al., 2000; Sprick et al., 2002). Caspase-8 associates with this complex through its death-effector domains (DED) and autoactivates at the receptor complex via induced proximity with other caspase-8 molecules (Muzio et al., 1998; Salvesen & Dixit.1999). Caspase-8 may cleave and activate the pro-apoptotic protein known as BID which can engage the intrinsic pathway, via Bax/Bak oligomerisation, to caspase activation by promoting

mitrochondrial cytochrome c release (Liu et al., 1996; Luo et al. 1998). Additionally, active caspase-8 can also directly process effector caspases. These executioner caspases (caspase-3/-7) in turn carry out the apoptotic dismantling of the targeted cell.

Granzyme B pathway

As an alternative to the engagement of death receptors on the surface of target cells, cytotoxic NK cells and CTLs may kill their targets through the delivery of cytotoxic granules to the target cell cytosol (Cullen & Martin 2008). Contained within these granules are two key constituent proteins, perforin and granzyme B. Perforin is thought to permeablilize the plasma membrane of the target cell, possibly through the formation of channels (Keckler, 2007), and this facilitates cellular entry of granzyme B, a proteolytic enzyme that can initiate apoptosis. This is achieved in part through the ability of granzyme B to cleave and activate the executioner caspases-3 and -7 (Adrain et al., 2005).

The Intrinsic pathway

The intrinsic pathway is centred on events occurring at mitochondrial membranes. Specifically, it is the release of cytochrome *c* from mitochondria that triggers the activation of the caspase cascade and essentially represents a point of no return for the dying cell (Liu et al., 1996; Slee et al., 1999). DNA damage, transcriptional/translational block, protein mis-folding or loss of growth factor signaling are some examples of events that can potentially lead to the activation of the intrinsic pathway (Martin et al., 1990, Masud et al., 2007, Youle & Strasser 2008). Regardless of the upstream signalling events, it is the interplay between members of the BCL-2 protein family that regulates the cell's response to stress. Oligomerization of two BCL-2 proteins, BAX and BAK, at the mitochondrial membrane, is the event that facilitates cytochrome *c* release (Kuwana et al., 2002). BAX and BAK are, in turn negatively regulated by other BCL-2 family members, which include BCL-2, BCL-xL and MCL-1. While anti-apoptotic BCL-2 family proteins inhibit BAX/BAK channel opening, a diverse group of pro-apoptotic BH3-

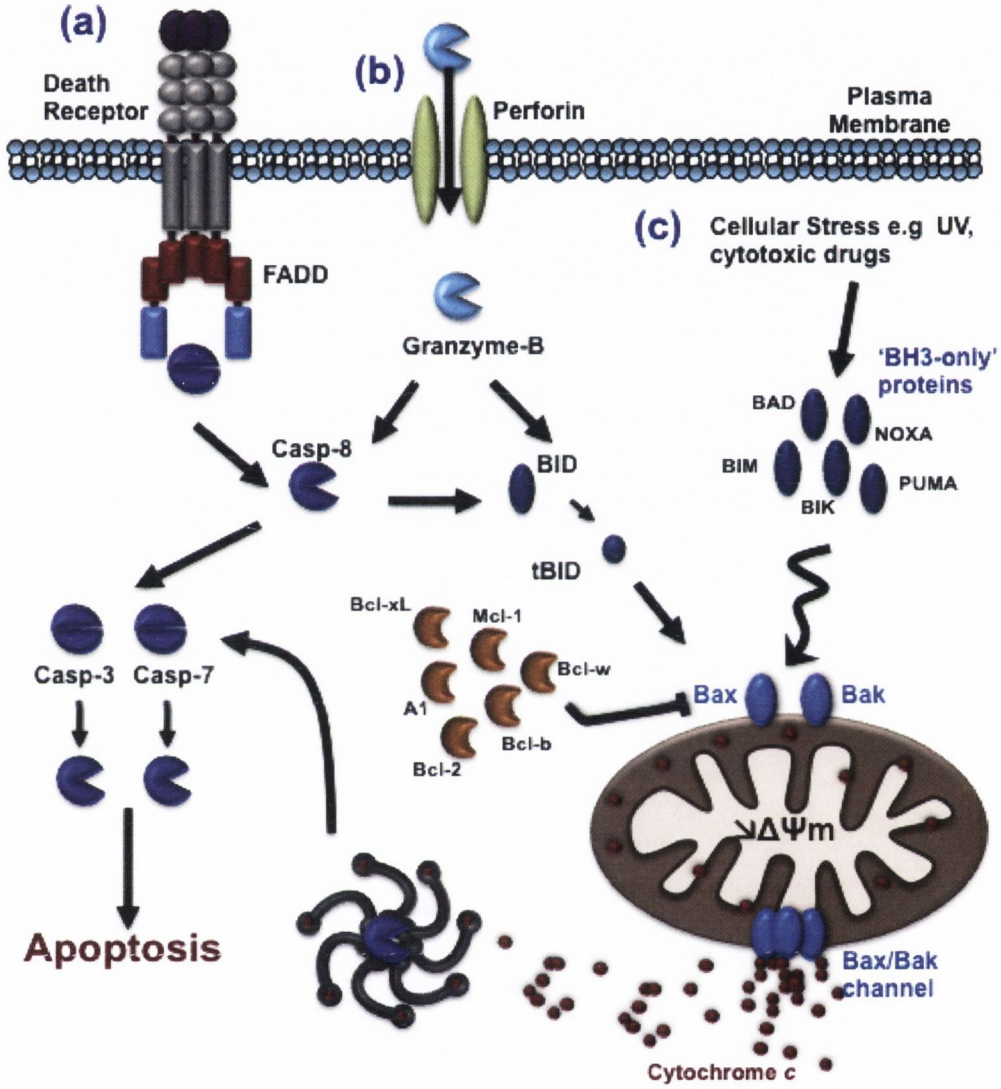


Figure 1.2 Major pathways leading to apoptosis
Pro-apoptotic stimuli are routed through three major pathways, namely **(a)** The extrinsic pathway mediated by pro-apoptotic molecules such as Fas/CD95 and TRAIL, **(b)** The granzyme-B pathway mediated by a pro-apoptotic granzyme delivered from NK and cytotoxic T-cells, and **(c)** The intrinsic pathway mediated by cytochrome *C* release from mitochondria as a result of mitochondrial outer membrane permeabilization (MOMP). The endpoint of each pathway results in activation of the caspase cascade and apoptotic cell death.

only proteins (such as BID) promote BAX/BAK oligomerization (Youle & Strasser 2008). Upon BAX/BAK oligomerization, cytochrome *c* is released into the cytoplasm and induces the oligomerization of the cytoplasmic protein APAF-1. This complex, referred to as the apoptosome, recruits and activates caspase-9 (**Fig. 1.2**), which can then act as an initiator of the caspase cascade by cleaving and activating caspase-3 and -7 followed by activation of additional caspases downstream (Li et al., 1997; Slee et al., 1999).

1.4 Caspases as modulators of inflammation

1.4.1 Death by a thousand cuts

Regardless of their individual specificities, together the effector caspases are implicated in the cleavage of hundreds of proteins within the cell (Lüthi & Martin 2007, Taylor et al., 2008). During the final phase of apoptosis their activity results in the wholesale demolition of the cell and can be regarded as the defining moment of programmed cell death. We can observe this demolition phase through hallmark events such as cell detachment and plasma membrane blebbing, nuclear condensation and fragmentation (Taylor et al., 2008; Henry et al., 2013). Although the identified substrates are numerous, it is a puzzling fact that only very few proteolytic events have been explicitly linked to phenotypic alterations occurring within apoptotic cells. Furthermore, the failure to cleave particular caspase substrates does not permit a cell to survive the events that precede caspase activation. This is mainly due to the fact that mitochondria are permanently compromised after cytochrome *c* release such that the cell is now destined to die (Green & Kroemer, 2004; Martin et al., 2012). Given the sheer number of caspase substrates (~700 so far identified), it would seem highly improbable that the majority of these proteins are targeted exclusively for the purpose of terminating cell viability.

1.4.2 Advertising a cell for removal

Although a clear understanding of the significance of most caspase-dependent cleavage events has yet to be achieved, a key endpoint must be the presentation of apoptotic cells and apoptotic bodies to the surveying phagocytes responsible for cleaning up the cellular debris. From the viewpoint of the immune system, the difference between necrotic and apoptotic cells appears to be one of stark contrast. While necrotic cell death is characterized by the release of DAMPs and subsequent inflammation, apoptosis is largely tolergenic (recognised as 'self' by the immune systems) or even refractory to an inflammatory response (**Figure 1.3**) (Birge & Ucker 2008). Therefore, if cytochrome *c* release alone is sufficient to kill a cell (Green & Kroemer, 2004), much of the caspase-dependent processing of substrates may be targeted towards preparing the dying cell to meet the immune system on good terms (Martin et al., 2012).

Detachment and fragmentation into apoptotic bodies is a key event that aids in the removal of apoptotic cells by phagocytes, however to achieve this, apoptotic cells must be labelled for removal. More specifically, the phagocyte must identify the dying cell among a sea of living ones. A number of candidate molecules, called 'eat-me' signals, are expressed on the membrane of apoptotic cells. These include phosphatidylserine (PS) and oxidized-low density lipo-protein (Martin et al., 1995, Chang et al., 1999, Greenberg et al., 2006). PS has received the most attention since its discovery by Fadok and colleagues, with PS exposure routinely used as a marker for apoptotic cells (Fadok et al., 1991), but whether PS exposure alone is sufficient for removal of apoptotic cells has recently come under question (Suzuki et al., 2010; Segawa et al., 2011). This would suggest that additional 'eat-me' signals are required for effective removal of apoptotic corpses by phagocytes.

Recent reports have suggested that apoptotic cells may also actively release soluble factors, dubbed 'find-me' signals, than can promote chemotaxis of phagocytic cells towards dying cells (Gregory and Pound, 2011; Ravichandran, 2011). These factors include ATP/UTP (Elliott et al., 2009; Chekeni et al., 2010), lysophosphatidylcholine (Lauber et al., 2003), fractalkine (CXCL3) (Trumen et al., 2003) and sphingosine-1-phosphate (S1P) (Gude et al., 2008) (**Fig. 1.4**).

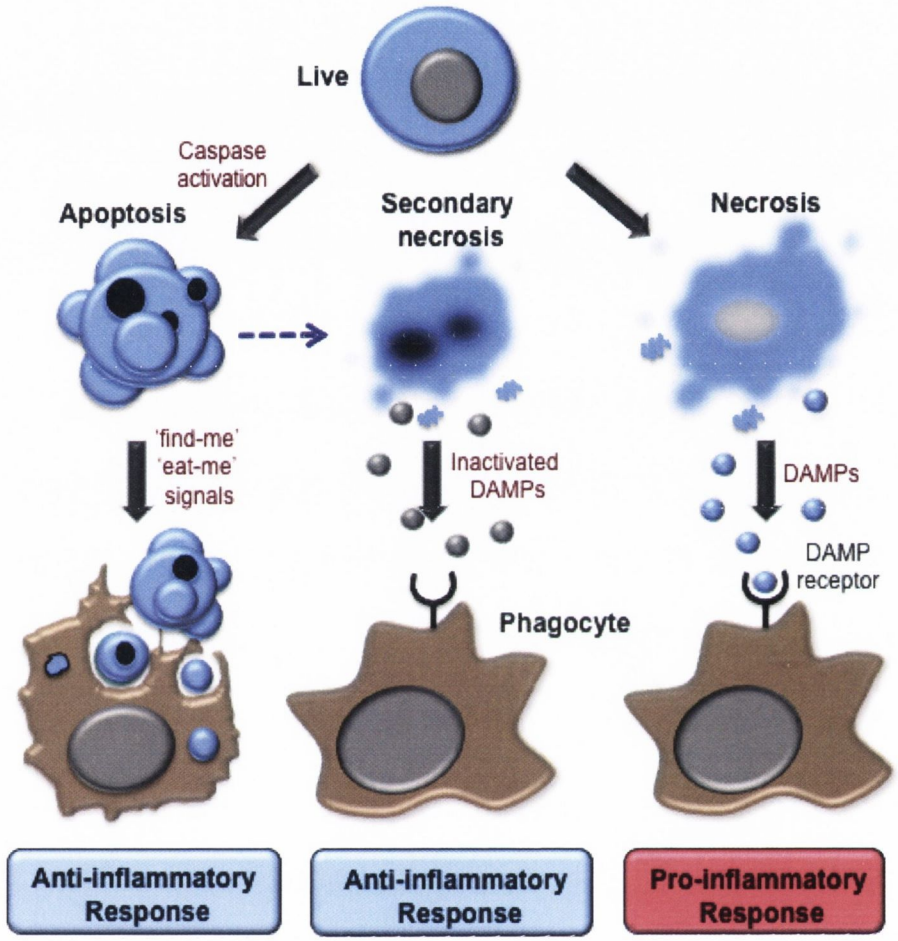


Figure 1.3 Different modes of cell death elicit distinct immune responses
Caspase activation coordinates the swift removal of apoptotic cells by phagocytes while at the same time actively suppressing immune responses. Caspase activation also ensures that secondarily necrotic cells are anti-inflammatory through inactivation of DAMPs. As caspases are not activated during necrosis, these cells exhibit potent pro-inflammatory properties.

Lysophosphatidylcholine (LPC), which is released in a caspase-dependent manner, was one of the first molecules to be implicated as a 'find-me' signal that is released during apoptosis (Lauber et al., 2003). LPC production by apoptotic cells results as a consequence of caspase-3-dependent cleavage of calcium-independent phospholipase A2 resulting in the hydrolysis of membrane phosphatidylcholine to produce LPC (Lauber et al, 2003). LPC can act as a chemoattractant for monocytic cells and macrophages and may help to guide phagocytes to dying cells. Ravichandran and colleagues have also implicated efflux of ATP and UTP as 'find-me' signals for monocytes (Elliott et al., 2009; Chekeni et al., 2010). It is worth noting that ATP has also been identified as a DAMP associated with necrosis (Idzko et al., 2007) but the magnitude of release during apoptosis (~2% total cellular ATP) appears to be much lower than that seen during necrosis (Elliott et al., 2009). Interestingly, the release of these molecules is dependent on caspases, however whether caspase involvement in this processing event is direct or indirect remains unclear for a number of these factors. However, it was reported that ATP secretion by apoptotic cells requires the cleavage of the membrane channel protein Pannexin 1 by caspase 3/7 (Chekeni et al., 2010).

Apoptosis *in vivo* is rarely associated with neutrophil influx and phagocytosis of apoptotic cells is thought to be mediated by tissue resident macrophages (Ravichandran, 2011). This selectivity in immune cell recruitment is particularly important as recruitment of neutrophils may risk eliciting an unwanted inflammatory response. A number of proposed 'find-me' signals have been known to stimulate neutrophil chemotaxis (Chen et al., 2006; Floray & Haskard, 2009). However, Gregory and colleagues have demonstrated that lactoferrin is released during apoptosis and this inhibits migration of neutrophils (Bournazou et al., 2009) (**Fig 1.4**). This is the first example of a 'stay away' signal, however its mechanism of release and whether it is specific to apoptotic cell death remains to be demonstrated.

1.4.3 Apoptotic caspases mediate the inactivation of danger signals

Another vital reason for ensuring that a dying cell is correctly packaged for removal is its potential antigenicity to the surrounding tissue. DAMPs released from necrotic cells may include conventional cytokines (e.g. IL-33, IL-36 or IL-1α) or cellular constituents that normally serve the intracellular physiology of healthy cells (e.g. HMGB1 or DNA) (Kono & Rock 2008; Martin, et al., 2012). DAMPs all share a common property in that they represent 'hidden self', thus their presence in the extracellular space is indicative of some gross departure from normality (Matzinger, 1994; Martin et al. 2012). These DAMPs come into contact with the immune system when they are released by deregulated rupture of the plasma membrane by necrosis. Unlike necrotic cells, apoptotic cells maintain plasma membrane integrity prior to their ingestion by phagocytes and this has been cited as the primary reason behind their lack of immunogenicity (Birge & Ucker, 2008). Although maintaining plasma membrane integrity is likely to have a significant effect on how the immune system responds to apoptotic cells, this does not appear to be the whole story. It has been observed in culture that cells undergoing apoptosis, with no phagocytes to clear them, eventually lose their membrane integrity and undergo secondary necrosis. It would stand to reason that if the plasma membrane was the only barrier to potential danger signals, then cells that have undergone secondary necrosis and leak their intracellular contents should activate the immune system in a similar manner as necrotic cells do. However, studies using bone marrow derived macrophages have found that exposure to late stage secondary necrotic cells does not stimulate a response comparable to that of primary necrotic cells (Patel et al., 2006). Furthermore, several laboratories have independently reported that apoptotic cells are also capable of profoundly attenuating responses to PAMPs delivered in parallel (Voll et al., 1997; Stuart et al., 2002; Lucas et al., 2003, 2006; Henson & Bratton, 2013). These data suggest that apoptotic cells are immunogenically deactivated, or switched to an anti-inflammatory state, from the inside out, a scenario that caspases have recently been implicated in (**Fig. 1.3**).

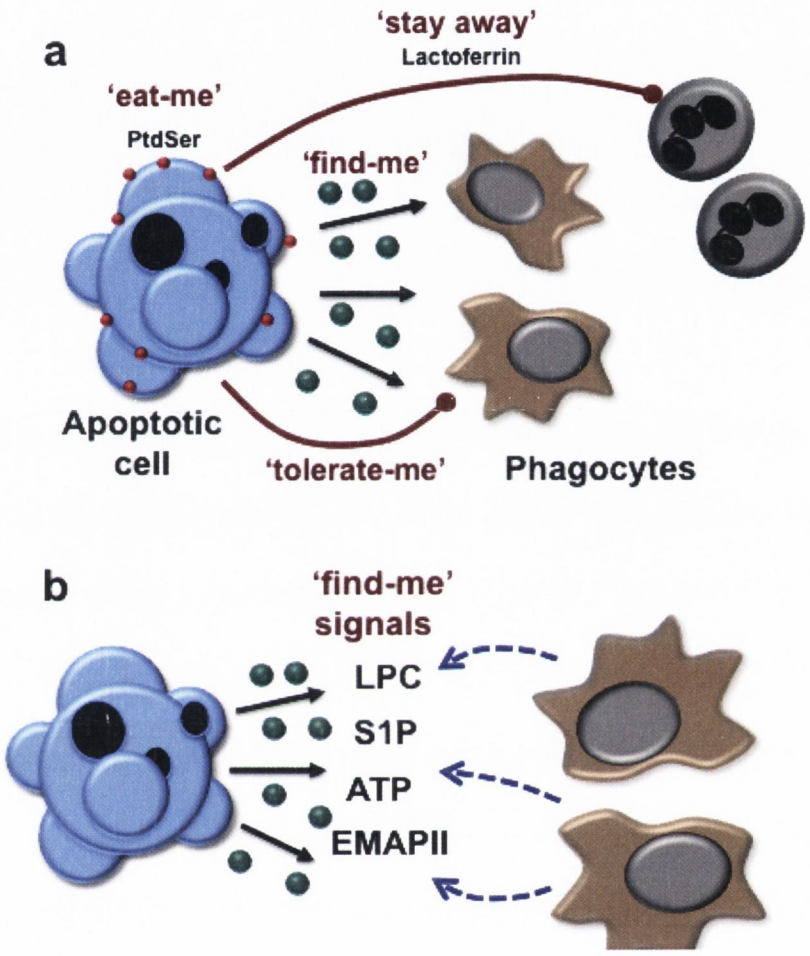


Figure 1.4 Apoptotic cells releases multiple signals to facilitate removal
a. Apoptotic cells generate a diverse set of signals which promote recruitment of phagocytes, keep out inflammatory neutrophils, to qualify this mode of cell death as harmless. **b.** Cells undergoing apoptosis release 'find me' signals such as ATP/UTP and lysophosphatidylcholine which attract the attention of professional phagocytes, and 'eat me' signals, to ensure swift removal of dying cells.

Examples of caspase-dependent inactivation of DAMPs are starting to emerge. Kazama and colleagues demonstrated that caspase-3-mediated proteolysis of the mitochondrial protein p75NDUF leads to accumulation of reactive oxygen species within apoptotic cells. These oxidizing species proved sufficient to deactivate the inflammatory potential of HMGB1, through oxidation of a critical cysteine residue (Kamaza et al., 2008). This provides a clear example of how caspase-mediated changes in the internal environment of apoptotic cells may reduce their inflammatory potential. Another key event is likely to be the fragmentation of genomic DNA, a key morphological feature of apoptosis (Kerr et al., 1972). Numerous studies have implicated genomic DNA, as well as DNA-protein complexes as a major source of autoimmune stimulation in diseases such as systemic lupus erythematosus (SLE) (Napirei et al., 2000), and DNA is also capable of inducing dendritic cell maturation and the cross presentation of self-antigens (Ishii et al., 2001). A particularly interesting finding relates to the mechanism of action of aluminum salts (Alum), an adjuvant long known for its capacity to provoke a robust immune response to antigens, which on their own fail to provoke immunity. A report by Marichal and colleagues demonstrates that administration of alum triggers necrosis of cells in local tissue, releasing genomic DNA that can act as a danger signal to alert local immune cells. In addition, isolated genomic DNA mimicked the adjuvant properties of Alum upon delivery into mice. Furthermore, the authors also found that degradation of DNA by the nuclease DNase I could attenuate the adjuvant affect of alum (Marichal et al., 2011). This exciting observation provides a clue as to why genomic DNA undergoes extensive degradation during apoptosis, but not necrosis. This degradation of DNA is mediated by caspase-dependent cleavage of ICAD, an inhibitor of the nuclease caspase-activated DNase (CAD). Upon ICAD inactivation, active CAD is released to chop up the genomic DNA into the characteristic ~200bp fragments observed during apoptosis (Enari et al., 1998). In addition, upon phagocytosis by macrophages, DNA from the dying cell is also degraded by DNase II, thus two separate DNases cooperate to ensure that genomic DNA is degraded (Kawane et al., 2003). Therefore, it seems plausible

based on these findings that short DNA fragments are less immunogenic than their high molecular weight counterparts and that caspases actively target DNA during apoptosis to dampen this immunogenic threat.

Thus far proteolysis of IL-33 is the only example of direct caspase-mediated inactivation of a danger signal (Luthi et al., 2009). IL-33, a recently described cytokine of the IL-1 family, appears to be a *bone fide* danger signal. It is released exclusively during necrosis, but undergoes caspase-dependent proteolysis during apoptosis (Luthi et al., 2009, Cayrol & Girard 2009). Although an initial report suggested that IL-33 was activated through caspase-1-dependent proteolysis (Schmitz et al., 2005), several laboratories have comprehensively demonstrated that this cytokine is constitutively active and is inactivated by caspase-3/-7 processing (Luthi et al., 2009; Cayrol & Girard 2009). A recent paper by Bonilla and colleagues, demonstrated that IL-33 is released during lymphocytic choriomeningitis virus (LCMV) infection as a consequence of lysis from virally infected cells. The presence of extracellular IL-33 enhanced the $CD8^+$ T-cell (CTL) response against viral infection, with mice defective in either $IL\text{-}33^{-/-}$ or the $ST2^{-/-}$ (IL-33 receptor) mounting defective CTL responses to LCMV infection. This is perhaps the first example of where a DAMP can directly mediate the adaptive immune response, through CTL activation, in the context of viral infection (Bonilla, et al., 2012).

While the full list of danger signals recognized by the immune system in times of crisis will no doubt expand, the emerging role of apoptosis in suppressing the activation of immune responses to dying cells suggests that the study of programmed cell death may help to identify new danger signals.

1.5 Alternative endpoints to death receptor signalling

1.5.1 TRAIL and Fas are immunostimulatory molecules

As outlined earlier, engagement of TRAIL receptors (DR4/DR5) and Fas/APO-1, members of the TNF superfamily, can result in apoptosis via a

caspase-8-dependent pathway (Wiley et al., 1995; Schneider et al., 1997; Sprick et al., 2000; Sprick et al., 2002; Wilson et al., 2009). The majority of studies exploring TRAIL and Fas interactions with their receptors have focused on cell death as the primary endpoint. As a consequence, this has overshadowed the role of death receptor engagement as a driver of other biological endpoints. For example, reports in the literature also suggest that TRAIL receptor stimulation results in the activation of multiple kinase pathways, including NF-κB, JNK and MAPK, with associated production of pro-inflammatory cytokines and chemokines (Schneider et al., 1997, Varfolomeev et al., 2005, Jin et al., 2006, Berg et al., 2009, Tang et al., 2009; Falschlehner et al., 2007; Kavuri et al., 2011). Other reported consequences of TRAIL receptor engagement include co-stimulation of $CD4^+$ T-cells (Hwei-Fang et al., 2004, Ai-Hsiang et al., 2001), proliferation of tumor cells (Ehrhardt et al., 2003), tumor invasion (Ishimura et al., 2006) and modulation of inflammatory diseases (Weckmann et al., 2007). Thus, much evidence suggests that signaling through the TRAIL receptor pathway can lead to endpoints other than cell death, but this aspect of TRAIL biology and its functional consequences are not well understood.

Owing to the cytotoxic effects on the liver, Fas has not been considered a viable option for cancer therapy. In contrast, TRAIL is typically non-cytotoxic to non-transformed tissues, however tumor cells are susceptible to TRAIL-induced killing. This has led to TRAIL therapeutics entering clinical trials for many different cancer types (Falschlehner et al., 2007; Ashkenazi, 2008). The conclusion that tumors are susceptible to TRAIL was somewhat premature as it emerged in time that many cancers, particular colon and pancreatic-derived, are highly resistant to TRAIL, in some circumstances as a result of the expression of TRAIL 'decoy receptors' (Ashkenazi, 2002, 2008). These decoy receptors, which include DcR1 and DcR2, are capable of binding TRAIL ligand but do not transduce a death signal due to the lack of a death domain (DD). These decoy receptors have received limited attention, relative to TRAIL-R1/DR4 and TRAIL-R2/DR5, but evidence suggests that they can contribute to cell survival by competing for ligand, but also by activating alternative pro-inflammatory and pro-

survival pathways such as NF-κB, underscoring the potential for TRAIL to regulate inflammation via multiple mechanisms (Ashkenazi, 2002).

TRAIL receptors are members of the TNF receptor superfamily, along with molecules such as Fas and TNF Receptor 1 (TNFR1), members of which play an important role in regulating cell lifespans but also in cell-cell communication within the immune system (Karin et al., 2009). For example, a key aspect of TNFα function is its potent ability to trigger the production of numerous pro-inflammatory cytokines and chemokines in the context of immune reactions, i.e. during viral or bacterial infections or autoimmune conditions (Brennan & McInnes, 2008). TNFα-induced cytokines and chemokines, such as IL-6, IL-8, GM-CSF and RANTES, can coordinate and amplify immune responses through triggering the production of acute phase proteins, recruitment of neutrophils and basophils to the site of inflammation and by promoting increased production of monocytes/macrophages from bone marrow (Delves et al., 2011).

Fas and TRAIL are best known as inducers of apoptosis in target cells via engagement of their respective receptors, but as for TRAIL, sporadic reports over the years have implicated Fas signalling in a range of non-death related functions. For example, Fas stimulation can result in the production of pro-inflammatory cytokines and chemokines (Choi et al., 2001; Park et al., 2003; Farley et al., 2006, Cullen et al., 2013). Other reported consequences of Fas engagement include: activation and maturation of dendritic cells (Rescigno et al., 2000), chemotaxis of neutrophils and monocytes via Fas-induced chemokines (Cullen et al., 2013), cell motility (Barnhart et al., 2005), and tumor invasion (Kleber et al., 2008). Fas stimulation has also been implicated, somewhat counterintuitively, as a driver of tumor proliferation (Chen et al., 2010). Thus, much evidence suggests that signaling through the Fas pathway, like the TRAIL pathway, can lead to endpoints other than cell death.

1.5.2 A paradoxical role for death receptors in tumorigenesis

An interesting and puzzling finding that has emerged from the vast array of cancer genomic and transcriptomic datasets compiled in the past decade has

been the expression of death receptors on tumors. Fas and TRAIL receptors are significantly upregulated in many different types of cancer including ovarian, renal, hepatocellular, pancreatic and colorectal cancers yet the reason why has remained obscure. Landmark studies by Marcus Peter and colleagues has shown that elimination of Fas receptor expression on several different cell types, including renal, ovarian and breast cancers, led to a reduction in proliferation both *in vitro* and *in vivo* and can even lead to an atypical from of cell death with necrotic-like features (Chen et al., 2010; Hadji et al., 2014). In addition the authors of this study demonstrated that in a *Kras Pten*-deleted mouse model of epithelial ovarian cancer, genetic deletion of Fas greatly diminished the incidence of tumorigenesis in these mice (Chen et al., 2010). Furthermore, in a chemical (DEN)-induced carcinogenesis model of hepatocellular carcinoma, loss of Fas expression greatly reduced the rate of tumor formation in these animals (Chen et al., 2010). A direct demonstration that Fas overexpression can be beneficial to tumor growth was demonstrated in a mouse model of Lewis lung carcinoma, where Fas overexpression in these tumors fails to sensitize to apoptosis but greatly accelerated tumor growth (Lee et al., 2003). However, how Fas mediates this pro-tumorgenic effect has not been elucidated. Similarly, it has been shown that TRAIL-mediated stimulation of certain leukemia cell types promoted survival and proliferation, which correlated with NF-κB expression (Ehrhardt et al., 2003). NF-κB-driven inflammation was speculated to be involved in another study which looked at mice that constitutively overexpress soluble Fas ligand (sFasL), where these mice developed hepatic tumors and a chronic inflammatory condition (O'Reilly et al., 2009). Therefore, it is interesting to speculate that blockade of Fas and/or TRAIL receptors in certain cancer types may slow growth and progression of a tumor, a view that challenges the current opinion that 'death receptor' expression is invariably detrimental to the tumor.

1.5.3 Inflammation and tumorigenesis

An emerging 'enabling hallmark' of tumor development is chronic inflammation. Indeed, it has long been recognised by pathologists that many

tumor types are often infiltrated with cells from the immune system, yet the implications remained obscure (Hanahan & Weinberg, 2011; Grivennikov et al., 2010). A major function of the immune system is to restore normal tissue integrity (or homeostasis) after infection or sterile injury by promoting wound healing (Chovatiya & Medzhitov, 2014). During both infection and sterile injury, cells of the innate immune system such as macrophages and dendritic cells secrete a array of growth and angiogenic factors, which stimulate the proliferation of local tissue for the purpose of replacing cells killed during the acute phase of microbial infection or after trauma-induced tissue damage (Chovatiya & Medzhitov, 2014). In the context of cancer, it is now emerging that macrophages can be recruited by tumors (dubbed 'Tumor-Associated Macrophages' or TAMs) and re-programmed towards a more M2-like 'wound-healing' phenotype characterised through production of immunosuppressive cytokines, such as TNF-β and IL-10, which in turn polarizes T-cells to a more Th2 type (secrete the M2 polarizing cytokine IL-4). TAMs also secrete pro-angiogenic VEGF and tissue remodelling proteases such as MMP-9 (**Fig 1.5**). Thus, tumors can subvert the host wound healing response by utilizing the growth-stimulating potential of these cells to promote angiogenesis and tissue remodeling (Murdoch et al., 2008; Mantovani et al., 2008). However, it is important to consider that many of the tumor-promoting cytokines (TNF, IL-6 and IL-1) are more akin to the more M1 pro-inflammatory phenotype. This suggests that TAMs are not simply defined by specific and hard wired differentiation pathways or lineages but represent multiple distinct populations with overlapping features. In addition, a wealth of recent findings have established that ~20% of cancers benefit from the recruitment of cells of the innate immune system (Hanahan & Weinberg, 2011; Murdoch et al., 2008; Mantovani et al. 2008). TAMs as well as newly defined cell type called myeloid-derived suppressor cells (MDSCs) are frequently associated with tumors and indicative of a bad prognosis, which appear to treat the tumor as damaged tissue in need of healing rather than destruction (Murdoch et al., 2008; Mantovani et al., 2008). MDSCs have the capacity to suppress activation of Natural Killer cells (NK cells) and also CD4/CD8 T-cells, therefore severely limiting any cytotoxic

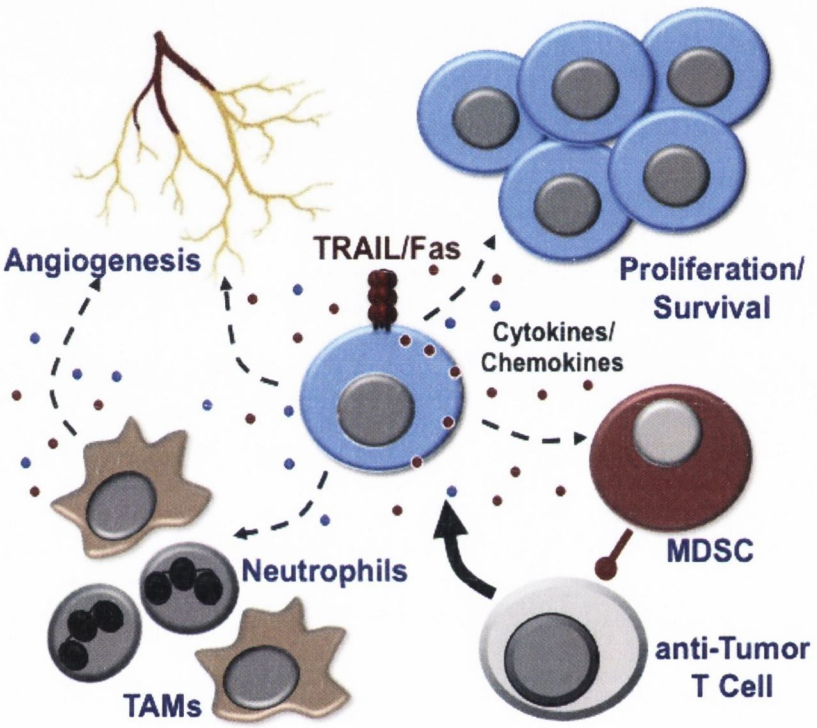


Figure 1.5 Death receptors may promote cancer through inflammatory signalling
Tumor cells that express death receptors may untilize the inherent pro-inflammatory properties of these receptors to promote tumorgenesis via multiple mechanims

potential of these cell types towards the tumor (Gabrilovich & Nagaraj, 2009) (**Fig 1.5**). In addition, MDSCs also contribute to tumor development and progression through the production of pro-angiogenic factors such as VEGF and tissue remodelling proteases such as MMPs. Interestingly, it has recently been shown that tumor-derived CXCL1, which acts to recruit MDSCs, when inhibited, slows the rate of tumor progression. Similarly, when tumor-derived GM-CSF, a cytokine that plays a role in MDSC development, is depleted, this renders tumors more susceptible to T-cell mediated killing and tumor regression (Pylayeva-Gupta et al., 2012).

Even before a tumor can develop, persistent or chronic inflammation is thought to be an important initiator of tumor formation (Karin, 2009). If an inflammatory response persists unchecked for months or years due to complex underlying genetic as well as environmental factors, as happens in inflammatory bowel disease (IBD) or viral hepatitis for example, this can greatly increase the risk of cancer development through genetic instability at the site of chronic inflammation (Karin, 2009; Grivennikov et al., 2010). Furthermore, the presence of inflammatory cytokines at sites of chronic inflammation such as TNF, IL-6 and IL-8 can further benefit a developing tumor through recruitment of TAMs and MDSCs along with other potentially tissue damaging and re-modeling cells types such as neutrophils and mast cells. In addition, many of these cytokines like IL-6 and IL-8 have autocrine survival and growth-promoting effects on nascent tumors. Finally, it is worth noting that many of these tumor-related cytokines (IL-6, IL8, CXCL1, GM-CSF, TNFα) have shown to be induced by both Fas and TRAIL suggesting that death receptor-induced cytokines may actively contribute to tumor development in contexts where tumors are expressing death receptors (**Figure 1.5)**.

1.6 Interleukin-1 family

1.6.1 Overview of IL-1 members

Interleukin-1α and Interleukin-1β (IL-1α & β) were the first interleukins to be molecularly defined during the mid-1980s and have since been implicated in a multitude of different biological activities, most notably within innate immune responses (Auron et al. 1984; March et al., 1985). Since the initial discovery of IL-1β, the family has dramatically increased in size, with 11 members defined to date (**Figure 1.6**). The expansion of the IL-1 family probably occurred through multiple gene duplications, with nine of the eleven IL-1-family cytokines lying on the same ~400 kilo-base region of chromosome 2 (IL-33 located on chromosome 9 and IL-18 located on chromosome 11). All possess a highly conserved gene structure, as well as a conserved protein structure with all members having 12-stranded β-barrels (Sims & Smith, 2010). In addition, the IL-1 family has a dedicated set of receptors that bind IL-1 family ligands (**Figure 1.6**) (Sims & Smith, 2010; Garlanda et al., 2014). The family also contain three receptor antagonists, namely IL-1 receptor antagonist (IL-1RA), IL-36 receptor antagonist (IL-36RA) and the recently described IL-38, which has been claimed to act as a receptor antagonist for IL-36R. These molecules serve as crucial regulators of IL-1 signalling, as patients with mutations in these molecules develop servere autoinflammatory conditions (Towne & Sims, 2012; Jesus & Goldbach-Mansky, 2014). Similar to TLRs, IL-1 receptors contain a Toll/IL-1 receptor (TIR) domain within their intracellular domains, which recruits the adaptor myeloid differentiation protein (MyD88) to initiate signalling (Cohen, 2014) (**Figure 1.7**). Therefore, while TLRs respond to pathogen-associated-molecular-patterns (PAMPs), and IL-1 receptors have defined host-derived ligands, the subsequent inflammatory signalling responses are highly similar, suggesting that the innate immune system has evolved similar responses to either foreign or host-derived inflammatory stimuli.

1.6.2 IL-1 signalling pathway

IL-1 family cytokines exert their pro-inflammatory effects through binding to a dedicated set of high affinity receptors. IL-1 family receptors are comprised of

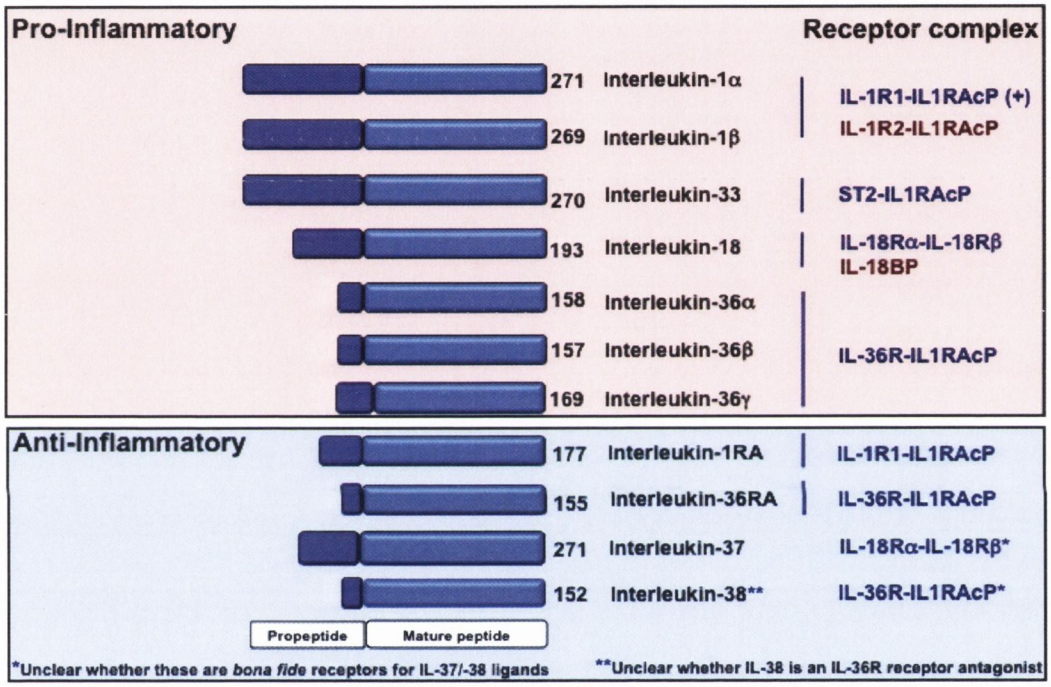


Figure 1.6 Members of the IL-1 family of cytokines.
All IL-1 family members grouped according to pro- or anti-inflammatory activity. Receptor complexes for IL-1 cytokines are indicated.

three extracellular immunoglobulin-like domains, while the intracellular portion contains a TIR domain (Dinarello, 2009). Similar to IL-1R and IL-33R, the IL-36R requires the IL-1 accessory protein (IL-1RAcP) to transduce signals (Towne et al., 2004). Upon receptor binding, these receptors aggregate with the IL-1RAcP signalling chain and trigger the formation of the signalling complex. A critical adaptor molecule recruited to IL-1/IL-33R/IL-36R receptors is MyD88, which binds to the TIR domain via its own TIR domain at the C-terminus of the protein. Mice deficient in MyD88 have dramatically attenuated responses to both IL-1 as well as certain Toll-like receptor agonists (Chen et al., 2007). After MyD88 recruitment, IRAK4 is recruited, followed by the recruitment of IRAK1 and IRAK2 to form the 'Myddosome' (Cohen, 2014) (**Figure 1.7**). IRAK1 is activated by IRAK4 via phosphorylation, which then undergoes autophosphorylation. This in turn promotes high affinity binding between IRAK1 and TRAF6, an E3 ubiquitin ligase. Because of its ubiquitin ligase activity, TRAF6 can catalyse the formation of Lys63-linked polyubiquitin chains (K63-pUb) on IRAK proteins (**Figure 1.7**). These K63-pUb chains subsequently recruit the TAK1/TAB1/TAB2/3 complex through TAB2/3 binding directly to ubiquitin chains. TAK1 becomes activated most likely as a result of induced conformational change after TAB2/3 binding. K63-pUb chains also result in the recruitment of the LUBAC complex via the HOIP subunit, which in turn promotes Methionine-1 (M1)-linked linear ubiquitin chains that are required for activation of the IKK complex (**Figure 1.7**). The K63 and M1 ubiquitin chains therefore bring TAK1 and the canonical IKK complex into close proximity and facilitate TAK1 activation of the IKKs (Cohen, 2014).

1.6.3 IL-1 cytokines

IL-1 family members, IL-1α, IL-1β, IL-33, IL-18, IL-36α, IL-36β and IL-36γ are all generated as leaderless cytokines, and as a consequence do not get secreted into the extracellular space via the classical secretary pathway (Sims & Smith, 2010). It is becoming increasing apparent that necrotic cell death is the major mechanism of release of these cytokines (Rock et al., 2011; Martin et al., 2012). In accordance with Matzinger's 'danger hypothesis', the IL-1 family of

cytokines are the archetypical DAMPs, whereby their presence in the extracellular space is indicative of cellular damage. It is highly appropriate from an evolutionary perspective that the presence of necrotic cells can instigate immune responses. Sudden cell rupture is typically caused by severe departures from normal physiology and can betray the activities of viral infection (many viruses cause cell lysis such as influenza and HIV) or the activities of bacterial toxins such as group-A streptococci toxins, which are cytotoxic to host cells (Matzinger, 1994; Kono & Rock, 2008; Henry et al., 2013).

IL-1α/β

The two original members of the family, IL-1α and IL-1β, bind to the same receptor (IL-1R1), have similar biological properties yet each possess key distinctive features that impact on how these molecules interact with the immune system. IL-1α can be found in its biologically active precursor form in many different tissues and upon release can affect virtually all cells and organs. IL-1α also possesses a nuclear localization signal (NLS) and has been shown to translocate to the nucleus in response to inflammatory stimuli (Wessendorf et al., 1993). IL-1α translocation to the nuclear compartment has also been demonstrated during apoptosis and may represent a mechanism to sequester this inflammatory cytokine within the apoptotic cell (Cohen et al., 2010). Also overexpression of IL-1α in cells has been shown to activate NF-κB in an IL-1R-independent manner, suggesting a role for IL-1α in regulating inflammatory signalling via intracellular signalling, although this is controversial (Werman et al., 2004). IL-1α is an apical cytokine that can mediate many of the features of inflammation, including elevated temperature (fever) through activation of the hypothalamus-pituitary-adrenal (HPA) axis, induction of acute phase proteins in the liver, prolonging the lifespan and effector function of macrophages and neutrophils, and the differentiation and function of key innate and adaptive lymphoid cells (e.g. DCs, Th17 cells) (Garlanda et al., 2013).

By comparison, IL-1β is inactive in its precursor form and requires activation by caspase-1-dependent proteolysis. Caspase-1 is recruited to macromolecular

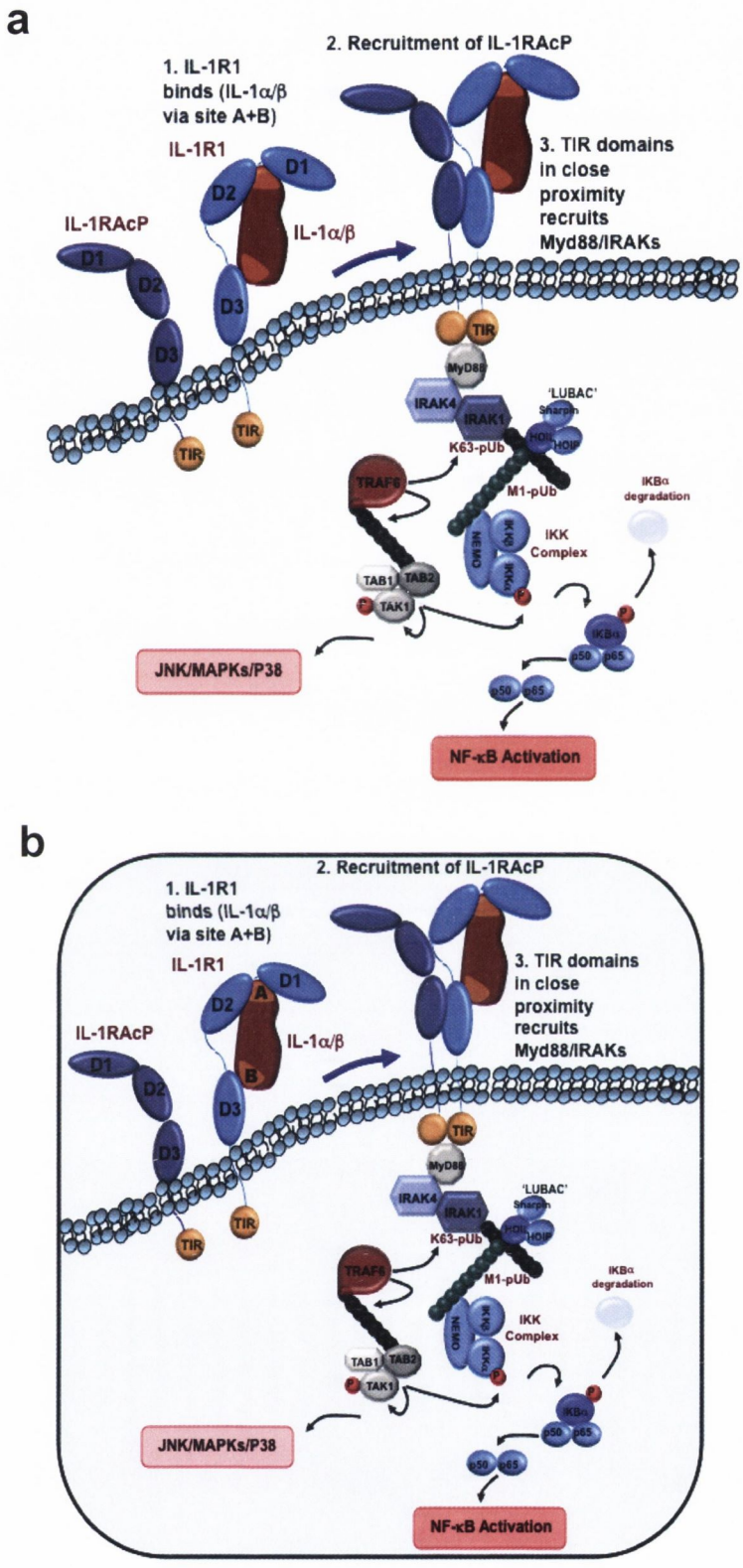


Figure 1.7 Current Model of IL-1 signalling

a. IL-1 agonists (IL-1α/β) have two points of contact with the IL-1 receptor 1 (IL-1R1) indicated as site A and B. Site A on the ligand interacts with the interface of domain 1 and 2 (D1/2) of the receptor while site B interacts with domain 3 (D3). IL-1RAcP is recruited to the ligand-receptor complex and physically interacts with both. This conformation brings the TIR domains in close proximity which promotes recruitment of MyD88 and IRAKs. **b.** IL-1 Receptor Antagonist (IL-1RA) does not transduce a signal through IL-1R1 upon binding. First, a critical loop region present on IL-1α/β that interacts with IL-1RAcP is absent on IL-1RA, thus recruitment of IL-1RAcP is prevented. Second, IL-1RA interacts with IL-1R1 only through site A.

complexes called 'inflammasomes' comprising of NOD-like receptor proteins (NLRs) such as NLRP3, NLRP1, or NLRC4 and the adaptor ASC, which stablizes the scaffold to recruit and activate caspase-1 (Lamkanfi & Dixit, 2014; Latz et al., 2013). It has now been firmly established that the NLRP3 inflammasome requires two signals for biologically active IL-1β to be released (Lamkanfi & Dixit, 2014; Latz et al., 2013). The first signal is typically a PAMP (e.g. LPS), which upregulates expression of NLRP3 and pro-IL-1β via NF-κB activation, followed by a second signal. Indeed, a large diversity of molecules have been implicated in NLRP3 activation. These include microbial-derived molecules such as peptidoglycan and pore forming toxins, as well as host-derived molecules such as uric acid crystals and ATP (Lamkanfi & Dixit, 2014). This second signal drives the assembly of the inflammsome complex and subsequent release of IL-1β. Our understanding of exactly how the inflammasome can 'recognise' these diverse stimuli is uncomplete but monitoring of host-derived factors, such as K^+ ion efflux, has been suggested as a possible trigger (Munoz-Planillo et al., 2013; Latz et al. 2013). Interestingly, a common feature of inflammsome activation in response to particular stimuli such as flagellin, is a caspase-1-dependent cell death dubbed 'pyroptosis', whereby activated IL-1β is released concomitantly with necrotic-like cell death (Bergsbaken et al. 2009; Latz et al. 2013). It is tempting to speculate that perhaps necrotic cell death is a common mechanism by which active IL-1β is released from cells in response to signal two agents (Cullen et al., 2014).

As a consequence of their release, IL-1α and IL-1β are major inflammatory mediators of the early innate immune response towards infection and sterile injury (Rock et al., 2011). The apical and pleotropic effects of these cytokines, that typically serve to alert our immune system to signs of damage and infection, also make IL-1α/β major pathogenic mediators of autoinflammatory, autoimmune, infectious and degenerative diseases (Gross et al., 2012; Lukens et al., 2013; Dinarello et al., 2012; Jesus et al., 2014). Indeed, the clinical implications of IL-1 biology are nowhere more apparent than in autoinflammatory diseases that are almost uniquely IL-1-mediated, and where anti-IL-1 therapies have yielded tremendous clinical benefits (Dinarello et al., 2012; Jesus et al., 2014).

IL-36 cytokines

IL-36α, IL-36β and IL-36γ are encoded by distinct genes and all three cytokines signal through the IL-36R/IL-1RAcP complex (Towne et al., 2004). Similar to IL-1, the IL-36 subfamily modulates signalling through its receptor via a receptor antagonist (IL-36RA), which binds IL-36R but does not transduce a signal. IL-36 cytokines and receptor are predominately expressed in barrier tissues, in particular the skin and lung (Towne & Sims, 2012). IL-36 cytokines contain a relatively short N-terminal domain compared with other IL-1 cytokines. Recently, Sims and colleagues demonstrated that full-length IL-36 cytokines display little biological activity, however truncation of IL-36 cytokines at specific residues within their N-terminal regions greatly increased the biological potency of these cytokines. This strongly suggests that the IL-36 cytokines are subject to proteolytic activation, as has been discovered for other IL-1 family members (Thornberry et al., 1992; Afonina et al., 2011; Lefrancais et al., 2012). Furthermore, it has recently been shown that immune cells respond to IL-36 by promoting Th1 and Th17 polarization and can also produce IL-36 in response to inflammatory stimuli (Vigne et al., 2011, 2012). Epithelial cells of the skin and lung are also an abundant source of these cytokines, which have been shown to mediate pathological conditions in these organs including psoriasis and *Aspergillus fumigatus* infection in the lung (Gresnight et al., 2013; Tortola et al., 2012).

IL-1 cytokines and inflammatory diseases

Over the past decade, the biology of the extended IL-1 family has become increasingly understood, especially in terms of their roles in inflammatory diseases (Towne & Sims, 2012; Dinerallo et al., 2012; Jesus & Goldbach-Mansky, 2014). The IL-36 cytokines have emerged as key inflammatory mediators in pathological skin diseases such as psoriasis, with patients presenting with elevated levels of these cytokines in affected areas (Johnston et al., 2011). A rare and extremely debilitating form of psoriasis, called generalized

pustular psoriais (GPP), has been linked to a number of hypomorphic mutations in the IL-36 receptor antagonist (IL-36RA), suggesting that deregulated IL-36 signalling is a major driver of GPP pathology (Marrakchi et al., 2011; Onoufriadis et al., 2011; Farooq et al., 2013). As of yet, there is no clinically approved drug (e.g. neutralizing antibody or receptor antagonist) to inhibit IL-36 signalling in a pathological setting.

Autoinflammatory diseases such as cryopyrin-associated periodic syndromes (CAPS) and deficiency in IL-1 receptor antagonist (DIRA) are caused by mutations in key regulators of IL-1 cyokines. CAPS are associated with gain-of-function mutations in the gene that encodes NLRP3. As a consequence, these patients have constitutive overactivation of the inflammasome and elevated IL-1β production. While CAPS represents a disease state characterised by overproduction of IL-1β, the inflammatory disease resulting from DIRA reflects an inability to regulate IL-1 signalling. DIRA patients have loss-of-function mutations in IL-1 receptor antagonist that produce a severe inflammatory phenotype present from birth, characterised by systemic inflammation in particular in bones and skin (Aksentijevich et al., 2009). DIRA patients are particularly susceptible to trauma or mechanical-induced inflammation in the skin. IL-1RA (absent in DIRA patients) is highly expressed in the epidermis but absent in DIRA patients and therefore cannot inhibit the pro-inflammatory effects of IL-1α when released as a consequence of trauma-induced necrosis. Targeting IL-1 in autoinfammatory diseases such as CAPS and DIRA has had some success. In particular, recombinant IL-1RA (Anakinra) as well as a soluble IL-1R-Fc fusion antibody (Rilonacept) have shown remarkable efficacy in both DIRA and CAPS patients, and in some cases have been successful at reducing systemic multi-organ inflammation (Jesus & Goldbach-Mansky, 2014). Interestingly, a neutralizing antibody against IL-1α (MABp1) has shown promise in a limited number of trials for type 2 diabetes, pustular psoriasis and occlusive vascular disease, demonstrating that anti-IL-1 therapies are likely to find use in a wide range of inflammatory diseases (Hong et al., 2011; Garlanda et al., 2013). Indeed, a diversity of inflammatory conditions such as type 2 diabetes, atopic dermatitis,

gout, graft-versus-host disease and rheumatoid arthritis all have a significant component of inflammation that is IL-1 driven. Many of these conditions are being treated in ongoing clinical trials with anti-IL-1 therapies and are showing promise (Dinerallo et al., 2012).

IL-36 cytokines and psoriasis

Psoriasis is a common inflammatory skin condition that effects ~1-3% of the Caucasian population (Frank et al., 2009). The most prevalent form of this condition, plaque psoriasis, accounts for approximately 80% of cases. Of those, the related psoriatic arthritis is encountered in 5-30% of individuals. Palmoplanter psoriasis is encountered in about 10% of psoriasis patients and a life-threatening severe form of psoriasis, generalized pustular psoriasis (GPP), accounts for less than 5% of cases (Gottlieb, 2005; Nestle et al., 2009). Psoriasis is characterised by hyperproliferation and impaired differentiation of keratinocytes, the most abundant cell type in the skin, leading to thickening of the skin in lesion areas (acanthosis). It is well established that psoriasis features excessive inflammatory reactions in the skin as a result of innate as well as adaptive immune cells infiltrating the affected area. This results in the pathological features of psoriasis. While the events that trigger the onset of psoriasis remain unclear, skin damage, viral and bacterial infection (e.g streptococcal bacteria in the throat) and inherited genetic susceptibilities are all major factors (Lowes et al., 2007; Pasparakis et al., 2014). Although a bewildering array of cytokines and chemokines have now been identified, several key cytokines have been implicated in many autoinflammatory and autoimmune disorders, including TNF, IL-12, IL-22, IL-23, IL-17, IL-1 and more recently IL-36 (Pasparakis et al., 2014; Jesus et al., 2014; Towne & Sims, 2012). While each of these cytokines have distinct and/or overlapping roles during the development of an inflammatory response, it is becoming increasingly clear that they are initiated in a cascade-like manner. Therefore, it is quite likely that in the case of psoriasis, damage to keratinocytes, whether by infection or damage, results in the release of IL-36/IL-1 and/or TNF cytokines triggering the production of further cytokine (IL-17C, TNF, IL-6) and

chemokines (IL-8, CXCL1) from keratinocytes in an autocrine/paracrine manner. This results in neutrophil and macrophage recruitment, activation of dendritic cells that polarize T-cell populations (via IL-12/IL-23) towards Th17 (IL-17 secretion) and Th1 (TNF, IFNγ secretion) (Lowes, et al., 2005) (**Fig 1.8**). It has recently been reported that keratinocytes can also produce IL-17C, which closely mimics the biological activity of IL-17A/F, while neutrophils act as innate immune source of IL-17A (Ramirez-Carrozzi et al. 2011; Taylor et al. 2014). The influx of neutrophils and T-cells into the skin, combined with the fact that IL-17, TNF and IL-23 can induce further production of IL-36 proteins from keratinocytes (Carrier et al., 2011), provoke a reinforcing cycle of cytokine production and further inflammation. Interestingly, biologics such as TNF, IL-23, IL-12 and IL-17 neutralizing antibodies have shown remarkable efficacy in psoriasis, with almost complete remission of symptoms in many patients (Lowes, et al., 2007, 2014; Crow, 2013). As mentioned above, recent studies have provided compelling evidence that IL-36 cytokines play an important role in psoriasis. Transgenic expression of IL-36α in the mouse leads to a psoriasis-like condition at birth that can be further exacerbated with the skin irritant, phorbol acetate (Blumberg et al., 2007, 2010). The most severe form of psoriasis, GPP, has recently been demonstrated to be associated with the inheritance of distinct hypomorphic mutations (partial loss-of-function) in IL-36RA a natural inhibitor protein that sets the threshold for IL-36 responses (Marrakchi et al., 2011; Onoufriadis et al., 2011; Farooq et al., 2013). The fact that a reduction in the function of the IL-36RA is sufficient by itself to provoke an extreme form of psoriasis attests to the importance of IL-36 signalling in the skin. Application of a TLR7 receptor agonist (Imiquomod) to the skin in humans and mice can provoke psoriatic outbreaks, which increase in severity when IL-36RA has been deleted in the mouse, however imiquomod-induced psoriasis is completely abolished in IL-36R deficient mice (Wu et al., 2004; Tortola et al., 2012). IL-36 proteins are highly expressed in keratinocytes and are upregulated further in response to IL-17, IL-22 and TNF, all of which are frequently overexpressed in psoriasis (Carrier et al., 2011; Johnston et al., 2011). Analysis of IL-36 expression in skin biopsies from psoriasis patients

has found dramatically elevated expression of IL-36 proteins compared with non-lesional skin from the same patients or healthy controls (Johnston et al., 2011; Schonthaler et al., 2013). Furthermore, transplantation of human psoriatic lesions into immunodeficient (SCID) mice produces a psoriatic-like condition that is greatly improved through blocking the IL-36 receptor (Blumberg et al., 2010). To date, anti-IL-36 biologics have not entered clinical trials, however given the apical nature of IL-36 signalling within the inflammatory cytokine cascade, one would expect to see a significant therapeutic benefit in psoriasis patients.

1.6.4 Proteolysis of IL-1 cytokines by immune-related proteases as a general mechanism to modulate their biological activity

Targeted proteolysis at specific amino acid residues or 'motifs' is an important means of specifically regulating the function of proteins. Proteases can regulate a diverse array of biological processes that include: apoptosis, wound healing, cell proliferation and immunity (Taylor et al., 2008; Martin et al., 2012; Levine, 2008). Unsurprisingly, given the importance of IL-1 cytokines in immune responses, these cytokines are subject to extensive proteolytic regulation by a number of distinct proteases that can alter the biological activity of these cytokines and shape subsequent immune responses (Martin et al., 2012; Lefrançais & Cayrol, 2012). Proteases that target IL-1 cytokines have been found to (1) activate inactive precursors in the case of caspase-1 and pro-IL1β (Thornberry et al., 1992), (2) further amplify the biological activity of active full-length cytokines, in the case of neutrophil-, mast cell- and cytotoxic T-cell (CTL)-derived proteases and IL-1α/IL-33 (Afonina et al., 2011; Lefrançais et al., 2012), or (3) inactivate biologically active cytokines, in the case of caspase-3/-7 and IL-33 (Luthi et al., 2009).

While activation of pro-IL-1β by caspase-1 is thought to take place mainly as an intracellular event, the activation of IL-1α and IL-33 is mediated predominantly in extracellular scenarios. Release of these cytokines, as a consequence of necrosis, brings them into close contact with immune proteases that are actively secreted from infiltrating immune cells such as neutrophils present at the site of

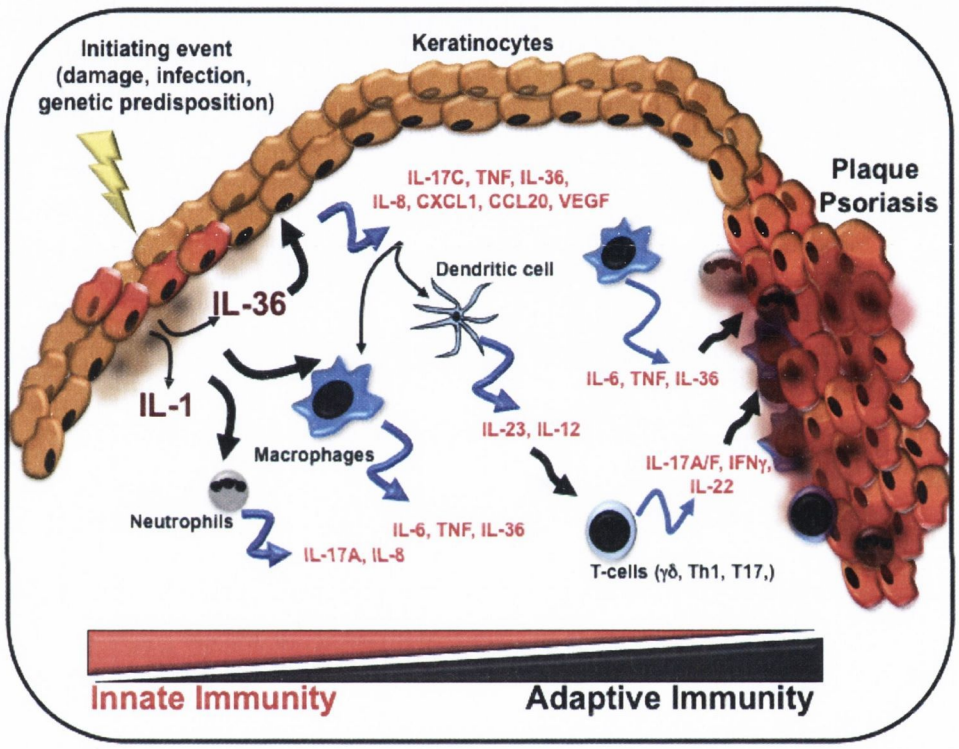


Figure 1.8 Cytokine network implicated in Psoriasis
Release of IL-1 cytokines from damaged keratinocytes activate tissue macrophages and local epidermal cells, which in term recruit neutrophils, to the site of damage. IL-1 also activates inflammatory and resident myeloid DCs produce IL-23. This drives production of IL-17 ligands (IL-17A and IL-17F) from $\alpha\beta$ and $\gamma\delta$ T cells (T17), and IL-22 by subsets of CD4+ (Th22) and CD8+ (Tc22) cells, whereas IL-12 drives production of IFNγ. These T cell derived cytokines can then activate the epidermis to produce further inflammatory chemokines and cytokines. Some will recruit cells into the skin: IL-8 and CXCL1 are neutrophil chemotaxins; CCL20 attracts chemokine CC receptor (CCR)6+ DCs and T17 cells; and vascular endothelial growth factor (VEGF) is important in inducing the vascular hyperplasia seen in psoriasis.

infection or injury. Interestingly, it has been reported that IL-1α is also processed into a more biologically potent form via necrosis-dependent activation of the intracellular protease calpain (Zheng et al., 2013). Furthermore, calpain activation of IL-1α was shown to be a cell type specific phenomenon, as cells that expressed the IL-1R2 (decoy receptor) bound IL-1α and protected it from calpain proteolysis, thus dampening the immunostimultory potential of these cells (Zheng et al., 2013). Nonetheless, in cells that do not express IL-1R2, this represents a novel mechanism by which the dying cell may 'boost' the activity of a danger signal.

1.7 Thesis Aims

The primary aim of the first part of this thesis was to explore how cells dying in response to physiologically relevant apoptotic stimuli might signal to immune cells and how these signals might be subsequently deciphered. We asked whether the pro-apoptotic cytokine TRAIL might play a role in preparing a dying cell for disposal by professional phagocytes through engagement of other signalling pathways. Chapter 3 describes describes a novel role for TRAIL in mediating the release of classical chemokines such as, IL-8 and MCP-1, that may serve as "find me" signals that attract phagocytes towards dying cells. Furthermore, we identified cell types that fail to undergo TRAIL-induced apoptosis but nonetheless respond to TRAIL with the secretion of pro-inflammatory mediators, suggesting that certain tumors may utilize the inherent pro-inflammatory properties of TRAIL to facilitate tumorigenesis.

Next, we focus on recently described members of the IL-1 family of cytokines, namely IL-36α/β/γ. IL-36-activating proteases had been speculated (Towne et al., 2011) however prior to this work such proteases had not yet been identified. Chapter 4 details the identification of neutrophil-derived proteases, elastase and cathepsin-G, as IL-36 activating enzymes. Using either purified proteases or activated neutrophil degranulates we demonstrate that these proteases potently activate IL-36 cytokines. As outlined above, IL-36 cytokines are likely to play a key role as initiators of inflammation in the skin barrier,

therefore inhibitors of IL-36 activation may have considerable potential for the treatment of inflammatory skin conditions, such as psoriasis. Importantly, psoriatic plaques are frequently associated with neutrophil infiltrates, suggesting that small molecule inhibitors of neutrophil granule proteases may have significant potential as inhibitors of IL-36 activation in psoriasis. The details of our analysis using novel small polypeptide inhibitors of IL-36 processing proteases are contained in chapter 4. Because IL-36 cytokines appear to play a key role as initiators of inflammation in the skin barrier, we next examined the effects of activated IL-36 in a range of physiological settings, including its inflammatory signature on primary keratinocytes, as well as exploring a potential role in the modulation of proliferation and differentiation of keratinocytes. Finally, we explore the endogenous expression of IL-36 cytokines in both primary keratinocytes and psoriasis biopsies. The details of our analysis are contained in chapter 5.

Chapter 2

Materials and Methods

2.1. Reagents

2.1.1 Recombinant protein, ELISA kits and chemicals

Recombinant Human and Mouse SuperKiller™ TRAIL was purchased from Enzo Life Sciences. Human and mouse ELISA kits were purchased from R&D Systems. Proteome profiler arrays™ were purchased from R&D systems Human Cytokine array ARY005 and Human Angiogenesis array ARY007. The pan-caspase inhibitor Z-VAD-fmk was purchased from Bachem. A/G Agarose was from Santa Cruz Biotechnology. Chemical inhibitors Cathepsin-G Inhibitor I (219415) and Elastase Inhibitor IV (324759) were purchased from Calbiochem (UK). Purified Neutrophil-derived Cathepsin-G was purchased from Calbiochem (UK). Purified Neutrophil-derived Elastase was purchased from Serva (Germany). Unless otherwise indicated, all other reagents were purchased from Sigma (Ireland) Ltd.

2.1.2 Antibodies

The following antibodies were used anti-IL-6, anti-MCP-1, anti-IL-1α, anti-RANTES, anti cIAP-1, anti-cIAP-, anti-IL-8 and anti-CXCL1 (R&D Systems); anti-IKKα, anti-IKBα/β anti-phospho IKKα/β, anti-MEK, anti-phospho MEK, anti-ERK, anti-phospho ERK, anti-p38, anti-phospho p38, anti-JNK, anti-phospho JNK (Cell Signalling); anti-RIPK1 (Santa Cruz Biotechnology). Polyclonal antibodies were generated against IL-36 α, β and γ by repeated immunization of rabbits with the full-length recombinant IL-36 proteins (Biogenes, Germany). Anti-IL-1α (MAB200), anti-IL1R1 (AF269) and anti-IL-1β (MAB201) were purchased from R&D systems (UK). anti-Actin (clone C4) was from MP Biomedicals, was from Sigma, anti-Cullin-3 (611848) was from BD antibodies.

2.1.3 Synthetic polypeptide synthesis

Synthetic peptides, Ac-DEVD-AMC, Ac-WEHD-AMC, and biotin-VAD-FMK were all purchased from Bachem (Germany); Suc(oMe)-AAPV-AMC was purchased

from Peptanova (Germany); biotin-VAD-FMK was purchased from ICN (UK). Novel synthetic peptides biotin-FLF-CMK, z-FLF-CMK, z-AFLF-CMK, z-EPF-CMK, z-GLF-CMK, z-KAL-CMK, z-GLK-CMK, z-GLW-CMK, z-AAPV, z-ARPV, z-API, z-APL, z-APZ, z-DTEF, z-PQR, z-RAV, z-RPI, z-RPL, and z-RPV were synthesized by Boston Open Labs (USA).

2.2 Recombinant proteins

2.2.1 Expression and purification of recombinant proteins in Escherichia coli

Full-length poly-histidine-tagged IL-36α, β and γ proteins was generated by cloning the human coding sequence in frame with the poly-histidine tag sequence in the bacterial expression vector pET45b. Protein was expressed by addition of 600 μM IPTG to exponentially growing cultures of BL21 strain E. coli followed by incubation for 3 h at 37°C. Bacteria were lysed by sonication and poly-histidine tagged proteins were captured using nickel-NTA agarose (Qiagen, UK), followed by elution into PBS, pH 7.2, in the presence of 100 mM imidazole. Modified forms of IL-36 where cloned that included a caspase-3-processing motif (DEVD) into the IL-36 sequences, N-terminal to the known processing sites (Towne et al., 2011). All IL-36 mutants were expressed and purified in the same way. Recombinant poly-histidine-tagged caspases –1, and -3, were also expressed and purified as described previously (Afonina et al., 2011).

2.2.2 LPS depletion

Triton X-114 was added to recombinant proteins to a final concentration of 1%. Proteins were incubated for 30 min at 4°C, followed by a 10 min incubation at 30°C. The protein fraction was then separated by centrifugation at 20 000 g for 10 min at room temperature. The procedure was repeated three times.

2.2.3 In vitro transcription/translation

^{35}S-labeled proteins were synthetised using a coupled *in vitro* transcription/translation system according to the manufacturer's instructions (Promega, UK). Plasmid template was added to the reaction containing rabbit reticulocyte lysate, amino acid mix (minus methionine), T7 RNA polymerase and ^{35}S-methionine (10 mCi/ml, Amersham). The reaction was carried out for 2 h at 30°C.

2.3 Protein detection

2.3.1 SDS-PAGE electophoresis

Proteins were typically subjected to sodium dodecyl sulphate polyacrylamide gel electrophoresis (SDS-PAGE) for analysis. Protein samples were denatured by boiling for 7 minutes in SDS loading buffer (2 % SDS, 50 mM Tris-HCl, pH 6.8, 10 % glycerol, 2.5 % β-mercaptoethanol) and loaded onto 12 % polyacrylamide gels. Electrophoresis was carried out at 55 V through the stacking gel, and 75 V through the separating gel. In order to visualise proteins with Coomassie Blue staining, SDS-PAGE gels were incubated in Coomassie Blue staining solution (45 % methanol, 10 % acetic acid, 0.25 % Coomassie Brilliant Blue) overnight. Gels were then incubated in destain solution (45 % methanol, 10 % acetic acid) to remove background staining. Radio-labelled Methionine proteins were visualised by enhanced fluorography using Amplify reagent (Amersham). Gels were fixed in fixative solution (45 % methanol, 10 % acetic acid) for 2 hours followed by incubation for 25 minutes in Amplify and vacuum drying onto blotting paper (Whatman) for 2 hours at 80°C. Gels were exposed to autoradiography film (Denville Scientific) at –70°C for 12 - 48 hours.

2.3.2 Tricine gels

Prepared gels according to protocol described by Schagger, 2006. Briefly, 30 ml of 10% resolving gel was prepared as follows: 10 ml of 3X gel buffer (Tris 3 M,

SDS 0.3 %, pH 8.45), 3 ml of 40% Glycerol, 6 ml of acrylamide/Bis-acrylamide 30 % (AB-30%), 250 μl of APS 10 %, 15 μl TEMED, up to 30 ml with dH_2O. To prepare 12 ml of stacking gel, 2 ml AB-30 %, 3 ml of 3X gel buffer, 150 μl of APS 10 %, 12 μl TEMED, up to 12 ml with dH_2O. Tricine running buffer was prepared as a 10X stock (60.55 g Tris, 89.6 g Tricine, 5 g SDS, up to 500 ml dH_2O).

2.3.3 Western immunoblotting

After protein separation using SDS-PAGE, proteins were transferred onto 0.45 μM nitrocellulose membranes (Schleider and Schull) at 35 mA overnight in transfer buffer (39 mM glycine, 48 mM Tris-HCL, pH 8.3, 0.037 % SDS, 20 % methanol). Membranes were next blocked with TBST (10 mM Tris-HCL, pH8.3, 150 mM NaCl, 0.05 % Tween-20) containing 5 % (w/v) non-fat dried milk for 1 h and then probed with the primary antibody at a typical concentration of 250 ng/ml for 2 h. Blots were then washed for 30 min in TBST and incubated with the appropriate horseradish peroxidase (HRP)-coupled secondary antibody (Jackson Labs, USA) for 1 h. Blots were washed again and incubated with Supersignal West, Peroxide and Enhancer solutions (Pierce). Proteins were visualised by exposing blots to autoradiography film. Immunoblotting of lysates and precipitated supernatants: To precipitate protein from supernatant, TCA was added at a 1:4 ratio to supernatant volume (250 μl to 1ml supernatant) and incubated on rotation for 10 min. Supernatants were centrifuged at 15,000 g for 10 min. Top layer was removed without disturbing the pellet. 200 μl pre-chilled acetone was added to each pellet and mixed by several inversions. Samples were centrigued for a further 10 min at 15,000 g. Samples were then put on heating block to burn off the acetone. 1 X SDS-PAGE loading buffer (2 % SDS, 50 mM Tris-HCl, pH 6.8, 10 % glycerol, 2.5 % β-mercaptoethanol) was added to each sample pellet. Samples were then boiled for a further 5 mins. Cell lysates were prepared using SDS-PAGE loading buffer and were electrophoresed on 8-13% SDS-polyacrylamide gels followed by transfer onto nitrocellulose membranes. Protein expression was subsequently examined by immunoblotting with the appropriate antibodies.

2.3.4 Protease Activity Assays

Reactions (50 µl final volume) were carried out in protease reaction buffer (50 mM Hepes, pH 7.4, 75 mM NaCl, 0.1 % CHAPS, 2 mM DTT) containing 50 µM Ac-DEVD-AFC, Ac-WEHD-AMC, Suc(oMe)-AAPV-AMC. Samples were measured by using an automated fluorimeter (Spectrafluor Plus; TECAN) at wavelengths of 430 nm (excitation) and 535 nm (emission). For suc-FLF-sBzl assay, substrate was diluted to a final concentration of 300 mM in protease reaction buffer (50 mM Hepes, pH 7.4, 75 mM NaCl, 0.1 % CHAPS, DTNB 300 mM). Samples were measured by automated fluorimeter (Spectrafluor Plus; TECAN) at an absorbance wavelength of 430 nM.

2.4 Cell-based assays

2.4.1 Cell culture

HeLa (human cervical epithelial carcinoma), HeLa.pcDNA3 and HeLa.BcL-xL cells (generated by Susan Logue in Martin laboratory) were cultured in RPMI media, supplemented with 5 % fetal calf serum. THP-1 (human monocytic) cells and HCT116 (human colorectal carcinoma) cells were cultured in RPMI media, supplemented with 10 % fetal calf serum. HT-29 (Human colon adenocarcinoma) cells, 3LL (mouse Lung Lewis carcinoma) cells, HEK293T (human embryonic kidney 293) cells, and PancTu-1 (human pancreatic carcinoma epithelial-like) cells were cultured in DMEM media, supplemented with 10 % fetal calf serum. HaCat (human transformed keratinocytes) were cultured in DMEM (Gibco) supplemented with FCS (10 %). Primary neonatal foreskin derived Keratinocytes P0 were purchased from Cell Systems (Germany) and cultured in serum-free Dermalife K media (Cell Systems, Germany). . All cells were cultured at 37°C in a humidified atmosphere with 5% CO_2.

2.4.2 Generation of HeLa cell lines stably expressing either Bcl-xL, IL-36R, NF-kB-SEAP

Briefly, HeLa (1 x 106) were nucleofected with 1-2 mg of plasmid, plated in 10cm2 culture dishes and left to recover for 48hrs. HeLa cells expressing plasmid was selected with G418 antibiotic (Sigma). Single cell clones expressing BcL-xL were generated by the limiting dilution method. Individual Bcl-xL clones were subsequently grown up and screened for Bcl-xL expression and apoptosis resistance. HeLa.vector or HeLa.IL-36R cell lines were generated by transfection with 5 mg pCXN2 or pCXN2.IL-1Rrp2(IL-36R) plasmids followed by selection using G418 antibiotic. IL-36R over-expressing clones were expanded from a single cell. Clones were selected by demonstration of acquired optimal responsiveness to active forms of IL-36 via ELISA. HeLa.IL-36R.SEAP cell line was generated by transfection with pNifty2-SEAP plasmid followed by selection using zeocin antibiotic. Clones were expanded from a single cell and tested for SEAP production. All cells were cultured at 37°C in a humidified atmosphere with 5 % CO2.

2.4.3 Bioactivity assay

Cells were plated at a density of 5 x 105 (HeLa, HT-29, 3LL) in a 6-well plate or 4 x 104 (HeLa) in a 24-well plate. The next day cells were incubated with the specified concentrations of TRAIL. Supernatants were subsequently collected for quantitative cytokine and chemokine analysis by ELISA. Pro-inflammatory activity of IL-36 was analysed in a similar way using HeLa, HaCat and primary keratinocytes (4 x 104 cells per treatment)

2.4.4 RNA interference

To ablate protein expression in HeLa/HT-29 cells, 0.5-1 x 10^6 cells/cuvette were transfected with 100-200 nM siRNA using nucleofection (Amaxa) as per manufacturers instructions. Cells were incubated with siRNA for 48 h followed by treatment with 50 ng/ml TRAIL for 18-24 h. siRNA were as follows: cIAP-1#1: sense: 5'-ggcaaaugcugcggccaaca-3', cIAP-1#2: sense: 5'-uucguacauuucucucuuua-3', cIAP-2#1: sense: 5'-guucaagccaguuacccuc -3', cIAP-2#2: sense: 5'-aagugguagggacuugugc-3', XIAP#1: sense: 5'-

gugguaguccuguuucagc-3', XIAP#2: sense: 5'-gcaguugacaaguguccca-3', RIPK1#1: sense: 5'-ggagcaaacugaauaaugaagagca-3', RIPK1#2: sense: 5'-guacuccgcuuucugua-3', RIPK3: sense: 5'-uaacuugacgcacgacauc-3', FADD#1: sense: 5'-gauuggagaaggcuggcuc-3', FADD#2: sense: 5'-gaacucaagcugcguuuau-3', Caspase-8#1: sense: 5'-guuccugagccuggacuac-3', Caspase-8#2: sense: 5'-aacuaccagaaagguauaccu-3', p65#1: sense: 5'-gauugaggagaaacguaaa–3', p65#2: sense: 5'-gcccuaucccuuuacguca–3', JNK1/2#1: 5'-aaagaauguccuaccuucu–3', JNK1/2#2: sense: 5'-ggcaugggcuacaaggaaa–3', ERK1: sense: 5'-gccgccgccgccgccau–3', and 5'-cgucuaauauauaaauuau–3' ERK1: sense: 5'-cagcugagcaaugaccaua–3', ERK2: sense: 5'-gacacaacaccucagcaau–3', and 5'-cacuugucaagaagcguua–3', p38#1: sense: 5'-guccaucauucaugcgaaa–3', p38#2: sense: 5'-ggucuaaaguauauacauu–3'.

2.4.5 ELISA

ELISAs were performed according to the manufacturer's instructions (R&D systems, UK). Briefly, 96-well polysterene plates were coated with corresponding capture antibody and incubated overnight at room temperature. Next day, plates were extensively washed and blocked with 1% bovine serum albumin (Roche) in PBS, pH 7.2. After blocking, plates were incubated with samples or standard cytokines, followed by the appropriate biotin-conjugated detection antibody. Finally, plates were incubated with HRP-conjugated streptavidin, after which HRP substrate was added. Reactions were stopped with 2N H_2SO_4 and optical density was measured on the automated plate reader (wavelength 430 nm). Cytokines and chemokines were measured from cell culture supernatants using specific ELISA kits obtained from R&D systems (human IL-6, IL-8, CXCL1, MCP-1, IL-17C). Each assay was repeated a minimum of three times and all cytokine assays were carried out using triplicate samples from each culture.

2.4.6 Human cytokine and angiogenesis Arrays

HeLa were plated at 2 x 10^6 on 10 cm dishes. After 24 h, cells were incubated with 100 ng/ml TRAIL for a further 24 h. Supernatants were harvested. Human Cytokine

array ARY005 and Human Angiogenesis array ARY007 were prepared according to manufactures instructions. Typically, arrays were incubated overnight at 4° with either control or TRAIL treated supernatants. Arrays were then washed and incubated with the appropriate horseradish peroxidase (HRP)-coupled secondary antibody for 1 h. Blots were washed again and incubated with Supersignal West, Peroxide and Enhancer solutions (Pierce). Arrays were visualised by exposing blots to autoradiography film.

2.4.7 Intracellular cytokine staining

Hela cells were plated on coverslips and treated with TRAIL for 12-14 h. Cells were then fixed in 3.7 % paraformaldehyde and permeabilized in 0.15 % Triton X-100 in PBS, pH 7.2. Cells were incubated in 2 % BSA for 30 min and antibodies added at 2.5 – 5 μg/ml for 1 h followed by PBS washing and addition of fluorescently-conjugated secondary antibodies. Final washings included incubation with 20 μM Hoechst (Sigma) for 10 min. Cells were mounted with Slow Fade (Molecular probes) and observed on a laser scanning microscope (Olympus FV1000) using a 488 nm Argon laser (green fluorescence) and a 405 nm LD laser (Hoechst). Confocal images were acquired with Fluoview 1000 V.1 application software, and images were processed with Indesign (Adobe).

2.5 Neutrophil degranulate preparations

2.5.1 Purification of primary cell populations and preparation of degranulates

Primary neutrophils were purified from donor human blood using the plasma-Percoll gradient method as described in Haslett et al., (1985). Purity of cell preparations (>90 %) was determined by Hematoxylin and Eosin staining of cytospins. To prepare degranulates, neutrophils (1 x 10^7 per treatment) were stimulated in the presence or absence of 50 nM PMA in HBSS/0.25 % BSA for 1-3 h at 37°C in a humidified atmosphere with 5 % CO_2. Supernatants were

harvested and clarified by centrifugation. Degranulate aliquots were stored at -80°C.

2.6 Chemotaxis assays

Chemotaxis assays were performed in Neuro Probe 10-Well Chemotaxis Chambers as per manufacturer's instructions. Briefly, supernatants were generated from HeLa cells stimulated with TRAIL for 24 h in RPMI, 0.5 % FCS. Supernatants (150 μl) were added to the bottom well of a chemotaxis chamber then 3-8 mm nitrocellulose filters placed on top and secured by application of the top chamber, to which 250 ml THP-1 monocytes, PBMCs or neutrophils were added at 1–2 x 10^6/ml. Total cells entering the bottom chamber were counted after 1-2 h. For antibody-mediated depletion of chemokines, supernatants were mock-depleted with A/G agarose for 1 h then incubated with neutralizing antibodies (1-2 μg/ml), 1 h, followed by depletion of the antibody-protein complexes from the supernatnts with A/G agarose. All depletions were confirmed by ELISA.

2.6.1 Detection/Inhibition of ATP in apoptotic supernatants

ATP was measured on the day of the experiment using the ENLITEN® ATP Assay System Bioluminescence Detection Kit (Promega) as per manufacturer's instructions. ATP was enzymatically degraded using Apyrase (New England Biotech) at the indicated concentrations for 30 min prior to chemotaxis assay then ATP concentration determined immediately after the experiment.

2.7 Cell death assays

2.7.1 Annexin V/propidium iodide staining

To quantify apoptosis, cells were resuspended in annexin V staining buffer (10 mM HEPES-NaOH, pH 7.4, 150 mM NaCl, 5 mM KCl, 1 mM $MgCl_2$, 1.8 mM $CaCl_2$) containing 1 μg/ml of annexin V-FITC. Propidium iodide was added prior

analysis to the final concentration of 10 μg/ml. Cell fluorescence was measured on a flow cytometer (FACSCalibur, Becton Dickinson, CA) and analysed using CellQuest software.

2.7.2 Morphological apoptosis assays

Cells were plated at 4 x 10^5 cells/well in 6-well plates and 24 h later were treated with TRAIL for a further 18-24 h prior to enumeration of apoptosis based on cell morphology (cell rounding, detachment from the plate, nuclear condensation and presence of apoptotic bodies). A minimum of 300 cells were counted in each treatment. Each assay was repeated three times. Where appropriate, cell lysates were prepared using SDS-PAGE loading buffer and protein expression was examined by Western Immunoblotting.

2.8 Site-directed mutagenesis

Site-directed mutagenesis was carried out using the QuikChange kit (Stratagene). Plasmids were verified by sequencing.

2.9 Generation and immunhistochemical analyses of organotypic skin equivalents.

Skin models were generated using 24 well inserts (Nunclon TM Δ, Nunc, Rochester, NY) in 24 well plates (Greiner-bio-one). Per insert 1 x 10^5 fibroblasts in GNL (322.5 ml 2x DMEM; 7,5 ml 3 M HEPES; 1.25 ml chondroitin-4-sulfate; 1.25 ml chondroitin-6-sulfate; 7.5 ml FCS) were mixed 1:3 with collagen I isolated from rat tails to a final volume of 500 μl and cultivated in DMEM/4.5 g/l glucose/1% L-glutamine/10 % FCS/-L-pyruvate over night at 37°C. Next day dermal gels were equilibrated with EGM/10 % FCS/1% PenStrep/10 mg/ml gentamycine for 2 h at 37°C. The medium was withdrawn and 1 x 10^5 keratinocytes in EGM carefully seeded on top and incubated for 1.5 h at 37°C to allow adhesion. Subsequently, skin equivalent were covered with EGM and

cultivated for 7 days – changing the medium every other day. At day 7 skin equivalents were transferred to 6 well plates and cultivated/treated (with IL-36) at the air-liquid interface in MM for 15 more days at 37 °C, changing the medium every other day. Skin reconstructs were fixed in Roti-Histofix (Roth; Karlsruhe, Germany) for 3 h at RT released from the insert and embedded into paraffin. Sections of 3 µm were cut using a RM 2145-microtome (Leica, Biberach, Germany), transferred onto slides (LABOnord; Greiner-bio-one) for hematoxylin-eosin (HE)-staining or onto sialynized slides (Menzel GmbH, Braunschweig, Germany) for immunhistochemical analysis and dried at 37°C over night. Sections were released from paraffin using Roticlear (Roth) and subjected to HE-staining at RT or were incubated with primary antibodies against keratin 10 (Dako, Hamburg, Germany), keratin 14, filaggrin (Biomedia, Singapore) and involucrin (Acris, Herford, Germany), respectively, as recommended by the manufacturer at 4°C over night. Secondary polyclonal goat-anti-mouse-FITC (Dako) or goat-anti-mouse-Cy3 IgG (Jackson ImmunoResearch) antibodies were used, slides mounted in ProLong® Gold with or without DAPI (MolecularProbes® life technologies™) and analyzed using an Apotom1-Axio Imager and CEN software (Zeiss).

2.10 Psoriatic patient samples

4 mm punch biopsies were obtained from 3 individuals presenting with clinical features of psoriais. The punch biopsies were obtained from uninvolved as well as involved areas of epidermis. Samples were homogenized using a dounce homogenizer in protease reaction buffer (50 mM Hepes, pH 7.4, 75 mM NaCl, 0.1 % CHAPS. 1 X SDS-PAGE loading buffer (Tris.Cl, 50 mM, SDS, 2 %, Glycerol 10 %, Bromophenol Blue, 0.05 %, β-mercaptoethanol, 2.5 %) was added to each sample pellet. Samples were then boiled for a further 5 mins. Cell lysates were prepared using SDS-PAGE loading buffer and were electrophoresed on 8-13% SDS-polyacrylamide gels followed by transfer onto nitrocellulose membranes.

Protein expression was subsequently examined by immunoblotting with the appropriate antibodies.

2.11 Gene expression analysis

2.11.1 Gene expression microarray

Primary human neonatal foreskin-derived Keratinocytes (P3) were used for gene expression analysis. Primary Keratinocytes were stimulated with IL-36β for 8 and 24 h timepoints. Cells were harvested with RNAprotect cell reagent (Qiagen) and stored at -80°. Analysis of samples were performed using SurePrint G3 Human Gene Expression 8x60K v2 Microarray using a one-color based hybridization protocol and preformed by IMGM Laboratories (Germany).

2.11.2 RNA analysis by Real-Time PCR (RT-PCR)

RNA was extracted from cells using the RNeasy Kit (Qiagen) as per manufacturer's instructions. cDNA was generated using the Omniscript RT Kit (Qiagen) and used to seed RT-PCR reactions (LightCycler® FastStart DNA Master Mix Sybr Green I). Quantification of cytokine gene products was preformed using the Roche Light Cycler 1.5 sortware and normalized to the β–Actin housekeeping gene.

2.11.3 Primers for RT-PCR

Primer sequence design for cytokine gene expression by real-time RT-PCR.
IL-17C Forward 5' TTG GAG GCA GAC ACC CAC C 3',
IL-17C Reverse 5' GAT AGC GGT CCT CAT CCG TG 3';
IL-36γ Forward 5' GAA ACC CTT CCT TTT CTA CCG TG 3',
IL-36 γ Reverse 5' GCT GGT CTC TCT TGG AGG AG 3';
IL-8 Forward 5' TCTGCAGCTCTGTGTGAAGG 3',
IL-8 Reverse 5' ACTTCTCCACAACCCTCTGA 3';
G-CSF Forward 5' GCT TAG AGC AAG TGA GGA AG 3',
G-CSF Reverse 5' AGG TGG CGT AGA ACG CGG TA 3';

GM-CSF Forward 5' GAG CAT GTG AAT GCC ATC CAG GAG 3',

GM-CSF Reverse 5' CTC CTG GAC TGG CTC CCA GCA GTC AAA 3';

β-defensin-2 Forward 5' ATG AGG GTC TTG TAT CTC CT 3',

β-defensin-2 Reverse 5' TAT CTT TGG ACA CCA TAG TT 3';

β-Actin Forward 5' ATGTTTGAGACCTTCAACAC 3',

β-Actin Reverse 5' CACGTCACACTTCATGATGG 3'

Chapter 3

TRAIL promotes pro-inflammatory cytokine and chemokine production

3.1 Introduction

Engagement of TRAIL receptors (DR4/DR5) with their ligand (TRAIL) results in apoptosis via a caspase-8-dependent pathway that is now well established (Wiley et al., 1995; Sprick et al., 2000; Sprick et al., 2002). The majority of studies exploring TRAIL signalling have focused on cell death as the primary endpoint and as a consequence have overshadowed the role of TRAIL receptor engagement as a driver of other biological endpoints. For example, sporadic reports in the literature also suggest that TRAIL receptor stimulation may result in the activation of multiple pro-inflammatory kinase pathways, including NF-κB and MAPK, and the production of pro-inflammatory cytokines and chemokines (Schneider et al., 1997; Varfolomeev et al., 2005; Jin et al., 2006, Berg et al., 2009; Tang et al., 2009; Falschlehner et al., 2007; Kavuri et al., 2011). Other reported consequences of TRAIL receptor engagement include co-stimulation of $CD4^+$ T-cells (Hwei-Fang et al., 2004; Ai-Hsiang et al., 2001), proliferation of tumor and non-transformed cells (Ehrhardt et al., 2003; Morel et al., 2005), tumor invasion (Ishimura et al., 2006) and as a modulator of allergic diseases (Weckmann et al., 2007). Thus, much evidence suggests that signaling through the TRAIL receptor pathway can lead to endpoints other than cell death, but this aspect of TRAIL biology and its functional consequences are not well understood.

TRAIL is a member of the TNF receptor superfamily, members of which play an important role in regulating cell life spans but also in cell-cell communication within the immune system (Aggarwal et al., 2003; Karin et al., 2009). A key aspect of TNF-α function is its potent ability to trigger the production of numerous pro-inflammatory cytokines and chemokines in the context of immune reactions, i.e. during viral or bacterial infections or autoimmune conditions (Aggarwal et al., 2003; Brennan & McInnes, 2008). TNF-α-induced cytokines and chemokines, such as IL-6, IL-8, GM-CSF and RANTES, can coordinate and amplify immune responses through triggering the production of acute phase proteins, recruitment of neutrophils and basophils to the site of inflammation and by triggering increased production of monocytes/macrophages from bone marrow. Because the TRAIL receptor-associated signalling complex shares several constituents in

common with the TNF receptor complex (Jin et al., 2006), we asked whether TRAIL receptor stimulation could also modulate inflammatory cytokine production and chemotaxis towards apoptotic cells.

Until recently, cells dying via apoptosis were considered to be immunologically inert or 'silent', differing from viable cells primarily on the basis of alterations to their plasma membrane that permit recognition and engulfment by phagocytes. In sharp contrast, necrotic cells are well known to communicate their presence through the uncontrolled release of intracellular molecules or DAMPs, which have the potential to activate the immune system (Matzinger, 1994). While the list of potential danger signals is long, the best described so far include IL-33, IL-1α, genomic DNA, HMGB1 and ATP. Recent reports suggest that apoptotic cells may also actively release soluble factors, dubbed 'find-me' signals, than can promote chemotaxis of phagocytic cells towards dying cells (Gregory and Pound, 2011; Ravichandran, 2011; Cullen et al., 2013). These factors, which include ATP/UTP (Elliott et al., 2009; Chekeni et al., 2010), lysophosphatidylcholine (Lauber et al., 2003), and fractalkine (CXCL3) (Trumen et al., 2003), represent somewhat unconventional chemotactic signals, but it is unclear whether conventional chemotactic factors are also released from apoptotic cells. Because TRAIL-R stimulation has been sporadically linked with the production of pro-inflammatory cytokines and chemokines—primarily from cells of the immune system—we wondered whether non-immunological cell types undergoing TRAIL-induced apoptosis also secrete conventional chemotactic factors to attract the attentions of phagocytes and coordinate removal of dying cells.

In this chapter, we show that TRAIL receptor stimulation induced the production of several pro-inflammatory cytokines and chemokines, a subset of which could trigger chemotaxis of phagocytic cells towards the source of these factors. Importantly, although we could uncouple TRAIL-induced cell death from production of cytokines and chemokines, TRAIL-dependent apoptosis was nonetheless accompanied by robust production of several conventional chemotactic factors. Importantly, we identify caspase-8 and FADD as critical components of TRAIL-induced cytokine and chemokine production. Furthermore,

we present data to support a role for RIPK1 and IAPs, along with NF-kB and p38 pathways, as modulators of TRAIL-induced inflammatory signalling. Thus, not all forms of apoptotic cell death may be immunologically silent, and certain stimuli, such as TRAIL, can actively engage the immune system through the secretion of conventional cytokines and chemokines from apoptotic cells

3.2 Results

3.2.1 TRAIL receptor engagement induces production of multiple cytokines and chemokines

As shown in **Figure 3.1 a,** stimulation of HeLa cells with TRAIL ligand triggered extensive apoptosis, as expected. Under the same conditions, HeLa cells also secreted large amounts of IL-6, IL-8, MCP-1, CXCL1 and MIF into the culture medium (**Figure 3.1 b**). In addition, cytokine arrays were used to identify TRAIL-dependent cytokine secretion. Of particular interest is the diverse range of soluble factors, including key angiogenic factors, such as amphiregulin and uPA, produced by HeLa cells in response to TRAIL (**Figure 3.2 a, b**). Thus, in parallel with its ability to provoke apoptosis, TRAIL-R stimulation is capable of triggering the production of diverse pro-inflammatory mediators from dying cells. Importantly, we also observed TRAIL-dependent production of cytokines and chemokines in several additional cell types, such as HT-29 colon adenocarcinoma cells (**Figure 3.5 a**), HEK239T embryonic kidney cells (**Figure 3.5 b**) and 3LL lung carcinoma cells (**Figure 3.5 c**), demonstrating that this is a general property of TRAIL-R engagement. It is important to note that TRAIL-induced cytokines/chemokines in HeLa cells failed to be attenuated through co-incubation with a neutralizing antibody against TNF, ruling out the possibility that TRAIL-induced cytokines/chemokine production was due to TRAIL-induced TNF production acting in an autocrine or paracrine manner (**Figure 3.6 a, b**).

3.2.2 TRAIL-dependent cytokine production is present in cells with features of apoptosis

Although TRAIL-induced cytokine and chemokine secretion could be uncoupled from apoptosis, as demonstrated above, it is important to note that cells undergoing TRAIL-induced apoptosis still produced substantial quantities of these inflammatory mediators (**Figure 3.1 a, b, Figure 3.4 a, b**). Indeed, immunostaining of cells undergoing TRAIL-induced apoptosis readily detected IL-6, IL-8 and MCP-1 being produced by cells with clear features of apoptosis, while unstimulated cells stained negative for the same proteins (**Figure 3.3 b**) with the exception of MIF, which is constitutively present in high amounts in the cytoplasm.

3.2.3 TRAIL-induced production of pro-inflammatory cytokines is cell death and caspase-independent

One interpretation of these results was that the observed release of cytokines and chemokines occurred secondary to TRAIL-induced cell death and represented passive, as opposed to active, release. Because caspase activation is essential for TRAIL-induced apoptosis, we explored whether inhibition of caspases suppressed cytokine release in response to TRAIL receptor ligation. However, while inhibition of caspase activation using the pan-caspase inhibitor zVAD-fmk, efficiently blocked TRAIL-dependent apoptosis, TRAIL-induced cytokine release was not suppressed under the same conditions (**Figure 3.4 a**). Indeed, caspase inhibition significantly enhanced the release of IL-6, IL-8 and MCP-1 from TRAIL-stimulated cells, most likely through protection from apoptosis, thereby extending the duration of cytokine production. We also attenuated TRAIL-induced apoptosis through stable over-expression of the anti-apoptotic Bcl-2 family member Bcl-xL, and this also resulted in enhanced release of IL-6, IL-8 and MCP-1 (**Figure 3.4 b**).

Finally, we could completely uncouple cytokine production from death under conditions where cells were resistant to TRAIL-induced cytotoxicity. Importantly, HT-29, 293T and 3LL cells were resistant to TRAIL-induced death but produced

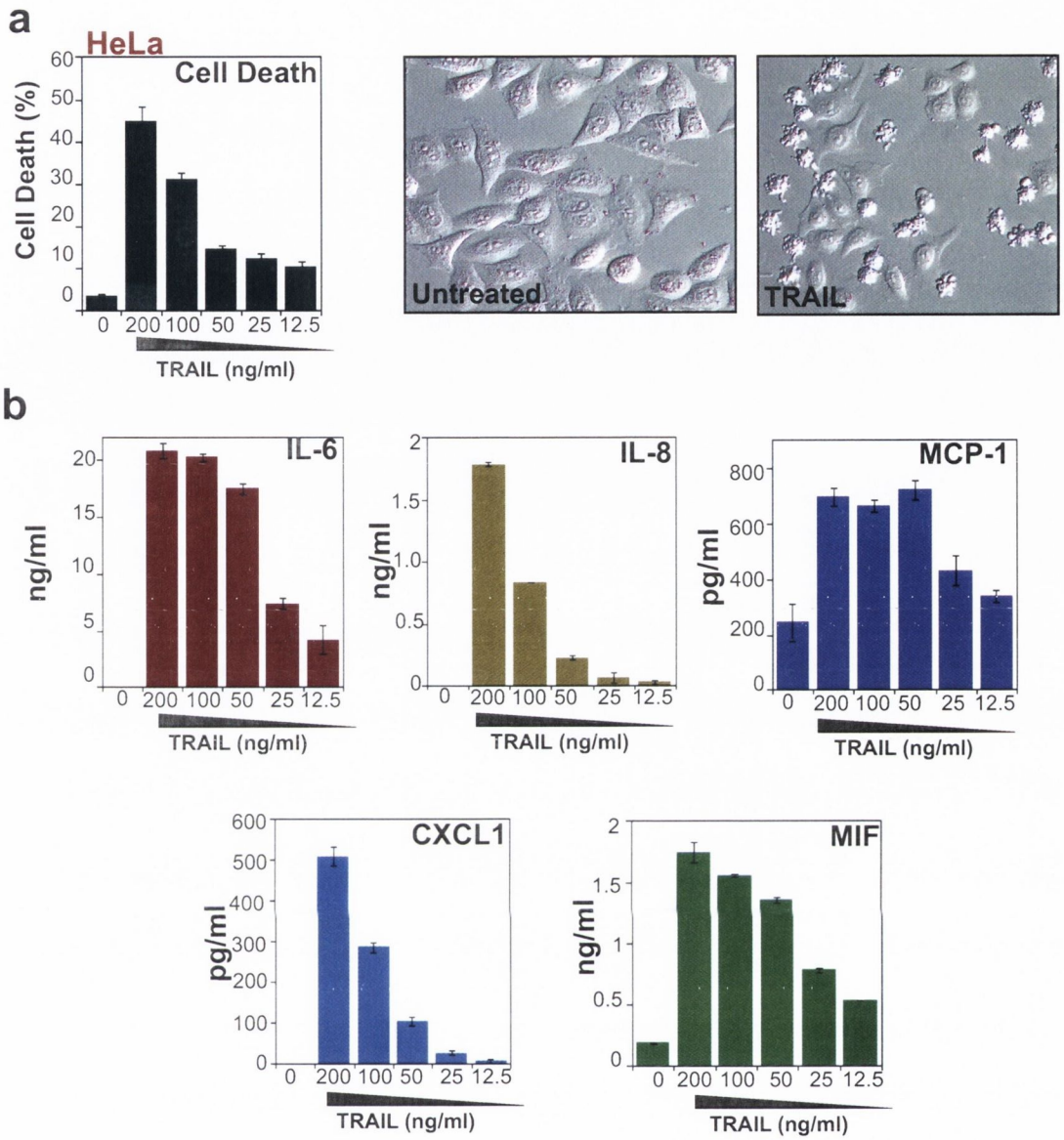


Figure 3.1 TRAIL stimulation induces apoptosis as well as multiple pro-inflammatory cytokine

a. HeLa were stimulated with TRAIL at the indicated concentrations. After 24 h, apoptosis was scored on cell morphology (cell rounding, detachment from the plate, nuclear condensation and presence of apoptotic bodies). **b.** Live and apoptotic cells in culture were visualized by phase-contrast microscopy at 12hrs. **c.** Cytokine concentrations in the culture supernatants were determined by ELISA. Results shown are representative of at least three independent experiments. Error bars represent the mean ±SEM of triplicate determinations from a representative experiment.

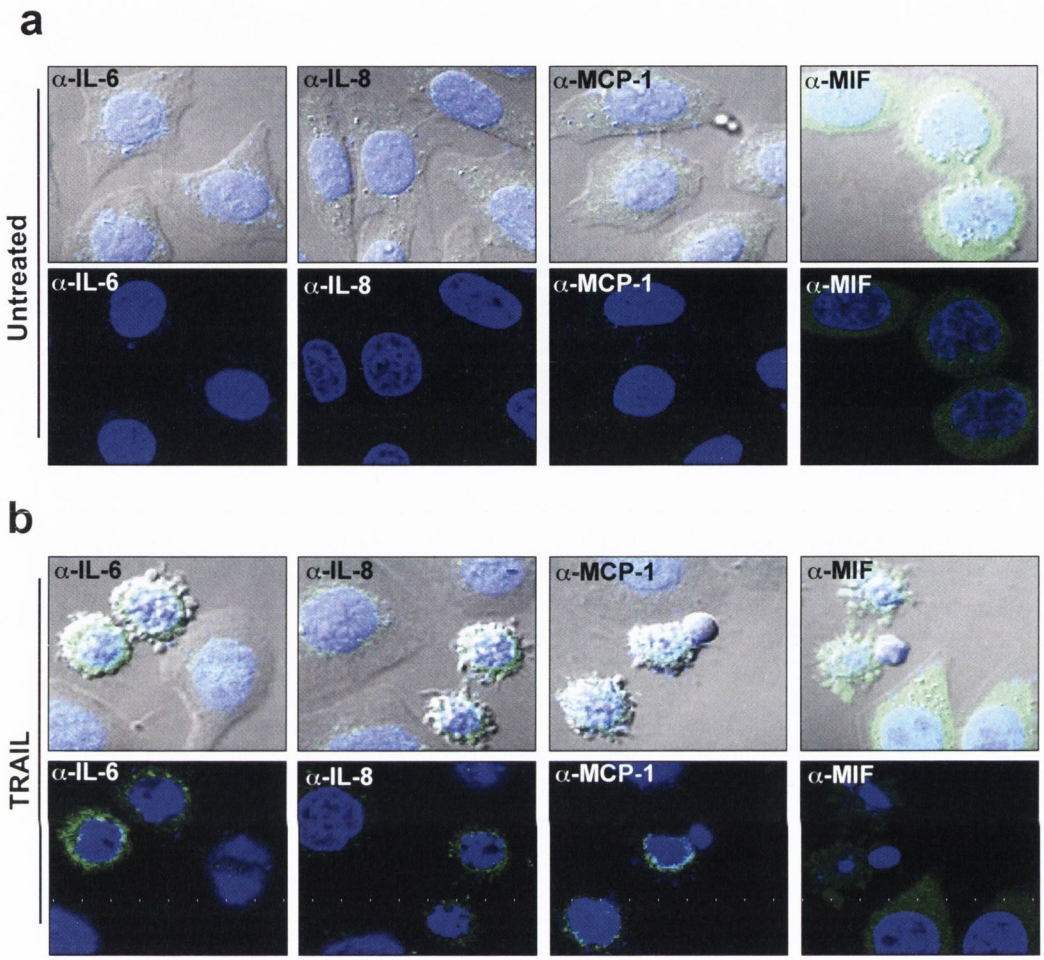


Figure 3.2 Pro-inflammatory cytokines and chemokines are produced by cells with clear features of apoptosis

(a-b) Representative confocal images of HeLa cells in the presence or absence of TRAIL (100 ng/ml) for 14 h followed by immunostaining for the indicated cytokines and chemokines and staining of nuclei with Hoechst 33342.

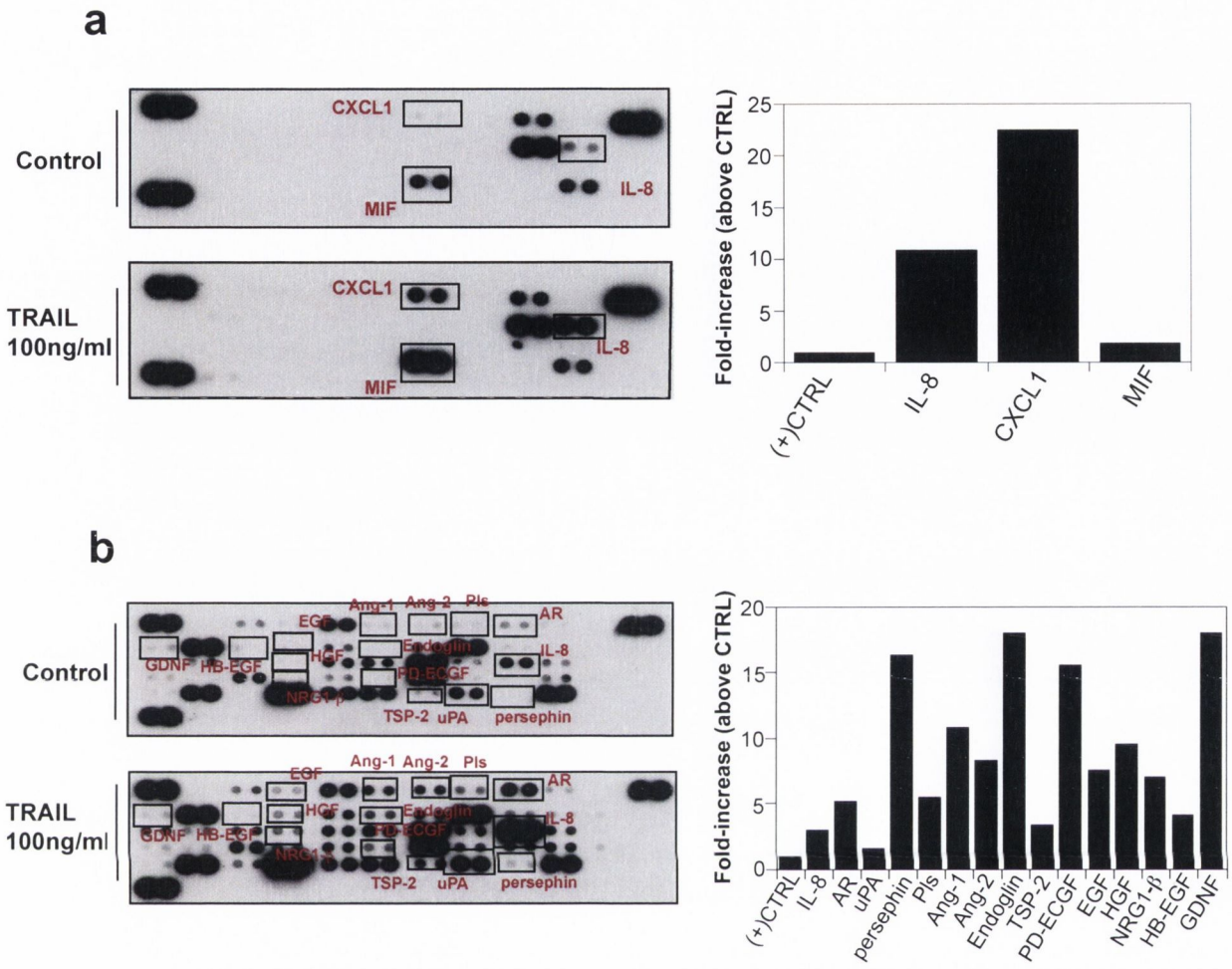


Figure 3.3 TRAIL stimulation induces the secretion of a diverse array of inflammatory cytokines

a. HeLa were stimulated with 100ng/ml TRAIL. After 24h, supernatants were harvested and incubated with a human cytokine antibody array. **b.** Supernatants were incubated with a human angiogenesis array.

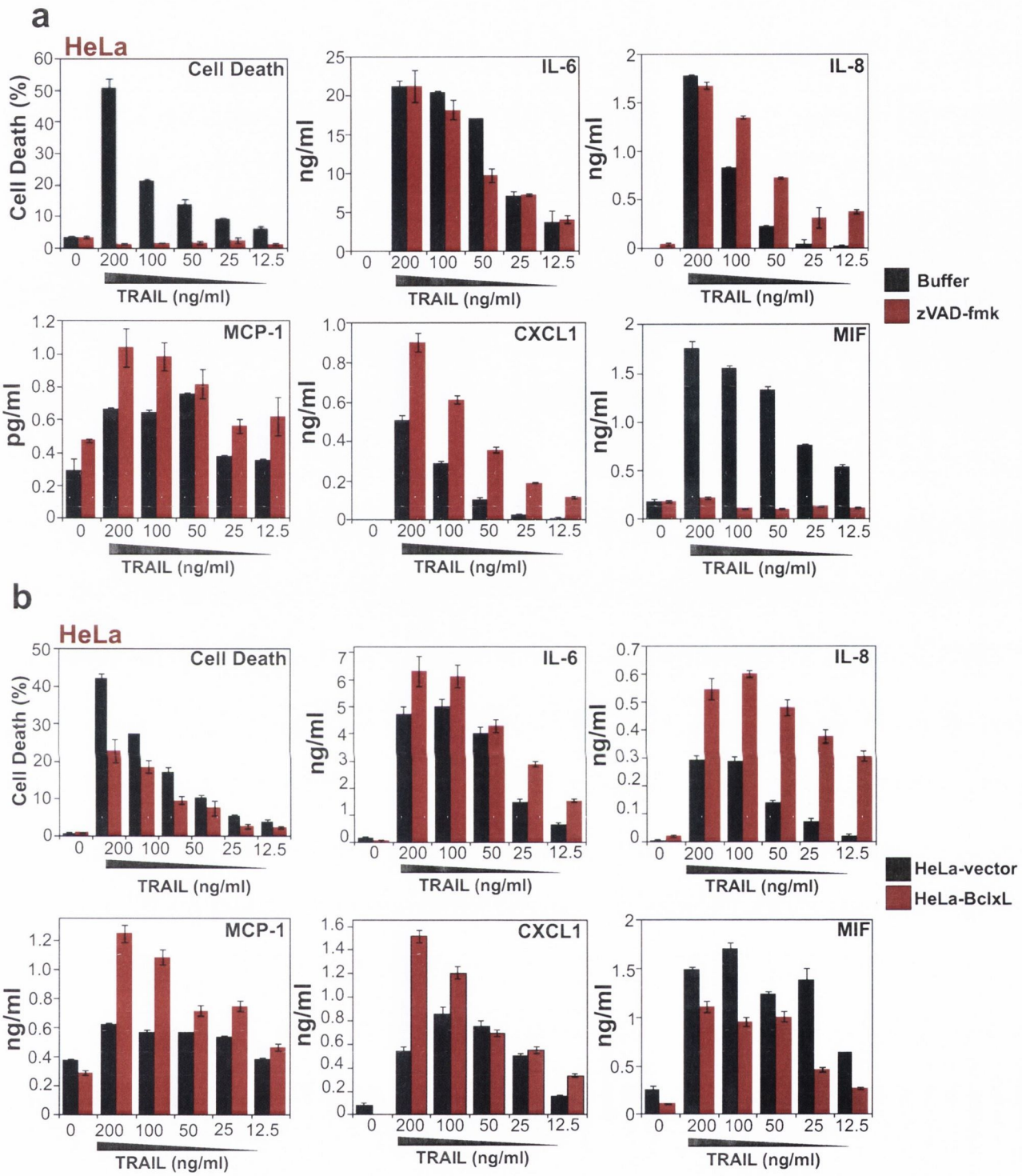


Figure 3.4 TRAIL production of pro-inflmmatory mediators is caspase-independent.
a. HeLa cells were treated with TRAIL at the indicated concentrations, in the presence or absence of zVAD-fmk (10 μM), as indicated. After 24 h, apoptosis was quantitated by annexin V/PI staining and cytokine concentrations in culture supernatants were determined by ELISA. **b.** HeLa cells were treated with TRAIL at the indicated concentrations, in the presence or absence of zVAD-fmk (10 μM), as indicated. After 24 h, apoptosis was quantitated by annexin V/PI staining and cytokine concentrations in culture supernatants were determined by ELISA. Results shown are representative of least three independent experiments. Error bars represent the mean ±SEM of triplicate determinations from a representative experiment.

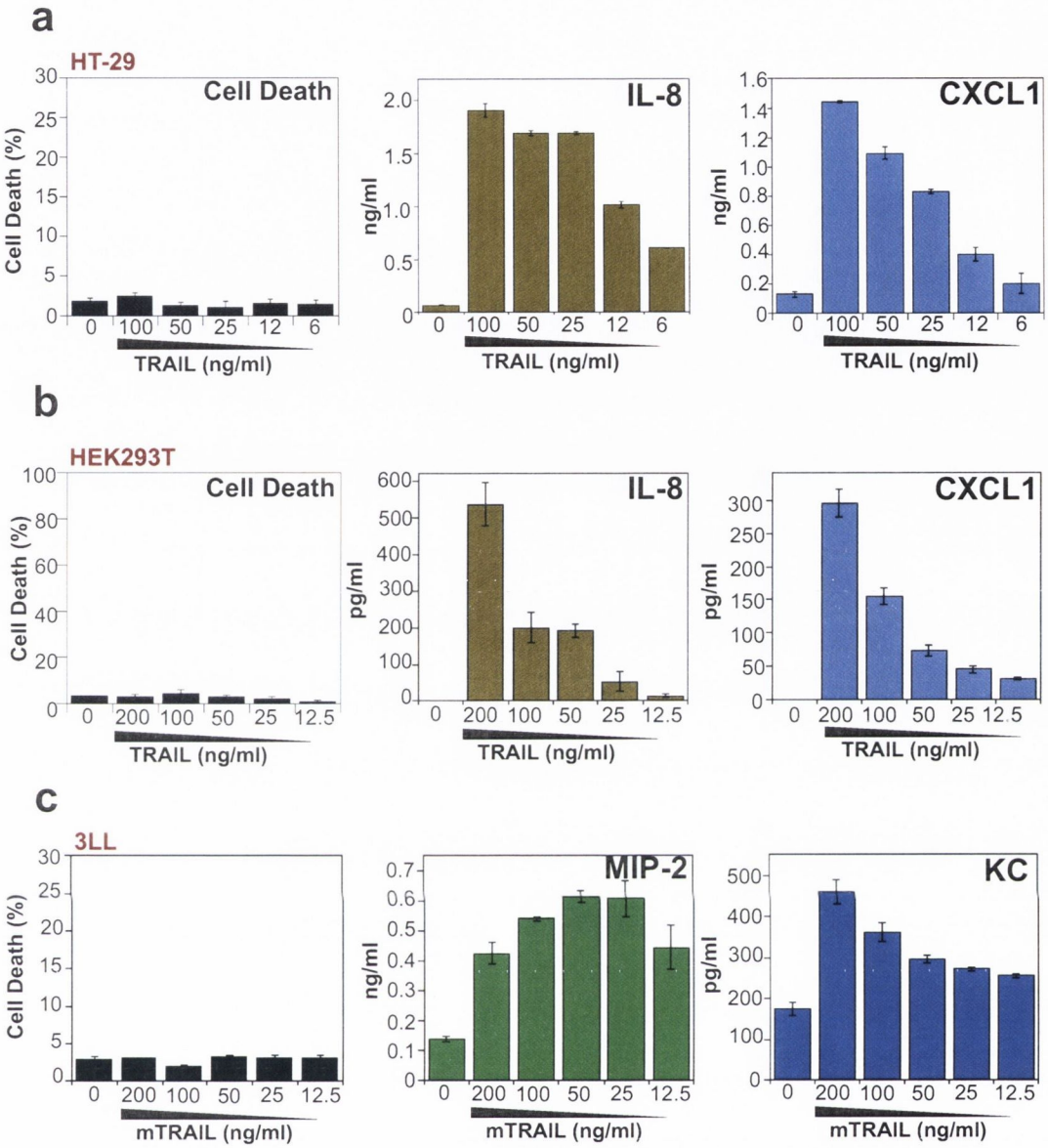


Figure 3.5 TRAIL receptor engagement in multiple cell types promotes the secretion of pro-inflammatory cytokines and chemokines
a. HT-29, **b.** 293T, **c.** 3LL cells were treated with TRAIL at the indicated concentrations. After 24 h, apoptosis was quantitated by annexin V/PI staining and cytokine concentrations in culture supernatants were determined by ELISA.

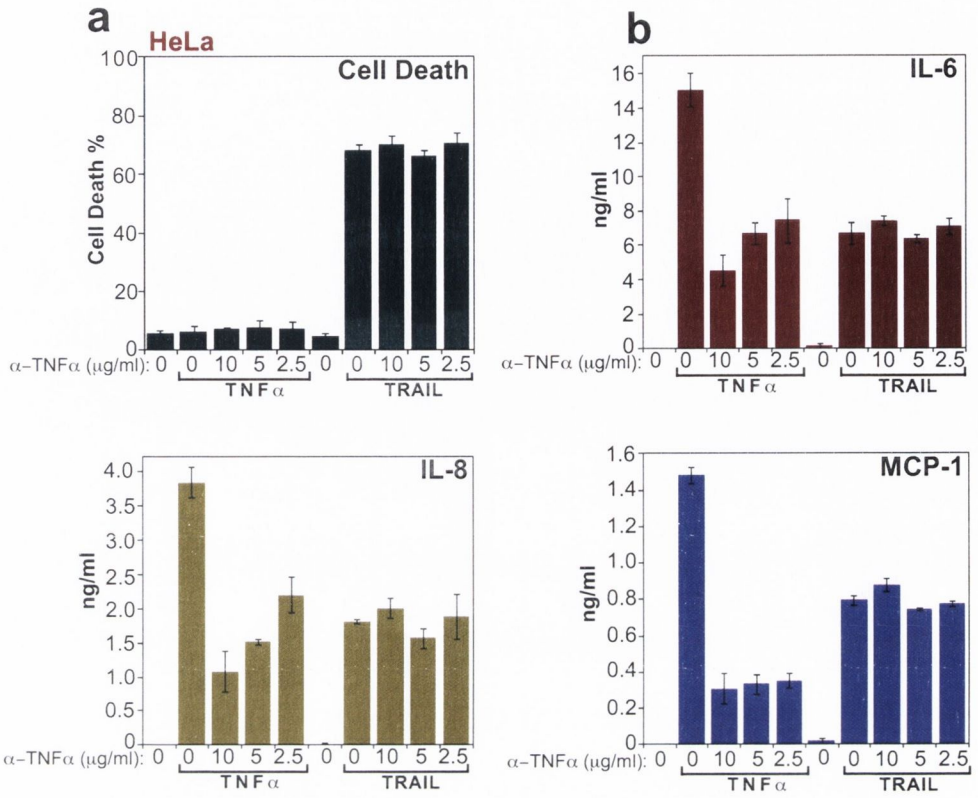


Figure 3.6 TRAIL-induced death and cytokines are not dependent on a TNFα-autocrine loop

a. HeLa cells were preincubated for 2 h with anti-TNFα neutralizing antibody before stimulation with TNFα (1ng/ml) or TRAIL (50ng/ml) and incubated for 24 h. Apoptosis was scored on cell morphology and was counted in triplicate fields of view. **b.** Supernatants were harvested and cytokine concentrations in the supernatant were determined by ELISA.

cytokines and chemokines (**Figure 3.6 a, b, c**). Thus, TRAIL-dependent inflammatory signalling can be uncoupled from caspase activity and cell death.

3.2.4 TRAIL-induced chemokine production can be inhibited through antagonism of IAPs

Recent studies have implicated inhibitor of apoptosis proteins (IAPs) as important regulators of TNF and TRAIL-induced apoptosis (Varfolomeev et al., 2007; Vince et al., 2007; Petersen et al., 2007; Bertrand et al., 2008). Thus, we wondered whether IAPs were also required for optimal TRAIL-induced production of cytokines and chemokines. To address this possibility, we used a bivalent small molecule IAP antagonist (BV6) that Vucic and colleagues have previously shown to promote the rapid degradation of cIAP-1, cIAP-2 and to a lesser extent XIAP (Varfolomeev et al., 2007). BV6 greatly sensitized HeLa cells to the apoptosis-inducing effects of TRAIL stimulation (**Figure 3.7 b**) and promoted essentially complete degradation of cIAP-1, cIAP-2 as well as partial degradation of XIAP (**Figure 3.7 a**) as observed by immunoblot.

Next we explored the impact of IAP antagonism on TRAIL-induced cytokine production. Importantly, TRAIL-induced production of IL-8 and CXCL1 were profoundly inhibited through addition of BV6 (**Figure 3.7 b**) yet IL-6 secretion was unaffected. This strongly suggests that IAPs are required for optimal TRAIL-induced cytokine production. Because TRAIL-induced apoptosis was dramatically enhanced in the presence of BV6 (**Figure 3.7 b**), it was possible that TRAIL-induced chemokine production was impaired merely as a consequence of cell death (i.e. less cells to make chemokines) rather than as a direct consequence of IAP antagonism. However, under conditions where TRAIL/BV6-initiated cell death was completely suppressed by zVAD-fmk (**Figure 3.7 c**), TRAIL-induced production of chemokines was still largely inhibited in the presence of BV6 (**Figure 3.7 c**). These results demonstrate a potentially important role for IAPs in TRAIL-dependent induction of chemokines.

3.2.5 RIPK1 and multiple kinase pathways regulate TRAIL-induced cytokines

The potent pro-inflammatory effects of TNF receptor stimulation are achieved through RIPK1-dependent activation of multiple kinases including, p38MAPK, MEK/ERK and the IKK complex (Haas et al. 2009). Indeed, we observed a similar range of kinase activation events in response to TRAIL-R stimulation, well before the activation of caspase-8, with the notable exception of NFκB activation that was detected relatively late in response to TRAIL-R engagement (**Figure 3.8**). In addition, caspase-8 autoactivation and processing to produce the active p18 fragment was observed. cIAP-1 and cIAP-2 have been implicated as regulators of RIPK1 poly-ubquitination and recruitment of downstream signalling intermediates in the context of TNF receptor and FasL/CD95 signalling (Haas et al. 2009, Hsu et al., 1996, Cullen et al. 2013). Because the preceding experiments found that IAP neutralization suppressed TRAIL-induced chemokine production, this suggested that RIPK1 may be important in this context. Thus, we asked whether RIPK1 could modulate TRAIL-induced chemokine production. Initially, we overexpressed RIPK1 and found that it sensitized to cell death but also induced cytokine and chemokine production (**Figure 3.9 a)**. Furthermore, RIPK1-induced death was attenuated in the presence of zVAD-fmk but this did not affect cytokine production, again suggesting that death and cytokine production can be functionally uncoupled (**Figure 3.9 b)**. Next, we knocked down RIPK1 expression in HeLa cells, and as **Figure 3.9** demonstrates, silencing of RIPK1 with two different siRNAs attenuated TRAIL-induced IL-8 and CXCL1 production suggesting that this kinase is required for the pro-inflammatory effects of TRAIL-R stimulation. Furthermore, we found that RIPK1-mediated cytokine/chemokine production was largely dependent on NF-κB as silencing of p65 completely ablated RIPK1-induced IL-6, IL8 and CXCL1 (**Figure 3.9 c)**. In addition, the downstream signalling components NF-κB and p38 MAP kinase also modulated TRAIL-, as well as Fas-, induced cytokine production, suggesting that TRAIL and Fas share similar downstream components to TNF via the recruitment of RIPK1 (**Figure 3.10 a, b**)

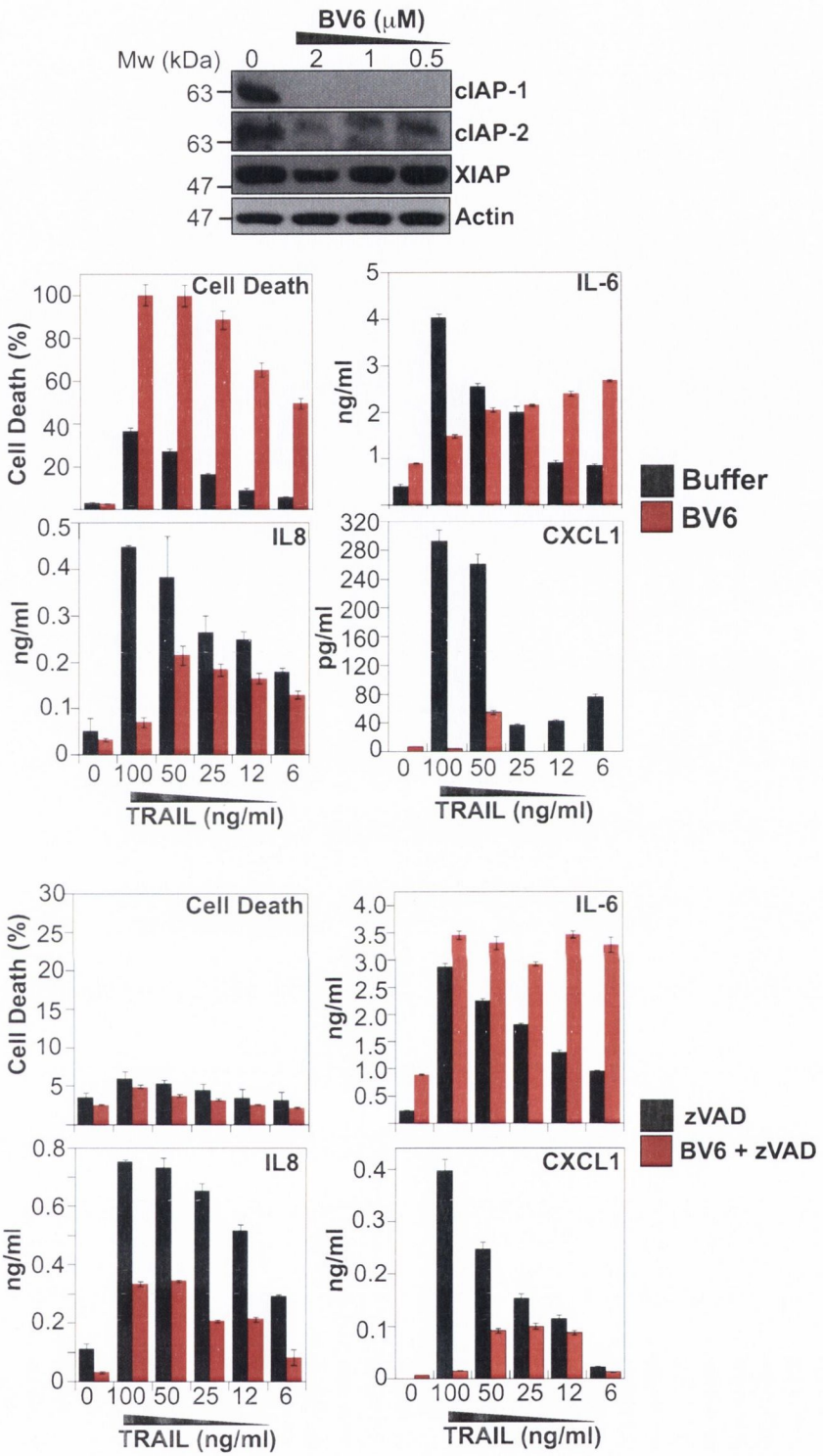


Figure 3.7 IAP antagonist BV6 modulates TRAIL-induced cytokine and chemokine production
a. HeLa cells were treated with indicated concentrations of BV6. Lysates were immunoblotted for IAPs. **b.** HeLa cells were treated with indicated concentrations of TRAIL +/- BV6 (2uM). After 18 h cytokines were measured by ELISA. **c.** As outlined in (B) with pan caspase inhibitor zVAD-fmk added to every treatment. Error bars represent the mean ±SEM of triplicate cell counts from a representative experiment.

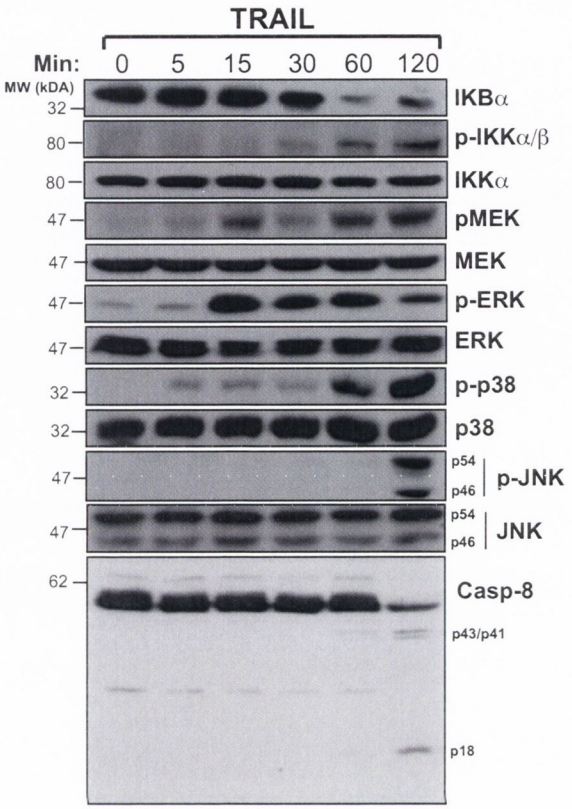


Figure 3.8 TRAIL receptor engagement activates multiple inflammatory signalling pathways

a. HeLa cells were treated with TRAIL (100 ng/ml). Whole cell lysates were prepared at the indicated timepoints and analysed by immunoblotting for the indicated proteins.

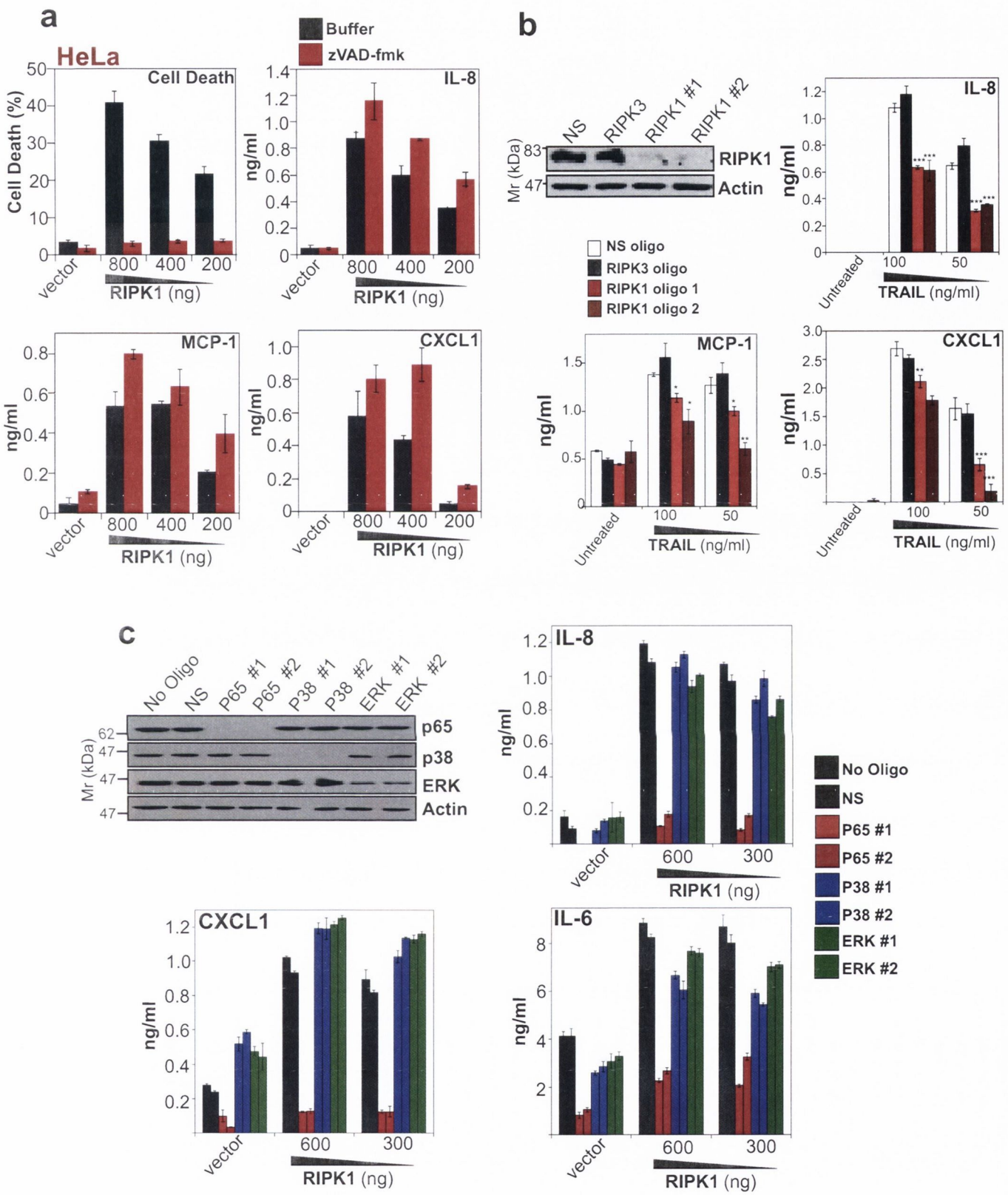


Figure 3.9 RIPK1 is required for optimal TRAIL induced cytokines and chemokines
a. HeLa cells were transfected with RIPK1 plasmid at the indicated concentrations, in the presence or absence of zVAD-cmk (10μM) and incubated for 36 h. Cytokine concentrations in the supernatant were determined by ELISA. **b.** HeLa cells were nucleofected with indicated with siRNAs. After 48 h cells were treated with indicated concentrated of TRAIL and zVAD-fmk (10 μM). After 18 h cytokine concentrations in the supernatant were determined by ELISA. **c.** HeLa cells were nucleofected with indicated siRNAs (200nM) and incubated for 48 h. Cells were then transfected with indicated concentrated concentrations of RIPK1 plasmid and incubated for a further 24 h. Cytokine concentrations in the supernatant were determined by ELISA.

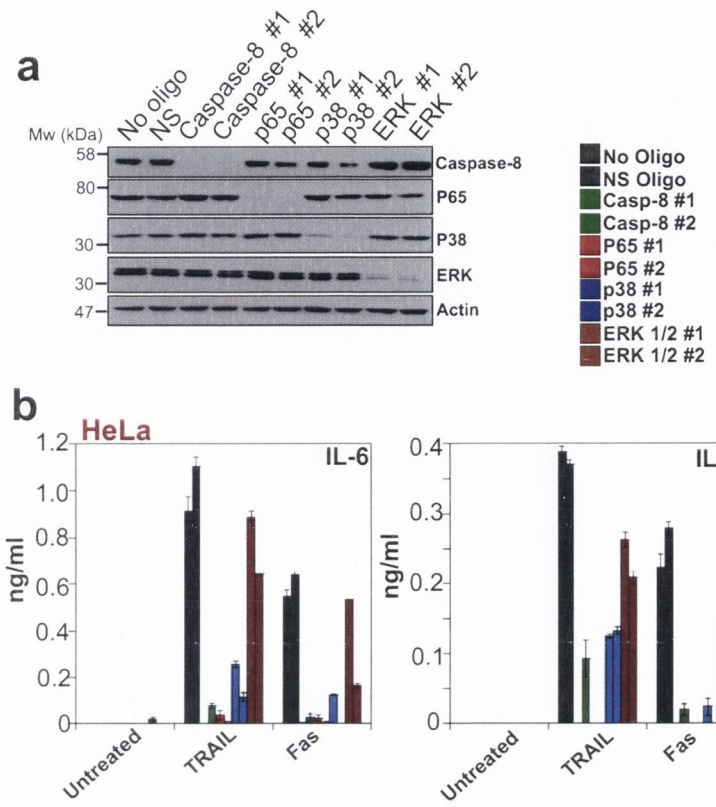


Figure 3.10 NF-kB and p38 are required for optimal TRAIL/FasL-induced cytokine and chemokine production

a. HeLa cells were nucleofected with indicated siRNAs (200nM) and incubated for 48 h. Lysates were immunoblotted for indicated proteins. Cells were then stimulated with TRAIL (50 ng/ml) and anti-Fas (CH-11) (100 ng/ml) and incubated for a further 24 h. Enumeration of apoptosis based on cell morphology and was counted in triplicate fields of view. Cytokine concentrations in the supernatants were determined by ELISA.

3.2.6 Components of the DISC differentially modulate cytokine production

In addition to RIPK1, we wished to explore the relative contributions of other adaptor molecules that are normally present at the DISC, namely caspase-8 and FADD. Through the overexpression of either RIPK1, caspase-8 or FADD, alone or in combination, we asked what effect this had on apoptosis as well as cytokine production. As demonstrated in **Figure 3.11 a, b, c**, overexpression of either RIPK1 or FADD induced death as well as cytokine production. Overexpression of caspase-8 induced cell death but did not promote cytokine production whereas overexpression of the caspase-8 catalytically inactive mutant (C>A) promoted cytokine production. Caspase-8 C>A mutant also triggered a small degree of cell death most likely as a result of interaction with and activation of endogenous caspase-8. Collectively, these data suggest that RIPK1, FADD and caspase-8 can promote cytokine production. Of particular note, caspase-8 C>A mutant was sufficient to drive cytokine production while wild-type caspase-8 was not. Note the latter mutant mimics the use of zVAD-fmk to block wild-type caspase-8 activity suggesting that it is the physical presence of caspase-8 at the DISC that is required for cytokine signalling and not its enzymatic activity.

3.2.7 Caspase-8 is critical for TRAIL/Fas-induced cytokines and is independent of its role in mediating apoptosis

To further explore whether caspase-8 was required for TRAIL- and Fas-induced cytokine production, we knocked down caspase-8. Although caspase-8 enzymatic activity was not required for TRAIL/Fas-induced cytokine production (**Figure 3.4**), knockdown of caspase-8 robustly attenuated TRAIL/Fas-induced cytokine production (**Figure 3.12 a, b**), suggesting a function for complex-associated caspase-8, but not enzymatically active caspase-8, for gene induction. Knockdown of FADD had a similar inhibitory effect on TRAIL- and Fas-induced cytokine production. Surprisingly, knockdown of FADD did not attenuate TRAIL-induced cell death, however Fas-induced death was completely abolished through FADD knockdown (**Figure 3.12 a, b**). This result raises the rather

exciting possibility that in some scenarios TRAIL may induce cell death in a FADD-independent manner. Collectively, these data suggest that TRAIL and Fas stimulation generates a FADD/caspase-8/RIPK1 complex, which is important for promoting cytokine and chemokine production.

3.2.8 Caspase-8/FADD/cFLIP are the key proteins that modulate TRAIL- and Fas-induced cytokines

Previous reports have implicated other death domain (DD) proteins, such as TRADD and MyD88, as modulators of TRAIL and Fas signalling (Cao et al, 2011, Altemeier et al, 2007). To explore this issue, we knocked down expression of TRADD, MyD88, $cFLIP_{S/L}$, RIPK1, FADD and caspase-8 in both HeLa and HT-29 cell lines. As we found previously, caspase-8 and FADD knockdown greatly impaired cytokine production while knockdown of TRADD and MyD88 had no reproducible effect (**Figure 3.13, Figure 3.14**). As has been reported previously by other groups, knockdown of $cFLIP_{S/L}$ resulted in increased sensitivity to cell death after TRAIL and Fas stimulation. In addition, $cFLIP_{S/L}$ knockdown also significantly enhanced production of cytokines (**Figure 3.13, Figure 3.14**). The absence of cFLIP at the DISC resulted in elevated cell death via the enhanced interaction and activation of caspase-8, which is typically kept in check by $cFLIP_{S/L}$ binding to form caspase-8/FLIP heterodimers, however the loss of $cFLIP_{S/L}$ and the subsequent effect on cytokine production was intriguing. This suggests that $cFLIP_{S/L}$ may negatively regulate the recruitment of molecules such as RIPK1 and IAPs to the FADD/caspase-8 complex in a similar manner as described for cFLIP regulation of 'Ripoptosome' formation (Feoktistova et al., 2011; Tenev et al., 2011). Collectively, these data suggest that TRAIL and Fas stimulation generates a soluble FADD/caspase-8/RIPK1/cFLIP complex, which is important for promoting NFκB-dependent cytokine production, with cFLIP acting as a negative regulator of this complex.

3.2.9 RIPK1 modulation of TRAIL/Fas-induced cytokines

During the course of the preceding experiments, we noticed that knockdown

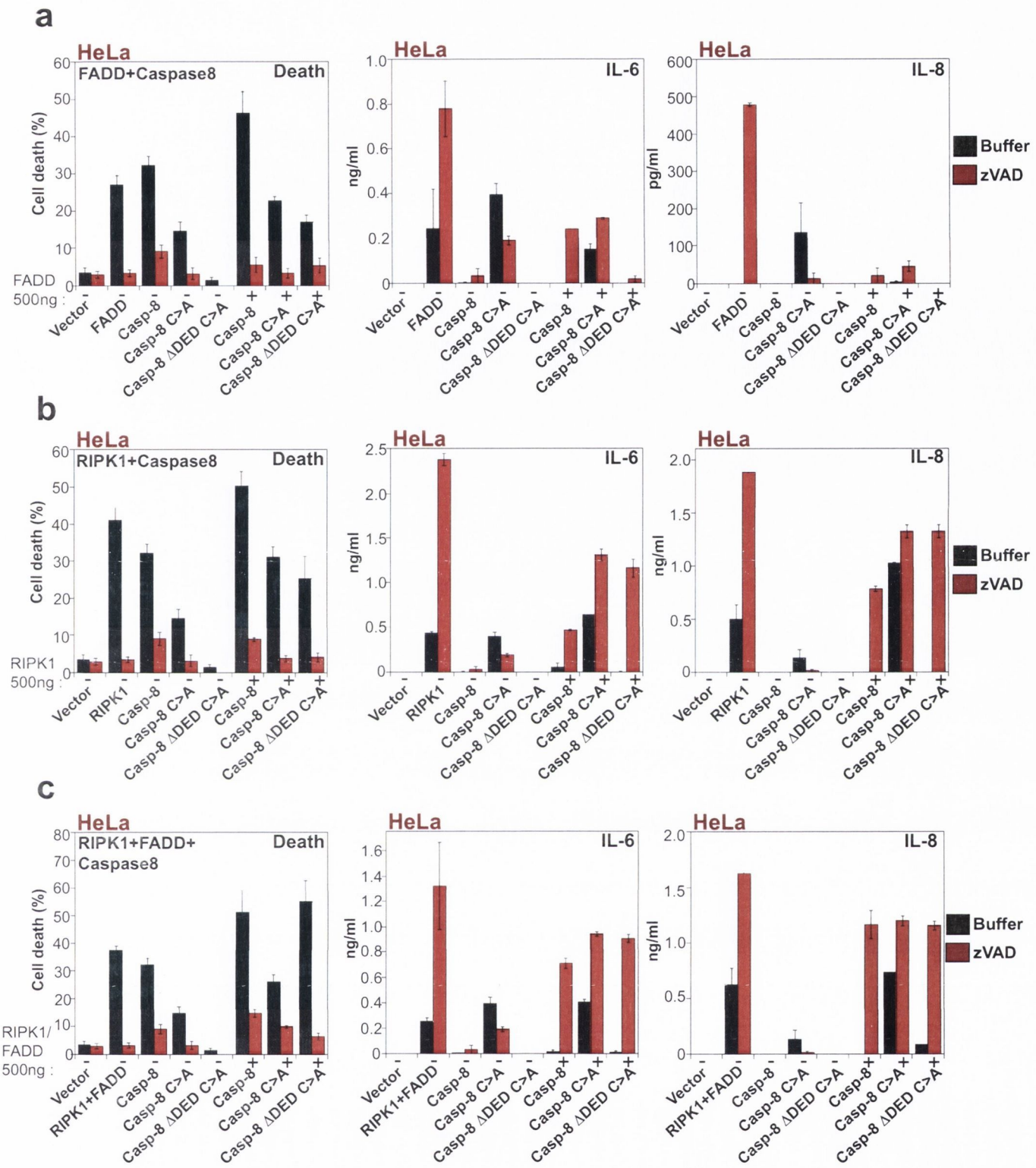


Figure 3.11 DISC adaptors caspase-8, FADD and RIPK1 are sufficient to drive cytokine production

a. HeLa cells were transfected, where indicated, with FADD plasmid (500ng), in the presence of either caspase-8 plasmid (500ng), caspase-8 C>A (500ng), Caspase-8 ΔDED C>A (500ng) and incubated for 24 h in the presence or absence of zVAD-cmk (10μM). **b.** HeLa cells were transfected, where indicated, with RIPK1 plasmid (500ng), in the presence of either RIPK1 plasmid (500ng), caspase-8 plasmid (500ng), caspase-8 C>A (500ng), Caspase-8 ΔDED C>A (500ng) and incubated for 24 h in the presence or absence of zVAD-cmk (10μM). **c.** HeLa cells were transfected, where indicated, with RIPK1+FADD plasmids (500ng), in the presence of either RIPK1 plasmid (500ng), in the presence of either RIPK1 plasmid (500ng), caspase-8 plasmid (500ng), caspase-8 C>A (500ng), Caspase-8 ΔDED C>A (500ng) and incubated for 24 h in the presence or absence of zVAD-cmk (10μM). Enumeration of apoptosis based on cell morphology and was counted in triplicate fields of view.

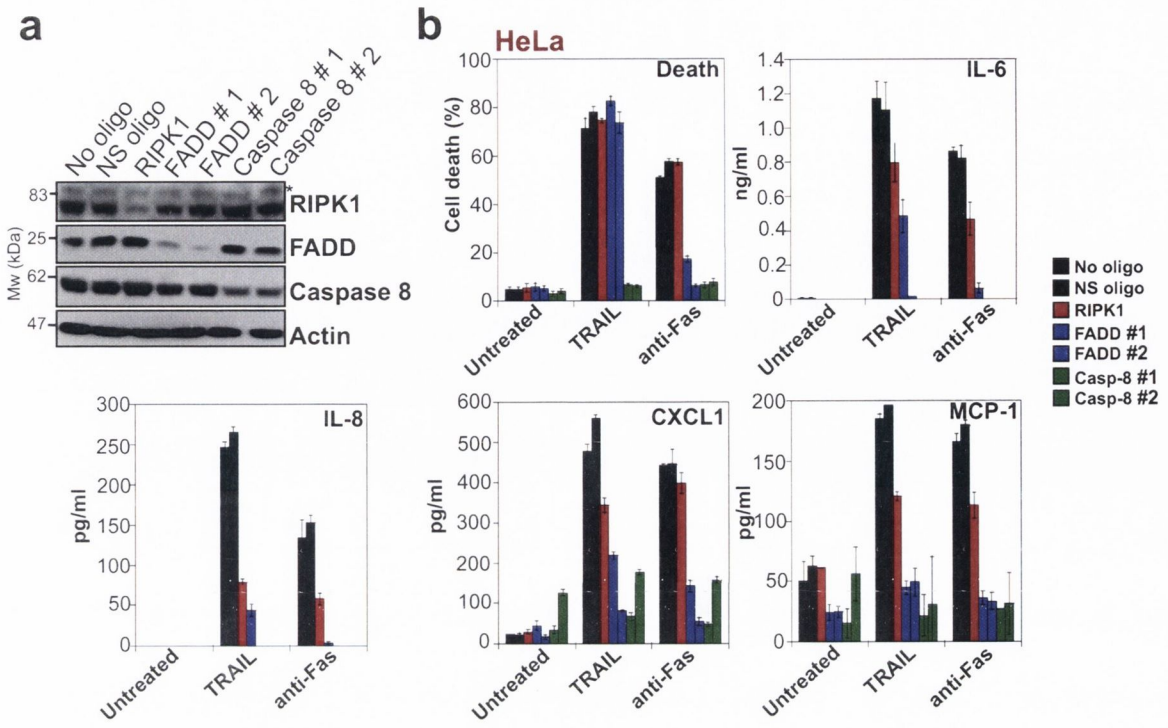


Figure 3.12 Caspase-8 and FADD are critical for TRAIL/Fas-induced cytokine and chemokine production a. HeLa cells were nucleofected with indicated siRNAs (200nM) and incubated for 48 h. Lysates were immunoblotted for indicated proteins. Cells were then stimulated with TRAIL (50 ng/ml) or anti-Fas (CH-11) (100 ng/ml) and incubated for a further 24 h. Apoptosis was scored on cell morphology (cell rounding, detachment from the plate, nuclear condensation and presence of apoptotic bodies) and was counted in triplicate fields of view. Cytokine concentrations in the supernatants were determined by ELISA.

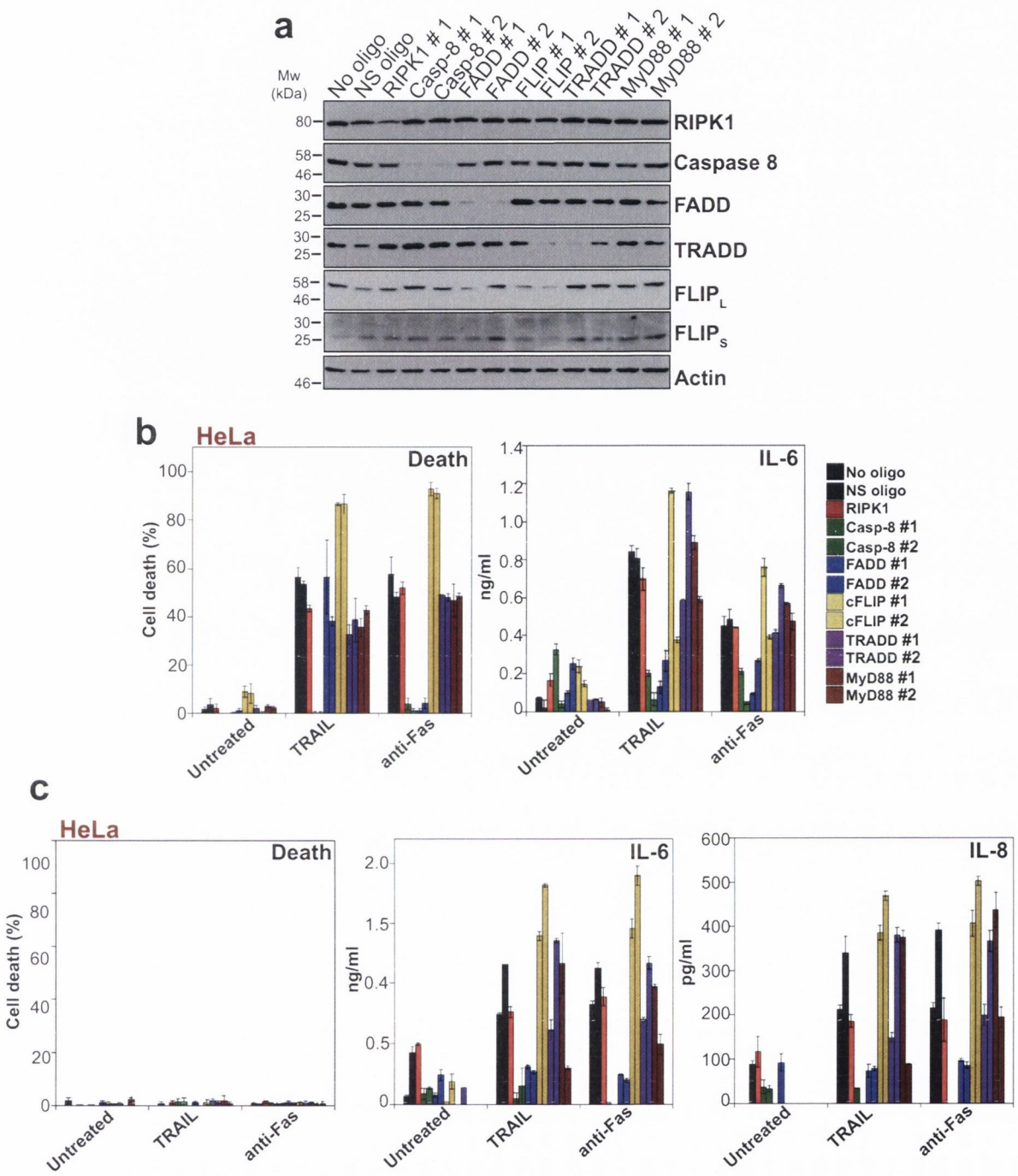


Figure 3.13 Caspase-8 and cFLIP modulate cytokine and chemokine production
a. HeLa cells were nucleofected with indicated siRNA (200nM) and incubated for 48 h. Lysates were immunoblotted for indicated proteins. **b.** Cells were then stimulated with TRAIL (50ng/ml) OR anti-Fas (CH-11) (100 ng/ml) and incubated for a further 24 h. Apoptosis based on cell morphology and was counted in triplicate fields of view. Cytokine concentrations in the supernatant were determined by ELISA. **c.** Cells were preincubated for 1 h with zVAD-fmk (10 μM) before stimulation with TRAIL (50 ng/ml) and anti-Fas (CH-11) (100 ng/ml) and incubated for a further 24 h. Cytokine concentrations in the supernatant were determined by ELISA

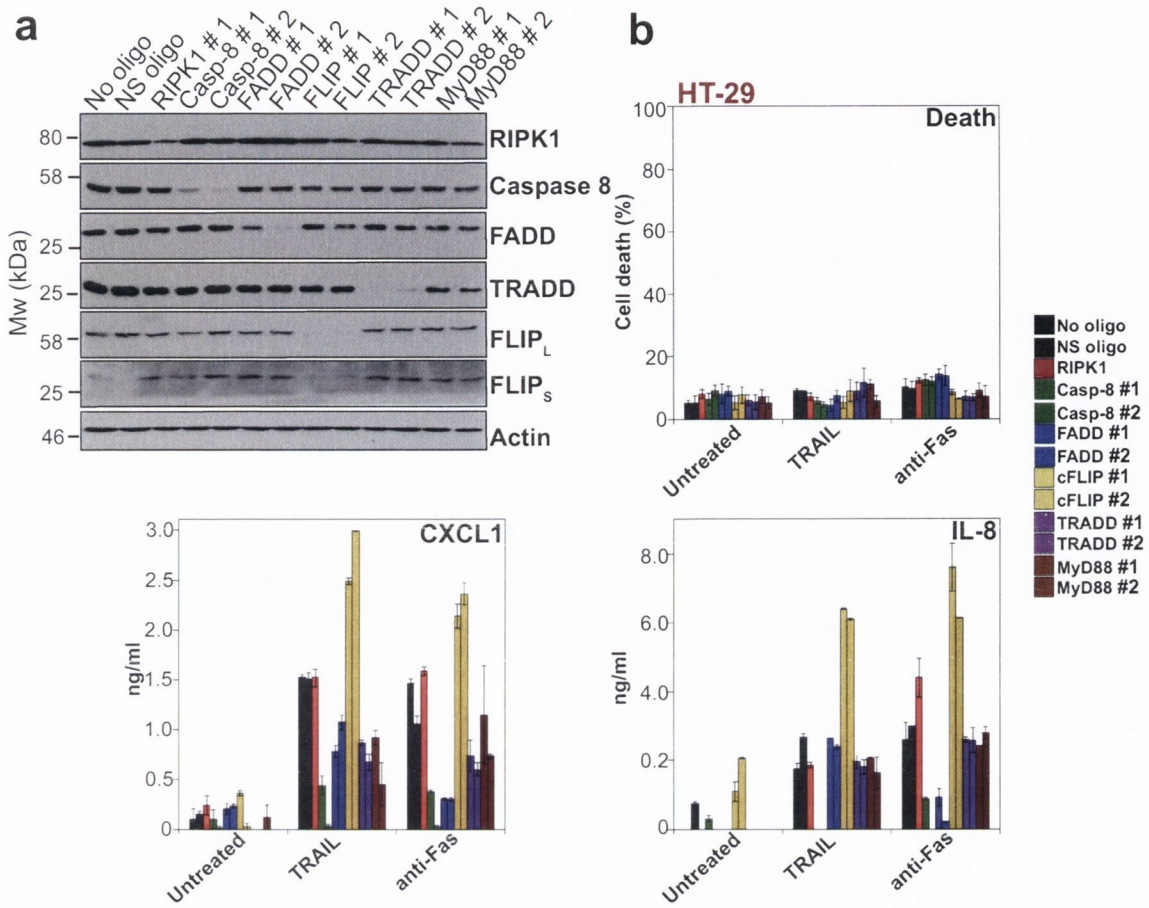


Figure 3.14 Caspase-8 is critical for chemokine production in the absence of death
a. HT-29 cells were nucleofected with indicated siRNAs (200 nM) and incubated for 48 h. Lysates were immunoblotted for the indicated proteins. **b.** Cells were then stimulated with TRAIL (50 ng/ml) and anti-Fas (CH-11) (100 ng/ml) and incubated for a further 24 h. Apoptosis was scored on cell morphology and was counted in triplicate fields of view. Cytokine concentrations in the supernatant were determined by ELISA.

of RIPK1 in HeLa reduced cytokine levels by ~30-50% with the most significant effects on IL-8 and CXCL1 secretion, while in HT-29 there was very little functional effect of RIPK1 knockdown on cytokine production (**Figure 3.12, 3.13, 3.14**). Therefore we explored the possibility that other RIP kinases may act either in conjunction with and/or instead of RIPK1 in HT-29. We knocked down RIPK1, RIPK2 and RIPK3 either alone or in combination. As **Figure 3.15 a, b** demonstrates, individual knockdown of RIPK1, RIPK2, or RIPK3 or the combined triple knockdown did not attenuate cytokine production to any significant degree in HT-29 cells. In comparison, knockdown of TAK1, a molecule implicated in TLR, IL-1 and TNF signalling through activation of IKK complex and MAPKs pathways, or knockdown of p65, significantly blunted CXCL1 and IL-8 production in response to TRAIL and Fas stimulation (**Figure 3.15 b)**.

3.2.10 Supernatants from TRAIL-stimulated cells promote phagocyte chemotaxis

Because multiple chemokines are secreted in response to TRAIL receptor stimulation, this suggested that cells undergoing TRAIL-dependent apoptosis might actively elicit the attention of neighbouring phagocytic cells, such as neutrophils and macrophages. To explore this issue, we asked whether supernatants from TRAIL-stimulated cells could promote chemotaxis of the monocytic cell line, THP-1. As **Figure 3.16** demonstrates, supernatants derived from TRAIL-stimulated HeLa cells were potently chemotactic for THP-1 cells. A previous study by Elliot and colleagues suggested that chemotaxis towards apoptotic cells may be mediated through caspase-dependent release of ATP, which is known to function as a monocyte chemoattractant (Elliot at el., 2009). Indeed as **Figure 3.17 a** demonstrates, THP-1 monocytes underwent chemotaxis towards exogenous ATP. To address whether TRAIL-dependent release of ATP was responsible for the chemotaxis observed in our experiments, we used two different approaches. First, we directly measured ATP in supernatants from TRAIL-stimulated cells, but these did not contain detectable amounts of ATP (**Figure 3.16 b**). A caveat of this experiment may be that the concentrations of

ATP in the supernatants may be below the range of detection of the assay but might still be responsible for the chemotaxis seen in response to TRAIL stimulation. To control for this possibility, we added the nucleotide-degrading enzyme, apyrase, to supernatants from TRAIL-stimulated cells and assessed the effect of this on chemotaxis. Apyrase efficiently degraded exogenously added ATP (**Figure 3.17 b**), and resulted in potent inhibition of THP-1 chemotaxis towards this nucleotide (**Figure 3.17 c**). However, treatment of TRAIL supernatants with the same concentrations of apyrase did not reduce their chemotactic capacity (**Figure 3.17 c**). In addition, because previous experiments found that IAP antagonism could suppress TRAIL-induced chemokine production, we generated TRAIL-apoptotic supernatants treated in the presence of BV6. As **Figure 3.17 d** demonstrates, removal of IAPs resulted in a suppression of THP-1 chemotaxis. Collectively, these data suggest that apoptotic supernatants are chemotatic but this chemotaxis is ATP-independent (**Figure 3.17 c**). These results motivated us to identify the soluble factor(s) responsible for chemotaxis.

3.2.10 TRAIL-induced MCP-1 and IL-8 serve as 'find me' signals for apoptotic cells

The preceding experiments suggested that one or more TRAIL-induced chemokines, rather than ATP, was responsible for the chemotaxis observed. To identify the factor responsible, we used antibody-mediated depletion of specific chemokines from TRAIL-stimulated HeLa supernatants, followed by assessment of chemotactic activity. To validate that the depletion strategy worked, antibody-treated supernatants were analysed by ELISA to confirm that the specific cytokine in question was depleted (**Figure 3.18**). While TRAIL-stimulated HeLa cells produced multiple chemokines (**Figure 3.1**), depletion of MCP-1 significantly blocked THP-1 chemotaxis, while IL-8 depletion inhibited THP-1 chemotaxis to a lesser extent (**Figure 3.19 a, b**). In addition, supernatants from TRAIL stimulated cells generated over a timecourse induced potent chemotaxis of THP-1 cells, which correlates closely with the appearance of MCP-1 and IL-8 in the supernatant (**Figure 3.20 a, c, d**). Immunodepletion of MCP-1 from 6 and 10

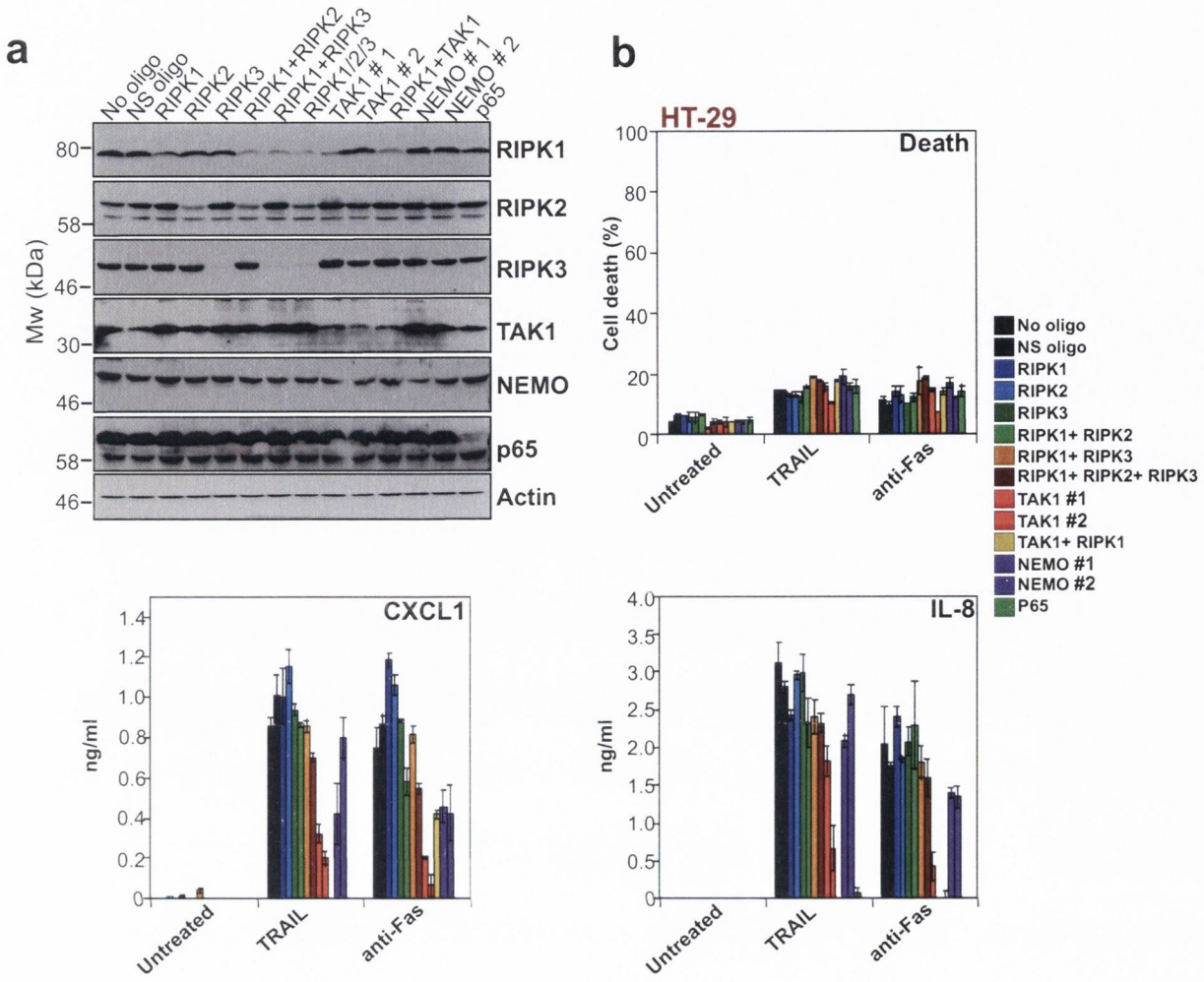


Figure 3.15 TRAIL/Fas-induced cytokines in HT-29 are independent of RIP kinases
a. HT-29 cells were nucleofected with indicated siRNAs (200 nM) and incubated for 48 h. Lysates were immunoblotted for the indicated proteins. **b.** Cells were then stimulated with TRAIL (50 ng/ml) and anti-Fas (CH-11) (100 ng/ml) and incubated for a further 24 h. Apoptosis was scored on cell morphology and was counted in triplicate fields of view. Cytokine concentrations in the supernatant were determined by ELISA.

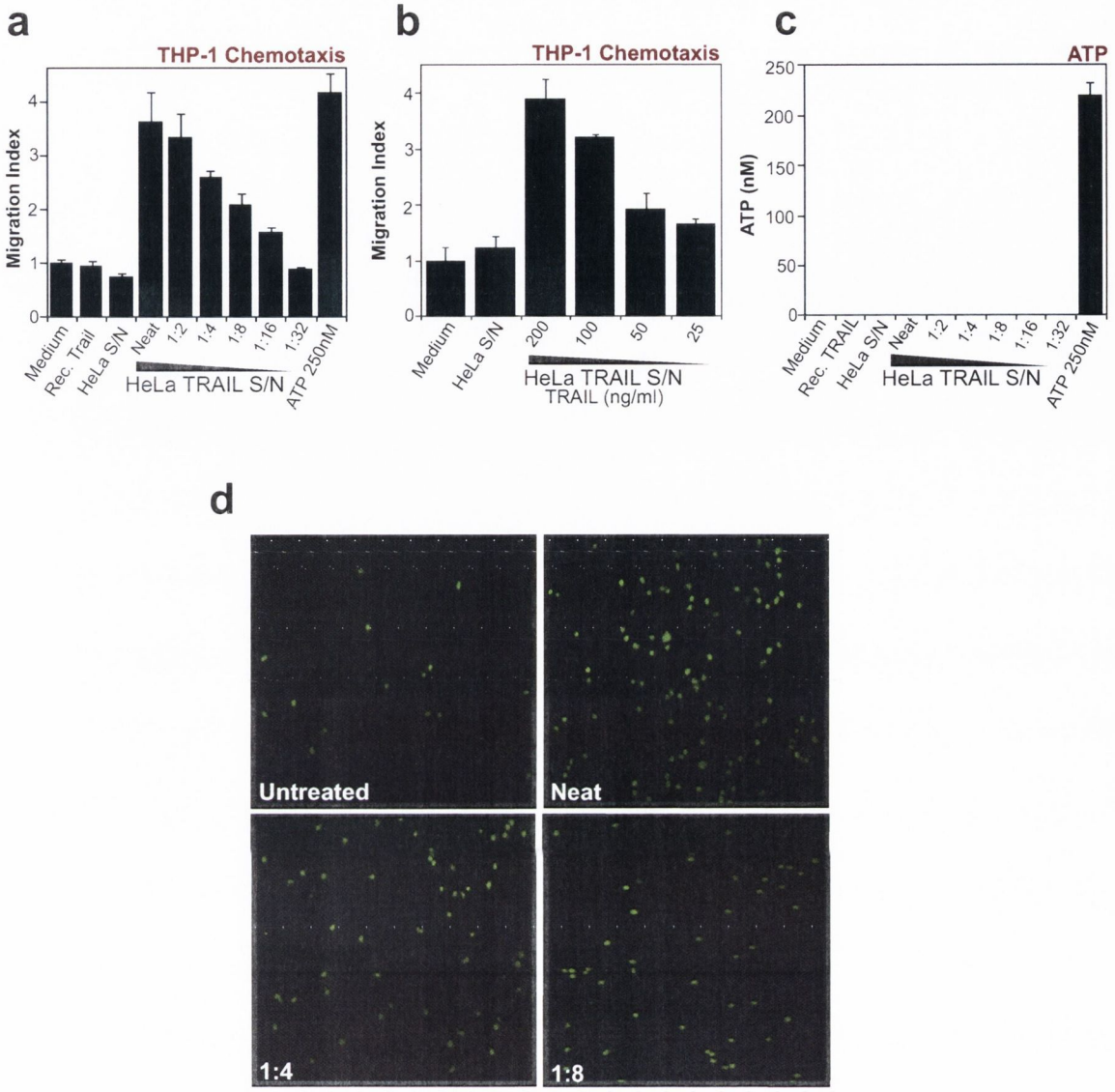


Figure 3.16 TRAIL-induced apoptosis elicits chemotaxis of THP-1 monocytes
a. HeLa Bcl-XL cells were stimulated with TRAIL (200 ng/ml) in RPMI, supplemented with 0.5 % FCS. After 24 h, culture supernatants were clarified by centrifugation and a chemotaxis assay was performed using the indicated dilutions of supernatant (S/N) from Fas-stimulated cells. THP-1 cells were used for the chemotaxis assay, separated from the cell supernatants by 8 µM nitrocellulose filters. Cells that had migrated into the bottom wells of the chemotaxis chambers were counted after 1-2 h and are expressed relative to the migration observed in the control wells. **b.** HeLa Bcl-XL cells were stimulated with a titration of TRAIL in RPMI, supplemented with 0.5 % FCS. After 24 h, culture supernatants were clarified by centrifugation and a chemotaxis assay was performed using the indicated dilutions of supernatant (S/N) from Fas-stimulated cells. Chemotaxis was preformed as in (a) **c.** ATP concentrations were determined by chemiluminescence from supernatants generated in (a). Results shown are representative of least three independent experiments. **d.** HeLa cells were treated as in (a) and a chemotaxis assay with THP-1 cells was performed except that THP-1 cells were labeled with the fluorescent dye CFSE to facilitate detection. CFSE-labeled THP-1 cells that had migrated into the bottom wells of the chemotaxis chamber from the experiment depicted in (A) were removed and photographed under UV microscopy. Error bars represent the mean ±SEM of triplicate cell counts from a representative experiment.

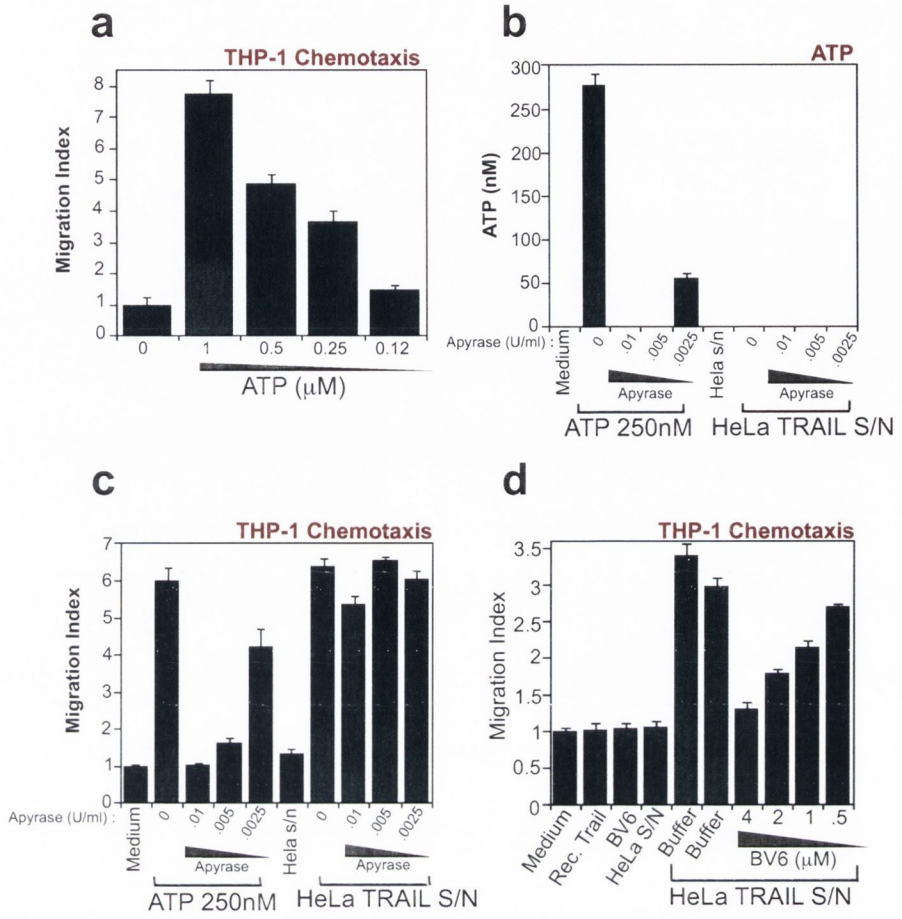


Figure 3.17 TRAIL-induced chemotaxis is ATP-independent

a. Exogenous ATP at indicated concentraions were used in a THP-1 chemotaxis assay. **b.** ATP or supernatants from TRAIL-treated HeLa were treated with the indicated concentrations of apyrase for 30 min, **c.** the resulting preparations were used in a THP-1 chemotaxis assay. Results shown are representative of least three independent experiments. **d.** HeLa were pretreated with IAP antagonist BV6 and zVAD-fmk (10 μM) for 1h prior to generation of TRAIL supernatants. THP-1 chemotaxis preformed as in (a). Results shown are representative of least three independent experiments. Error bars represent the mean ±SEM of triplicate cell counts from a representative experiment.

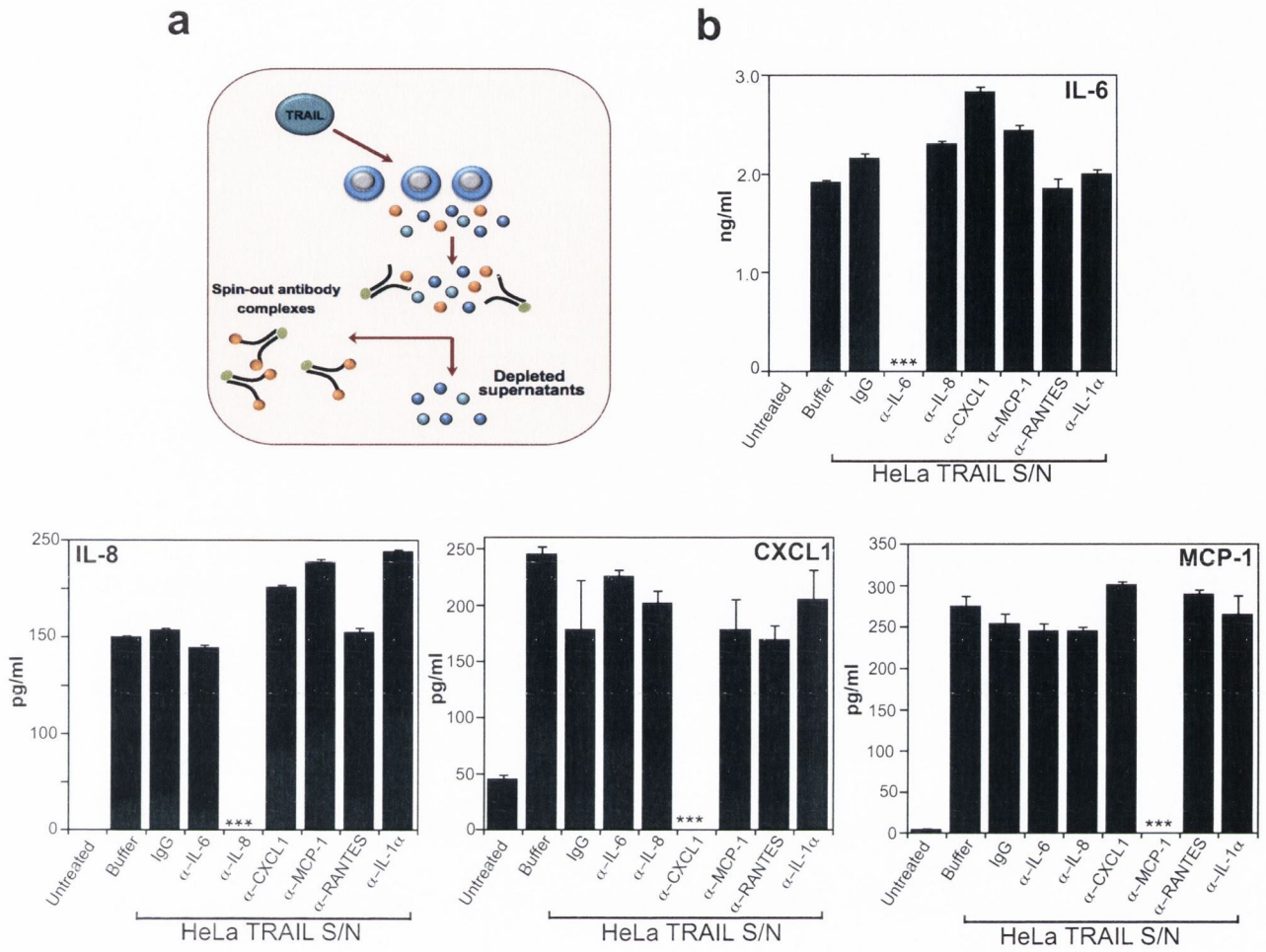


Figure 3.18 Depletion of specific cytokines and chemokines from apoptotic supernatants

a. Schmatic of the cytokine/chemokine depletion strategy using antibodies specific to each protein. **b.** HeLa Bcl-XL cells were either left untreated or were treated with TRAIL (200 ng/ml) in RPMI, supplemented with 0.5 % FCS. After 24 h, culture supernatants were depleted of indicated cytokines and chemokines.THP-1 chemotaxis assay was then performed with depleted supernatants.

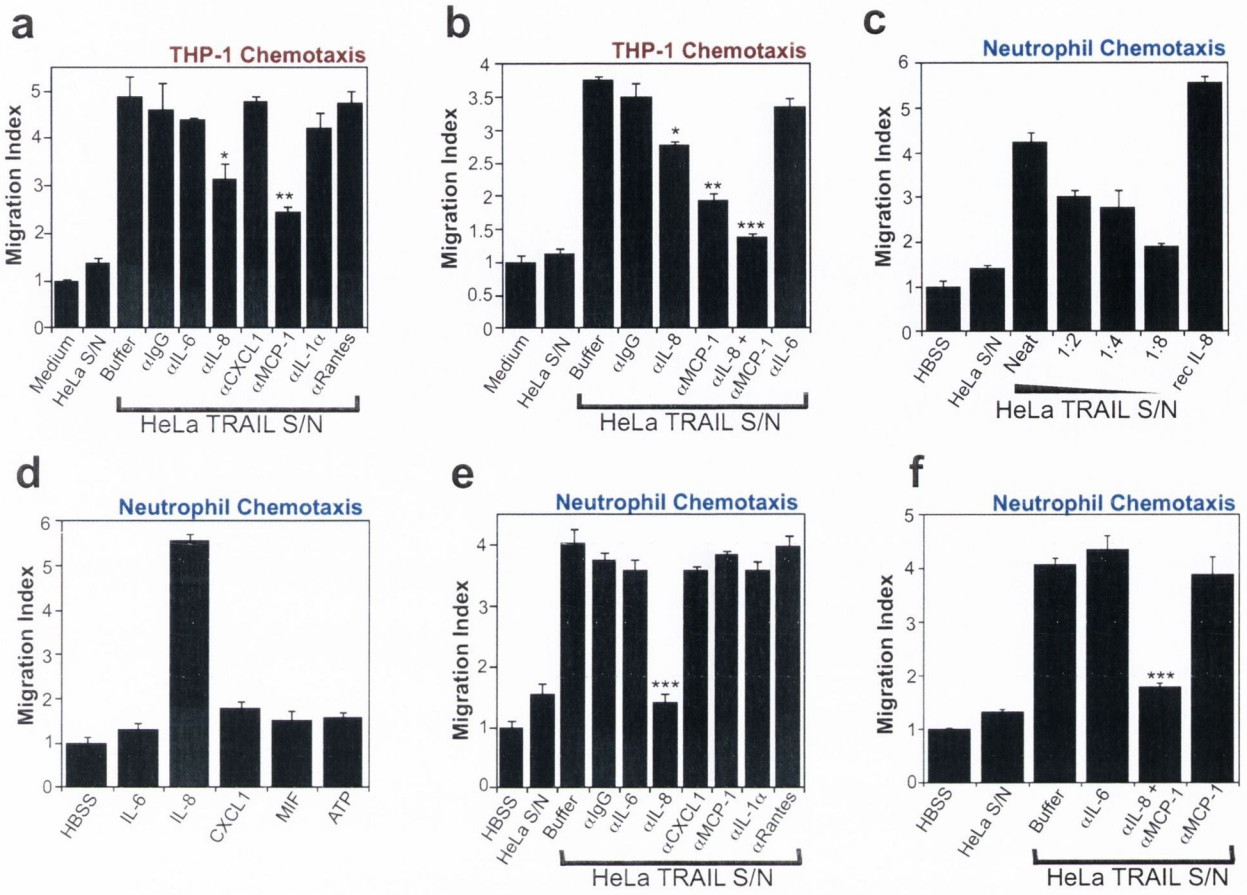


Figure 3.19 TRAIL-induced chemotaxis is dependent on chemokines IL-8 and MCP-1
a. HeLa Bcl-XL cells were stimulated with TRAIL (200 ng/ml) in RPMI, supplemented with 0.5 % FCS. After 24 h, culture supernatants were depleted of indicated cytokines and chemokines. THP-1 chemotaxis assay was then preformed with depleted supernatants. **b.** Neutrophil chemotaxis assay was then preformed with TRAIL treated supernatants. IL-8 (100ng/ml) served as a postitive control. **d.** Neutrophil chemotaxis assay was then preformed with indicated recombinant proteins IL-6 (100ng/ml), IL-8 (100ng/ml), CXCL1 (100ng/ml), MIF (100ng/ml), ATP (250nM). **e.** HeLa cells were either left untreated or were treated with TRAIL (200 ng/ml) in HBSS, supplemented with 0.5 % BSA. After 24 h, culture supernatants were depleted of indicated cytokines and chemokines. **f.** HeLa cells were either left untreated or were treated with TRAIL (200 ng/ml) in HBSS, supplemented with 0.5 % BSA. After 24 h, culture supernatants were double-depleted of indicated cytokines and chemokines. Neutrophil chemotaxis assay was then preformed with depleted supernatants. Results shown are representative of least three independent experiments. Error bars represent the mean ±SEM of triplicate cell counts from a representative experiment.

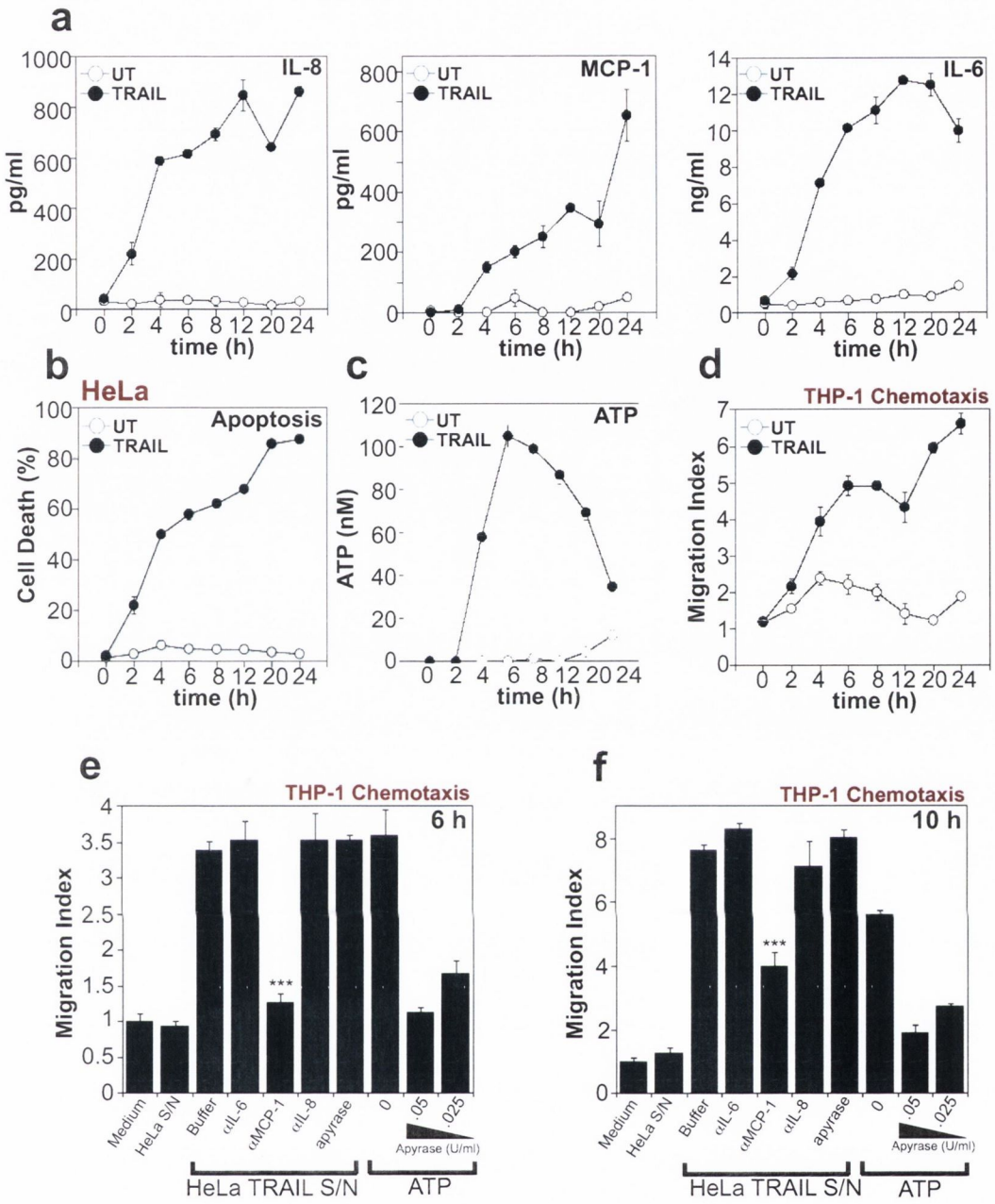


Figure 3.20 MCP-1 release from apoptotic cells promotes chemotaxis of THP-1 monocytes
a. HeLa cells were stimulated in the presence or absence with TRAIL (100 ng/ml) in RPMI, supplemented with 0.5 %FCS. At indicated timepoints culture supernatants were harvested. Cytokine concentrations in the supernatant were determined by ELISA. **b.** cell death were determined by annexin V/ PI staining. **c.** ATP concentrations were determined by chemiluminescence from harvested supernatants **d.** THP-1 chemotaxis assay was then preformed with supernatants. **e-f.** culture supernatants were depleted of indicated cytokines and chemokines at indicated timepoints. THP-1 chemotaxis assay was then preformed with depleted supernatants. Results shown are representative of least three independent experiments. Error bars represent the mean ±SEM of triplicate cell counts from a representative experiment.

hour supernatants significantly attenuated THP-1 chemotaxis (**Figure 3.20 e, f**). Following on from these experiments with THP-1 monocytes, we switched to a more physiological cell type, namely *ex vivo* primary human peripheral blood neutrophils, to explore whether these cells also migrated towards MCP-1 and/or IL-8 within TRAIL-stimulated cell supernatants. As **Figure 3.19 c, e** illustrates, these experiments revealed that IL-8 was essential for migration of human neutrophils towards supernatants derived from TRAIL-stimulated cells. In addition, neutrophils also migrated towards recombinant IL-8 but not to other chemokines such as CXCL1 and MCP-1 (**Figure 3.19 d)**. It is also important to note that neutrophils did not migrate towards 250nM exogenous ATP, a concentration that induces potent chemotaxis of THP-1 cells (**Figure 3.19 d, Figure 3.17 a**).

Collectively, these results demonstrate that TRAIL-induced apoptosis is associated with production of several pro-inflammatory factors, a subset of which can trigger chemotaxis towards dying cells (**Figure 3.19, Figure 3.20**). Thus, conventional chemokines, such as MCP-1 and IL-8, may serve as 'find me' signals for apoptotic cells.

3.3 Discussion

3.3.1 TRAIL is a pro-inflammatory molecule

In this chapter we have shown that engagement of the TRAIL receptor complex can activate a pro-inflammatory programme, resulting in the expression and secretion of multiple cytokines and chemokines that runs in parallel with the events leading to cell death. TRAIL-induced production of cytokines and chemokines was critically dependent on caspase-8 and FADD. In addition, we provide data to support a role for RIPK1, TAK1, cFLIP and IAPs as additional components of the TRAIL inflammatory signalling complex. Downstream kinase signalling pathways such as NFκ-B and p38/MAPK also contribute to death receptor-induced cytokine production. Cells dying in response to TRAIL stimulation produced several chemokines (MCP-1, IL-8, and CXCL1), some of which promoted chemotaxis of phagocytes towards the source of these factors in an *in vitro* setting.

3.3.2 TRAIL-induced chemokines as potential 'find-me' signals for apoptotic cells

Previous studies have suggested that apoptotic cells release 'find me' signals that promote chemotaxis of phagocytic cells towards dying cells (Gregory & Pound, 2011; Ravichandran, 2011). These include ATP, fractalkine, lysophosphatiylcholine, EMAPII and sphingosine-1-phosphate (Kao et al., 1994, Lauber et al., 2003; Truman et al., 2008; Gude et al., 2008, Elliott et al., 2009). A recent study by Elliott and colleagues demonstrated that Fas-induced cell death was associated with efflux of ATP and UTP via caspase-3/-7-mediated opening of pannexin 1 membrane channels, with these factors serving as 'find me' signals for monocytes in this context (Chekeni et al., 2010). We did observe a transient ATP release in response to TRAIL-stimulation under our experimental conditions, however addition of apyrase failed to attenuate chemotaxis towards supernatants from TRAIL-stimulated cells. Instead, depletion of MCP-1 and IL-8 potently inhibited TRAIL-induced chemotaxis towards monocytic cells and neutrophils,

respectively, implicating these molecules as potential 'find-me signals'. Additionally, we found that exogenously added ATP did not induce chemotaxis of human neutrophils even at concentrations that were potently chemotatic for THP-1 cells.

Interestingly, It has been reported by others that while ATP can promote monocyte chemotaxis, ATP by itself is not a chemoattractant (Chen et al., 2006, Corriden et al., 2008 Isfort et al., 2011). In a 2006 study, Chen and colleagues found that ATP release by neutrophils in response to chemotatic signals like IL-8 or formyl-methionine-leucine-phenylalanine-peptide (FMLP), facilitates gradient sensing by activating multiple P2Y2 receptors in an autocrine/paracrine manner, which controls cell orientation in an existing chemotatic gradient. Interestingly, incubation of apyrase with neutrophils was sufficient to prevent chemotaxis of neutrophils towards FMLP in chemotaxis assays, suggesting that neutrophil-derived ATP is necessary for chemotaxis. Furthermore, chemotaxis of neutrophils was dramatically attenuated using general inhibitors of P2-receptors (P2X and P2Y receptors) and A3 receptors, suramin and MRS 1191. Also, neutrophil chemotaxis from *A3*$^{-/-}$ and *P2Y2*$^{-/-}$ mice was also attenuated compared with wild-type littermates (Chen et al., 2006). Thus, Elliott and colleagues observation in *P2Y2*$^{-/-}$ mice, of attenuated macrophage/neutrophil migration towards apoptotic supernatants, could be interpreted as simply a failure of macrophages/neutrophils to migrate efficiently towards any chemotactic stimulus, rather than specific requirement of the P2Y2 receptor in sensing ATP release from dying cells. Additionally, upon release *in vivo*, ATP is rapidly degraded to AMP and ADP (~5-10 min) by neutrophil-derived ecto-nucleotide hydrolases such as E-NTPDase1 (Corriden et al., 2008). The authors of this study also provide evidence that hydrolysis of ATP to AMP/adenosine is critical for neutrophil chemotaxis (Corriden et al., 2008). This rapid extracellular hydrolysis of ATP by a family of ecto-nucleotide hydrolases may potentially limit ATP extracellular range as a 'find-me' signal for dying cells (Yegutkin et al., 2008, Isfort et al., 2011). Thus, the proposed model of ATP as a chemoattractant released by dying cells is a controversial one. A cell type used by Ravichandran and colleagues is the

Jurkat T-cell line. In agreement with these authors, our laboratory has found that Jurkat cells release ATP in response to Fas stimulation over a timecourse, however we did not observe any significant THP-1 migration in response to these apoptotic supernatants. Furthermore, Jurkat cells did not produce chemokines such as IL-8 and MCP-1 (Cullen et al., 2013). We hypothesize that in a context where cells are dying in response to TRAIL or Fas and producing conventional chemokines, these will be the dominant 'find-me' signals that coordinate the chemotaxis of phagocytic cells. Nonetheless, ATP efflux may serve as a 'find-me' signal for apoptotic cells in contexts where dying cells fail to make chemokines and where the extracellular concentration of ATP is above a threshold to form a stable chemotatic gradient.

3.3.3 Key components of the TRAIL inflammatory signalling complex

A consistent and striking finding was the absolute requirement for caspase-8 and FADD for TRAIL and Fas-induced inflammatory signalling. The idea that caspase-8 is a key modulator of inflammation is an idea that has received a lot of experimental validation in recent years. For example, Wallach and colleagues find that mice with conditional knockout of caspase-8 in the skin develop a severe inflammatory condition dependent upon hyperactivation of the RIG-I-RIPK1 complex. The authors demonstrate that caspase-8 is the critical enzyme that typically keeps this inflammatory complex in check through proteolysis and inactivation of RIPK1 (Kovalenko et al., 2009). Caspase-8 and FADD have also been implicated in another form of cell death, necroptosis, for which these molecules act to prevent the assembly of a RIPK3-MLKL complex necessary for necroptosis (Green et al., 2011). Here, we identify caspase-8 and FADD as critical components of TRAIL induced inflammatory signalling. Loss of these molecules completely suppressed TRAIL- and Fas-induced cytokines. A striking and unexpected finding was that caspase-8 and FADD were also necessary for cytokine production in HT-29 cells that were completely refractory to TRAIL-induced cytotoxicity. These findings are in agreement with our earlier data where we find that in the presence of zVAD-FMK, HeLa still respond to TRAIL by

making cytokines and chemokines. Thus, these data suggest that the enzymatic activity of caspase-8 is not required for inflammatory signalling but is required for cell death. This dependency for inflammatory signalling on caspase-8 and FADD suggests these molecules acts as molecular 'scaffolds' to recruit additional components necessary for signalling. Indeed, we find that molecules such as TAK1, RIPK1, and IAPs are capable of modulating cytokine production in this context. Recent studies have shown that RIPK1-mediated signalling is enhanced through cIAP-1 and cIAP-2-dependent ubiquitination of RIPK1 (Dynek et al., 2010), which promotes recruitment of the LUBAC signalling complex required for optimal RIPK1-dependent signal transduction (Haas et al., 2009). Consistent with a role for IAP dependent ubiquitination in TRAIL signalling, we have also found that interfering with IAP function using a small molecule IAP antagonist (BV6) attenuates TRAIL-induced production of IL-8 and CXCL1. Moreover, supernatants derived from TRAIL-stimulated cells that were treated with BV6 elicited less potent chemotaxis compared to supernatants from the same cells treated with TRAIL alone. A number of reports have also suggested that RIPK1 is recruited to the TRAIL-receptor complex and is required for optimal signal transduction (Varfolomeev et al., 2005, Jin et al., 2006, Kavuir et al., 2011; Cullen et al., 2013). In agreement with these studies we found that knockdown of RIPK1 in HeLa cells attenuated TRAIL- and Fas-induced production of IL-8 and CXCL1, however in HT-29, the removal of RIPK1 did not inhibit chemokine production. Furthermore, related molecules such as RIPK2 and RIPK3 did not modulate death-receptor induced cytokines in HT-29. This cell type specificity for RIPK1 in modulating TRAIL-indcued cytokines has been hinted at in the literature with Lin and colleagues finding that TRAIL-induced NF-κB activation depends on RIPK1, however both RIPK1 and TRAF2 were required for optimal TRAIL-mediated JNK activation (Lin et al., 2000). Another study found that knockdown of RIPK1 does not influence TRAIL-induced JNK activation, whereas p38 MAPK and NF-κB signalling were inhibited (Varfolomeev et al., 2005). RIPK1 is the major target for ubiquitination (both K63-pUb and M1-pUb linkages) in TNF signalling, however it is still somewhat obscure what the major targets of ubiquitination are in TRAIL

and Fas signalling. While our laboratory and others have demonstrated that RIPK1 is ubiquinitated at the Fas receptor (Cullen et al., 2013; Kavuri et al., 2011), it is not clear whether it is the only target of ubiquitination. It is highly likely that additional ubiquitination substrates exist at TRAIL and Fas receptor complexes, with caspase-8 and FADD as leading candidates.

3.3.4 Implications of TRAIL-induced cytokines and chemokines

Previous studies have also implicated TRAIL receptor stimulation as a trigger for non-apoptotic signalling pathways and the production of chemokines and cytokines from diverse cell types (Varfolomeev et al., 2005, Jin et al., 2006, Berg et al., 2009, Kavuri et al., 2011). While these studies have implicated TRAIL ligand as a modulator of pro-inflammatory cascades in multiple settings to promote outcomes such as cell survival, proliferation, migration and invasion, the implication arising from TRAIL stimulation, in terms of the broad range of cytokines and chemokines produced, and their significance in the context of apoptotic cell clearance has not previously been appreciated or explored. The role of inflammation in the initiation and subsequent progression of cancer is an area of reseach that has yielded some fascinating findings that implicate the collaboration of the immune system in certain tumor settings. The phenomenon of 'smouldering inflammation' to describe many solid tumors is an apt one, with a substantial part of the mass of a tumor being comprised of cellular infiltrates from the immune system. While this phenomenon has been known to pathologists for decades, tumor-associated immune cells and the implications for cancer biology has remained obscure until recently. Recruitment of cells of the immune system can provide a tumor with much needed support to facilitate further progression. For example, KRAS-postive tumors secrete GM-CSF that can promote the development of MDSCs. These MDSCs are capable of suppressing the cytotoxic potential of CD8 and NK cells, thus providing the tumor with the opportunity to develop with miminal interference from the tumor killing capacity of cytotoxic immune cells (Pylayeva-Gupta et al., 2012).

Cancer cells are highly evolved cells that have discarded and/or re-wired many of the fail-safe mechanisms that serve to prevent cancer from emerging. Malignant cells must undergo an extreme selection process, enabled by mutation, to attain immortality. The paradoxical findings that many tumor types, in particular colon, pancreatic and neural-derived tumors, overexpress Fas and TRAIL receptors is one that until recently has been without an easy explanation. The recent findings that both Fas and TRAIL, much like TNF, are capable of driving pro-inflammatory signalling may begin to explain the potential benefit of tumors to select for expression of these receptors. As we have demonstrated here, tumor cells that are refractory to TRAIL cytotoxicity still respond to TRAIL stimulation by producing inflammatory cytokines. This observation is intriguing and may suggest why tumors select for these receptors.

Here we have shown that TRAIL-induced cell death is an immunologically active process where secreted factors can communicate to immune cells. Recent studies from Kroemer and colleagues have also suggested that certain chemotherapeutic drugs, particularly those belonging to the anthracyclin family, may also trigger a form of apoptosis that elicits immune activation termed 'immunogenic cell death' (Casares et al., 2005, Obeid et al., 2006, Obeid et al., 2007). Anthracyclin-induced surface exposure of the ER chaperone, calreticulin was implicated as the main trigger of immune infiltration of tumors. How calreticulin initiates an immune response to tumors remains unclear. It is worth noting that in these studies, the role of cytokines and chemokines released by the tumor cells was not explored or even considered. Going forward, it will be important to determine whether apoptosis induced by these anthracyclins is also associated with the production of particular chemokines or other chemotactic factors. Thus, the production of pro-inflammatory cytokines and chemokines by tumor cells dying in response to certain classes of cytotoxic drugs may be responsible for conferring 'immunogenic cell death' in tumor cells.

In conclusion, we have demonstrated that cells dying in response to TRAIL receptor stimulation express and release multiple cytokines and chemokines, a subset of which attract the attentions of phagocytic cells. Thus, contrary to the

classical view that apoptotic cells are immunologically silent, certain pro-apoptotic signals, in particular TRAIL and Fas, may orchestrate the production of chemokines from dying cell that coordinate the efficient removal of dying cells through acting as 'find me' signals for such cells.

Chapter 4

Identification and characterization of IL-36 activating enzymes

4.1 Introduction

IL-1 family cytokines, which include the recently described IL-36α, β and γ proteins, play major roles as initiators of inflammation and are frequently among the first cytokines produced in response to infection or injury (Kono & Rock, 2008; Sims & Smith, 2010; Lukens et al., 2012). IL-1 family cytokines are capable of triggering complex cascades of additional cytokine production from diverse cells types, such as resident tissue macrophages and dendritic cells, as well as keratinocytes and endothelial cells lining local blood vessels (Towne et al., 2004; Martin et al., 2009; Dinarello, 2009; Vigne et al., 2011; Milovanovic et al., 2012; Vige et al., 2012; Debets et al., 2001). IL-36α, IL-36β and IL-36γ are encoded by distinct genes and evidence is rapidly accumulating to suggest that these cytokines play a key role in skin inflammation, particularly in psoriasis (Blumberg et al., 2007; Blumberg et al., 2010; Johnston et al., 2011; Tortola et al., 2012; Towne & Sims, 2012; Marrakchi et al., 2011; Farooq et al., 2013; Frey et al., 2013). Individuals that carry hypomorphic mutations in the IL-36RA display a severe and highly debilitating form of psoriasis called generalized pustular psoriasis (Marrakchi et al., 2011; Farooq et al., 2013; Onoufriadis et al., 2011; Kanazawa et al., 2013). This suggests that deregulated IL-36 cytokine signalling is sufficient to drive aggressive skin inflammation and also that IL-36 is an important barrier cytokine. Moreover, analysis of IL-36 mRNA expression in skin biopsies from individuals with the most common form of psoriasis, psoriasis vulgaris, found dramatically elevated expression (100-fold) of all three IL-36 transcripts compared with non-lesional skin from the same individuals, or non-affected controls (Johnston et al., 2011). Consistent with the idea that elevated IL-36 activity is an initiating event in psoriasis, transgenic expression of IL-36α in the mouse leads to a psoriasis-like condition at birth that can be further exacerbated with the skin irritant, phorbol acetate (Blumberg et al., 2007; Blumberg et al., 2010). Application of a TLR7 agonist (imiquomod) to the skin in humans and mice can provoke psoriasis outbreaks (Wu et al., 2004), which are increased in severity in *IL-36RA*$^{-/-}$ mice (Tortola et al., 2012). Furthermore, imiquomod-induced psoriasis in mouse models is completely abolished on an *IL-*

36R$^{-/-}$ background (Tortola et al., 2012). Finally, transplantation of human psoriatic lesions onto immunodeficient (SCID) mice produces a psoriasis-like condition that is greatly improved through blocking the IL-36 receptor (Blumberg et al., 2010).

IL-36α, IL-36β and IL-36γ are all generated as leaderless cytokines that lack biological activity (Towne et al., 2004; Towne et al., 2011). Thus, proteolytic processing of IL-36 proteins is required to unleash the pro-inflammatory potential of these cytokines, similar to other members of the IL-1 family, such as IL-1β and IL-18. Sims and colleagues have shown that removal of a small number of residues from the N-termini of IL-36α, IL-36β and IL-36γ increases their biological activity by greater than 10,000-fold (Towne et al., 2011). Because IL-36 cytokines appear to play a key role as initiators of inflammation in the skin barrier, inhibitors of IL-36 processing activation are therefore likely to have considerable potential for the treatment of inflammatory skin conditions. However, the protease(s) responsible for activation of IL-36 proteins are currently unknown. Because psoriatic plaques are frequently associated with neutrophil infiltrates (Teru et al., 2000; Murphy et al., 2007; Nestle et al., 2009; Ikeda et al., 2013), we wondered whether proteases derived from neutrophils might be capable of processing and activating IL-36 cytokines.

In this chapter, we demonstrate that the neutrophil-derived proteases, cathepsin-G and elastase are IL-36 activating proteases. Futhermore, because of the established association of neutrophils and inflammatory skin conditions, this suggests that targeted inhibition of neutrophil proteases might have significant potential as inhibitors of IL-36 activation in skin conditions, such as psoriasis. We present data that utilize novel tri-/tetra-peptides as potent inhibitors of neutrophil proteases capable of preventing activation of IL-36 cytokines.

4.2 Results

4.2.1 Production of recombinant interleukin-36 ligands

In order to screen for proteases that may activate IL-36 proteins we first cloned all three human IL-36 genes, namely IL-36α/β/γ, into a bacterial expression vector pET45b. Clones were selected and sequence validated before expressing the individual proteins in BL21 bacteria. As **Figure 4.1 a** demonstrates, all three full-length proteins were highly soluble under standard induction conditions with yields typically in the range of >2-3mg per 250 ml of culture.

4.2.2 Production of artifically truncated interleukin-36 ligands: Activation upon caspase-3 proteolysis

Sims and colleagues have reported that artificial truncations of IL-36α, β and γ at particular N-terminal residues dramatically increase the activity of these proteins (Towne et al., 2011). We engineered modified forms of IL-36α, β and γ by inserting a caspase-3 cleavage motif, DEVD, proximal to the residues identified by Sims and colleagues (**Fig. 4.1 b**). Similar to full-length cytokines, all three DEVD-modified forms of IL-36 were highly soluble. To confirm that these DEVD-modified forms of IL-36 are sensitive to caspase-3 proteolysis, we titrated caspase-3 with all three cytokines and analysed proteolysis via immunoblot. As **Fig. 4.2 a, b, c** illustrates, DEVD-modified IL-36α (IL-36α^{DEVD}), DEVD-modified IL-36β (IL-36β^{DEVD}) and DEVD-modified IL-36γ (IL-36γ^{DEVD}) were readily processed by caspase-3, whereas IL-36α^{wt}, IL-36β^{wt} and IL-36γ^{wt} were not.

4.2.3 Establishment of an IL-36 bioactivity assay with truncated IL-36 ligands

Next, we established an *in vitro* assay whereby we could reliably screen for IL-36 biological activity. HeLa-vector or HeLa-IL-36R cell lines were generated by transfection with pCXN2 (Vector) or pCXN2-IL-1Rrp2 (IL-36R) plasmids followed by selection using the G418 antibiotic. Vector and IL-36R over-expressing clones

were expanded from single cells. 21 clones were selected for screening of acquired responsiveness to active forms of IL-36 via ELISA (**Figure 4.3 a, b**). From this screen we indentified clone 16 as an optimal responder and expanded this clone for use in future assays. Clone 16 was subsequently used to establish an NF-κB-SEAP reporter HeLa subline, as a readout for the activation of the NF-κB inflammatory signalling pathway (**Figure 4.3 c**). Upon stimulation with IL-36, cells activate NF-κB and release secreted alkaline phosphatase (SEAP) into the medium, which is collected and detected with a colorimetric substrate. Specifically, the HeLa-IL-36R-SEAP cell line was generated by transfection with pNifty2-SEAP plasmid followed by selection using zeocin antibiotic. Clones were expanded from a single cell and tested for SEAP production (**Figure 4.3 d**).

4.2.4 Proteolytic processing of DEVD-modified IL-36 confers biological activity

As discussed above, Sims and colleagues have reported that artificial truncation of IL-36α, β and γ at particular N-terminal residues dramatically increases the activity of these proteins (Towne et al., 2011). In a cell-based bioassay, $HeLa^{wt}$ cells failed to respond to either full length or caspase-3-cleaved IL-$36\alpha^{DEVD}$, IL-$36\beta^{DEVD}$, IL-$36\beta^{DEVD}$, while $HeLa^{IL\text{-}36R}$ cells secreted multiple cytokines in response to caspase-3-processed IL-36^{DEVD} proteins, but not full length unprocessed IL-36^{DEVD} proteins (**Fig. 4.4 a**). Similar data were obtained for DEVD-modified forms of IL-36β and IL-36γ (**Fig. 4.4 b, c**). Furthermore, the transformed keratinocyte cell line HaCat, which naturally expresses IL-36R, also responded to the caspase-3-cleaved IL-36^{DEVD} forms (**Fig. 4.5**). These data confirmed that proteolytic processing of IL-36α, β and γ dramatically increase the biological activity of these cytokines, and established a bioassay to screen for proteases that naturally process and activate IL-36 cytokines.

4.2.5 Neutrophil-derived proteases activate IL-36 cytokines

One of the hallmarks of psoriatic lesions is persistent infiltration of the epidermis by neutrophils (Teru et al., 2000; Murphy et al., 2007). Neutrophil

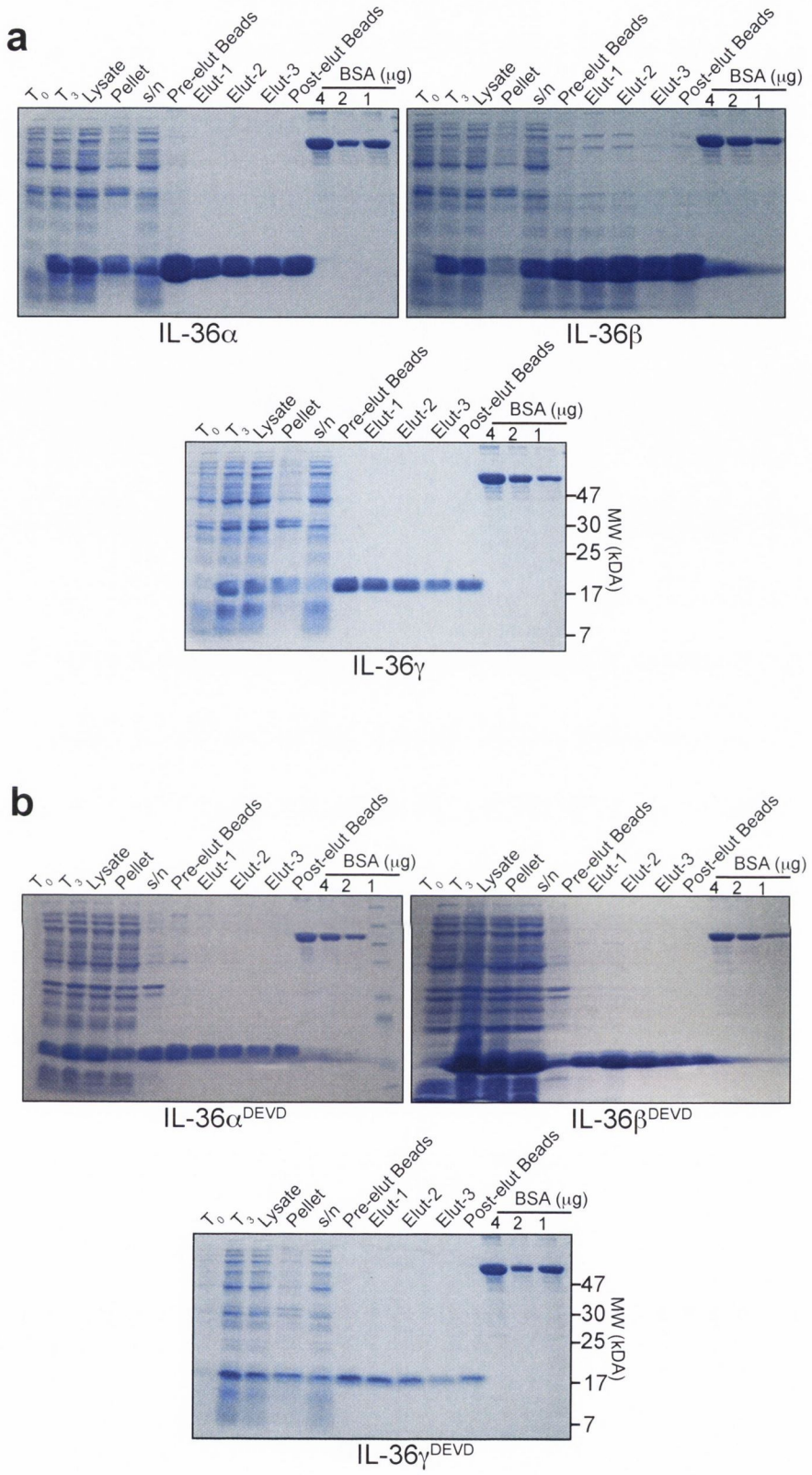


Figure 4.1 Recombinant IL-36 and DEVD-modified IL-36 expression and purification from bacteria

a. Full-length IL-36 expression was induced in *E.coli* BL21 by the addition of IPTG (600µM) for 3 h at 37°C. **b.** DEVD-modified IL-36 expression was induced in *E.coli* BL21 by the addition of IPTG (600µM) for 3 h at 37°C.

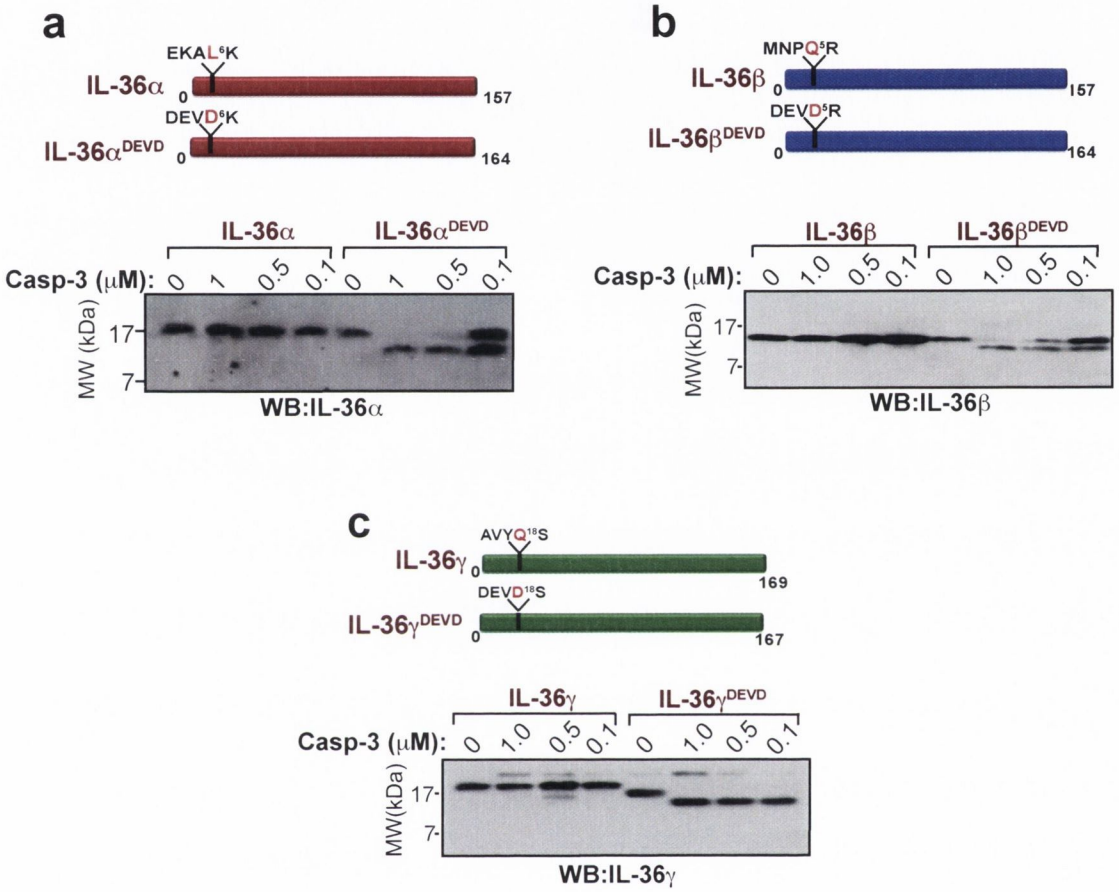


Figure 4.2 DEVD-modified IL-36 versions cleaved by caspase-3
(a-c). Schematic of modified forms of IL-36α, IL-36β and IL-36γ where a caspase-3-processing motif (DEVD) was inserted into the IL-36 sequence, N-terminal to the putative-processing sites. **b.** DEVD-modified IL-36 expression as in (a). IL-36α,β,γ and DEVD-IL-36α,β,γ were incubated at 37°C for 2 h, either alone or in the presence of indicated concentrations of recombinant caspase-3, followed by analysis by immunoblot

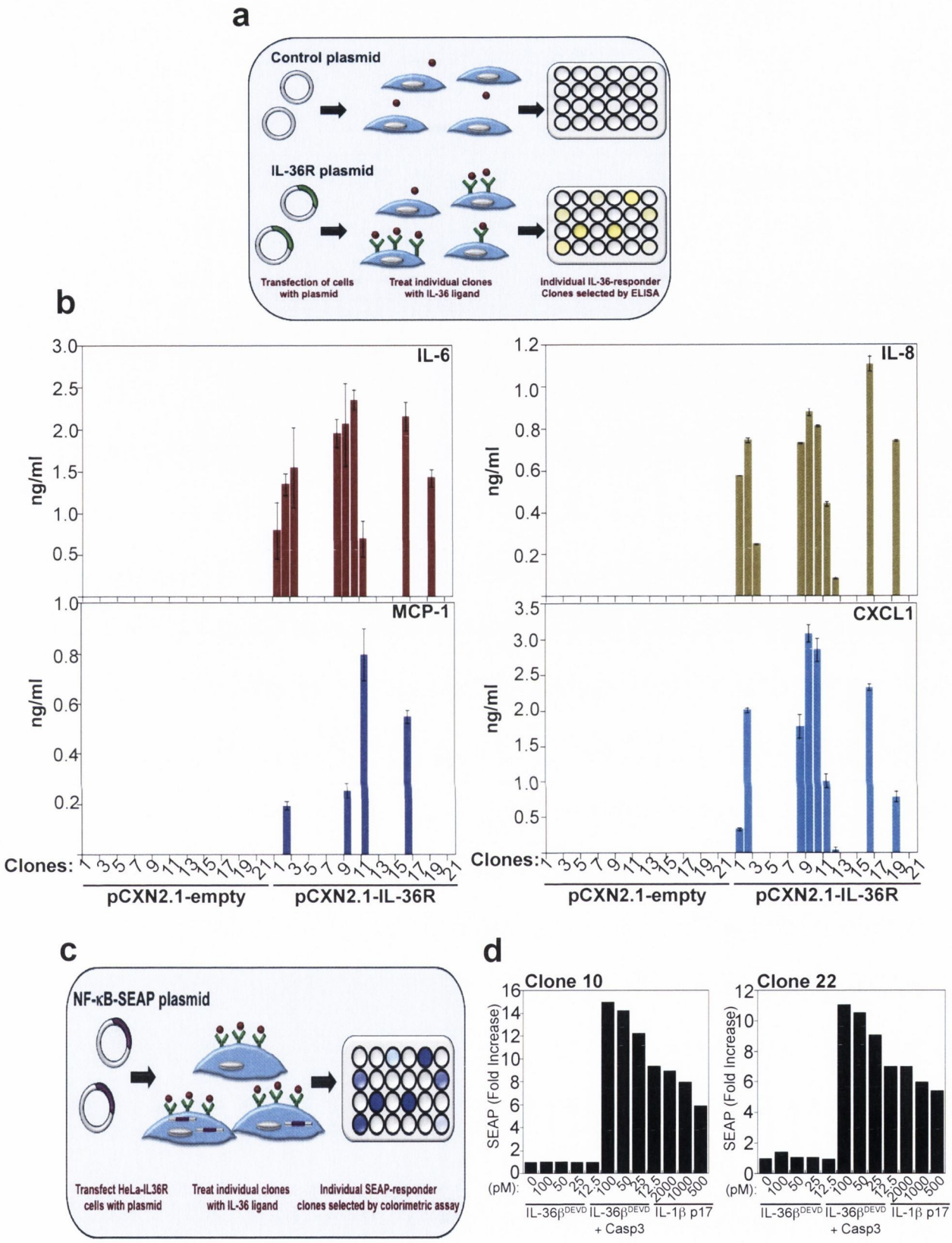


Figure 4.3 Establishment of HeLA$^{IL\text{-}36R}$ cell lines

a. HeLa-vector or HeLa-IL-36R cell lines were generated by transfection with 5 µg pCXN2.1 or pCXN2.1-IL-1Rrp2(IL-36R) plasmids followed by selection using G418 antibiotic (Sigma). IL-36R over-expressing clones were expanded from a single cell. **b.** Clones were selected by demonstration of acquired optimal responsiveness to IL-36γ^{DEVD}+Casp-3 (500pM) via ELISA. Supernatants were harvested at 24 h. **c.** HeLa-IL-36R-SEAP cell lines were generated by transfection with 5 µg pNiFty-SEAP plasmid followed by selection using Zeocin (Sigma). SEAP over-expressing clones were expanded from a single cell. **d.** Clones were selected by demonstration of optimal responsiveness to IL-36β^{DEVD}+/-Casp-3 and IL-1β p17 via QuantiBlue colorimetric assay. Supernatants were harvested at 24 h. (Danielle Clancy provided panel (**d**))

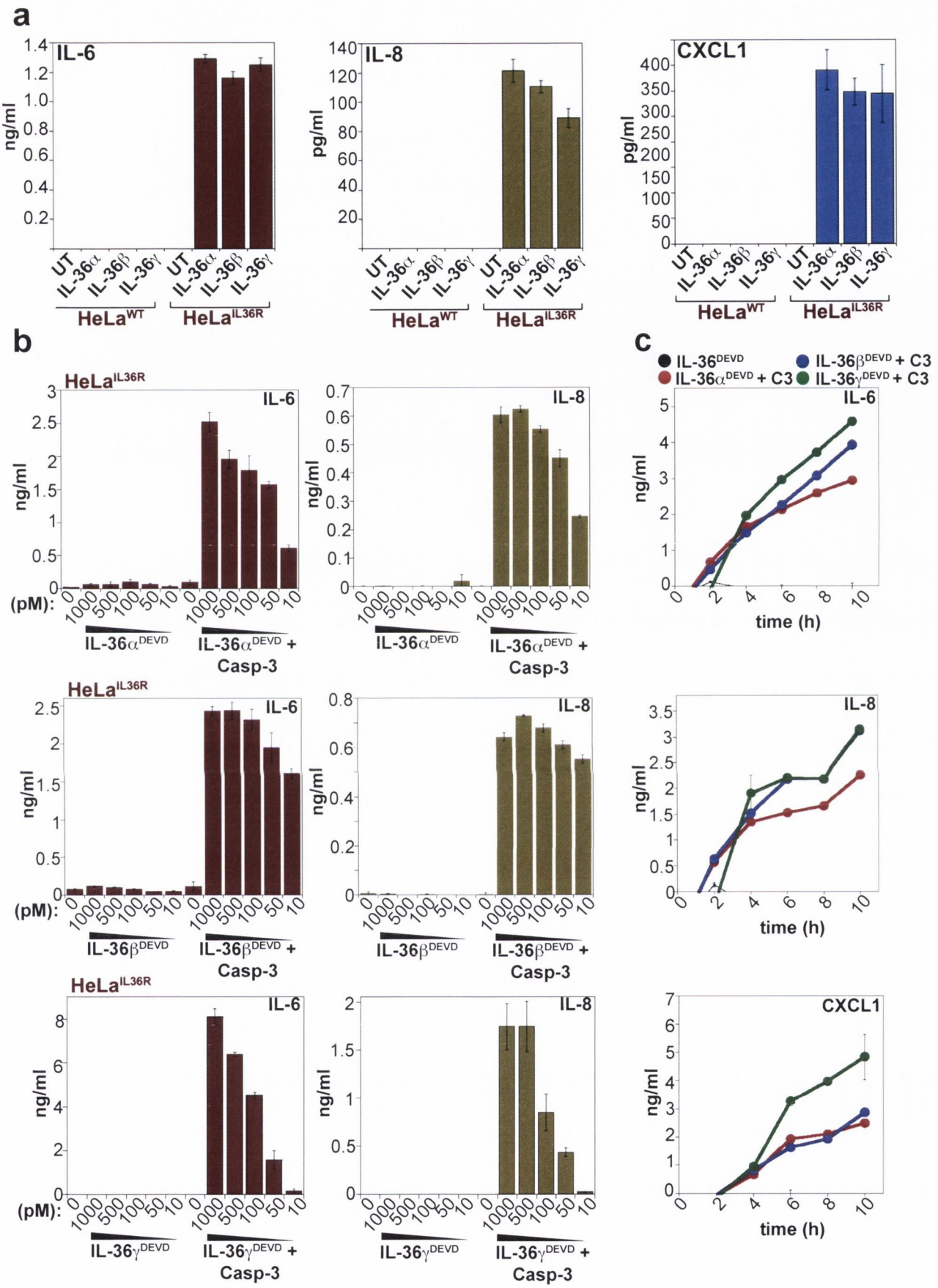


Figure 4.4 Proteolytic processing of DEVD-modified IL-36 releases biological activity
a. HeLa^{Vector} and HeLa^{IL36R} were stimulated with caspase-3 cleaved DEVD-IL36α, β and γ. After 24 h, cytokine concentrations in the culture supernatants were determined by ELISA. **b.** HeLa^{IL36R} were stimulated with full-length or caspase-3 cleaved DEVD-IL-36α, β and γ at the indicated concentrations. After 24 h, cytokine concentrations in the culture supernatants were determined by ELISA. **c.** HeLa^{IL36R} were stimulated with full-length or caspase-3 cleaved DEVD-IL-36α, β and γ over a timecourse. Cytokine concentrations in the culture supernatants were determined by ELISA.

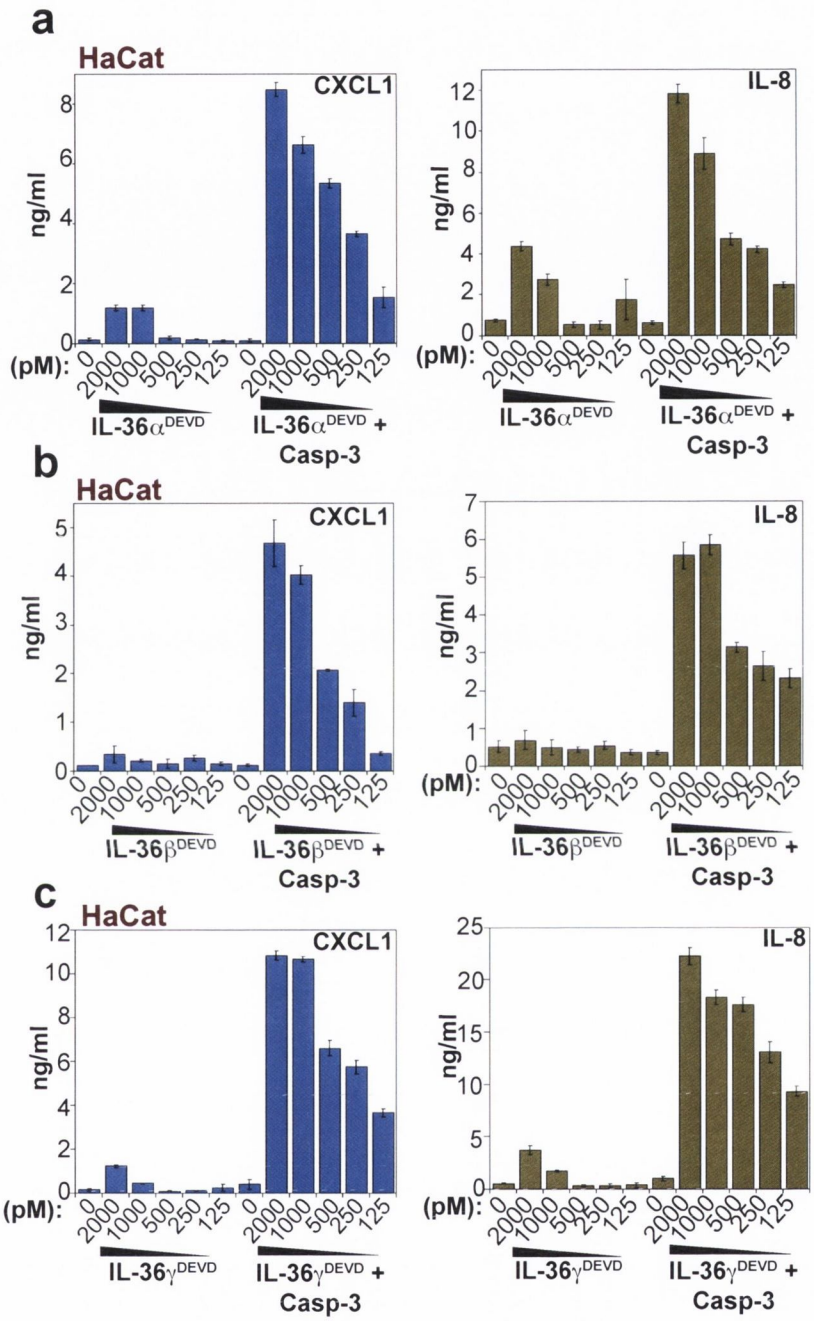


Figure 4.5 HaCat keratinocytes respond to DEVD-modified IL-36 cytokines (a-c). HaCat were stimulated with full-length or caspase-3 cleaved DEVD-IL-36α, β and γ at the indicated concentrations. After 24 h, cytokine concentrations in the culture supernatants were determined by ELISA.

azurophilic granules contain three major seine proteases (elastase, cathepsin-G and proteinase-3) that are involved in bacterial killing as well as in the processing of certain cytokines and chemokines (Kortmaz et al., 2010). Indeed, previous studies have found that neutrophil elastase can process and activate IL-1α (Afonina et al., 2011) and that cathepsin-G and elastase can activate IL-33 (Lefrançais et al., 2012). To explore whether neutrophil-derived proteases can process and activate IL-36 cytokines, we purified human peripheral blood neutrophils and induced degranulation with PMA (**Fig. 4.6 a, b**), thereby liberating granule proteases and generating reactive oxygen species (ROS) (Brinkmann et al., 2004). Robust ROS production and protease activity was found in supernatants from PMA-treated neutrophils, as expected (**Fig 4.6. c, d**). Purified full-length IL-36α, β and γ were then incubated with supernatants from untreated versus PMA-treated neutrophils, followed by assessment of IL-36 activity using $HeLa^{IL\text{-}36R}$ cells. As shown in **Fig. 4.6 e**, incubation of IL-36 cytokines in the presence of PMA-activated neutrophil degranulates resulted in robust activation of IL-36β and IL-36γ, whereas IL-36α was only weakly activated under the same conditions.

4.2.6 Identification of IL-36-activating proteases

To identify the nature of the protease(s) involved in IL-36 activation, we initially used a panel of broad-spectrum protease inhibitors. As **Figure 4.7** illustrates, the serine protease inhibitor PMSF robustly inhibited the activation of IL-36α, IL-36β and IL-36γ by neutrophil-derived proteases. A specific chemical inhibitor of cathepsin-G inhibited the activation of IL-36α and IL-36β whereas a specific chemical inhibitor of elastase inhibited the activation of IL-36γ by activated neutrophil degranulates.

4.2.7 Purified cathepsin-G and elastase activate IL-36 cytokines

We next compared the ability of purified cathepsin-G and elastase to process and activate IL-36 cytokines. The activity of all purified proteases employed was confirmed using synthetic substrate peptides (**Fig. 4.8 a**). As

Figure 4.8 b demonstrates, cathepsin-G selectively promoted IL-36β activation, whereas elastase preferentially activated IL-36γ. In contrast, IL-36α failed to be activated by either of these proteases (**Fig. 4.8 b**). Because caspase-1 processes and activates the IL-1 family cytokines, IL-1β and IL-18, we also explored whether caspase-1 or caspase-3 could process and activate IL-36 family cytokines. However, as **Figure 4.8 b** illustrates, neither caspase activated any of the IL-36 cytokines. To exclude the possibility that the concentrations of IL-36α we used in the above experiments were too low to detect biological activity, we also titrated IL-36 cytokines over a wide concentration range in the presence and absence of cathepsin-G and elastase. As **Figure 4.8 c** shows, once again cathepsin-G was found to preferentially activate IL-36β and elastase to preferentially activate IL-36γ, with cathepsin-G also exhibiting modest activation of IL-36γ at higher molar concentrations.

4.2.8 Depletion of IL-36 processing activity using a biotin-FLF-CMK peptide

To explore the identity of the IL-36 processing protease(s) further, we generated a biotin-conjugated form of the cathepsin-G synthetic substrate, biotin-FLF-CMK, to ask whether this depleted the IL-36β activating activity from neutrophil degranulates. As **Figure 4.9 a** illustrates, selective depletion of cathepsin-G activity from PMA-treated neutrophil degranulates using biotin-FLF-CMK largely eliminated activation of IL-36β but not of IL-36γ (**Fig. 4.9 b**). Furthermore, we exposed IL-36β and IL-36γ to purified neutrophil enzymes alone or in combination, and examined the effect of biotin-FLF-CMK. As **Figure 4.10** demonstrates, biotin-FLF-CMK selectively inhibited the activation of IL-36β mediated by both cathepsin-G and neutrophil degranulates but did not attenuate IL-36γ activation under the same conditions.

4.2.9 Design and functional validation of novel neutrophil protease inhibitors

Next, we designed a panel of peptides based upon optimal cathepsin-G and elastase cleavage motifs. The basic design of these peptides included a N-

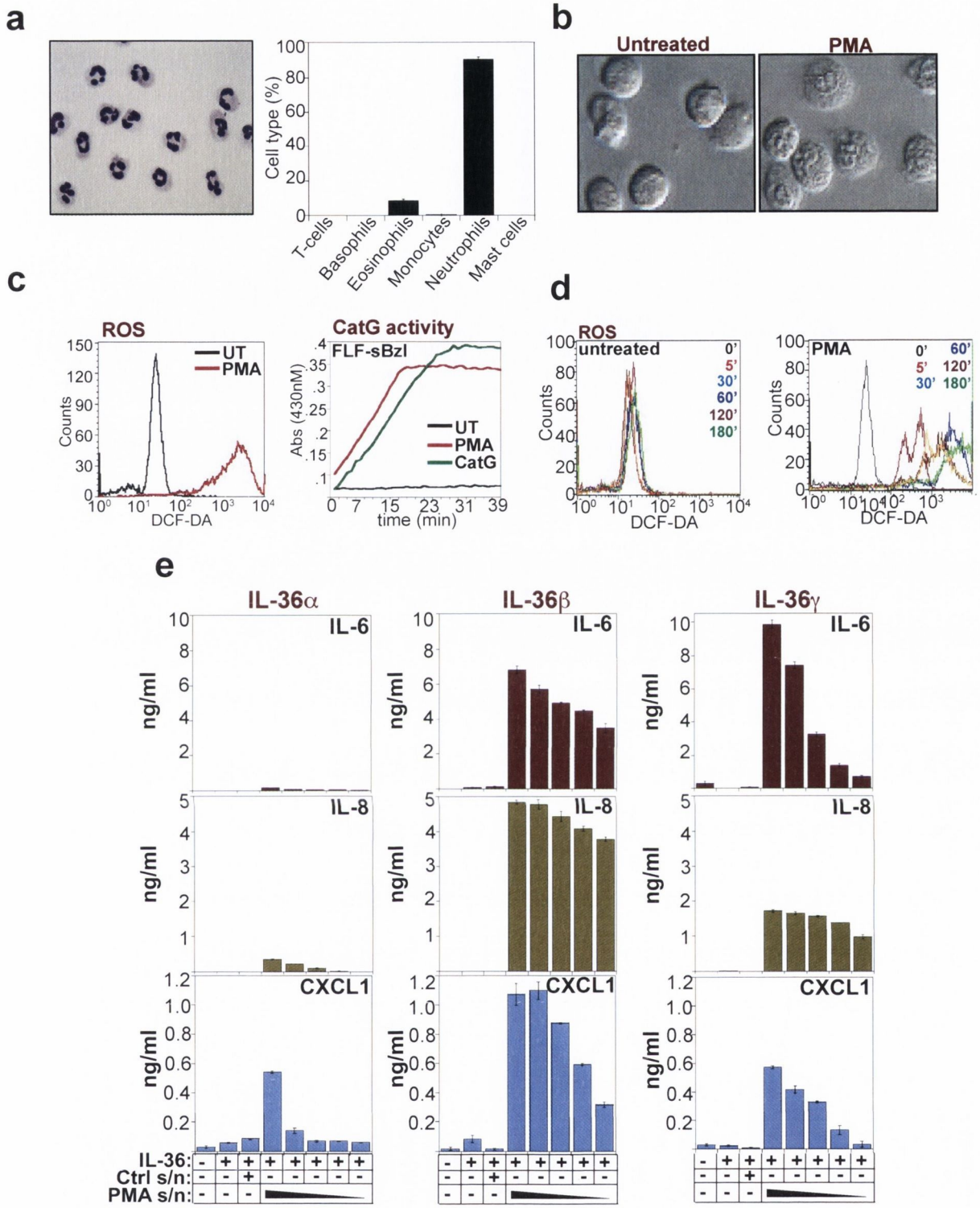


Figure 4.6 Neutrophil-derived proteases activate IL-36 cytokines

a. Phase contrast microscope image of purified blood-derived neutrophils and a quantification of immune cell types (triplicate fields-of-view counts) **b.** Primary human neutrophils were stimulated with PMA (50 nM) for 3 h. After 1 hr, cells were visualised by phase contrast microscopy. **c.** Primary human neutrophils stimulated with PMA as in (b). ROS-positive cells were measured via DCF-DA staining by flow cytometry (**c)** and cathepsin-G enzymatic activity was measured by suc-FLF-sBzl hydrolysis assay (**d**). **e.** HeLa^{IL36R} were stimulated with 500 pM IL36α, β and γ pre-incubated for 2 h at 37° with indicated dilutions of either control or PMA-activated degranulates. After 24 h, cytokine concentrations in culture supernatants were determined by ELISA.

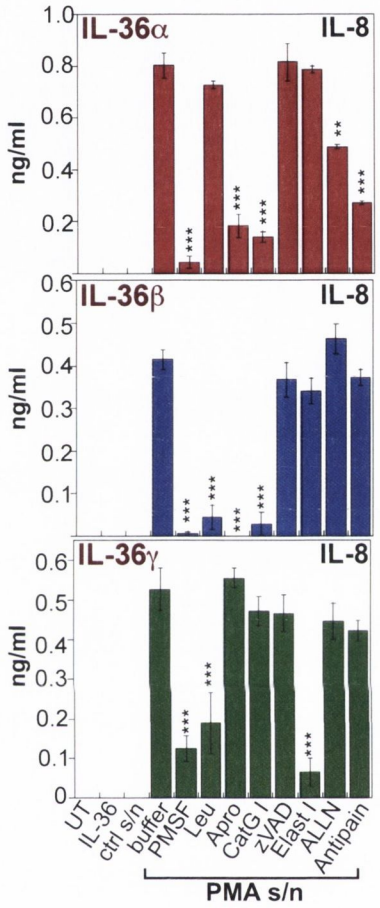


Figure 4.7 Inhibitor screen of IL-36 activation using neutrophil degranulates
HeLa^{IL36R} were stimulated with IL-36α (1 nM), IL36β (250 pM) or IL36γ (250 pM), pre-incubated for 2 h at 37° with neutrophil degranulates in the presence or absence of PMSF (1 mM), leupeptin (10 µg/ml), aprotinin (10 µg/ml), Cathepsin G inhibitor 1 (5 µM), zVAD-fmk (10 µM), Elastase Inhibitor IV (5 µM), ALLN (5 µM), antipain (100 µM). After 24 h, cytokine concentrations in culture supernatants were determined by ELISA. Asterisk(s) indicate significance levels, *** = $p < .0001$, ** = $p < .001$, * = $p < .1$, by Student's t test.

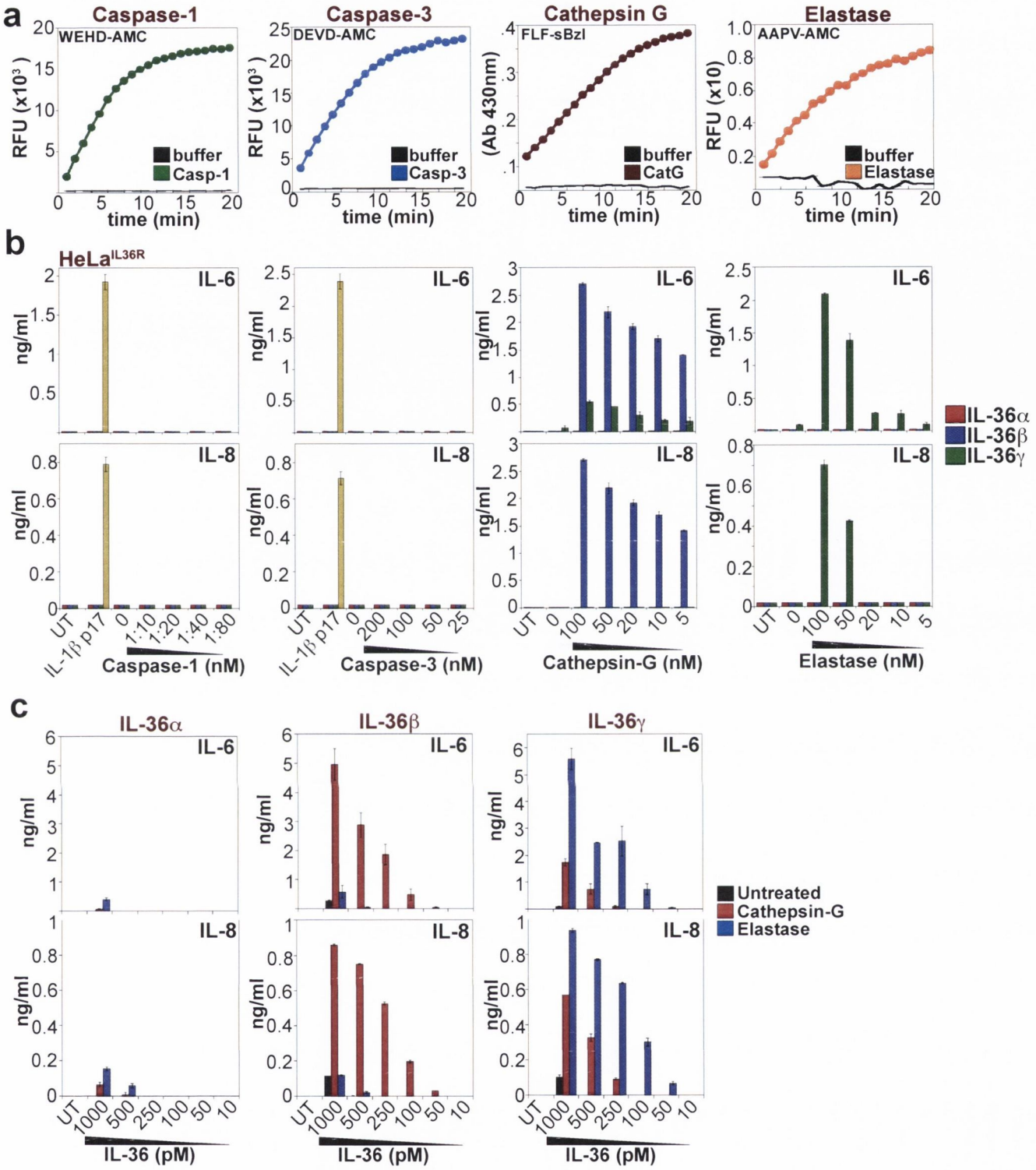


Figure 4.8 Identification of IL-36-activating proteases

a. Hydrolysis of synthetic substrates (WEHD-AMC, DEVD-AMC, FLF-sBzl, AAPV-AMC) by recombinant caspase-1 (1:20),-3 (400 nM), cathepsin-G (20 nM) and elastase (50 nM). **b.** HeLa^{IL36R} were stimulated with 500 pM IL36α, β and γ pre-incubated for 2 h at 37° with indicated concentrations of recombinant caspase-1,-3 or purified cathepsin-G and elastase. IL-1β p17 served as a positive control for caspase titrations. After 24 hr, cytokine concentrations in culture supernatants were determined by ELISA. **c.** HeLa^{IL36R} were stimulated with a titration of IL36α, β and γ pre-incubated for 2 hr at 37° with fixed concentrations of purified cathepsin-G (50 nM) and elastase (200 nM). After 24 hr, cytokine concentrations in culture supernatants were determined by ELISA.

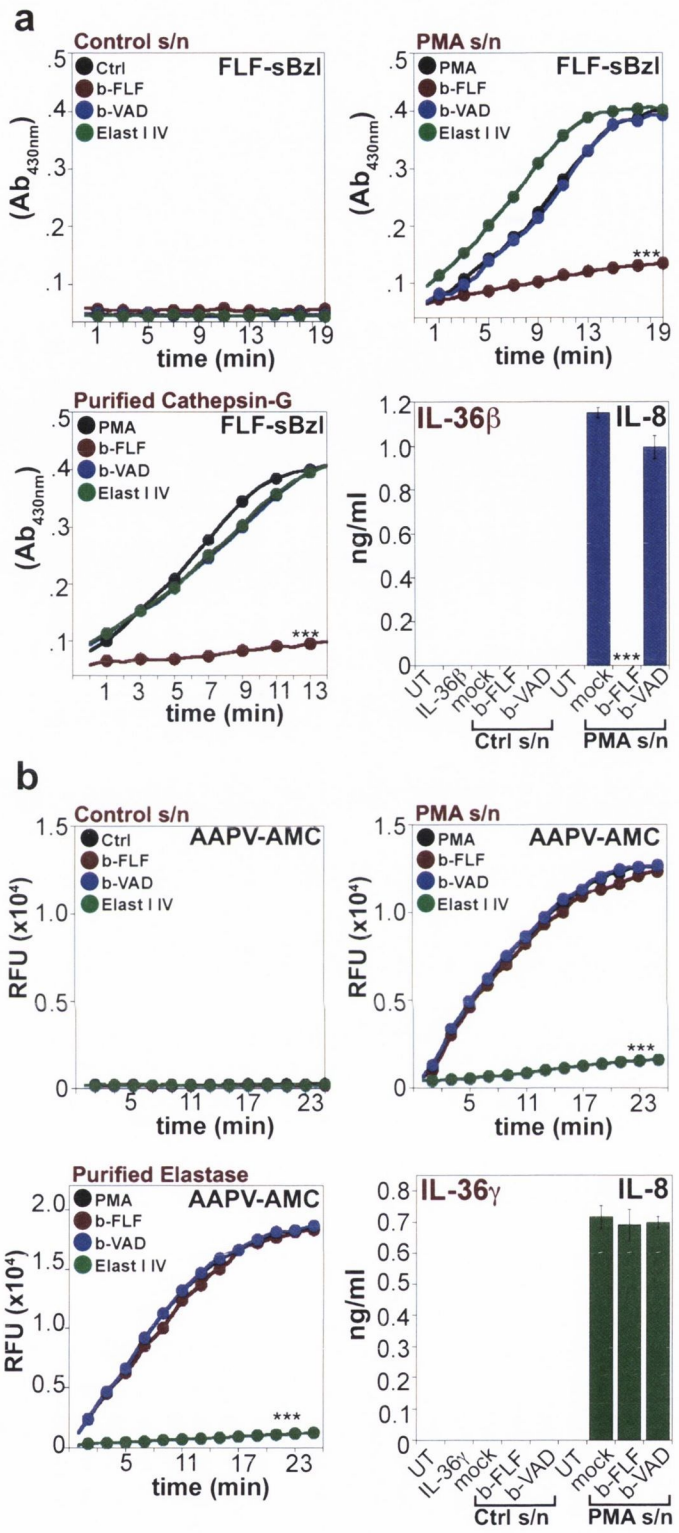


Figure 4.9 Selective depletion of neutrophil degranulates with biotin-tagged FLF-CMK pepetide specifically attenuates IL-36β activation

a. Control and PMA-activated neutrophil degranulates were pre-incubated with biotin-VAD-CMK (10 μM), biotin-FLF-CMK (10 μM) or Elastase Inhibitor IV (10 μM) for 30 min on ice followed by incubation with strepavidin agarose beads. Degranulates were subsequently assessed for cathepsin-G activity by FLF-sBzl hydrolysis assay (a) or elastase activity was assessed by AAPV-AMC hydrolysis (b). HeLa^{IL36R} were stimulated with IL36β (a) or IL36γ (b) pre-incubated for 2 h at 37° with mock, biotin-VAD-CMK (10 μM) or biotin-FLF-CMK (10 μM) treated degranulates. After 24 h, cytokine concentrations in culture supernatants were determined by ELISA. Results shown are representative of at least three independent experiments. Asterisk(s) indicate significance levels, *** = $p < .0001$, ** = $p < .001$, * = $p < .1$, by Student's t test.

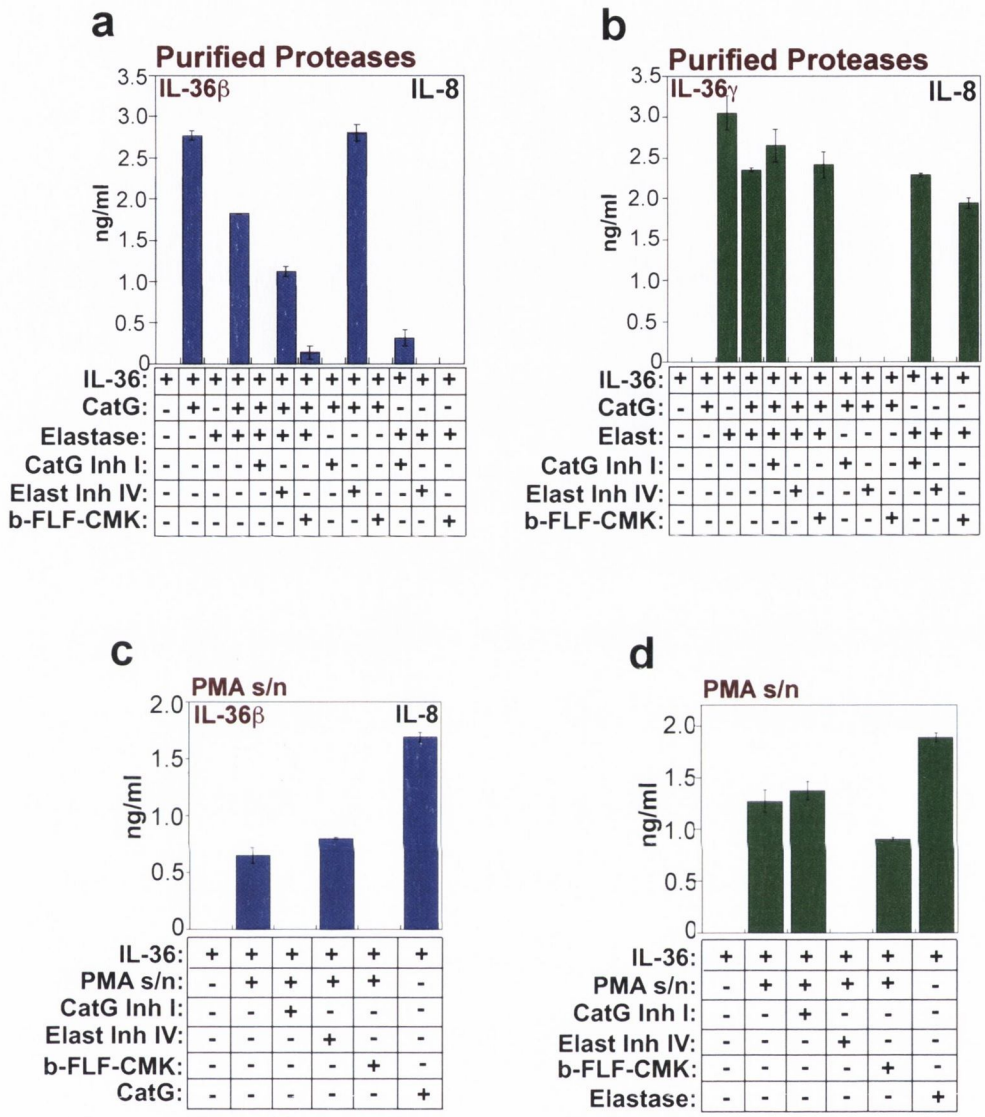


Figure 4.10 Inhibitiors of neutrophil proteases attenuate IL-36 activation
(a-b). HeLa^{IL36R} were stimulated with IL36β or IL36γ pre-incubated for 2 h at 37° with purified cathepsin-G and elastase (where indicated) in the presence or absence of Cat-G inhibitor 1 (10 μM), Elastase Inhibitor IV (10 μM), and biotin-FLF-CMK (5 μM). **c.** HeLa^{IL36R} were stimulated with IL36β pre-incubated for 2 h at 37° with neutrophils degranulates in the presence or absence of Cat-G inhibitor 1 (10 μM), Elastase Inhibitor IV (10 μM), and biotin-FLF-CMK (5 μM). Purified cat-G (50 nM) served as a positive control for activation. **d.** HeLa^{IL36R} were stimulated with IL36γ pre-incubated for 2 h at 37° with neutrophils degranulates as in (c). Purified elastase (100 nM) served as a positive control for activation. After 24 h, cytokine concentrations in culture supernatants were determined by ELISA.

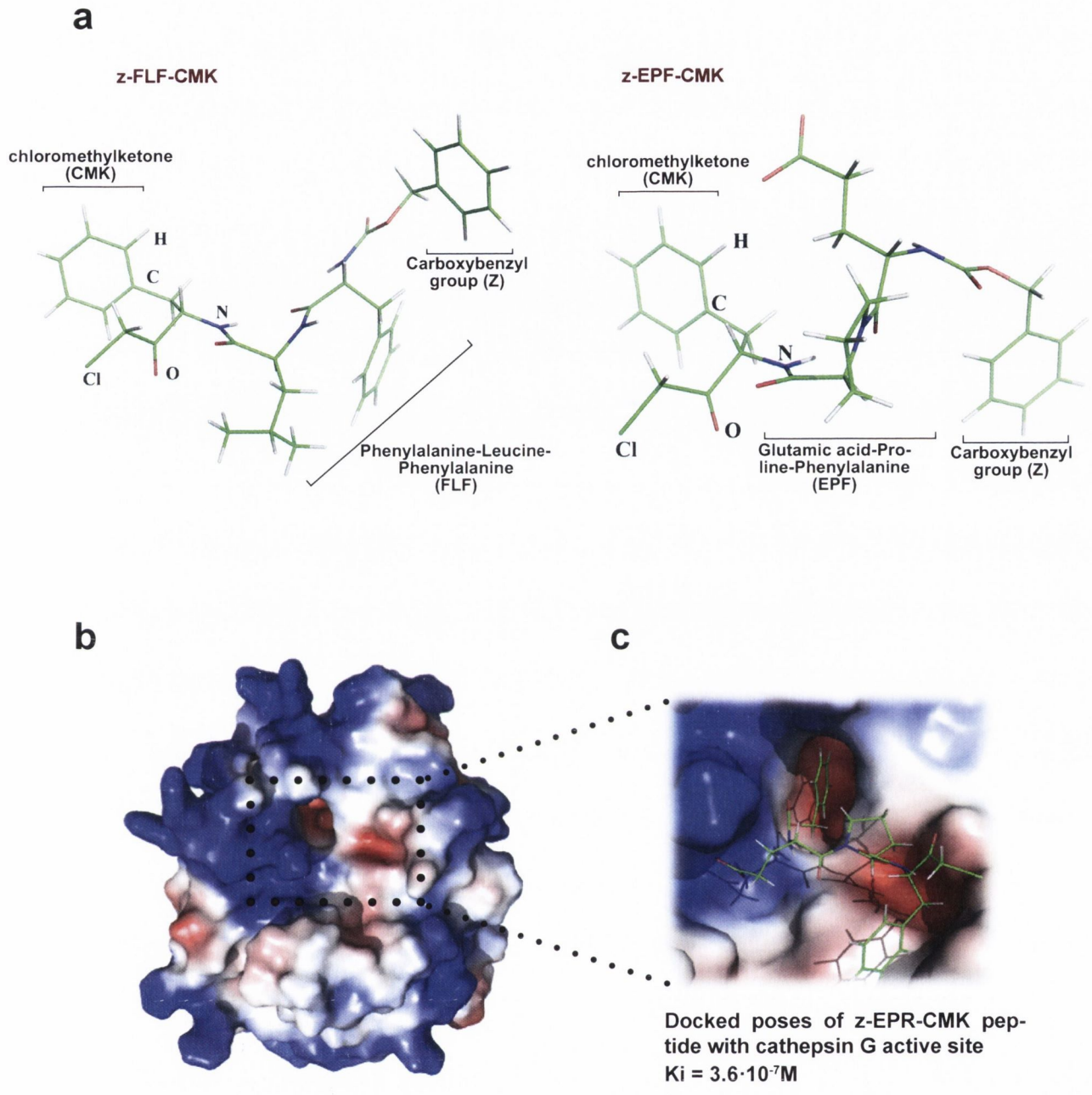


Figure 4.11 Design of peptide inhibitors
a. 3D modelling of basic peptide design for FLF and EPF. **b.** Representation of molecular electrostatic potential for cathepsin-G, with the enzymatic pocket indicated by dotted line. **c.** Docking of z-EPF-CMK with cathepsin-G enzymatic pocket. Data generated by Pavel Davidovich, Laboratory of Cell Biotechnology, Saint-Petersburg Institute of Technology.

benzyloxycarbonyl protective group (Z) at the N-terminus followed by the specificied tri-/tetra-peptide sequence, with a subset of peptides having a chloromethyketone (CMK) group at the C-terminal end. This CMK moiety allows for irreversible binding of the peptide to the enzyme active site through covelant binding of the active histidine residue (**Fig. 4.11**). These peptides were then assessed for the ability to inhibit activation of IL-36 cytokines by PMA-activated neutrophil degranulates. As **Figures 4.12 & 4.13** demonstrate, the peptides z-KAL-CMK and z-EPF-CMK appeared to inhibit IL-36α activation, while the peptides z-FLF-CMK, z-AFLF-CMK, z-GLF-CMK, and z-EPF-CMK proved to be the most potent inhibitors of IL-36β activation by neutrophil degranulates. In contrast, IL-36γ activation was not inhibited by these peptides but was antagonized by a specific chemical inhibitor of elastase (**Fig. 4.14**). Furthermore, the peptides z-API, z-DTEF, z-RPI, z-APV and z-PQR, which were designed around preferred elastase cleavage residues, proved to be the most potent inhibitors of IL-36γ activation by neutrophil degranulates (**Fig. 4.15**), whereas these same peptides did not inhibit activation of IL-36β (**Fig. 4.16**).

4.2.10 IL-36 receptor antagonist attenuates IL-36-induced cytokines

Sims and colleagues have reported that truncation of IL-36 receptor antagonist (IL-36RA) after the starting amino acid methionine dramatically increases the activity of this protein to antagonise IL-36 signalling (Towne et al., 2011). We engineered a modified form of IL-36RA by inserting a caspase-3 cleavage motif, DEVD, proximal to the residue identified by Sims and colleagues. (**Fig. 4 18 a**). To confirm that the DEVD-modified form of IL-36RA (IL-36RA^{DEVD}) was sensitive to caspase-3 proteolysis, we titrated caspase-3 with IL-36RA and analysed proteolysis via coomassie staining. As **Figure 4.18 a** illustrates, IL-36RA^{DEVD} was readily processed by caspase-3. To explore the functional effect of IL-36RA on IL-36 signalling, we incubated HeLa^{IL36R} cells with IL-36RA prior to exposure to activated forms of IL-36. As **Figure 4.18 b** demonstrates IL-36RA potently blocked IL-36-induced cytokines but did not inhibit IL-1 signalling. IL-

36RA was also capable of inhibiting IL-36 across a broad range of concentrations (**Fig. 4.18 c, d**).

4.2.11 Mapping of cathepsin-G and elastase cleavage sites in IL-36 cytokines

To identify the cathepsin-G cleavage site(s) within IL-36β that result in its activation, we performed Edman degradation sequencing of cathepsin-G-treated IL-36β preparations. This analysis identified two candidate sites at Arg5 and Phe53 (**Fig. 4.19 a, b**). We generated point mutations at both of these sites to assess their role in cathepsin-G-mediated activation of IL-36β. We initially tested each mutant for resistance to proteolysis by cathepsin-G. As **Figure 4.19 d** shows, IL-36β^{F53A} suppressed the appearance of the two major cleavage bands (~10 and ~4 kDa), yet still generated a third cleavage band (~16.5 kDa) just below the full-length protein. In contrast, IL-36β^{R5A} largely attenuated the appearance of the ~16.5 kDa band just below the full-length band, while the appearance of the cleavage bands (~10 and ~4 kDa) were significantly diminished. Furthermore, **Figure 4.20 a** demonstrates that mutation of Phe53 had no effect on cathepsin-G-mediated IL-36β activation, while mutation of Arg5 dramatically abolished activation of this cytokine (**Fig. 4.20 b, c**). Furthermore, mutation of Arg5 also abolished activation of IL-36β by PMA-activated neutrophil degranulates (**Fig. 4.21**). Using a similar approach, we identified Val15 in IL-36γ as the residue cleaved by elastase to promote activation of the latter (**Fig. 4.22**). Mutation of this residue also significantly attenuated activation of IL-36γ by elastase, as well as by PMA-activated neutrophil degranulates (**Fig. 4.23 & 4.24**).

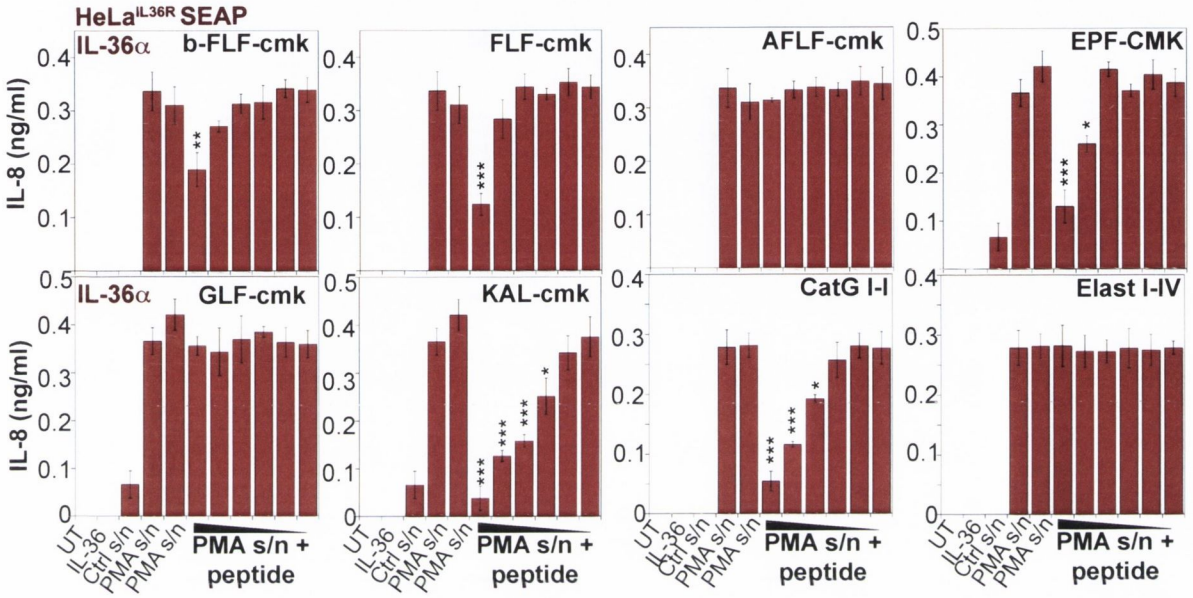


Figure 4.12 Screen of novel cathepsin-G targeted peptide inhibitors with IL-36α
Neutrophil degranulates were pre-incubated for 30 min on ice in the presence or absence of a titration of peptide (20, 10, 5, 2.5, 1.25, 0.625 μM) followed by addition of IL36α for 2 h at 37°. HeLa^{IL36R} were stimulated for 24 h. IL-8 cytokine concentrations in culture supernatants were determined by ELISA. Asterisk(s) indicate significance levels, *** = $p < .0001$, ** = $p < .001$, * = $p < .1$, by Student's t test. Results shown are representative of at least three independent experiments. Error bars represent the mean ±SEM of triplicate determinations from a representative experiment. (Graeme Sullivan provided data).

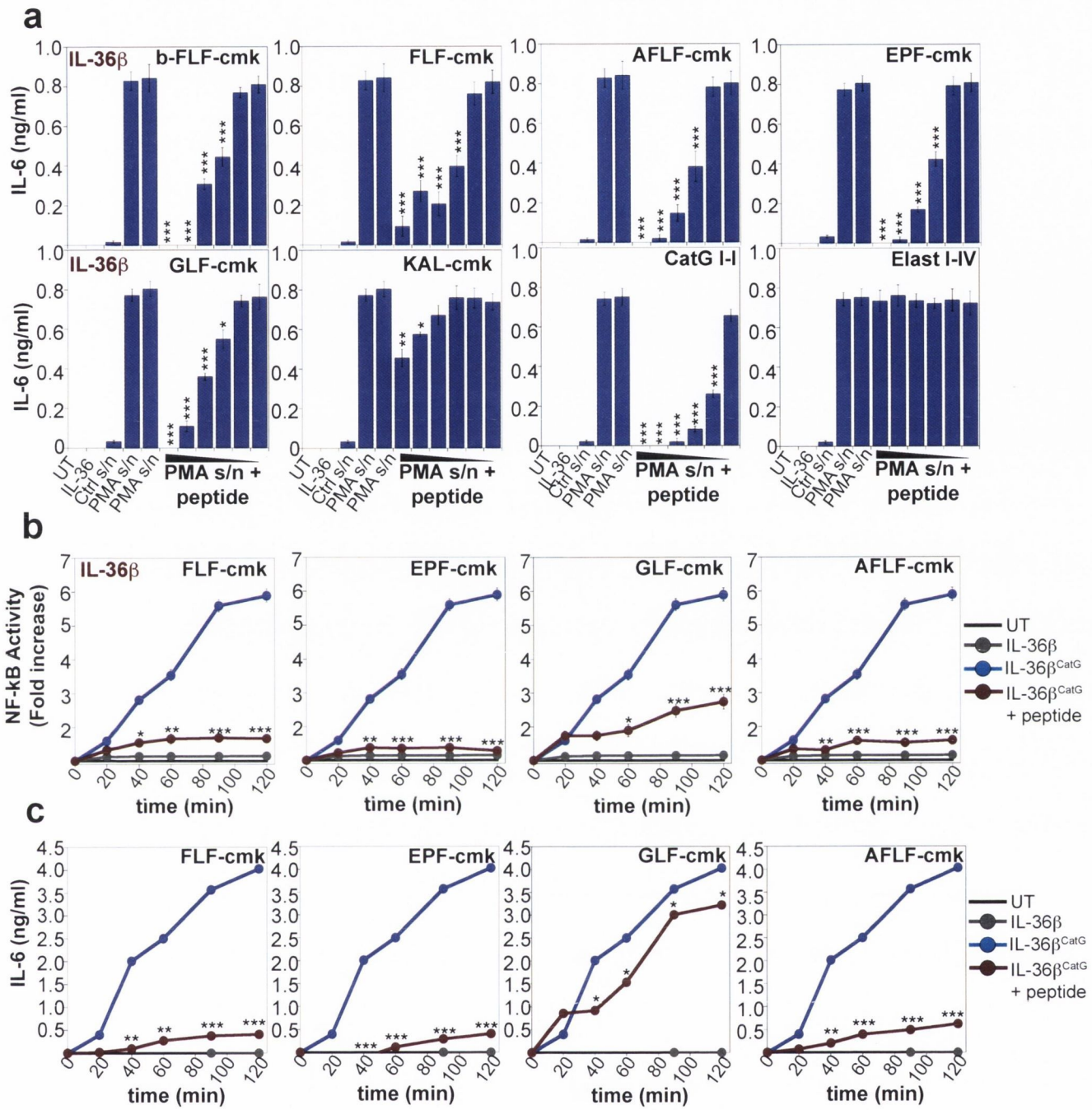


Figure 4.13 Screen of novel cathepsin-G targeted peptide inhibitors with IL-36β

a. Neutrophil degranulates were pre-incubated for 30min on ice in the presence or absence of a titration of peptide (20, 10, 5, 2.5, 1.25, 0.625 μM) followed by addition of IL36β for 2 h at 37°. HeLa^{IL36R} were stimulated for 24 h. IL-6 cytokine concentrations in culture supernatants were determined by ELISA. **b.** Cathepsin-G was pre-incubated for 30 min on ice in the presence or absence of peptide (10 μM) followed by incubation with IL36β. HeLa^{IL36R}SEAP were stimulated with samples of each reaction taken at indicated timepoints. NF-kB activity was measured as a fold induction of SEAP in the supernatant and (c) cytokine concentrations in culture supernatants were determined by ELISA. Asterisk(s) indicate significance levels, *** = $p < .0001$, ** = $p < .001$, * = $p < .1$, by Student's t test. Results shown are representative of at least three independent experiments. Error bars represent the mean ±SEM of triplicate determinations from a representative experiment. (Graeme Sullivan provided data).

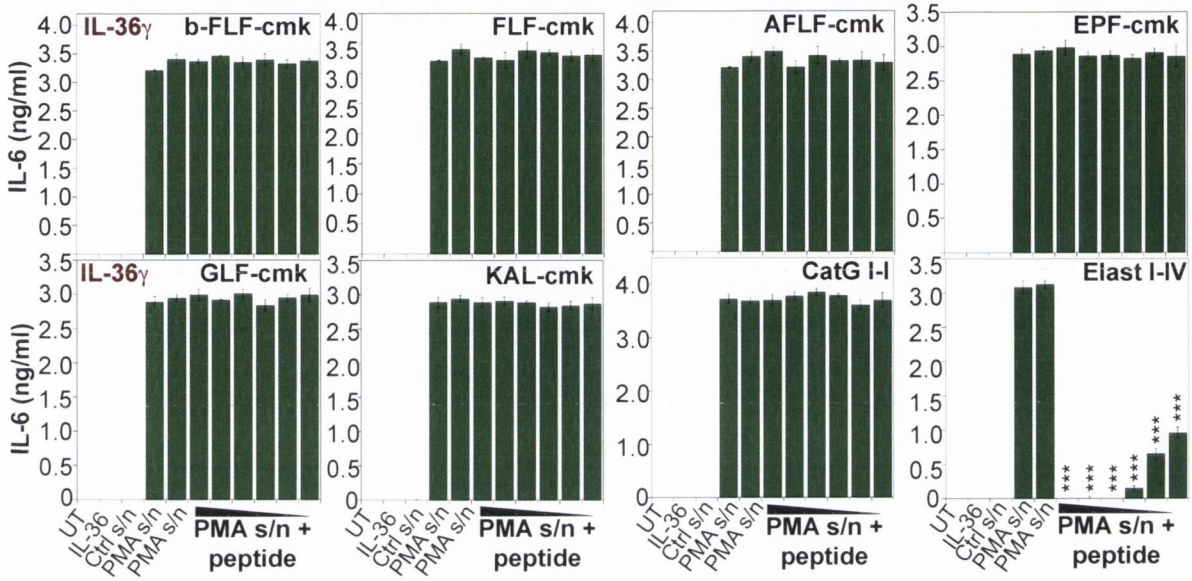


Figure 4.14 Novel cathepsin-G targeted peptide inhibitors do not block neutrophil degranulate activation of IL-36γ

Neutrophil degranulates were pre-incubated for 30 min on ice in the presence or absence of a titration of peptide (20, 10, 5, 2.5, 1.25, 0.625 μM) followed by addition of IL36γ for 2 h at 37°. HeLa^{IL36R} were stimulated for 24 h. IL-6 cytokine concentrations in culture supernatants were determined by ELISA. Asterisk(s) indicate significance levels, *** = $p < .0001$, ** = $p < .001$, * = $p < .1$, by Student's t test. Results shown are representative of at least three independent experiments. Error bars represent the mean ±SEM of triplicate determinations from a representative experiment. (Graeme Sullivan provided data).

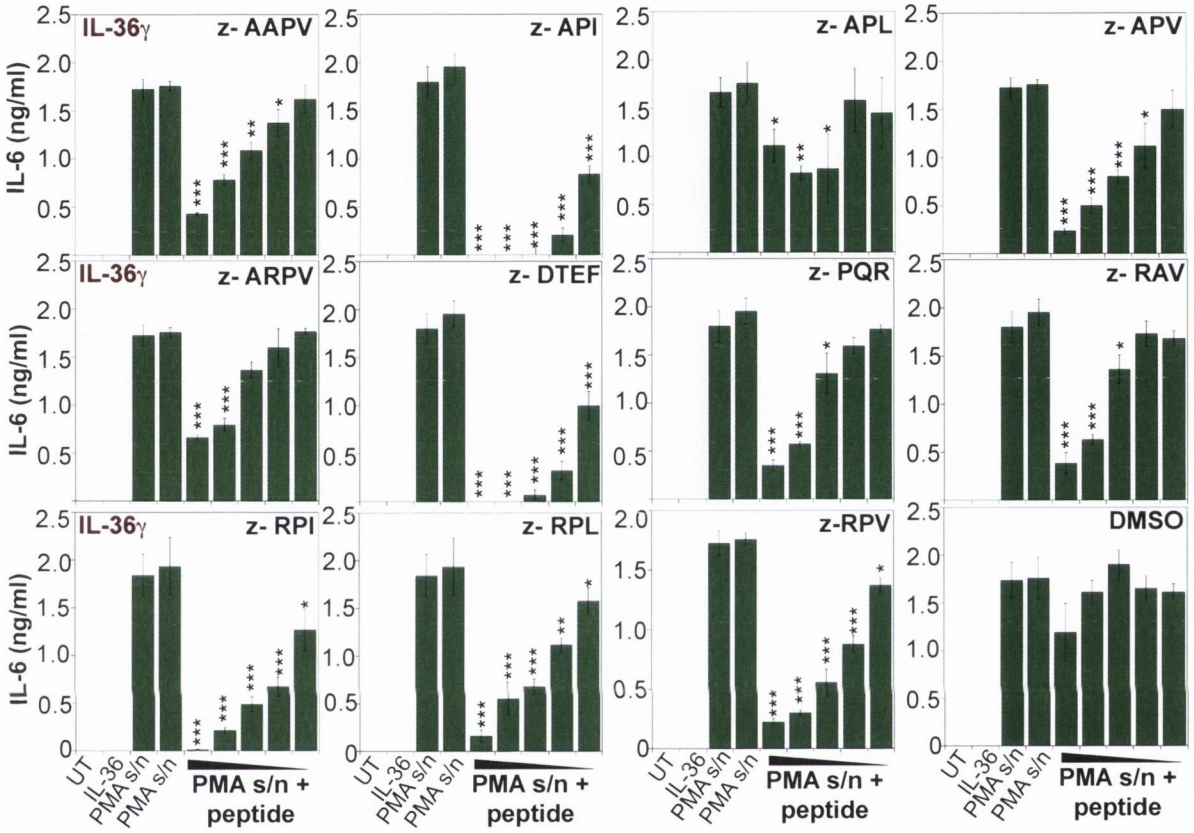


Figure 4.15 Screen of novel elastase targeted peptide inhibitors with IL-36γ
Neutrophil degranulates were pre-incubated for 30 min on ice in the presence or absence of a titration of peptide (100, 50, 25, 12.5, 6.25 μM) followed by addition of IL36γ for 2 h at 37°. HeLa^{IL36R} were stimulated for 24 h. IL-6 cytokine concentrations in the culture supernatants were determined by ELISA. Asterisk(s) indicate significance levels, *** = $p < .0001$, ** = $p < .001$, * = $p < .1$, by Student's t test. Results shown are representative of at least three independent experiments. Error bars represent the mean ±SEM of triplicate determinations from a representative experiment. (Graeme Sullivan provided data).

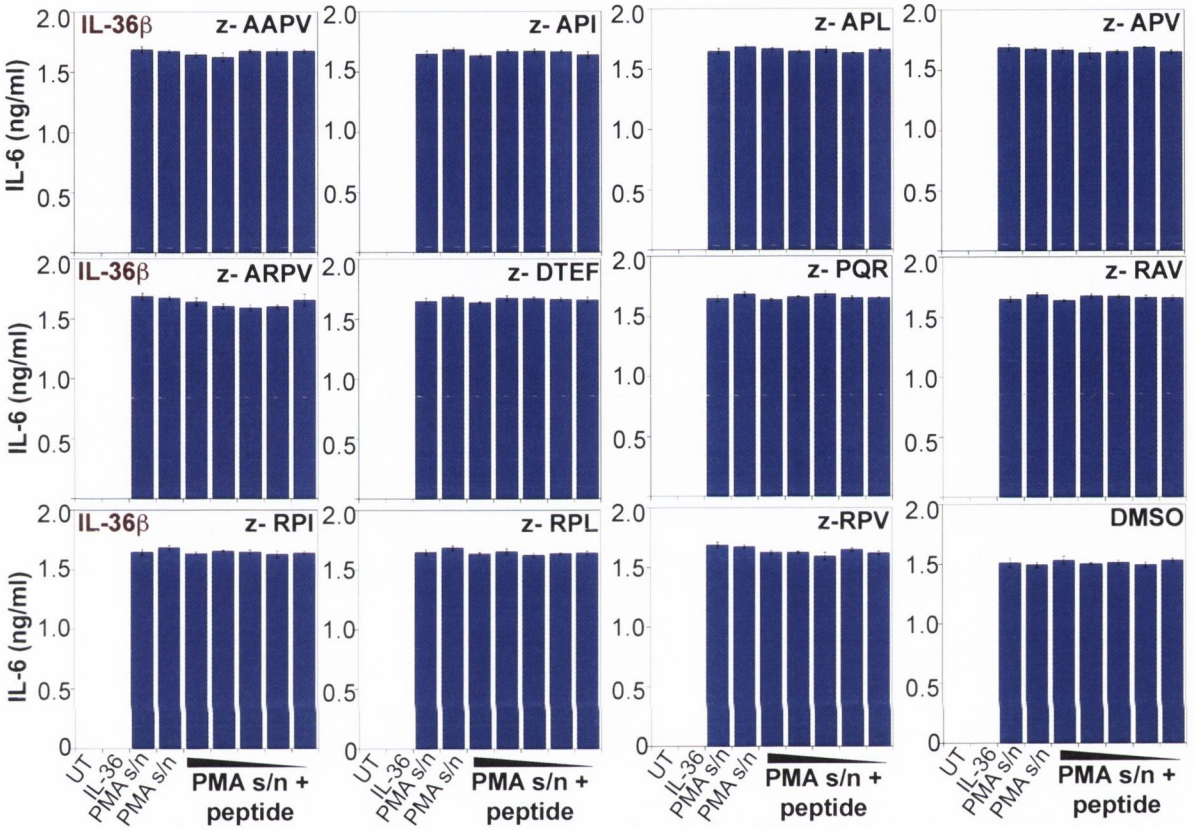


Figure 4.16 Novel elastase targeted peptide inhibitors do not block neutrophil degranulate activation of IL-36β

Neutrophil degranulates were pre-incubated for 30 min on ice in the presence or absence of a titration of peptide (100, 50, 25, 12.5, 6.25 μM) followed by addition of IL36β for 2 h at 37°. HeLa^{IL36R} were stimulated for 24 h. IL-6 cytokine concentrations in the culture supernatants were determined by ELISA. Asterisk(s) indicate significance levels, *** = $p < .0001$, ** = $p < .001$, * = $p < .1$, by Student's t test. Results shown are representative of at least three independent experiments. Error bars represent the mean ±SEM of triplicate determinations from a representative experiment. (Graeme Sullivan provided data).

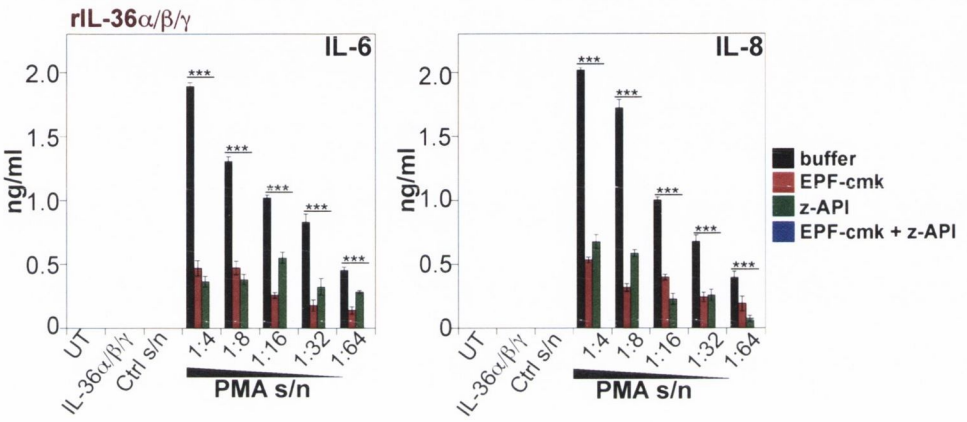


Figure 4.17 Mixing of cathepsin-G and elastase-targeted peptides block IL-36 activation by neutrophil degranulates

Neutrophil degranulates were pre-incubated for 30 min with z-EPF-CMK (10 μM), or z-API (100 μM) or both combined, followed by addition of equal molar amounts of IL36α/β/γ for 2 h at 37°. HeLa^{IL36R} were stimulated for 24 h. IL-6 cytokine concentrations in the culture supernatants were determined by ELISA. Asterisk(s) indicate significance levels, *** = $p < .0001$, ** = $p < .001$, * = $p < .1$, by Student's t test. Results shown are representative of at least three independent experiments. Error bars represent the mean ±SEM of triplicate determinations from a representative experiment. (Graeme Sullivan provided data).

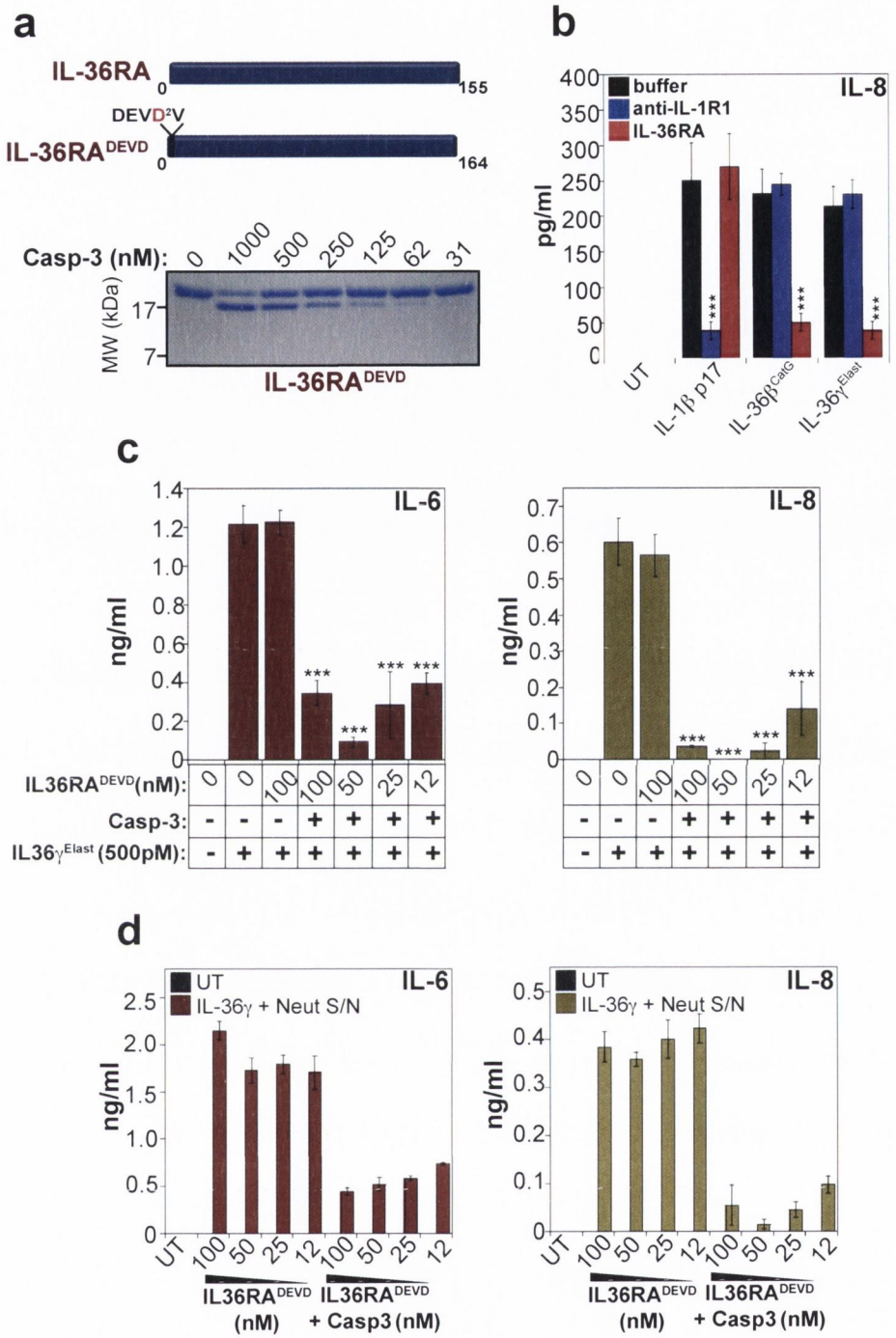
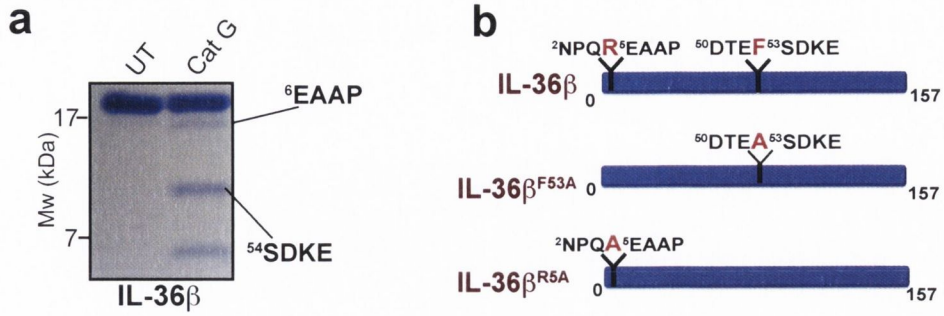


Figure 4.18 IL-36 receptor antogonist attenuates IL-36 signalling

a. Schematic of modified form of IL-36RA where a caspase-3-processing motif (DEVD) was inserted into the IL-36 sequence, N-terminal to the known processing sites. Recombinant IL-36RA^{DEVD} was incubated with indicated concentrations of caspase-3 Samples were resolved by Coomassie stain. **b.** HeLa^{IL36R} were preincubated with IL-36RA (50 nM) for 2 h prior to addition of IL-1β p17 (25 nM), IL-36β^{CatG} (500pM) and IL-36γ^{Elastase} (500pM). After 24 h, cytokine concentrations in culture supernatants were determined by ELISA. **c.** HeLa^{IL36R} were preincubated with a titration of IL-36RA^{DEVD} for 2 h prior to addition of IL-36γ^{Elastase} (500pM). After 24 h, cytokine concentrations in culture supernatants were determined by ELISA. **d.** HeLa^{IL36R} were preincubated with a titration of IL-36RA^{DEVD} (+/- caspase-3) for 2 h prior to addition of neutrophil degranulate cleaved IL-36γ (500pM). After 24 h, cytokine concentrations in culture supernatants were determined by ELISA



c

IL-36β

MAHHHHHHAGVMNPQ**R**[5]EAAPK SYAIRDSRQMVWVLGNSLIAAPLSRSIK
PVTLHLIACRDTE**F**[53]SDKEKGNMVYLGIKGKDLCLFCAEIQGKPTLQLKEKNI
MDLYVEKKAQKPFLFFHNKEGSTSVFQSVSYPGWFIATSTTSGQPIFLTK-
ERGITNNTNFYLDSVE

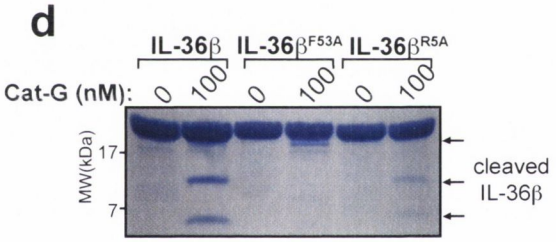


Figure 4.19 IL-36β is cleaved by cathepsin G after arginine 5
a. Recombinant IL-36β was incubated with cathepsin-G (50 nM). Samples were resolved by Coomassie stain. Indicated bands were analysed by Edman degradation sequencing. **b.** Schematic representing $NPQR_5$ and $DTEF_{53}$ cleavage motifs. Representative gel is shown from at least two independent experiments. **c.** Schematic representing recombinant IL-36β amino acid sequence with novel N-termi highlighted in red. 6 x His-tag is highlighted in green. **d.** Recombinant IL-36β, IL-36β^{F53A} and IL-36β^{R5A} were incubated with fixed concentration of cathepsin-G, as indicated, followed by analysis by SDS-PAGE and Coomassie stain. Representative gel is shown from at least two independent experiments.

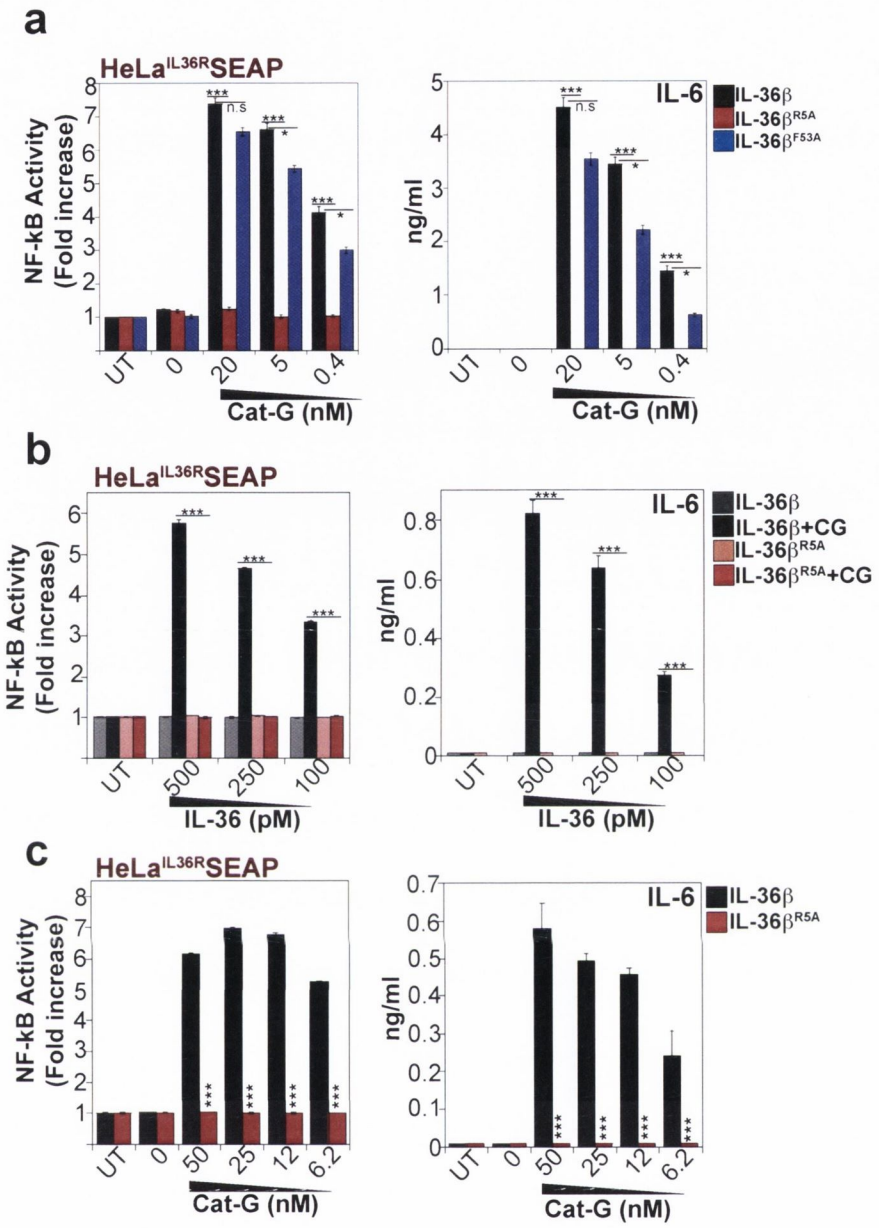


Figure 4.20 IL-36β is activated by cathepsin-G after arginine 5

a. HeLa^{IL36R}SEAP were stimulated with 500 pM of IL36β, IL-36β^{R5A} and IL36β^{F53A} pre-incubated for 2 h at 37° with a titration of cathepsin-G. After 24 h, NF-kB activity was measured as a fold induction of SEAP in the supernatant and cytokine concentrations in culture supernatants were determined by ELISA. **b.** HeLa^{IL36R}SEAP were stimulated with a titration of IL36β and IL36β^{R5A} pre-incubated for 2 h at 37° with cathepsin-G (50 nM). After 24 h, NF-kB activity was measured as a fold induction of SEAP in the supernatant and cytokine concentrations in culture supernatants were determined by ELISA. **c.** HeLa^{IL36R}SEAP were stimulated with 500pM of IL36β and IL36β^{R5A} pre-incubated for 2 h at 37° with a titration of cathepsin-G. After 24 h, NF-kB activity was measured as a fold induction of SEAP in the supernatant and cytokine concentrations in culture supernatants were determined by ELISA. Asterisk(s) indicate significance levels, *** = $p < .0001$, ** = $p < .001$, * = $p < .1$, by Student's t test.

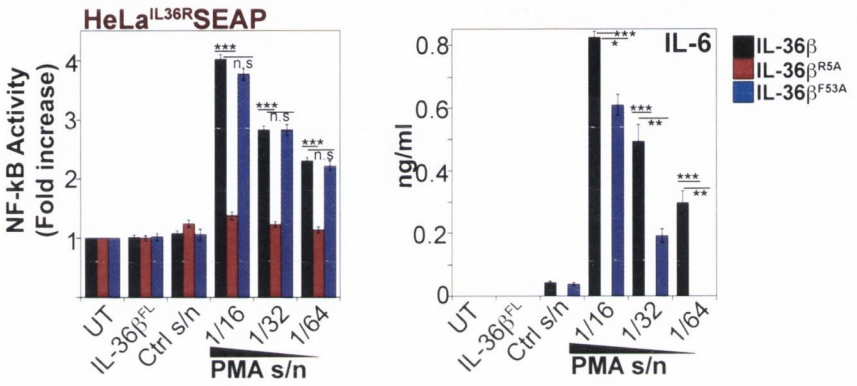


Figure 4.21 IL-36β is activated by neutrophil degranulates after arginine 5
HeLa^{IL36R}SEAP were stimulated with 500 pM of IL36β, IL-36β^{R5A} and IL36β^{F53A} pre-incubated for 2 h at 37° with a titration of PMA-activated neutrophil degranulate. After 24 hr, NF-kB activity was measured as a fold induction of SEAP in the supernatant and cytokine concentrations in culture supernatants were determined by ELISA. Asterisk(s) indicate significance levels, *** = $p < .0001$, ** = $p < .001$, * = $p < .1$, by Student's t test.

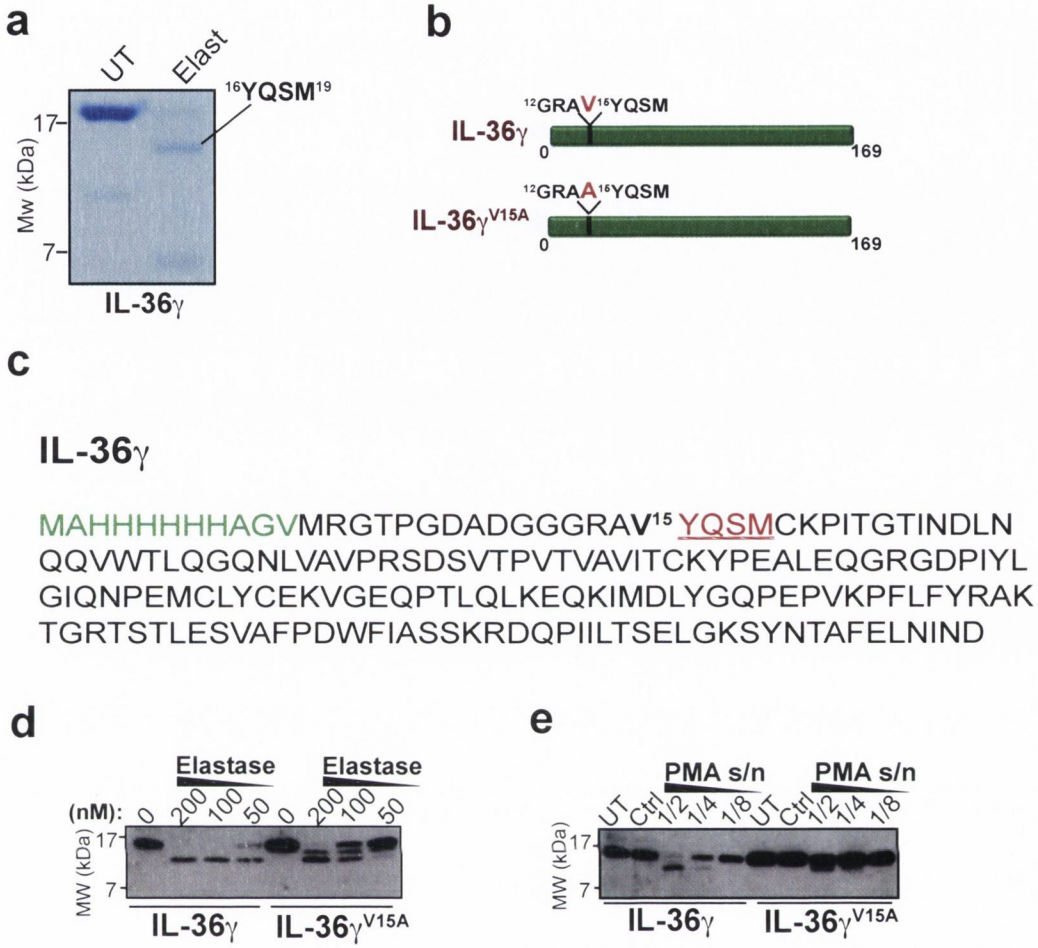


Figure 4.22 IL-36γ is cleaved by elastase after valine 15

a. Recombinant IL-36γ was incubated with elastase (100 nM). Samples were resolved by Coomassie stain. Indicated bands were analysed by Edman degradation sequencing. **b.** Schematic representing $GRAV_{15}$ cleavage motif. Representative gel is shown from at least two independent experiments. **c.** Schematic representing recombinant IL-36γ amino acid sequence with novel N-terminus highlighted in red. 6 x His-tag is highlighted in green. **d.** Recombinant IL-36γ and IL-36γ^{V15A} were incubated with a titration of elastase, followed by analysis by SDS-PAGE and immunoblot. **e.** Recombinant IL-36γ and IL-36γ^{V15A} were incubated with a titration of neutrophil degranulate, followed by analysis by SDS-PAGE and immunoblot.

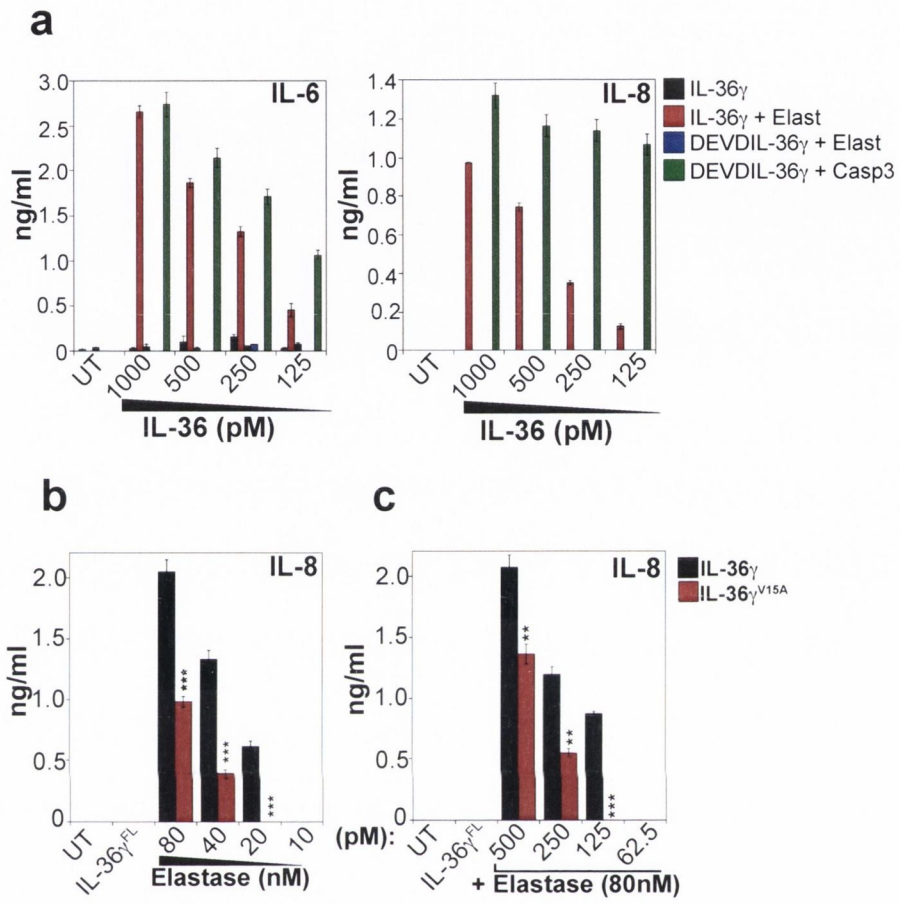


Figure 4.23 IL-36γ is activated by elastase after valine 15

a. HeLa^{IL36R}SEAP were stimulated with a titration of IL36γ and DEVD-IL36γ pre-incubated for 2 h at 37° either cathepsin-G (50 nM) or caspase -3 (800 nM). After 24 h, cytokine concentrations in culture supernatants were determined by ELISA. **b.** HeLa^{IL36R}SEAP were stimulated with 500pM of IL36γ and IL36γ^{V15A} pre-incubated for 2 h at 37° with a titration of elastase. After 24 h, cytokine concentrations in culture supernatants were determined by ELISA. **c.** HeLa^{IL36R}SEAP were stimulated a titration of IL36γ and IL36γ^{V15A} pre-incubated for 2 h at 37° with elastase (80 nM). After 24 h, cytokine concentrations in culture supernatants were determined by ELISA. Asterisk(s) indicate significance levels, *** = $p < .0001$, ** = $p < .001$, * = $p < .1$, by Student's t test.

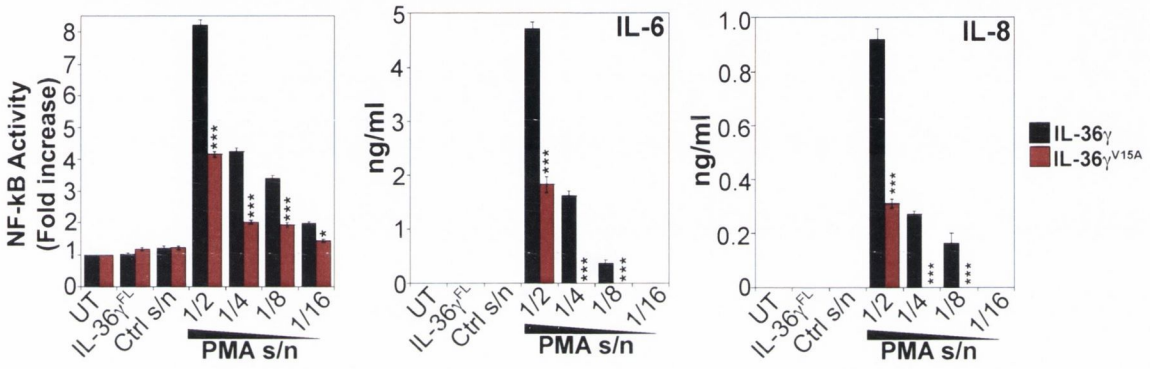


Figure 4.25 IL-36γ is activated by neutrophil degranulate after valine 15
HeLa^{IL36R}SEAP were stimulated with 500 pM of IL36β, IL-36β^{R5A} and IL36β^{F53A} pre-incubated for 2 h at 37° with a titration of PMA-activated neutrophil degranulate. After 24 hr, NF-kB activity was measured as a fold induction of SEAP in the supernatant and cytokine concentrations in culture supernatants were determined by ELISA. Asterisk(s) indicate significance levels, *** = $p < .0001$, ** = $p < .001$, * = $p < .1$, by Student's t test.

4.3 Discussion

4.3.1 IL-36 cytokines are activated by neutrophil proteases

It has recently been established that IL-36 proteins require processing at their N-terminal regions to release the biological activity of these cytokines, yet the protease(s) that do this have remained obscure (Towne et al. 2011). In addition, IL-36 cytokines have also caught the attention of scientists and clinicians due to the striking inflammatory skin phenotype displayed by patients with mutations in the IL-36 receptor antagonist, the clearest evidence yet for a role for IL-36 in skin inflammatory disease. In conjunction with these human genetic data, and in light of the discovery of Sims and colleagues (Towne et al., 2011), there has been a number of recent studies that have started to look at the pro-inflammatory effects of IL-36 cytokines in genetic mouse models as well as profiling IL-36 gene expression in psoriatic patient cohorts (Vigne et al., 2012; Tortola et al., 2012; Blumberg et al., 2010; Johnston et al., 2010). A caveat of these published data has been the use of artificially truncated versions of these cytokines that display enhanced biological activity but may not represent versions of these cytokines found in nature (Vigne et al., 2012, Tortola et al., 2012). Therefore, the identification of protease(s) required for IL-36 activation would begin to open up new contexts in which to explore IL-36 biology. Here we show that IL-36 cytokines are activated by neutrophil granule proteases. IL-36β and IL36γ are processed by cathepsin-G and elastase, respectively, and proteolysis of these cytokines releases their biological activity. Furthermore, we demonstrate that IL-36 activation can be blocked through the use of novel peptide inhibitors designed to inhibit the enzymatic activity of cathepsin-G and elastase.

4.3.2 Effects of proteolysis on IL-36 signalling

Proteolysis of IL-36 cytokines may induce a conformational change in these proteins that increase their affinity for the IL-36 receptor, thereby increasing biological potency. Alternatively, the IL-36 N-termini may partly occlude the receptor binding domain, removal of which permits a more stable interaction with

the IL-36R complex. Previously, Hazuda and colleagues have reported that IL-1α and IL-1β cytokines undergo profound conformational changes upon removal of their N-termini and, as a consequence, the mature regions of these molecules switch from a proteinase K-sensitive to a proteinase K-insensitive state. This change is most likely reflected in an altered conformation that increased IL-1 receptor affinity (Hazuda et al., 1991). Notably, IL-1β and IL-1AcP contacts are made through residues in loops connecting beta-strands 4 and 5 (β4/5) and β11/12 and it is these loop regions that are the major structural difference between IL-1β and the IL-1RA. Because of the reliance of IL-36 cytokines on IL-1AcP for signalling, it has been presumed to function analogously to IL-1 signalling. However, the recent resolution of the crystal structure for IL-36γ and chimeric versions of the protein with IL-36RA loop regions has revealed a fine specificity to IL-36 agonistic and antagonistic signalling that is distinct from IL-1 signalling (Guenter & Sunderberg, 2014). Substitution of both β4/5 and β11/12 loops of IL36γ with those of IL-36RA did not remove all agonist activity suggesting that additional sites in IL-36γ are needed for agonistic activity. This is in striking constrast to IL-1 whereby the same experiment between IL1β and IL-1RA converts IL-1β to an antagonist. The molecular basis of IL-36RA antagonism of the IL-36R is markedly different compaired with the IL-1RA and IL-1R1. A striking feature of IL-36RA is that it has a greatly extended β11/12 loop compaired with IL-36 agonists, likely blocking interaction with the IL1AcP. Furthermore, IL-1RA antagonism is highly dependent on a lysine (K145) residue C-terminal to its β11/12 loop (Ju et al., 1991). Mutation of this residue to an aspartic acid (K145D) grealy diminishes IL-1RA antagonism and switched it to a partial agonist, however IL-36RA has an aspartate at this position, which in principle could interact with IL-1RAcP. Strikingly, mutation of the homologous residue in IL-1β aspartic acid (D145) to a lysine (K) converts IL-1β to antagonist. The explanation for this apparent contradation may lie with the extended β11/12 in IL-36RA, which may simply shield the aspartate residue from IL-1AcP. Of note, the authors use the artificially truncated version of IL-36γ, identified by Sims and colleagues, as a

source of protein (Towne et al., 2011). Nonetheless, this study has provided the first insights into IL-36 signalling (Guenter & Sunderberg, 2014). The further resolution of IL-36 ligand structures, both in their full-length as well as their processed forms by proteases such as cathepsin-G and elastase will help to elucidate how exactly these molecules interact with the IL-36R/IL-1AcP receptor complex.

4.3.2 Neutrophils as critical drivers of inflammation

Immune cell infiltration is a hallmark of a number of skin-related inflammation disease pathologies. In particular, psoriatic plaques are heavily infiltrated with neutrophils, dendritic cells, macrophages, and T-cells (Teru et al., 2000; Murphy et al., 2007; Nestle et al., 2009; Kanbara et al., 2013; Frank et al., 2009). It has become increasingly clear that there exists a complex and extensive crosstalk between epithelial, stromal and immune cells that cooperate to ensure effective host defence and to maintain tissue homeostasis. In addition, the microbes and viruses that inhabit the skin continually interact with epithelial and immune cells, influencing host immunity and in some instances may act as important contributors to subsequent inflammatory skin pathologies (Pasparakis et al., 2014). Neutrophils are critical first responder cells in our innate immune arsenal and are continually on alert for signs of tissue damage. They harbour highly sophisticated and complex mechanisms to perform their role in immune defence and inflammation that include: engulfment and destruction of microbes via ROS production, release of neutrophil extracellular traps to sequester and kill microbes, migratory machinery that permits swift infiltration to sites of damage or infection, release of cytokines to orchestrate immune responses, as well as the production of a vast repertoire of antimicrobial molecules such as defensins, and granule proteases like elastase and cathepsin-G (Brinkmann et al., 2004; Pham., 2006; Borregaard et al., 2007; Koloaczakowska et al., 2013). Furthermore, mice deficient in neutrophil granule proteases cathepsin-G and elastase have deficiencies in bacterial clearance as well as increased mortality to streptococcus, pseudomonas and mycobacterial infections (Hahn et al., 2011; Steinwede et al.,

2012). Furthermore, patients that lack functional neutrophil proteases as a result of loss-of-function mutations in dipeptidyl peptidase I (DPPI), an enzyme critical for their activation, are prone to repeated microbial infection, high morbidity and increased mortality (Bardoel et al., 2014). While the degranulation and release of neutrophil proteases exerts profound antimicrobial and protective effects during infection, in excess they can cause extensive tissue damage through ROS production, inflammatory cytokines and protease degradation of the extracellular matrix (Korkmaz et al., 2010). Excessive protease activity is typically prevented by serum antiproteases such as α-1-antitrypsin and α-2-macroglobulin that are synthesized in great quantities during an inflammatory response (Korkmaz et al., 2010). In addition to their cytotoxic effects on microbes and degradation of viral virulence factors, another important function of neutrophil granule proteases is proteolytic modification of chemokines and cytokines. For example, elastase, cathepsin-G and proteinase 3 have been reported to process interleukin-8 (IL-8) to enhance its chemotatic potency (Padrines et al., 1994), while interleukin-33 (IL-33) proteolysis by elastase and cathepsin-G results in a switch from a basal level of activity to a greatly elevated biological activity (Lefrançais et al., 2012). The demonstration that IL-36 is also subject to proteolytic regulation by neutrophils proteases may begin to illuminate the role of IL-36-driven inflammation in neutrophil dominated skin inflammatory diseases such as psoriasis.

4.3.4 Targeting neutrophil protease activity using peptide inhibitors

An exciting possibility that emerged during the course of this work was that we might develop a way in which to 'shut-down' activation of IL-36 cytokines through targeted inhibition of neutrophil proteases. Because of the emerging role of IL-36 cytokines in the development of inflammatory skin diseases such as psoriasis, we reasoned that a strategy to limit their biological activity in this context might hold some therapeutic benefit. Neutrophils are a major component of the immune infiltrate seen in psoriatic tissue (Teru et al., 2000; Murphy et al., 2007). The presence of this inflammatory cell type strongly implicates these cells in disease pathology. Interestingly, therapeutic depletion of neutrophils show

protective effects in patients with generalized pustular psoriasis (Ikeda et al., 2013). With these issues in mind, we designed a strategy that involved the generation of tri-/tetra-peptides based upon optimal recognition sequences for the neutrophil proteases, cathepsin-G and elastase. This way we could 'bait' the proteases with these peptides, neutralizing their enzymatic activity and protecting IL-36 cytokines from proteolysis. There was clear precedent for this type of approach as peptide inhibitors have been developed to inhibit caspases (Thornbury et al., 1992; Nicholson et al., 1993). Examples of such peptides include z-VAD-FMK, z-DEVD-FMK, z-WEHD-CHO, all of which have been used extensively in apoptosis research as potent blockers of apoptosis *in vitro* and *in vivo* (Hara et al., 1997; Henry et al., 2013). Another attractive reason to use tri-/tetra-peptides is their relatively small molecular weight <400 kDa. In a therapeutic context size restriction is a major limiting factor for many types of protease inhibitors, especially those that have to cross the skin barrier. We identified a number of promising lead peptides that are potent inhibitors of cathepin-G and elastase, including z-EPF-CMK, z-AFLF-CMK, z-API, and z-APV. Importantly, we found that these not only inhibited purified preparations of these neutrophil proteases but also inhibited endogenously expressed cathepsin-G and elastase found in neutrophil degranulates. We found that chemical modifications, such as the addition of CMK moiety at the C-terminal end of the peptide, greatly enhanced the efficiency of the peptide to inhibit protease activity. This can be explained by the irreversible binding through a covalent bond that CMK promotes upon access to the catalytic residue within the active site of the enzyme. Therefore, efficient inhibition can be achieved with low micromolar concentrations of the peptide inhibitor with a CMK modification. While we have targeted neutrophil proteases because of their capability to process IL-36 cytokines, it is worth noting that selective inhibition of elastase may prove useful in a wide range of inflammatory diseases such as chronic obstructive pulmonary disease (COPD), cystic fibrosis (CF), acute lung injury (ALI) and acute respiratory distress syndrome (ARDS), all of which are characterised by excessive elastase activity as a result of infections in the lung.

4.3.5 Sequence mapping of neutrophil cleavage sites witin IL-36

Sims and colleagues demonstrated that IL-36 cytokines have limited biological activity as full-length proteins and require processing at their N-termini to activate them. However, the authors did not identify the proteases that naturally process and activate these cytokines, but mapped their active forms using artificial truncations. Therefore, a caveat of these results is that the residues identified as critical for activation of IL-36 cytokine may not represent activation sites found in nature. Following the identification of neutrophil proteases as activators of IL-36 it was important that we mapped the cleavage sites with IL-36 cytokines. Through Edman degradation sequencing we identified arginine 5 (R5) as the critical residue required for IL-36β activation by cathepsin-G, consistant with cathepsin-G preference for aromatic or positively charged residues at P1 position (phenlyalanine (F), arginine (R), lysine (K) or tyrosine (Y)). In addition, we identified another cleavage site phenyalinine 53 (F53) but found through point-mutation, where phenylalanine was replaced with alanine (F53A), that this site was not required for activation. Furthermore, replacement of the arginine with an alanine (R5A) completely abolished the ability of cathepsin-G to activate IL-36β. These data suggest that cathepsin-G cleaves IL-36β after arginine 5 at P1 position to release biological activity. Importantly, we have also recently identified another cathepsin protease (cathepsin-K) as an IL-36β-activating enzyme and found that it too cleaves and activates IL-36β after arginine 5, indicating that this residue is a conserved site for activation for at least two distinct proteases (data not shown). Of note, Sims and colleagues identified a truncation mutant of IL-36β starting with arginine 5 (R5) as having greatly enhanced biological activity. This would predict an enzyme that can process after the preceding amino acid glutamine 4 (Q4) at P1 position. Our findings suggest that this region of amino acids is indeed critical for the activation of IL-36β.

Repeating the process, we also mapped the elastase cleavage site within IL-36γ and identified valine 15 as the critical residue required for activation of this cytokine. We generated a point-mutant, where we replaced valine with an

alanine (V15A), and this significantly attenuates activation of IL-36γ. We observed that we did not get complete suppression of activation with the V15A mutant. One possible explanation for the residual activation is that alanine is one of the preferred residues that elastase is known to cleave after. Other examples include small hydrophobic residues such as valine (V), alanine (A), cysteine (C), methionine (M), isoleucine (I), leuine (L) and serine (S) at P1 position (Korkmaz et al., 2010). Another potential explanation is that there may be another cryptic site within the N-terminal region of IL-36γ required for full activation that we did not identifiy during our analysis. Sims and colleagues identified a truncation mutant of IL-36γ starting with serine 18 (S18) as having greatly enhanced biological activity. This would predict an enzyme that can cleave after the preceding amino acid glutamic acid 17 (Q17) in the P1 position. Notable, Sims and colleagues generated truncations upstream and downstream of the S18 and found that these mutants had similar activity to the full-length cytokine, suggesting that IL-36γ beginning with S18 is quite specific for activation, however the authors did not generate a truncation down as far as valine 15 to test whether the cytokine would gain biological activity.

In conclusion, we have demonstrated that IL-36 cytokines are activated by the neutrophil proteases, cathepsin-G and elastase, and similar to other IL-1 family members (IL-1 and IL-33) this proteolysis significantly increases their biologically activity. Collectively, these data indicate a conserved role for neutrophil proteases as potent amplifiers and activators of IL-36 cytokines and suggest that targeted inhibition of these proteases may have therapeutic benefits in inflammatory skin conditions such as psoriasis.

Chapter 5

Exploring the functional role of IL-36

5.1 Introduction

In the previous chapter, we identified IL-36 cytokines as novel substrates of neutrophil proteases. In the past few years a number of studies have been published that have begun to explore the physiological roles of IL-36 cytokines *in vivo*. This has been facilitated by the generation of transgenic mice overexpressing IL-36 cytokines, mice deficient in the IL-36 receptor, and the identification of truncated versions of both the human and mouse proteins that display dramatically increased bioactivity *in vivo* (Blumberg et al., 2010; Tortola et al., 2012; Towne et al., 2011). As introduced previously, it is becoming increasingly apparent that the IL-36 phenotype is most pronounced in the epidermis of patients deficient in IL-36RA developing a distinct and severe inflammatory skin condition, GPP. In agreement with a role for these cytokines in skin inflammatory disease, IL-36 is highly unregulated in both genome and proteome studies on psoriatic tissues (Blumberg et al., 2010; Johnston et al., 2011; Schonthaler et al., 2013). Cytokines from the IL-1 family such as IL-1α, IL-33 and IL-36, along with TNF, are 'apical' cytokines, in that these cytokines can orchestrate an extremely diverse set of immune responses, through initiation of an inflammatory cascade that serves to activate distinct immune cell types such as macrophages, dendritic cells and T-cells that cumulatively drive an immune response. IL-1 cytokines have been implicated in a whole range of immune responses from the allergic response (IL-33) to priming and activation of inflammatory T-cell subtypes (IL-1). Similar to IL-1, it has been recently demonstrated that IL-36 cytokines can also activate dendritic cells and induce the proliferation and polarization of T-cells towards the Th1 lineage (Vigne et al., 2011 & 2012). It is because of the 'apical' function of IL-1 cytokines as initiators of inflammation that these cytokines are being targeted for therapeutic benefits in a diverse range of inflammatory conditions.

In this chapter, we sought to explore the biological effects of activated IL-36 cytokines and show that IL-36 is capable of inducing an extensive inflammatory gene induction signature similar to TNF. In addition, activated IL-36 can perturb normal proliferation and differentiation in an organotypic skin model. Finally, we

explore the endogenous expression of IL-36 in keratinocytes and in psoriatic patient biopsies.

5.2 Results

5.2.1 Activated IL-36 promotes robust cytokine production by keratinocytes

To explore the biological activity of IL-36β in a physiologically relevant cell type, we used transformed HaCat keratinocytes as well as primary human keratinocytes to ask whether cathepsin-G processed IL-36β or elastase processed IL-36γ were capable of triggering the production of pro-inflammatory cytokines from these cells. As illustrated in **Figure 5.1**, whereas full length IL-36β or IL-36γ evoked a poor response from HaCaT cells, cathepsin-G-processed IL-36β and elastase-processed IL-36γ induced robust production of chemokines from these cells. Essentially identical results were seen with primary human keratinocytes (**Figure 5.2**). The inconsistent results in relation to IL-36α between the HaCat and keratinocyte systems relates to an issue with the solubility of IL-36a during the course of this work. We had solved this issue of solubility by the time the keratinocytes experiments were conducted.

5.2.2 IL-36 and TNF drive distinct inflammatory gene signatures in primary keratinocytes

To broaden our understanding of the potential biological effects of IL-36, we conducted genome wide gene expression array analysis using a physiological relevant cell type, primary keratinocytes. In addition, we compared the effects of TNF on primary keratinocytes as the role for TNF in skin inflammatory diseases is well established, with TNF-neutralization therapies (e.g etanercept) having hugely beneficial effects in patents. As **Figure 5.3** demonstrates, activated IL-36β induced robust expression of a diverse array of pro-inflammatory genes from these cells. Of particular note, IL-36 induced strong transcriptional upregulation of IL-17C (~50-fold within 8 hours), a cytokine that has been implicated as a key

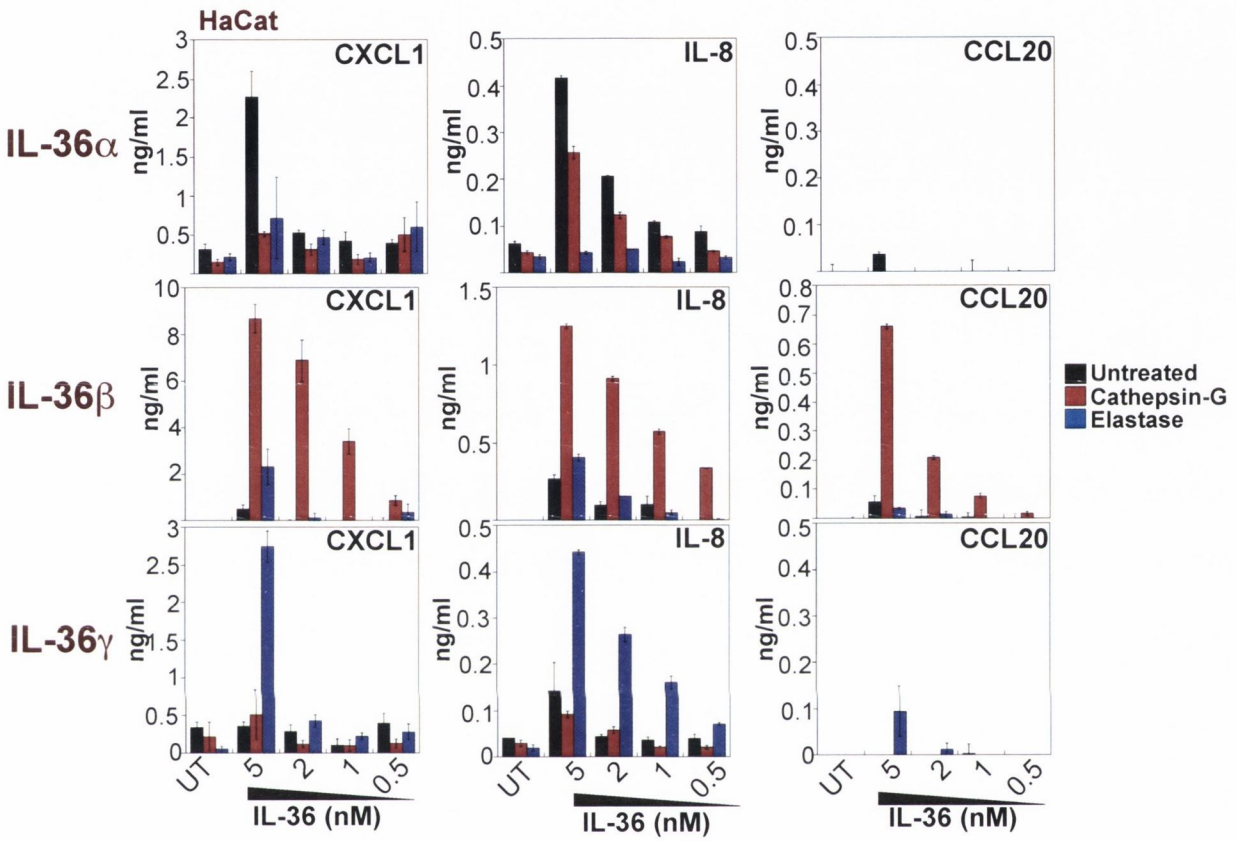


Figure 5.1 IL-36 cytokines are biologically active on HaCat keratinocytes
HaCat were stimulated with indicated concentrations of IL36α, β and γ pre-incubated for 2 h at 37° with cathepsin-G (50 nM), or elastase (100 nM). After 24 h, cytokine concentrations in culture supernatants were determined by ELISA.

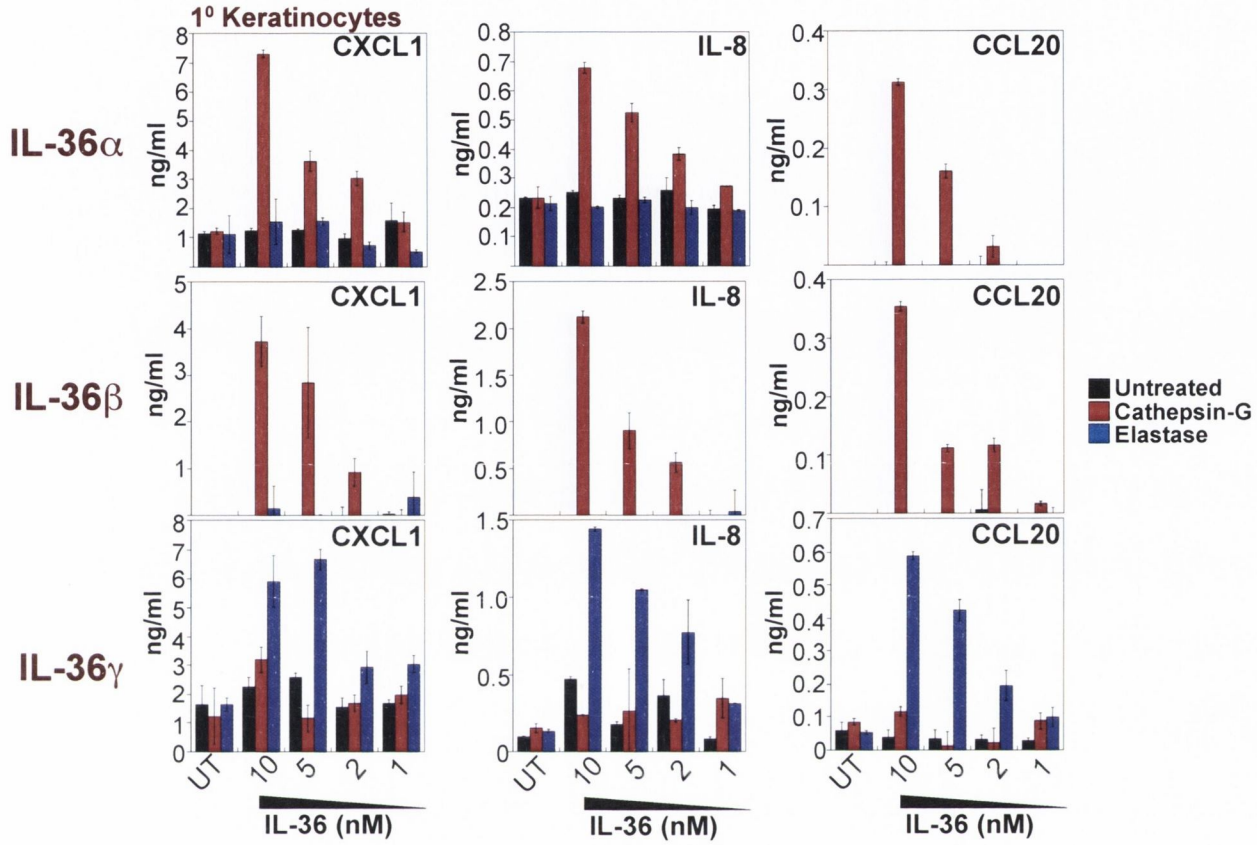


Figure 5.2 IL-36 cytokines are biologically active on primary keratinocytes
a. Primary keratinocytes were stimulated with indicated concentrations of IL36α, β and γ pre-incubated for 2 h at 37° with cathepsin-G (50 nM) or elastase (100 nM). After 24 h, cytokine concentrations in culture supernatants were determined by ELISA.

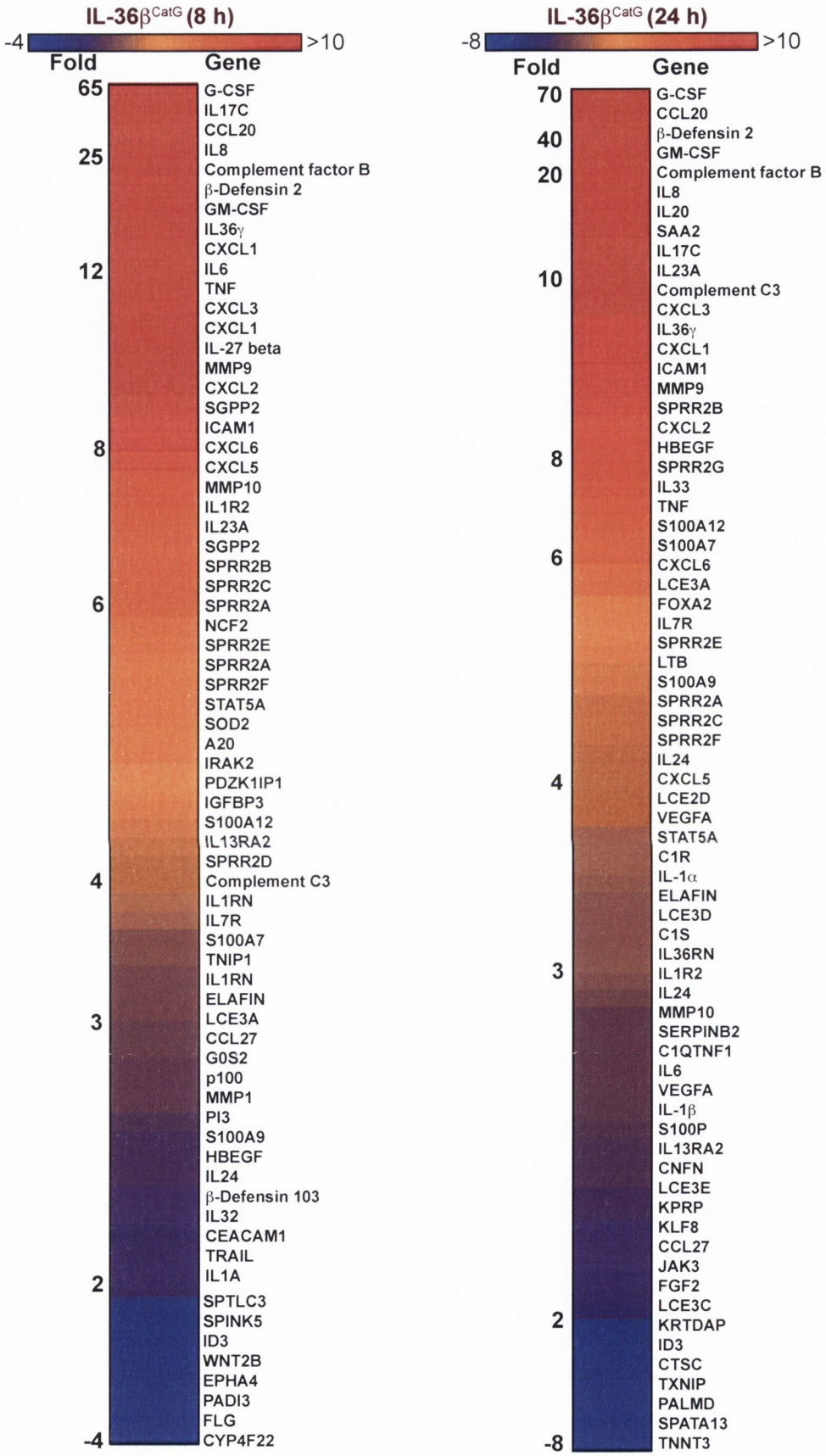


Figure 5.3 IL-36-induced gene expression array heat maps
Heat map analysis of significantly upregulated/downregulated genes from primary keratinocytes stimulated with IL-36β^{CatG} (5 nM) after 8 and 24 h.

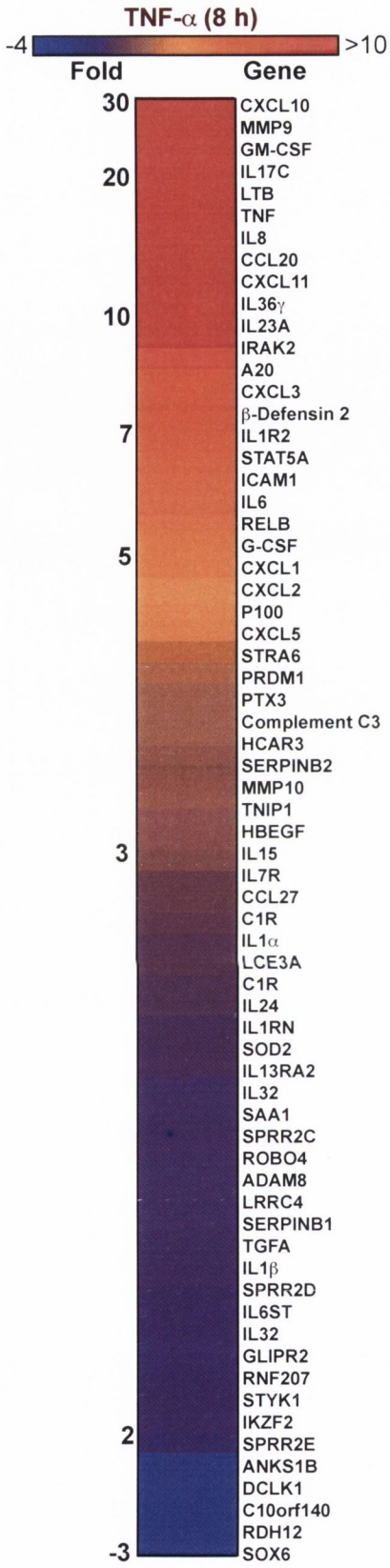


Figure 5.4 TNF-induced gene expression array heat map
Heat map analysis of significantly upregulated/downregulated genes from primary keratinocytes stimulated with TNF-α (10 ng/ml) after 8 h.

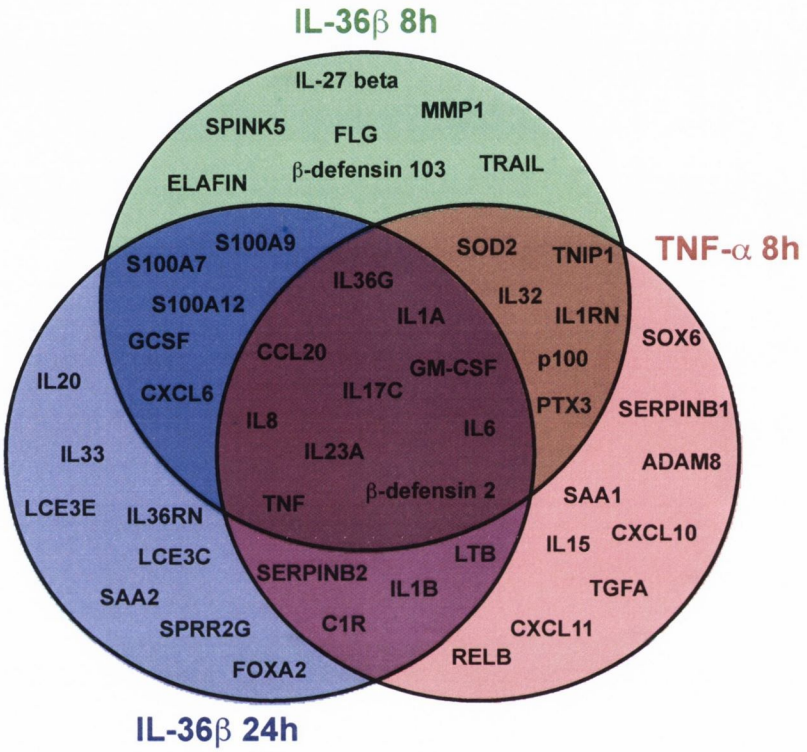


Figure 5.5 IL-36 and TNF induce distinct gene expression profiles with a subset of overlapping genes

Venn diamgrams of 67 genes from IL-36β (8 h), IL-36β (24 h) and TNF (8 h) datasets. Software website: *http://www.cmbi.ru.nl/cdd/biovenn/index.php*

driver of the pathology observed in psoriasis and related conditions (Carrozzi et al., 2011; Johnston et al., 2013). IL-36β also induced robust expression of multiple additional inflammatory factors, such as IL-17C, CCL20, β-defensin-2, S100A9, TNFα, and G-CSF, which are frequently elevated in lesional skin from psoriatic patients, as well as proteins required for differentiation such as small-proline rich repeat proteins (SPRR) (**Fig. 5.3**). Interestingly, we also found that IL-36β induced a strong signature of IL-36γ upregulation in primary keratinocytes, suggesting that this cytokine can promote a positive feedback loop for its own expression. Of particular note, we observed that the TNF gene expression array produced an overlapping but highly distinct pattern of pro-inflammatory gene expression compared with IL-36. As **Figures 5.5, 5.6** demonstrate, there are marked qualitative and quantitative differences between IL-36 and TNF.

5.2.3 Validation of genome wide gene array data

We subsequently validated several of these IL-36-induced genes identified in the gene array experiment at the mRNA level (**Fig. 5.7 a**), and at the protein level (**Fig. 5.7 b**). These data confirmed the hits we identified from the gene expression dataset. Interestingly, IL-17C can itself promote cytokine production from primary keratinocytes (**Fig. 5.8**), indicating that cytokines induced by IL-36 can themselves further propagate the inflammatory response through induction of multiple cytokines and chemokines.

5.2.4 Activated IL-36 does not modulate keratinocyte proliferation

Hyperproliferation and impairment of terminal differentiation of keratinocytes is one of the hallmarks of psoriasis (Frank & Nestle, 2009). Initially, we investigated whether IL-36 may be capable of modulating keratinocyte proliferation in a monoculture setting. We seeded keratinocytes at a low density in basal medium (low serum or lack of growth factors) conditions. As **Figure 5.9** shows, HaCat seeded in low serum media did not have an altered proliferation rate in the presence of activated IL-36. Similar data was found with primary keratinocytes (**Fig. 5.10)**.

5.2.5 Calcium-induced proliferative arrest and differentiation of keratinocyte monolayer is not modulated by IL-36

Calcium gradients within the epidermis are critical for normal differentiation of keratinocytes and serve as a potent terminal differentiation signal for these cells that results in proliferative arrest and upregulation of differentiation genes such as involucrin, filaggrin and transglutaminase. All mammalian epidermis displays a calcium gradient with low levels at the basal layer increasing steadily towards the upper granular layer and declining again in the cornified layer. We utilized this phenomenon of calcium-induced proliferative arrest to explore if IL-36 may modulate this effect. Initially, we titrated calcium onto keratinocytes in order to achieve an optimal concentration in which to see features of differentiation. As **Figure 5.11** shows, calcium as low as 0.5 mM induced pronounced morphological changes in keratinocytes that included flattening of the monolayer and becoming more elongated and wavy, indicative of a pronounced rearrangement of the cytoskeleton network. Next, we took an optimal dose of calcium (1.6 mM) and incubated cells in the presence or absence of IL-36. As **Figure 5.12** demonstrates, keratinocyes cultured in the presence of calcium, induce the expression of the differentiation marker involucrin, which became more extensively cross-linked in a time-dependent manner. Activated IL-36 did not appear to alter this differentiation process. Finally, we assessed the effect of IL-36 on proliferation in the presence or absence of calcium. As **Figure 5.13** shows, calcium dramatically arrested keratinocyte proliferation however IL-36 did not modulate this effect.

5.2.6 Activated IL-36 perturbs proliferation and differentiation in a three-dimentional (3D) skin model

A major caveat to the preceeding experiments was the fact that we were using a non-physioloigcal system in which to investigate keratinocyte proliferation. Co-culture of both keratinocytes and fibroblasts is required for optimal proliferation of keratinocytes as proliferation is highly dependent upon a complex

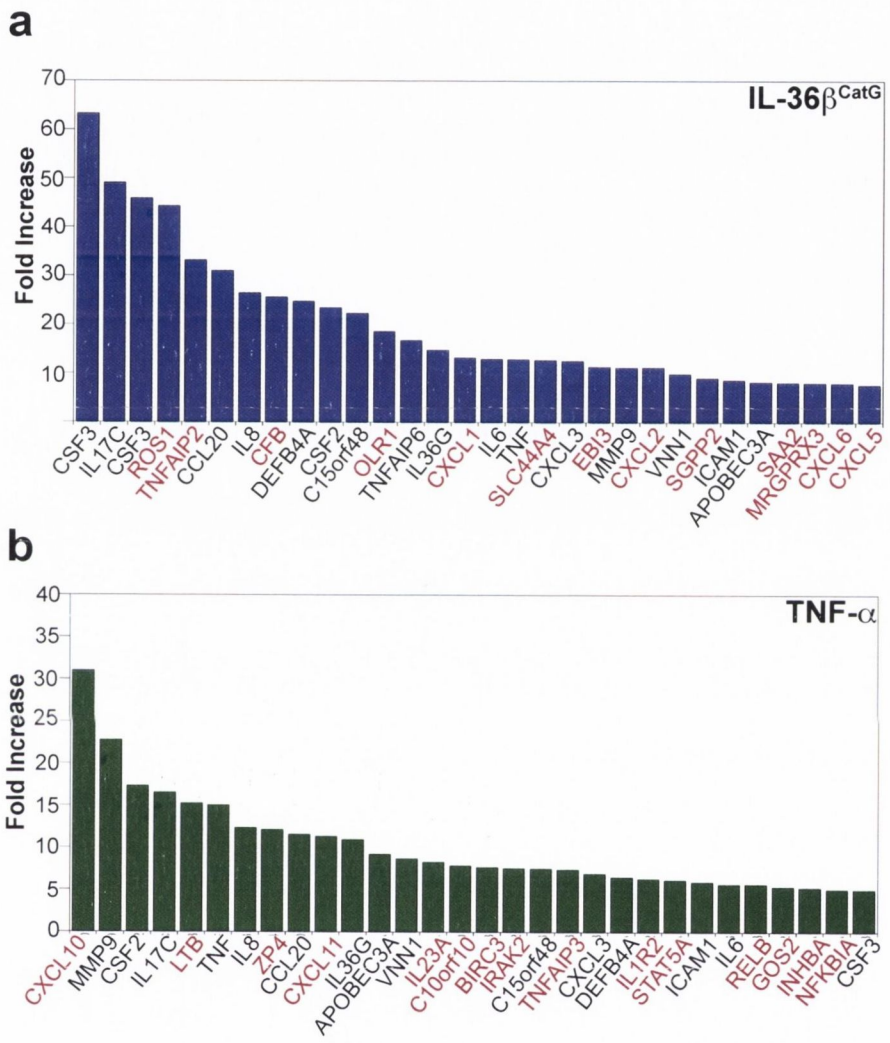


Figure 5.6 IL-36 and TNF display distinct pro-inflammatory gene profiles
(a-b) Comparison of fold expression of top 30 significantly upregulated genes from primary keratinocytes stimulated with IL-36β^{CatG} (5 nM) and TNF-α (10 ng/ml) after 8 h. NB: Highlighted in red are genes unique to the dataset analysed.

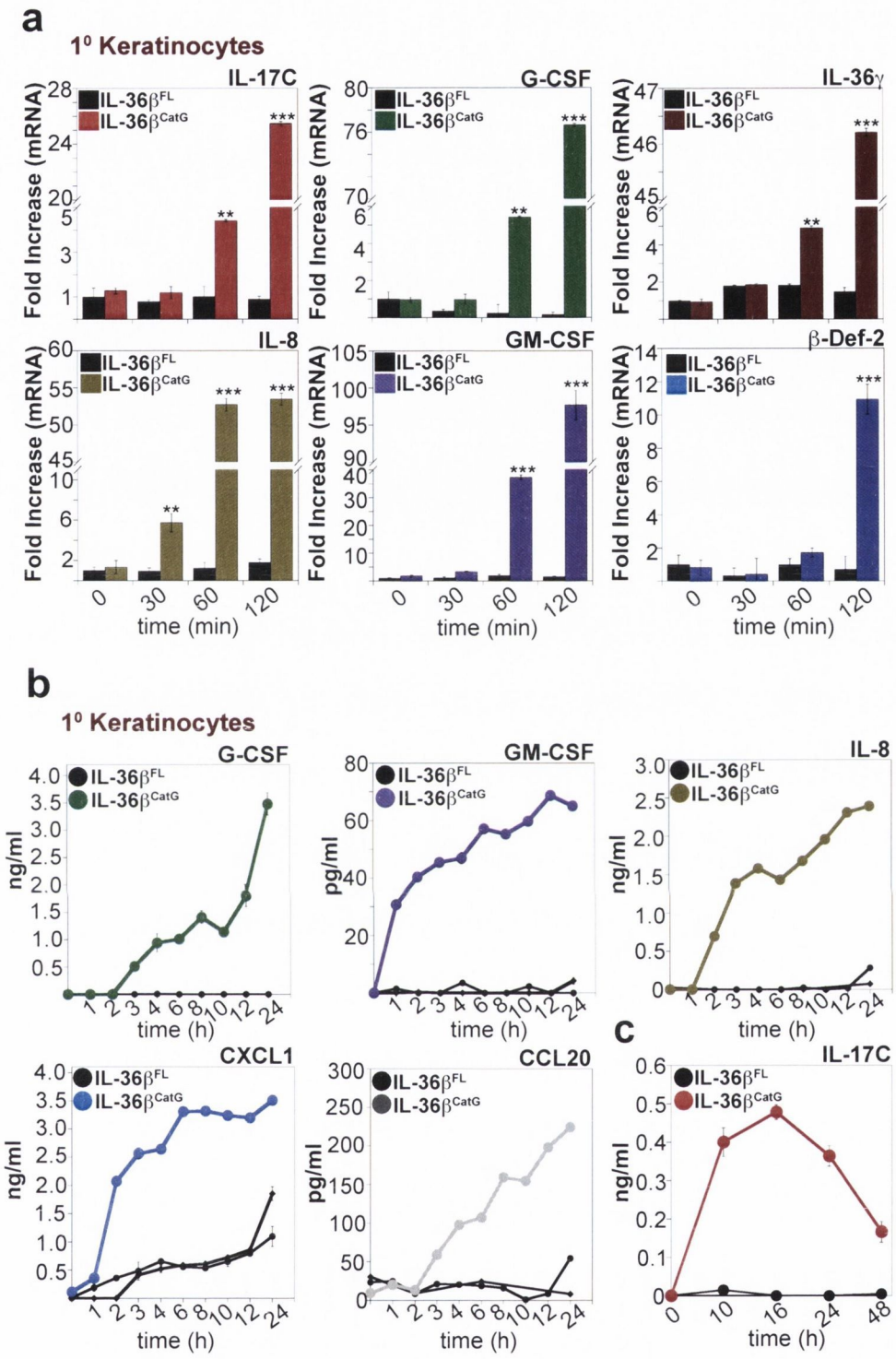


Figure 5.7 Primary keratinocytes upregulate multiple pro-inflammatory genes at both the RNA and protein level

a. Primary keratinocytes were stimulated with IL-36β^{FL} and IL-36β^{CatG} (5 nM). At indicated time-points levels of cytokine were determined by RT-PCR. **b.** Primary keratinocytes were stimulated with 5 nM IL-36β^{FL} and IL-36β^{CatG}. At indicated time-points concentrations of cytokine in the supernatant were determined by ELISA

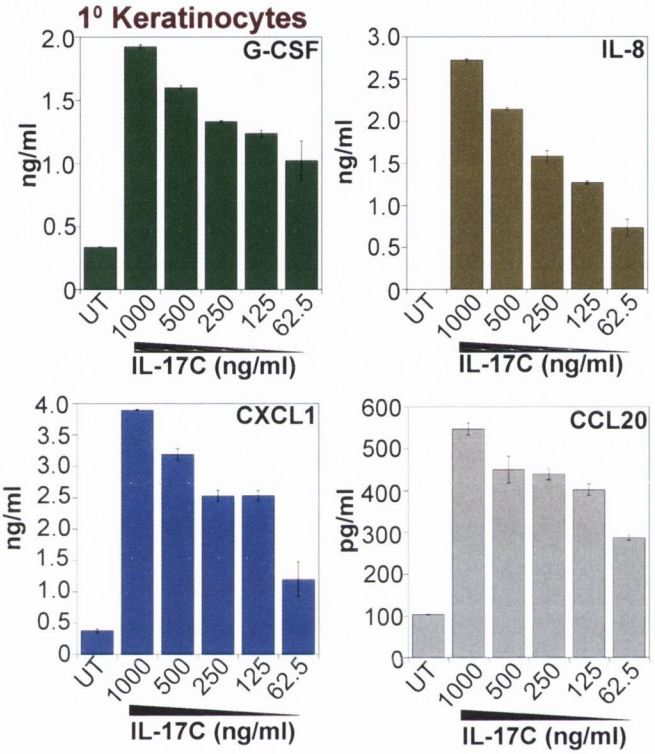


Figure 5.8 IL-17C promotes cytokine production from primary keratinocytes
Primary keratinocytes were stimulated with indicated concentrations of recombinant human IL-17C. After 48 h, cytokine concentrations in culture supernatants were determined by ELISA.

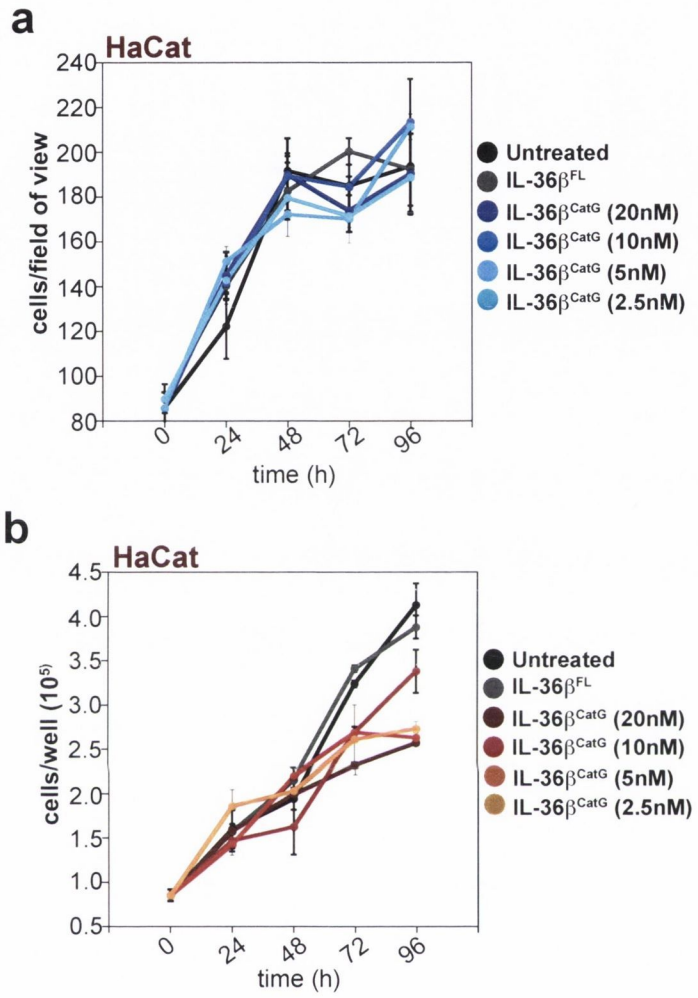


Figure 5.9 IL-36 does not modulate HaCat proliferation in monoculture
(a-b). HaCat were seeded in basal medium (DMEM +1 % FCS) and stimulated with indicated concentrations of IL-36β. Cells were counted per field of view **(a)** or trypinised and counted by haemocytometer **(b)** at indicated time-points. Data generated by Danielle Clancy (Martin Laboratory)

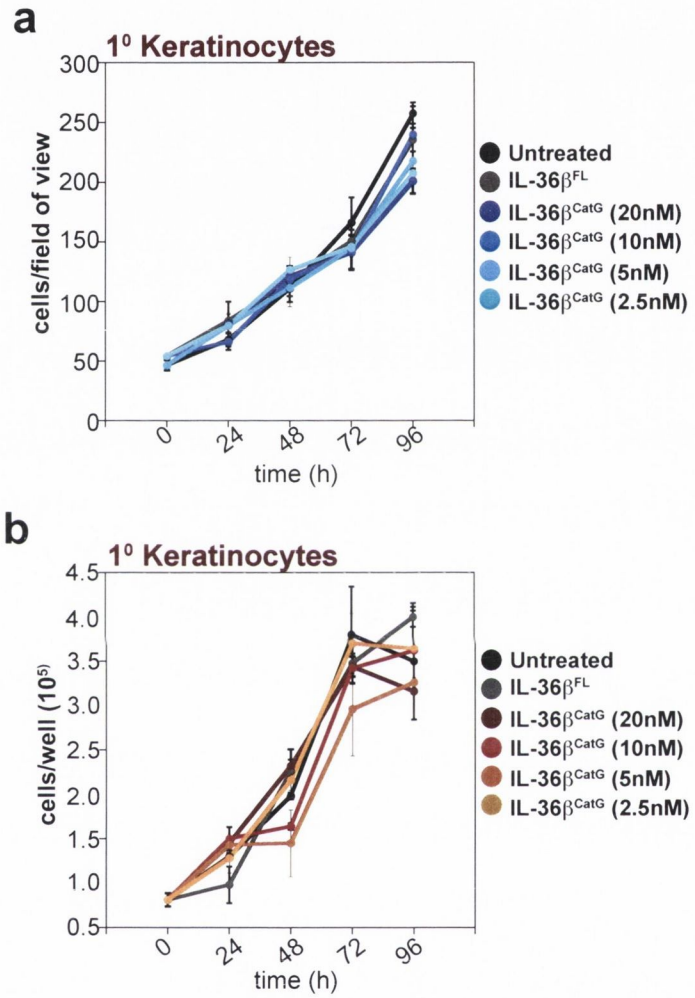


Figure 5.10 IL-36 does not modulate primary keratinocyte proliferation in monocluture

(a-b). Primary keratinocytes were seeded in basal medium and stimulated with indicated concentrations of IL-36β. Cells were counted per field of view **(a)** or trypinised and counted by haemocytometer **(b)** at indicated time-points. Data generated by Danielle Clancy (Martin Laboratory)

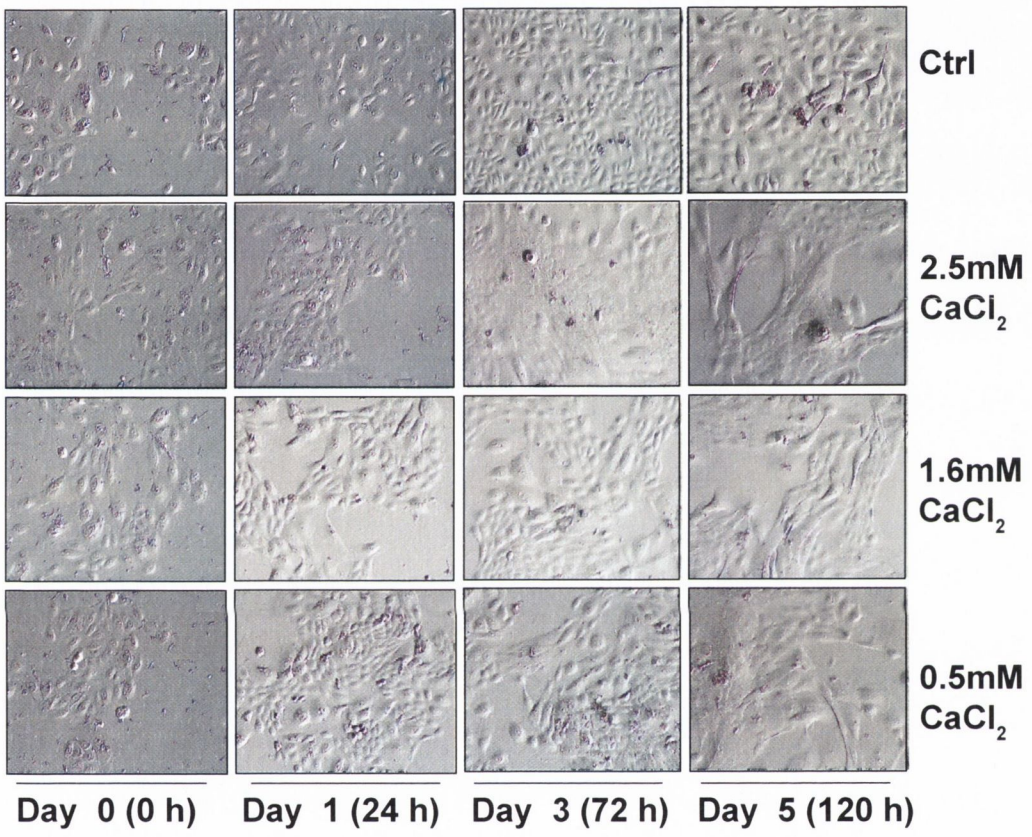


Figure 5.11 Morphological features of calcium-induced differentiation of primary keratinocytes

Keratinocytes seeded at $5x10^5$ on coverslips. $CaCl_2$ added to keratinocyte medium as indicated. Images acquired with phase microscope at indicated time-points.

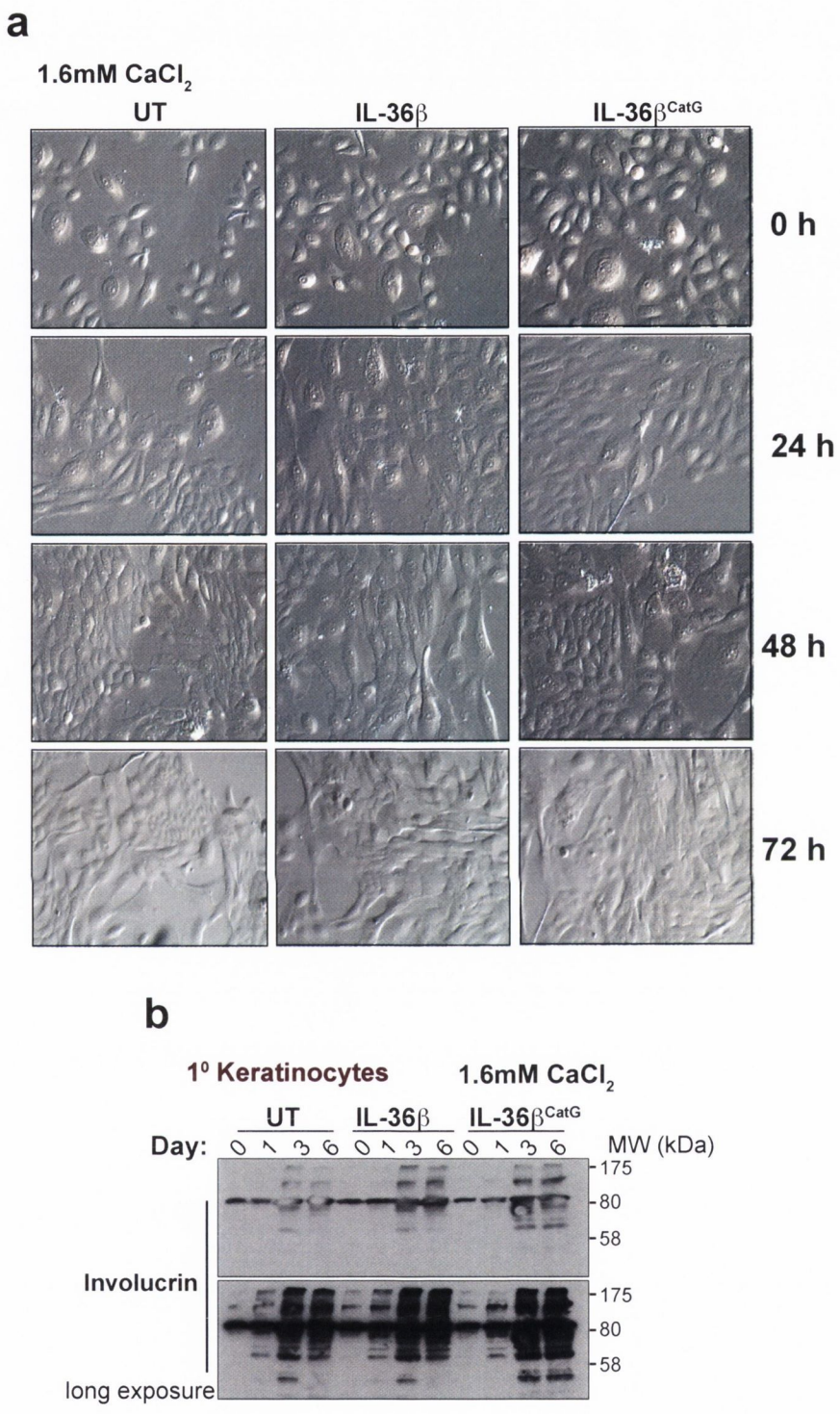


Figure 5.12 Calcium-induced differentiation or primary keratinocytes is not modulated by IL-36 in monoculture

a. Primary keratinocytes were treated with $CaCl_2$ (1.6 mM) over an indicated time-course in the presence or absence of IL-36β^{FL} or IL-36β^{CatG} (5 nM). **b.** Primary keratinocytes were incubated with $CaCl_2$ (1.6 mM) over the indicated time-course in the presence or absence of IL-36β^{FL} or IL-36β^{CatG} (5 nM). Indicated proteins were analysed by immunoblot.

interaction between both keratinocytes and dermal fibroblasts, which acts as a vital source of growth factors such as KGF, EGF and TGFα. Interestingly, it has been previously reported that keratinocytes only proliferate in an organtypic model when fibroblasts are present. Keratinocytes did not proliferate without fibroblasts even in the presence of exogenously added KGF or IL-1, highlighting the critical role of fibroblasts in this model (Maas-Szabowski et al., 2000). Furthermore, keratinocytes do not proliferate in monocultures in response to IL-1 stimulation, again suggesting that these cells require the presence of growth factors from fibroblasts not available to them otherwise (Maas-Szabowski et al., 1999). Therefore, to more accurately model an *in vivo* setting we used a 3D organtypic model to investigate any potential effects of IL-36 on proliferation and differentiation. Strikingly, using this system we found that activated IL-36β was sufficient to perturb normal epidermal proliferation and differentiation, producing features resembling psoriasis, such as diffuse epidermal hyperplasia and hyperkeratosis of the cornified layer (**Fig. 5.14**).

5.2.7 Human IL-36 is does not activate the mouse IL-36R

In order to address whether mouse IL-36 cytokines were activated by neutrophil proteases we needed to identify a mouse cell line that was IL-36 responsive. To achieve this, we cloned and purified a caspase-3 cleavable version of mIL-36β (mIL-36β^{DEVD}), to produce a truncated version of the protein previously described by Sims and colleagues (**Figure 5.15 a)**. Next, we incubated mIL-36β^{DEVD} with caspase-3 and could see robust proteolysis as determined by Coomassie stained gel (**Figure 5.15 a**). Using this active form of mIL-36β, we identified mouse embryonic fibroblasts (MEFs) as a mIL-36-responsive cell line (**Figure 5.15 d**). Importantly, cathepsin-G activated human IL-36β is not capable of inducing cytokine from MEFs even at high molar concentrations (**Figure 5.15 d**). These data suggest that human IL-36 is unable to signal through the mouse IL-36R.

5.2.8 Mouse IL-36β is cleaved but not activated by neutrophil proteases

Following the identification of a mouse cell line capable of responding to IL-36 we were in a position to test whether neutrophil proteolysis and activation of IL-36β is conserved between human and mouse. Initially, we assessed proteolysis by autoradiography and found that mIL-36β was cleaved when incubated with activated neutrophil degranulates, however mIL-36β^{DEVD} was not processed under the same conditions, suggesting proteolysis in the N-terminal region of the protein (**Fig. 5.15 b, c**). Next, we assessed the impact of proteolysis of mIL-36β using the MEF bioassay. As **Figure 5.16 a, b** demonstrate, neutrophil proteases do not activate mIL-36β under conditions where the cells were responding to the mIL-36β^{DEVD} version of the protein. These data suggest that mIL-36β is cleaved by neutrophil proteases but does not generate an active cytokine.

5.2.9 Endogenous IL-36 cytokines are induced by IL-36 and TLR signalling

As discussed previously, the phenotype of deregulated IL-36 signalling is most apparent in the epidermis. In addition, RT-PCR datasets from a number of screens of psoriatic patient tissue have indicated that IL-36 cytokines are overexpressed. To explore the expression of endogenous IL-36 proteins in keratinocytes, we generated polyclonal antibodies against all three IL-36 cytokines (**Fig. 5.17**). Whereas little endogenous IL-36α or β could be detected constitutively, IL-36γ was detected in primary keratinocytes (**Fig. 5.18 a, b**). However, treatment of these cells with IL-36, PMA or the TLR3 agonist Poly:(IC) robustly induced the expression of endogenous IL-36γ (**Fig. 5.18 a, b**). HaCat cells were also found to upregulate IL-36γ after IL-36 and PMA treatment (**Fig. 5.19**). Primary human keratinocytes are reported to express the full-length forms of pro-IL-1α and pro-IL-1β at the protein level. Indeed, we detected both pro-IL-1α and pro-IL-1β constitutively expressed in primary keratinocytes. Furthermore, these cytokines were upregulated further in response to IL-36 and Poly:(IC) (**Fig. 5.18**). Similar observations were made with HaCat cells (**5.19**).

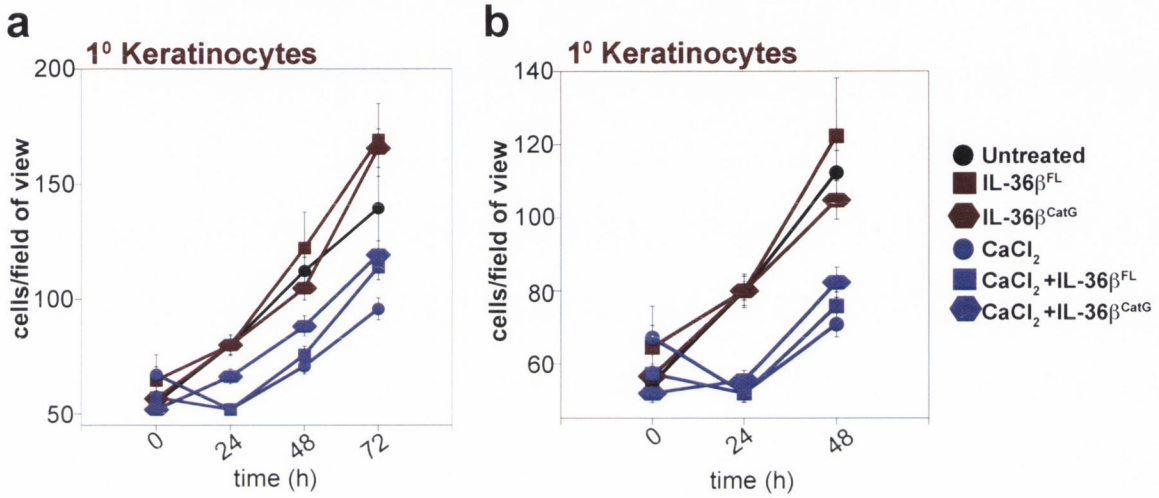


Figure 5.13 IL-36 does not modulate primary keratinocyte proliferation in the presence of calcium

a. Primary keratinocytes (1 x 10^4) were incubated in the presence or absence of $CaCl_2$ (1.6 mM) and stimulated with IL-36β^{FL} or IL-36β^{CatG} (5 nM) over the indicated timecourse. **b.** Primary keratinocytes (0.5 x 10^4) were incubated in the presence or absence of $CaCl_2$ (1.6 mM) and stimulated with IL-36β^{FL} or IL-36β^{CatG} (5 nM) over indicated timecourse. Cells were counted in triplicate field of view

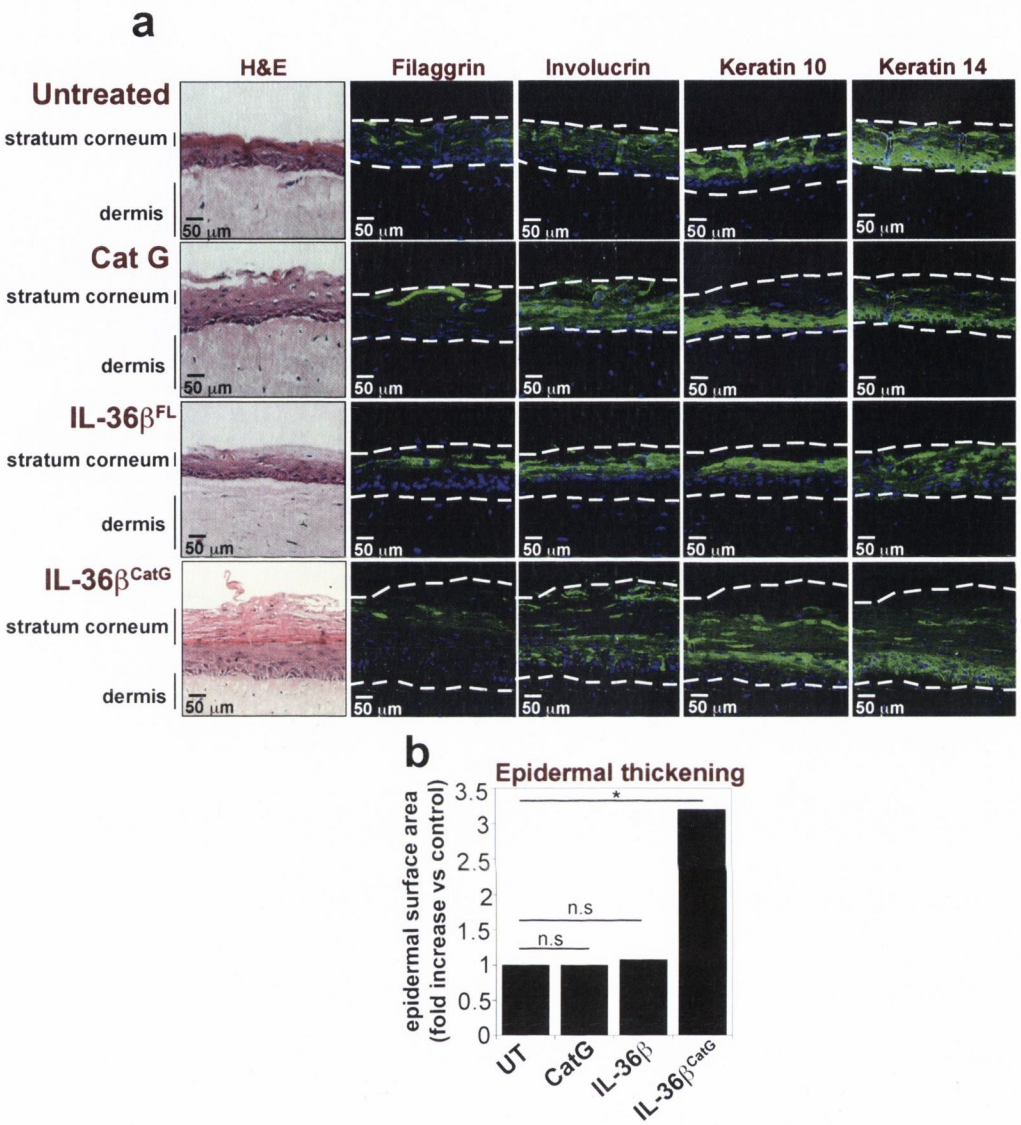


Figure 5.14 Activated IL-36 impairs differentiation in a 3D organotypic skin model
a. Organotypic skin reconstructs cultivated at the air to liquid interface were topically stimulated with either cathepsin-G alone (We applied 2 µl in 10 µl MM), 0.5 nM and 2 nM IL-36β^{FL} or IL-36β^{CatG} in a volume of 10 µl MM, respectively, every other day. Application of 10 µl MM only served as negative control. After 15 days skin reconstructs were harvested, fixed in paraffin, and sections stained with H&E, against filaggrin, involucrin, cytokeratin 10 and 14 as indicated to display epidermal thickness and differentiation. **b.** Quantification of epidermal thickness using IMAGEJ software.

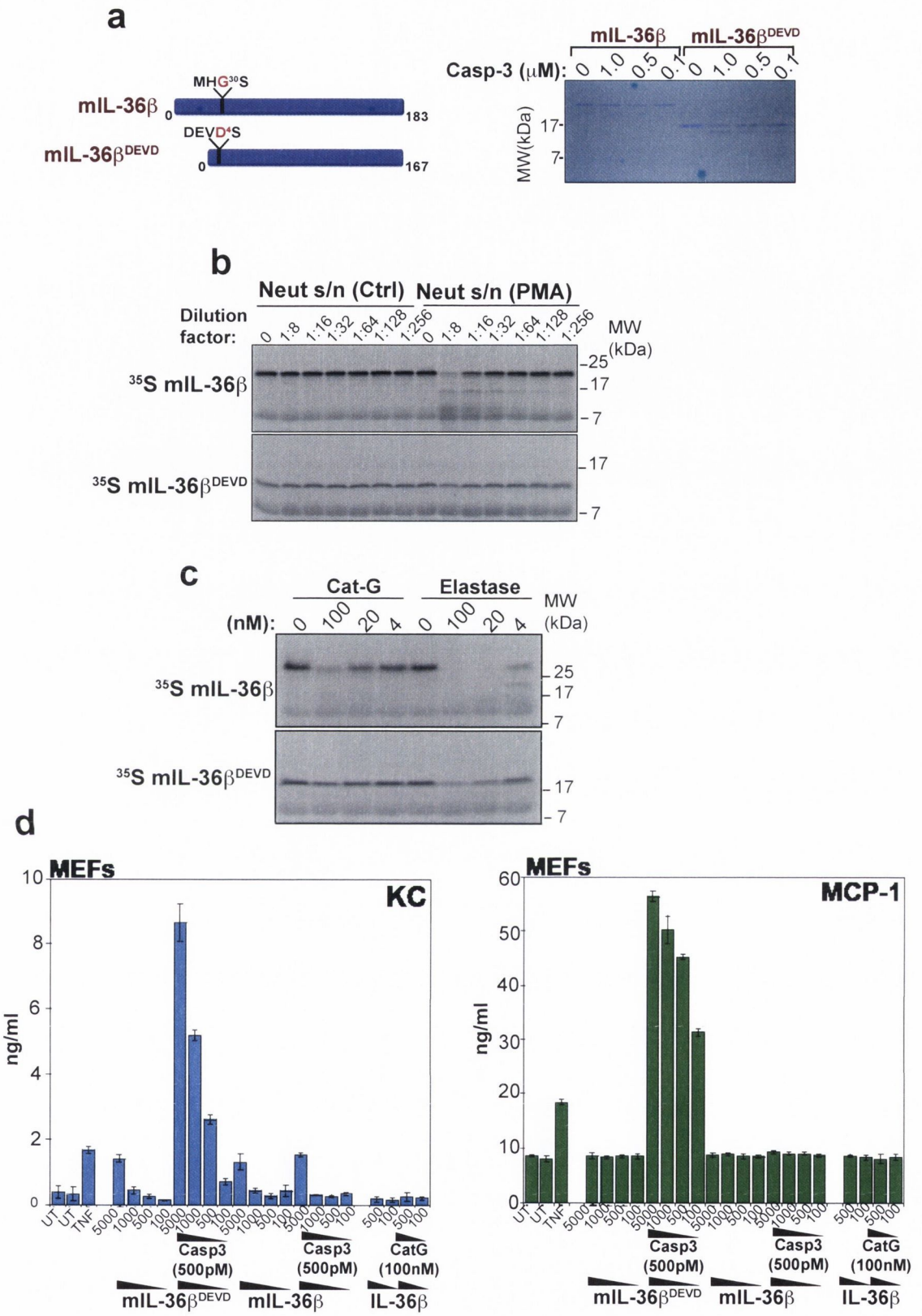


Figure 5.15 Mouse IL-36β is cleaved by neutrophil proteases

a. Schematic of modified form of mIL-36β where a caspase-3-processing motif (DEVD) was inserted into the IL-36 sequence, N-terminal to the known processing sites. mIL-36β and DEVD-mIL-36β were incubated at 37°C for 2 h, either alone or in the presence of indicated concentrations of recombinant caspase-3, followed by analysis by Coomassie staining **b.** mIL-36β was incubated with indicated concentrations of neutrophil degranulate s/n or cat-G or elastase (c) at 37°C for 2 h, followed by analysis by autoradiography gel. **d.** MEFs were stimulated with indicated concentrations of either mouse IL-36β^{DEVD}, mouse IL-36β, or human IL-36β. After 24 h, cytokine concentrations in culture supernatants were determined by ELISA.

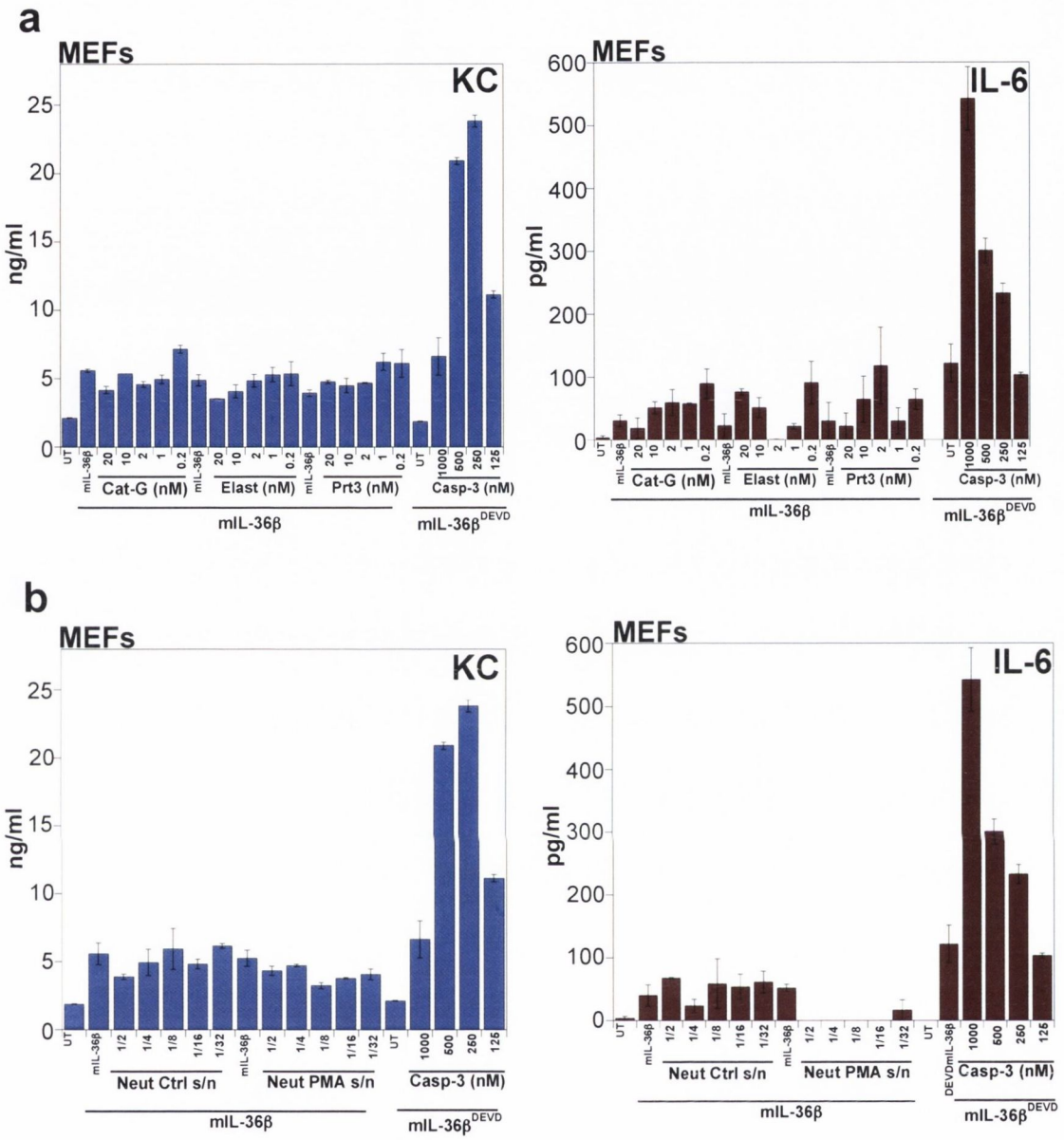


Figure 5.16 Mouse IL-36β is not activated by neutrophil proteases
a-b. MEFs were stimulated with indicated concentrations of either mouse IL-36β^{DEVD}, mouse IL-36β cleaved with a titration of cat-G, elastase (a), or neutrophil degranulates (b). After 24 h, cytokine concentrations in culture supernatants were determined by ELISA.

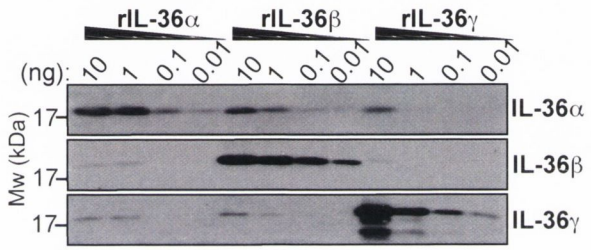


Figure 5.17 Validation of rabbit polyclonal antibodies raised against IL-36 proteins
Specificity and cross-reactivity of IL-36 rabbit polyclonal antibodies were tested against indicated protein amounts of recombinant IL-36 ligands.

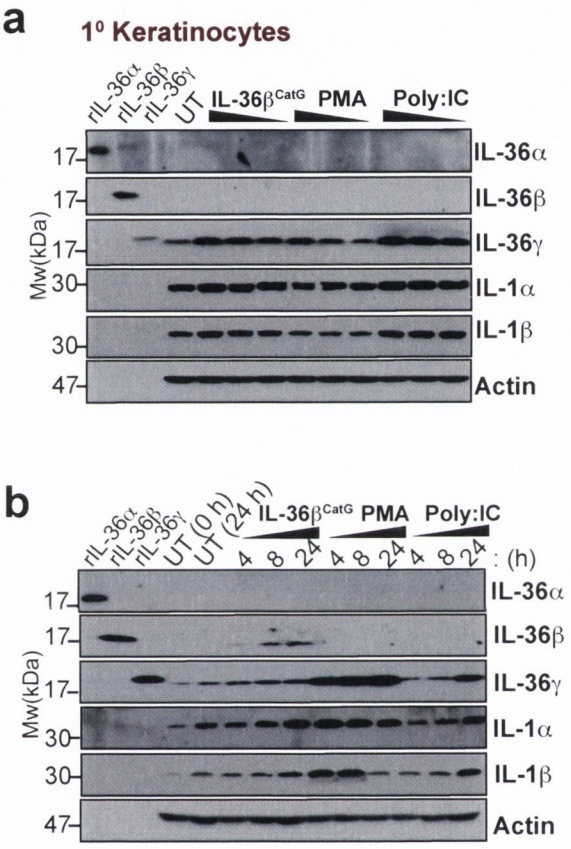


Figure 5.18 IL-36 stimulates upregulation of IL-1 family cytokines in primary keratinocytes in a dose and time-dependent manner

a. Primary keratinocytes were treated with a titration of IL-36β^{CatG} (10, 5, 2.5 nM), PMA (40, 20, 10 nM) and Poly:IC (100, 50, 25 μg/ml). Recombinant IL-36 (500pg) serves as a positive control for each immunoblot. **b.** Primary keratinocytes were treated with fixed concentrations of IL-36β^{CatG} (5 nM), PMA (20 nM) and Poly:(IC) (100 μg/ml) over indicated time-points. Recombinant IL-36 (500 pg) serves as a positive control for each immunoblot.

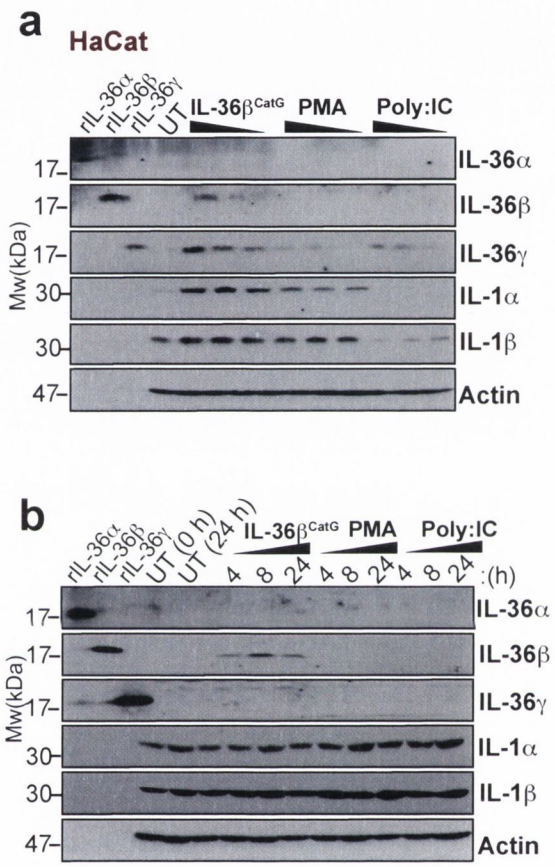


Figure 5.19 IL-36 stimulates upregulation of IL-1 family cytokines in HaCat in a dose and time-dependent manner

a. HaCat were treated with a titration of IL-36β^{CatG} (10, 5, 2.5 nM), PMA (40, 20, 10 nM) and Poly:IC (100, 50, 25 μg/ml). Recombinant IL-36 (500 pg) serves as a positive control for each immunoblot. **b.** HaCat were treated with fixed concentrations of IL-36β^{CatG} (5 nM), PMA (20 nM) and Poly:IC (100 μg/ml) over indicated time-points. Recombinant IL-36 (500 pg) serves as a positive control for each immunoblot.

5.2.10 Calcium-induced differentiation upregulates endogenous IL-36 expression

In vivo keratinocytes comprise the bulk of the epidermis, with defined layers within the epidermis under the control of a complex differentiation gene cascade. We were intrigued by the possibility that IL-36 expression may be altered during keratinocyte differentiation. To address this issue, we treated primary keratinocytes with different concentrations of calcium and followed the cells over a number of days. As **Figure 5.20** demonstrates, cells undergoing differentiation, evident by cross-linked involucrin, dramatically upregulate IL-36γ. These preliminary data raise the possibility that the 'DAMP profile' of the epidermis is dependent upon the differentiation state of keratinocytes, with cells of the lower epidermis (low calcium) having less IL-36 relative to the upper layers of epidermis.

5.2.11 IL-1 cytokines are released during necrotic cell death

IL-1 proteins lack a secretory signal and so how this important group of cytokines get into the extracellular space in order to mediate inflammatory responses has been a subject of intense debate. Necrotic cell death, or the sudden rupture of the plasma membrane is thought to be the major way in which IL-1 cytokines are released (Kono & Rock, 2008; Luthi et al., 2009; Martin et al., 2012; Bersbaken & Fink, 2009; Lamkanfi & Dixit, 2014). As previously mentioned, necrosis of tissue represents a gross departure from normal homeostasis and is indicative of pathogen activity that may result in the increased risk of infection. Therefore, it is entirely appropriate that our immune systems have evolved to respond to necrosis. To assess the behaviour of IL-1 proteins during necrosis, we treated primary keratinocytes with streptolysin-O (SLO), a strepotocccol-derived lytic protein, capable of inducing necrosis in cells. As **Figure 5.21 a** demonstrates, SLO induced necrosis of keratinocytes in a dose-dependent manner. We immunoblotted the supernatants and cell pellets and found that endogenous IL-1α, IL-1β and IL-36 were released as cells underwent

necrosis. IL-1 proteins were also released in their full-length forms suggesting that these proteins do not undergo proteolysis by endogenous proteases during necrosis. In addition, we also observed the release of other cytoplasmic proteins, such as cullin-3 and actin, indicative of the non-selective nature of membrane permeabilization during necrosis (**Fig. 5.21 a**). We also observed similar results using another necrosis-inducing agent LLOme (**Fig 5.21 b**).

5.2.12 Endogenous IL-36γ is cleaved by neutrophil proteases

To explore if IL-36γ is subject to cleavage by neutrophil elastase both intracellularly and extracellularly, we generated cell extracts and supernatants followed by incubation with neutrophil proteases. As **Fig. 5.22** illustrates, IL-36γ incubated with elastase resulted in robust IL-36γ proteolysis both intracellularly as well as extracellularly, with the resulting cleavage fragments running at a similar mobility to that produced through proteolysis of recombinant IL-36γ by elastase. Endogenous pro-IL-1α was also cleaved by elastase to generate a ~p17 fragment, while pro-IL-1β was cleaved by both elastase and cathepsin-G to generate ~p17 fragments similar to the caspase-1 generated form (**Fig. 5.22**). Furthermore, endogenous IL-36γ was also cleaved by neutrophil degranulates (**Fig. 5.23**). Collectively, these data indicate a conserved role for IL-1 cytokines as targets of neutrophil serine proteases.

5.2.13 Overexpressed IL-36 is cleaved and activated by neutrophil proteases

To further explore the effects of IL-36 in a cellular context, we overexpressed IL-36 proteins in 293T cells. As **Figure 5.24 a** shows, GFP-IL-36β and IL-36γ contructs are very well expressed in 293T. To assess proteolysis of overexpressed IL-36 proteins, we prepared necrotic lysates through SLO lysis of 293T, and incubated them with neutrophil proteases. As **Figure 5.24 b** demonstrates we see robust IL-36β and γ proteolysis, with the resulting cleavage fragments running at a similar mobility to that produced through proteolysis of recombinant IL-36 proteins. Furthermore, we incubated HeLa^{IL36R} cells with IL-36

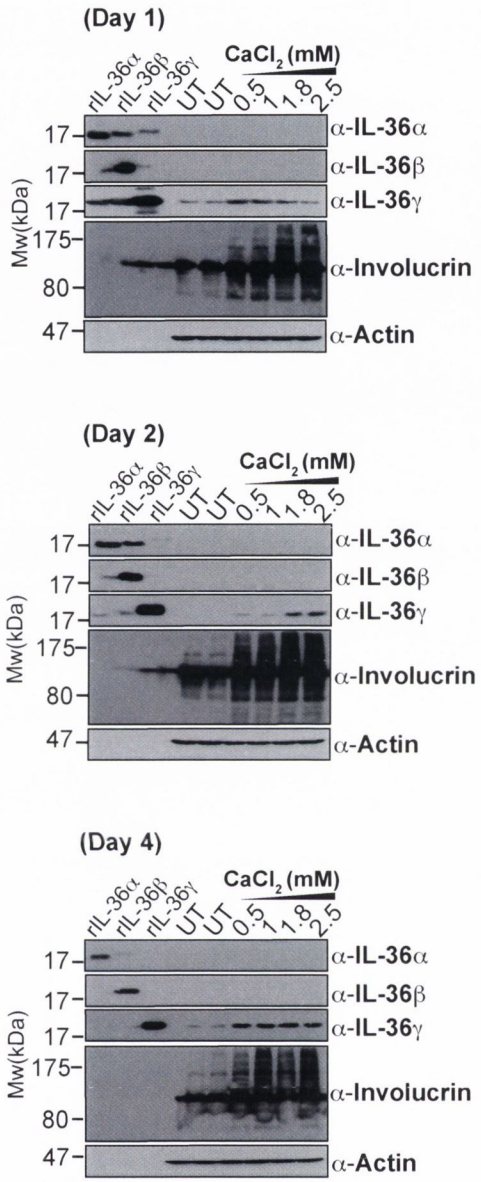


Figure 5.20 Expression of IL-36 proteins during calcium-induced differentiation of primary keratinocytes

Primary keratinocytes were stimulated with indicated concentrations of $CaCl_2$ and lysates were taken at indicated time-points. Indicated protein were analysed by immunoblot. Recombinant IL-36 (500pg) serves as a positive control for each immunoblot.

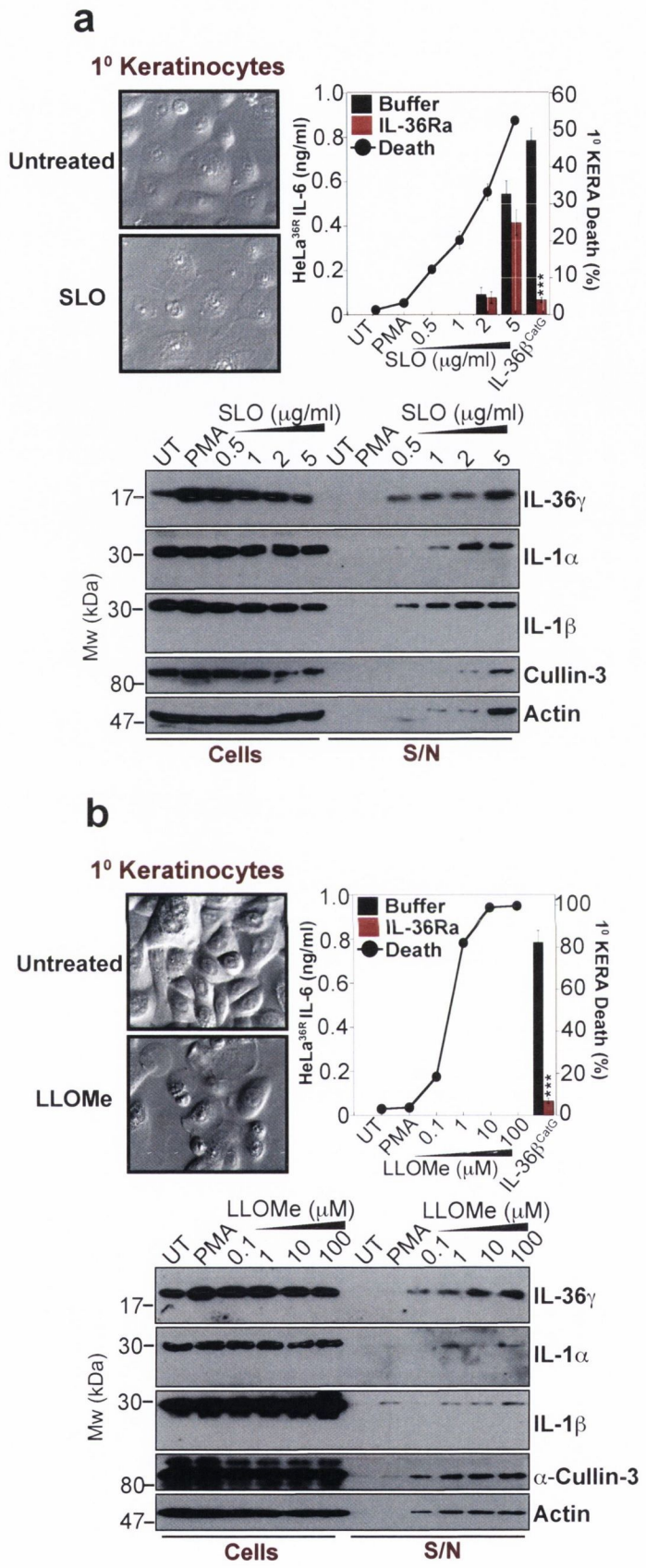


Figure 5.21 IL-36 is released during necrosis of primary keratinocytes a. Primary keratinocytes were incubated in the presence or absence of PMA (20 nM) for 12 h. Cells were then lysed over 1 h with indicated concentrations of SLO. Cells and supernatants were analysed for indicated proteins by immunoblot. **b.** Treated as in (a), then lysed for 1 h with LLOMe with indicated concentrations. Cells and supernatants were analysed for indicated proteins by immunoblot.

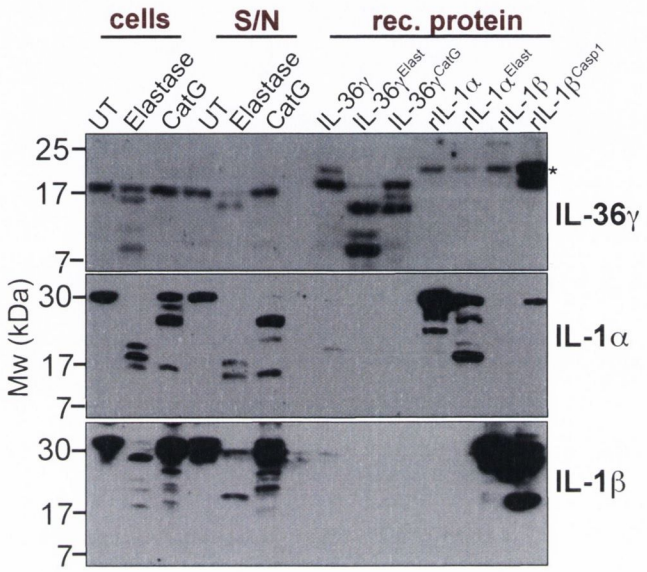


Figure 5.22 Endogenous IL-1 family cytokines are cleaved by neutrophil proteases
Primary keratinocytes were incubated in the presence of PMA (20 nM) for 12 h. Cells were disrupted by sonication (cells) or SLO-lysed cell supernatant (S/N), followed by incubation with elastase (100 nM) or cathepsin-G (50 nM). Cells and supernatants were analysed for indicated proteins by immunoblot. Recombinant proteins served as controls for proteolysis.

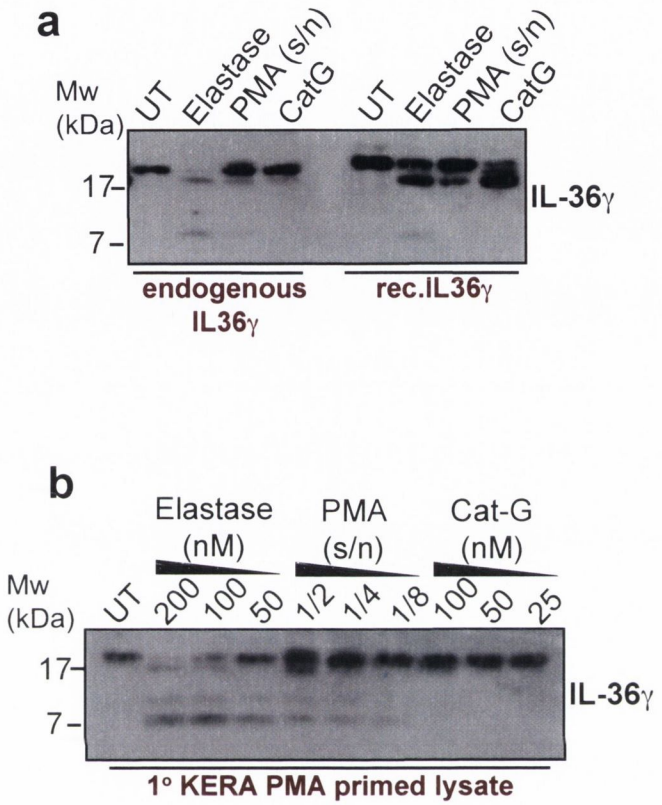


Figure 5.23 Endogenous IL-36γ is cleaved by elastase and neutrophil degranulates
a. Primary keratinocytes were incubated in the presence PMA (20 nM) for 12 h. Cells were disrupted by SLO lysis, followed by incubation with elastase (100 nM), neutrophil degraulate (PMA S/N) (1/4 dilution), or cathepsin G (50 nM). **b.** Primary keratinocytes were incubated in the presence of PMA (20 nM) for 12 h. Cells were disrupted by SLO lysis, followed by incubation with indicated concentrations of elastase, neutrophil degraulate (PMA S/N), or cathepsin-G (50 nM). Supernatants were analysed for indicated proteins by immunoblot.

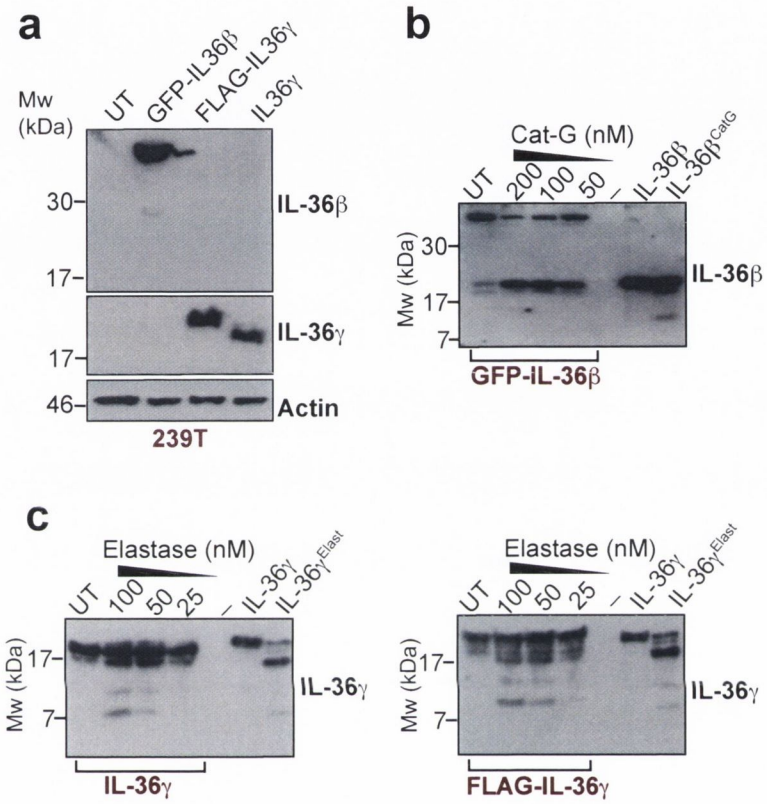


Figure 5.24 IL-36 cytokines are cleaved by neutrophil proteases in 293T lysates
a. 293T were transfected with vector (2 μg plasmid), GFP-IL-36β (2 ug plasmid), IL-36γ (2 ug plasmid) or FLAG-IL-36γ (2 ug plasmid). After 48 h, lysates were analysed for indicated proteins by immunoblot. **b.** 293T-GFP-IL-36β lysates were incubated with indicated concentrations of cathespin-G. Lysates were analysed for indicated proteins by immunoblot. **c.** 293T-IL-36γ & 293T-FLAG-IL-36γ lysates were incubated with indicated concentrations of elastase. Lysates were analysed for indicated proteins by immunoblot.

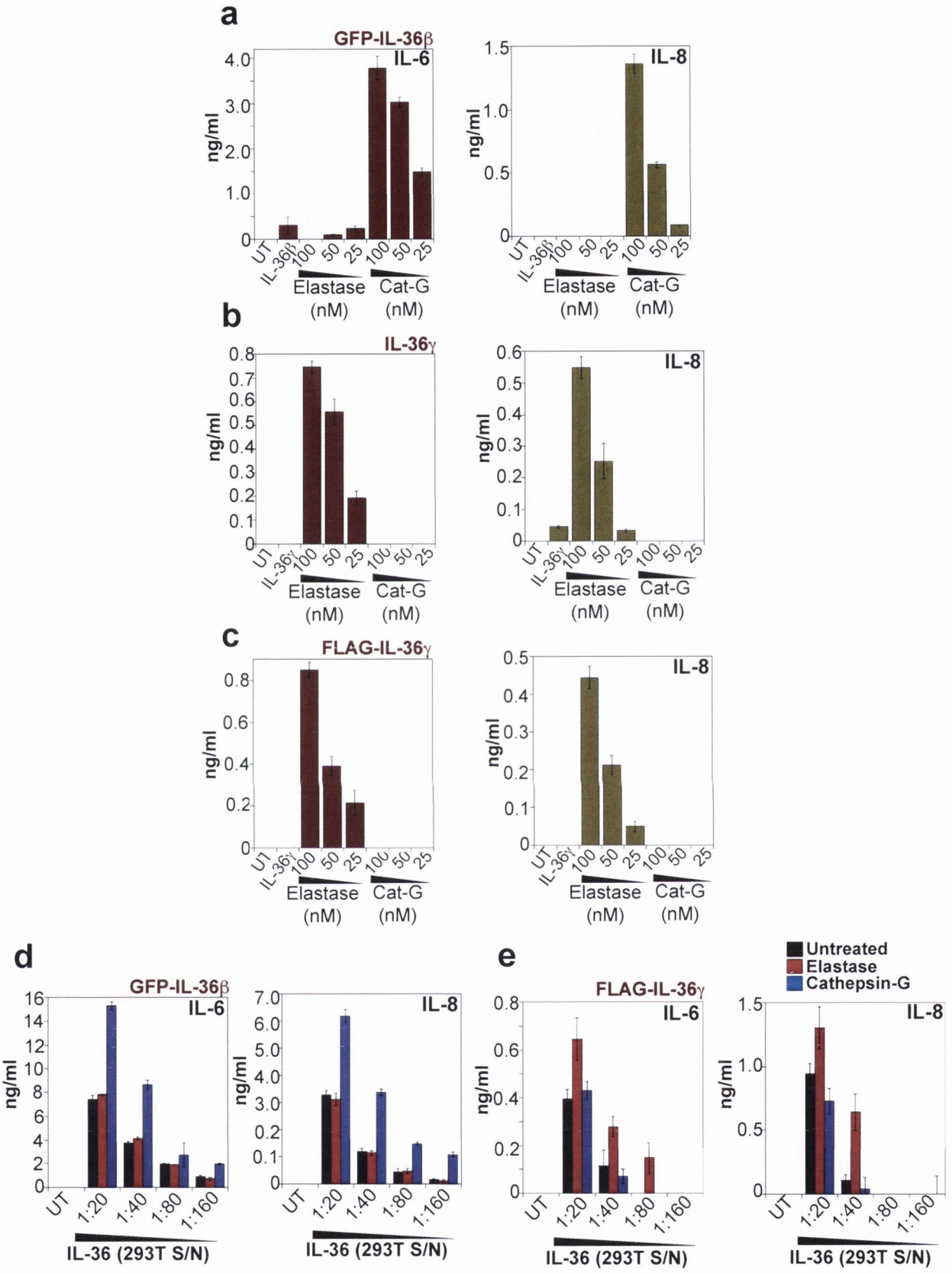


Figure 5.25 IL-36 cytokines are activated by neutrophil proteases in 293T lysates
a-c. 293T were transfected with GFP-IL-36β (2 ug plasmid), IL-36γ (2 ug plasmid) or FLAG-IL-36γ (2 ug plasmid). After 48 h, cells were lysed with SLO (5 ug/ml) and incubated with indicated concentrations of cathespin-G and elastase followed by addition (1/80 dilution) to HeLa$^{IL\text{-}36R}$. **(d-e)** Cells were lysed with SLO (5 ug/ml) and incubated with cathespin-G (100 nM) and elastase (50 nM) followed by titration of lysates onto HeLa$^{IL\text{-}36R}$. After 24 h, cytokine concentrations in culture supernatants were determined by ELISA.

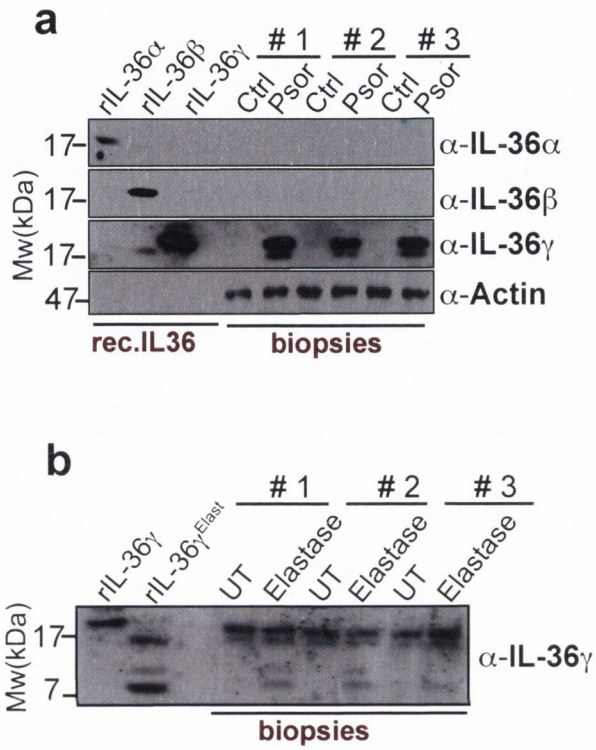


Figure 5.26 IL-36γ is highly expressed in biopsy samples from patients with plaque psoriasis
a. Uninvolved and involved psoriatic lysates were analysed for indicated proteins by immunoblot. Recombinant IL-36 (500pg) serves as a positive control for each immunoblot. **b.** Involved psoriatic lysates were incubated with elastase (100 nM) for 30 min at 37^0 and analysed for indicated proteins by immunoblot.

derived from 293T and could see robust activation of cathepsin-G cleaved IL-36β and elastase cleaved IL-36γ (**Fig. 5.25**).

5.2.14 IL-36γ is greatly elevated within lesional skin from psoriasis patients

To explore whether IL-36 cytokines were present in lesional skin from psoriatic individuals, we generated homogenates from skin samples obtained from uninvolved as well as involved areas from three psoriasis patients. As **Figure 5.26 a** shows, these experiments revealed that IL-36γ was greatly elevated in psoriatic tissue, while IL-36α and IL-36β were undetectable in these patient samples. Furthermore, incubating these psoriatic homogenates with neutrophil elastase resulted in IL-36γ proteolysis, with the resulting cleavage fragments running at a similar mobility to that produced through proteolysis of recombinant IL-36γ (**Fig. 5.26 b**).

5.3 Discussion

5.3.1 Proteolytic processing of IL-36 drives a potent inflammatory response in primary keratinocytes

It has previously been shown for IL-1 cytokines that proteolysis has dramatic effects on their biological activity. IL-1β and IL-18 require proteolysis by caspase-1 to unlock their potent biological activity, while IL-1α and IL-33, which have activity as full-length molecules, can gain further biological activity through proteolysis from a diverse set of proteases such as calpain, elastase, cathepsin-G and granzyme-B. We have demonstrated in the previous chapter that IL-36 proteins are also subject to this proteolytic switch mechanism. In order to gain an insight into the range of inflammatory effects of active IL-36, we sought to explore IL-36-induced inflammation in a physiological relevant cell type. Keratinocytes are the most abundant cell type in the epidermis and through a tightly controlled differentiation programme form the protective outer cornified layer, which acts as the front line of defence against potential threats from the outside world. These cells not only serve as a physical barrier to exterior insults, but also are highly immunocompetent cells in their own right, capable of detecting diverse pathogen challanges through expression of multiple pathogen recognition receptors such as TLRs and NODs (Pasparakis et al., 2014). It is now well appreciated that keratinocytes are capable of directly responding to damage or infection by releasing a number of key cytokines, such as IL-1α, IL-1β and IL-36 cytokines, to activate local macrophages and dendritic cells (Vigne et al., 2012; Pasparakis et al., 2012). We conducted genome wide expression array analysis of keratinocytes treated with active IL-36 and TNF, choosing the latter cytokine for its well established role in skin inflammatory conditions, most notably in the use of anti-TNF therapies in the treatment of inflammatory skin conditions, such as psoriasis. We found that activated IL-36 induced a potent gene expression programme that included a wide variety of gene subsets, such as pro-inflammatory cytokines and chemokines, inflammatory related transcription factors and differentiation-related genes (**Appendix II**). A striking feature of the

gene profile induced by IL-36 was the extent of inflammatory related cytokines and chemokines, such as TNF, IL-6, GM-CSF, IL-8, β-defensin, S100 proteins, IL-36γ, and IL-17C, that have been repeatedly implicated in skin inflammatory conditions, in particular psoriasis. We further validated a subset of these 'hits' from our gene expression dataset by RT-PCR and ELISA, introducing further robustness to the findings of the microarray. IL-17C was a particularly interesting gene that was highly enriched in our IL-36 dataset and is a recently described member of the IL-17 family, a group of cytokines within the psoriasis inflammatory network heavily implicated in driving inflammatory-associated pathology in psoriasis patients. Interestingly, a number of anti-IL-17 therapies are currently making their way through clinical trials and showing remarkable effects in ameliorating inflammation (Lowes et al., 2012). IL-17C has been shown to possess similar biological effects to IL-17A/F, however IL-17C is selectively secreted by cells of the barrier layer including the epidermis in response to bacterial challenge, while IL-17A/F are produced by specialized T-cell subtypes (Th17, α/γ T-cells), along with the recent identification of neutrophils as an innate immune source of these cytokines (Taylor et al., 2014). Furthermore, as demonstrated by Pappu and colleagues, and confirmed during the course of our own analysis, IL-17C is capable of inducing a potent inflammatory response from epidermal keratinocytes. Pappu and colleagues have also shown that mice deficient in IL-17C display significantly less inflammation and epidermal tissue thickening in a mouse model of psoriasis. In addition, upon intradermal injection, IL-17C promotes an extensive inflammatory response resembling features of psoriasis (Ramirez-Carrozzi et al., 2011). Other highly enriched genes in our IL-36 dataset include members of the IL-1 family, IL-1α, IL-1β and IL-36γ, suggesting that IL-36 was capable of inducing further synthesis of DAMPs. This is particularly relevant in the context of alerting neighbouring cells to potential danger, as the presence of extracellular IL-1α and IL-36γ would be indicative of necrosis and potential infection. Therefore, 'arming' of neighbouring cells to further upregulate DAMPs in the event of necrotic rupture would been an extremely prudent immune defense mechanism to evolve. We also found IL-36

to induce a large number of potent chemotatic molecules including the T-cell and DC chemokine, CCL20, and the neutrophil chemokine, IL-8. This gene expression data suggests that IL-36 is capable of driving a potent inflammatory response that is further amplified by molecules such as IL-17C, IL-6, GM-CSF, G-CSF, TNF and IL-8, either by direct induction of further inflammatory mediators or through recruitment of inflammatory cell types such as neutrophils, macrophages and T-cells.

5.3.2 The apicial cytokines IL-36 and TNF promote overlapping yet distinct inflammatory profiles

During the course of analysing the IL-36 and TNF gene expression datasets, we noted that these cytokines induced some of the same genes, albeit at different quantities, however a significant number of distinct genes were found within each dataset. This suggested a qualitative difference in the cohort of genes induced by these apicial cytokines. As discussed earlier, cytokines such as IL-1 and TNF are apex cytokines capable of inducing a diverse array of pro-inflammatory cascades that initiate inflammation, a property of these cytokines that in certain settings leads to the development of autoinflammatory conditions, with individual members of the IL-1 or TNF family playing predominant roles in particular disease settings (Jesus & Goldbach-Mansky, 2014). Indeed, the divergent nature of the inflammatory response induced by these apicial cytokines is particularly interesting given the dominant role they play in diverse inflammatory diseases and suggest that in principle it may be possible to stratify patients according to which apicial cytokine signature they present with. Indeed, a major limitation with the current clinical use of cytokine biologics is how to predict whether a patient will respond favourably to a particular therapy. A predictive indicator based on apicial cytokine profiles may assist in the treatment of individual patients with specific cytokine biologics.

5.3.3 Active IL-36 perturbs normal epidermal proliferation and differentiation

IL-1 has been implicated as a key factor that regulates the normal development of the epidermal layer. Fibroblasts serve as essential support cells and are the source of a diverse array of growth factors implicated in promoting the proliferation of keratinocytes (Blanton et al., 1989; Eller et al., 1995; Mass-Szabowski et al., 2000). In conditions where excess IL-1 is present, for example in psoriasis patients, this can promote excessive proliferation and thickening of the epidermis. Owing to the growing evidence for a role of IL-36 in epidermal inflammation, we asked the question whether IL-36, like IL-1, may be capable of modulating keratinocyte proliferation and differentiation. We initially began with simple monocultures of keratinocytes, looking to see if IL-36 may be sufficient to promote a hyperproliferative phenotype, however we failed to observe any modulation of proliferation under these conditions. We also failed to see any modulation or proliferation by IL-36 in conditions where we added calcium to mimic a highly simplified version of the differentiation program. These negative data suggested that additional factors may be required. This requirement for additional factors has support in the literature, where it has been demonstrated that co-culturing of keratinocytes with fibroblasts is necessary for proliferation of keratinocytes, owing to the capacity of fibroblasts to supply relevant cytokines and growth factors in a paracrine manner (Eller et al., 1999; Mass-Szabowski et al., 2000). Thus, co-culturing of keratinocytes and fibroblasts, especially in three-dimensinal organotypic models, has been demonstrated as providing highly similar conditions to those found *in vivo*, including the necessary growth factors such as KGF and EGF proteins, in addition to a functioning Ca^{2+} gradient (Fusenig, 1994; Mass-Szabowski et al., 2000). Under these more physiological conditions, we observed a profound perturbation of epidermal development with a significant epidermal thickening and expanded stratum layers similar to the hyperproliferative pathology of psoriasis. Therefore, IL-36 signalling may be capable of driving altered proliferative and differentiation programmes in keratinocytes *in vivo*.

5.3.4 IL-1 cytokines are released during necrosis

All IL-1 family members are generated as leaderless cytokines (Sims & Smith, 2010; Dinarello, 2009). Thus, these cytokines do not get secreted into the extracellular space via the classical secretory pathway. There have been a number of mechanisms suggested for the release of leaderless cytokines but it is becoming increasingly clear that sudden membrane rupture or necrotic cell death is the principal way in which these cytokines are released (Kono & Rock, 2008; Martin et al., 2012). In accordance with Matzinger's 'danger hypothesis', the IL-1 family of cytokines are the archetypical DAMPs in this respect, whereby their presence in the extracellular space is indicative of cellular damage (Martin et al., 2012; Matzinger, 1994). Furthermore, the IL-1 receptor and the TLR complexes share a number of key structural features such as a TIR domain, as well as recruitment of a similar repertoire of adaptor molecules such as MyD88, IRAK2/4 and TRAF6. Thus, IL-1 and TLR signalling activate many of the same signalling pathways during an inflammatory response (Kono & Rock, 2008). DAMPs are normally sequestered within healthy cells and only become released upon rupture of cells (i.e., necrosis), whereupon such molecules spill out into the extracellular space and trigger immune activation (Kono & Rock, 2008; Martin et al., 2012). During the course of this chapter, we have presented data that demonstrates that IL-1 cytokines, including IL-1α, IL-1β and IL-36γ, are released during necrosis of primary keratinocytes. Furthermore, IL-36 cytokines released from necrotized cells into the extracelluar space can be subsequently activated by neutrophil proteases, and drive the production of inflammatory cytokines. Indeed, it is highly appropriate that the presence of necrotic cells can instigate immune responses, as sudden cell rupture is typically only caused by severe departures from normal physiology. Moreover, necrotic cell death can betray the activities of viral infection as many viruses cause cell lysis, such as influenza and HIV, as a mechanism of release of new viruses, or the activities of bacterial toxins such as group A streptococci toxins, which are cytotoxic to host cells. Interestingly, the onset of psoriasis, in particular acute guttate psosiasis (AGP), often follows a streptococcal A infection (Whyte & Baughman, 1964; Telfer et al., 1992;

Valdimarsson et al., 1995), which is likely to be associated with both necrosis of infected tissue, as well as surrounding tissue, and with robust neutrophil and macrophage infiltration. If necrosis is not a direct consequence of pathogen activities, necrosis of barrier tissues as a result of compression injuries or burns are likely to lead to infection, thus the immune system recognizes this as potential danger and mounts an innate immune response characterized by the infiltration immune cells such as neutrophils and macrophages into the site of injury (Kono & Rock, 2008). Curiously, clinicians have reported for decades that psoriatic lesions can develop as a result of the epidermis experiencing physical injuries such as lacerations, burns or surgical incisions. This trauma-induced psoriasis is often described as the 'Koebner phenomenon', which was first described in 1877 (Weiss et al., 2002). An important clinical feature that unites all of the above diverse scenarios is that in each case, injury and infection respectively, are capable of triggering necrotic cell death to varying degrees in the epidermis. As a consequence of necrosis, DAMPs such as IL-36, IL-33 and IL-1α, may be released into the extracellular space where they can act on local epithelia to drive further inflammation. Concurrent with this is robust activation of cells of the immune system such as neutrophils, macrophages and mast cells, which infiltrate into the damaged tissue to guard against potential infection (Kono & Rock, 2008; Lukens et al., 2012; Pasparakis et al., 2012; Martin et al., 2012). It is under these conditions that extracellular IL-36 cytokines may encounter and get processed by neutrophil proteases since these proteases are frequently found at elevated levels within psoriatic lesions (Wiedow et al., 1992). Keratinocytes make up the majority of cells within the epidermis, which constitutes a very important barrier against infection. In addition to serving as a physical barrier against the entry of microorganisms, it is now well appreciated that keratinocytes are capable of directly responding to damage or infection by releasing a number of key inflammatory mediators, such as IL-1α, IL-8 and CCL20, to activate local macrophages and dendritic cells to initiate immune responses (Vigne et al., 2012; Pasparakis et al., 2012). In this respect keratinocytes serve as key sentinel cells that alert the immune system to potential danger. We have demonstrated during

the course of this chapter that IL-1 family members are constituvely present within keratinocytes and are subject to further regulation upon cellular stress or PAMP stimulation. We would argue that the presence of IL-1 cytokines in these cells is to be expected given the role of keratinocytes as a barrier cell type, subject to a wide variety of environmental insults and which must be appropriately armed, ready to alert the immune system.

In addition, we have demonstrated that IL-36γ is also significantly overexpressed in psoriatic lesion tissue, which is consistent with previous studies that implicate IL-36 in playing a key role in the instigation and/or amplification of psoriasis (Towne & Sims, 2012). Interestingly, we could not detect expression of other IL-1 members including IL-36α/β and IL-1α in these patient samples (data not shown). This may be due to the genuine absence of these cytokines or that these cytokines are present below the detectable range for western blot with the available antibodies. Furthermore, it is widely appreciated that IL-1 cytokines are extremely difficult to detect *in vivo*, as they are typically found at very small quantities (picomolar) even in diseased tissue where they are known to mediate a pathological effect (Dinarello, 2009). In psoriasis-susceptible individuals who carry various genetic polymorphic mutations, such as those with mutations in IL-36RA, an IL-36 inflammatory reaction may proceed uninhibited, thus seeding a destructive self-amplifying inflammatory loop.

Chapter 6

General Discussion

6.1 Introduction

How the immune system recognizes and deciphers different modes of cell death is of paramount importance to protect multicellular organisms from cellular injury and infection, breakdown of tolerence and to ward off the ravages of autoimmunity. Throughout this thesis we have focused on the activity and regulation of two distinct cytokine families in the context of cell death. The primary goal of the first part of this thesis was to contribute to our current understanding of how dying cells might signal to immune cells in the context of TRAIL stimulation. We asked whether the pro-apoptotic cytokine TRAIL might play a role in preparing a dying cell for disposal by professional phagocytes through engagement of non-apoptotic signalling outcomes. In chapter 3, we demonstrated a novel role for TRAIL in mediating the release of classical chemokines IL-8 and MCP-1 that may serve as 'find me' signals that attract phagocytes towards dying cells.

In the second part of this thesis, we focus on the IL-1 family of cytokines, namely IL-36$\alpha/\beta/\gamma$. In chapter 4, we identified the neutrophil-derived proteases elastase and cathepsin-G as IL-36 activating enzymes. We demonstrated this by using either purified proteases or activated human neutrophil degranulates, which both enhanced the biological activity of IL-36 cytokines in cell-based assays. IL-36 cytokines are likely to play a key role as initiators of inflammation in the skin barrier, therefore inhibitors of IL-36 activation are likely to have considerable potential for the treatment of inflammatory skin conditions. Importantly, psoriasis plaques are frequently associated with neutrophil infiltrates, which suggested that peptide inhibitors of neutrophil granule proteases may have significant potential as inhibitors of IL-36 activation in psoriasis. We also designed novel small molecule inhibitors of neutrophil proteases that could selectively inhibit these proteases as a method to attenuate IL-36 biological activity.

Because IL-36 cytokines appear to play a key role as initiators of inflammation in the skin barrier, we next examined the effects of activated IL-36 in a range of physiological settings. We conducted genome wide gene expression analysis on primary keratinocytes and discovered that IL-36 is capable of

inducing the expression of hundreds of pro-inflammatory genes, providing strong evidence for this cytokine as an apical inducer of inflammatory responses. Furthermore, we demonstrated that IL-36 is capable of promoting an altered proliferative and differentiation phenotype in a 3D skin model similar to psoriatic tissue, supporting the emerging role that IL-36 is thought to play in skin biology, and in particular its pathological effects in diseases such as psoriasis. Finally, we explored the endogenous expression of IL-36 cytokines in both primary keratinocytes and psoriatic biopsies. We demonstrated that IL-36γ is constitutively expressed in keratinocytes and that its expression within cells is subject to modulation by inflammatory stimuli as well as the differentiation state of the cell.

6.2 Death receptor-induced apoptosis and its immunological consequences

Cells dying by apoptosis *in vivo* die for many reasons including growth factor deprivation, DNA damage, pH imbalance, and viral infection, all of which are subject to monitoring by cells of the immune system, in particular tissue resident macrophages. Apoptotic cells share particular biochemical and morphological features, such as caspase activation, PS exposure, DNA fragmentation and extensive membrane blebbing, therefore the immunological response is likely determined by additional signals, which are differentially produced by apoptotic cells dying from different stimuli. In addition to responding to signals from the apoptotic cells, the immune system interprets the context in which the cell is dying from signals from the surrounding tissue. Therefore, macrophages may select from a number of reponses ranging from silent removal of the cell to the induction of an inflammatory reponse. This capacity for a measured and varied response to apoptosis *in vivo* makes intuitive sense as it would not be appropriate to repond in the same way to an apoptotic cell dying as part of normal homeostasis compared with an apoptotic cell dying due to viral infection or as a result of cellular damage.

In chapter 3, we used a physiological trigger of apoptosis, namely TRAIL, a member of the TNF cytokine family. We demonstrated that TRAIL-induced

apoptosis is accompanied by the release of pro-inflammtory cytokines and chemokines. Through use of chemotaxis assays we provided evidence that monocytes and neutrophils are capable of migrating towards these apoptotic supernatants in a manner dependent on MCP-1 and IL-8. Previous studies have established that both TRAIL and Fas/CD95 have critical functions in maintaining homeostasis in multicellular organisms through their immune-related functions. For example, Fas/CD95 signalling mediates the culling of autoreactive T-cells in the thymus during development, deficiencies in which lead to the develoment of a progressive and debilitating autoimmune condition (Takahashi et al., 1994). Furthermore, TRAIL and Fas/CD95 are key molecules within the arsenal of NK and CTL cells to eliminate damaged and/or transformed cells, thus preventing tumorigenesis. This is particularly striking in mice deficient in TRAIL signalling, where the incidences of metastasis during epithelial tumorigenesis is dramatically increased, implicating TRAIL as a key metastasis suppressor gene (Grosse-Wilde et al., 2008). Recently, a novel role for TRAIL within the immune system has been discovered, implicating this cytokine as a key component in the neutrophil response against bacterial infection in the lung. TRAIL was found to be released from activated neutrophils to target and kill macrophages infected with *Streptococcus pneumoniae*, thus limiting bacterial spread and dampening the inflammatory response (Steinwede et al., 2012). However, the role of TRAIL during infection is somewhat of a double-edged sword as can be seen in studies that have looked at influenza, *Listeria monocytogenes* bacterium and west Nile virus infections (Herold et al., 2008; Zheng et al., 2004; Shrestha et al., 2012). Mice deficient in TRAIL ligand have enhanced inflammatory responses at early stages after infection resulting in better control of the infection compared to wild-type mice, however if the infection is not cleared at these early stages, then adaptive immunity mediated by CTLs is comprised, clearance is delayed and increased tissue damage occurs (Benedict & Ware, 2012). The above observations may well have an inflammatory component in that TRAIL-induced killing of infected or damaged cells may release cytokines such as IL-6, IL-8 and MCP-1 to qualify this apoptosis as distinct from apoptosis in housekeeping or

developmental settings. How a macrophage behaves when it encounters a cell that has died in response to TRAIL during infection and the phenotype and signals the macrophage subsequently produces will be extremely interesting to investigate. Therefore, one aspect of TRAIL signalling may be to limit infections through elimination of the cell by apoptosis, however whether the apoptotic cell also produces inflammatory signals and how they might contribute to the ongoing immune response is unknown.

6.3 Non-apoptotic outcomes of TRAIL signalling

During the course of chapter 3, we also demonstrated that certain tumor cell lines were refractory to TRAIL killing, however still responded to TRAIL by producing cytokines and chemokines. This was a particularly intriguing observation as it underscored the idea that apoptosis is only one aspect to TRAIL biology. This is supported by the observation that tissues are typically refractory to TRAIL cytotoxicity *in vivo*, suggesting that the main role here may be an inflammatory one. As is common in biology, we frequently obtain insights into a particular biological process by looking at situations where it has gone awry. For example, a study by Lawrie and colleagues implicated TRAIL signalling in the progression of pulmonary arterial hypertension (PAH). Previously, it had been established that chronic inflammation plays a vital role in the progression of PAH, yet the molecules involved remained obscure. Using a number of rodent models including neutralizing antibodies, as well as mice deficient in TRAIL, the authors implicate TRAIL in the progression of PAH through it capability of promoting the proliferation and migration of vascular smooth muscle cells (Hameed et al., 2012). Indeed, it had been previously demonstrated that TRAIL can promote the proliferation of smooth muscle cells as well as vascular endothelial cells in the absence of apoptosis. This was dependent on ERK and AKT signalling pathways (Kavurma et al., 2008; Secchiero et al., 2003). Collectively, these studies support a role for TRAIL-induced inflammatory signalling in the progression of vascular disease.

The ability of TRAIL to induce inflammatory signalling in the absence of death also has implications for another pathological setting, namely tumorigenesis. While TRAIL's apoptosis-inducing effects have been extensively explored in multiple tumor models, the inflammatory component of TRAIL signalling has largely been ignored. Many solid tumors present with what is known as 'smouldering inflammation', with a substantial part of the mass of a tumor comprised of innate immune cells. Recent findings, including those demonstrated in this work, suggest that Fas and TRAIL are capable of driving pro-inflammatory signals, may begin to explain the potential benefit to tumors of selecting for expression of these receptors. Furthermore, given the accumulating evidence for TRAIL as a potent proliferative and remodelling factor in the vasculature, it is becoming clearer that the non-apoptotic functions of TRAIL may have significant benefits for a tumor. TRAIL's inherent pro-inflammatory properties are particularly relevant considering the use of TRAIL therapies for the treatment of cancers. While the use of TRAIL as a chemotherapeutic is focused on the cytotoxic capabilities of this molecule, the potential inflammatory effects of TRAIL in therapeutic settings have not been fully explored. Furthermore, given the role of inflammation in assisting the progression of tumors, TRAIL therapies may have unwanted pro-inflammatory side effects, which could well be detrimental to patient survival.

6.4 Proteolysis of IL-36 cytokines

As demonstrated in chapters 4 and 5, we have discovered an important mechanism of regulating the biological activity of IL-36 cytokines by neutrophil proteases. We have defined the biochemical and cellular effects of neutrophil protease-mediated proteolysis of IL-36 cytokines in a number of cell-based assays, as well as exploring the IL-36 inflammatory network via genome wide gene expression array anaylsis. In addition, we have demonstrated that activated IL-36 can produce epidermal thickening and altered differentiation in a 3D skin model, echoing its emerging role in psoriasis. Of course, the skin is an organ made up of many parts, and so exactly how IL-36 perturbs the epidermis is a key

question to be addressed in future experiments. The benefit of an *in vitro* skin model is that such systems are well defined and relatively simple. With two cell types, an upper keratinocyte layer and a lower fibroblast layer, it is likely that IL-36 modulates the extensive crosstalk that exists between these cells, resulting in the overproduction of particular growth factors and inflammatory mediators that results in a perturbed epidermis. In furture experiments, it will be important to identify these factors to gain a better understanding of how active IL-36 can modulate differentiation and proliferation in the skin.

Going forward, it is highly likely that additional proteases that process IL-36 will be discovered. Immune cell types such as mast cells, macrophages, NK cells and CTLs, which also have their own stores of distinct proteases broadly related to neutrophil proteases, are promising candidates for the discovery of additional IL-36 processing proteases. Of note, we have recently discovered that another cathepsin protease, cathepsin-K, can also activate IL-36β at the same amino acid residue as cathepsin-G, suggesting proteolysis in this particular region of the N-terminus is critical for its activation. This particular cathepsin has been reported to be expressed in a number of diverse cell types, including macrophages, fibroblasts and also osteoclasts. Interestingly, expression of cathepsin-K is elevated during inflammatory responses within fibroblast cells (Zavasnik & Turk, 2006; Quintanilla-Dieck et al., 2009). Furthermore, cysteine cathepsins are traditionally thought of as lysosomal proteases, responsible for degradation of cellular debris and also bacteria/viruses in the lysosome, however it is becoming increasingly clear that these cathepsins are also secreted and have important roles in the immune response. For example, during antigen processing and maturation of MHC II molecules, but also as regulators of cytokine activity (Zavasnik & Turk, 2006; Conus & Simon, 2010). Cathepsin-K has attracted a lot of attention recently because of its expression and activity in osteoclasts and its role as a potent remodelling protease of the extracellular matrix and bone matrices, with excessive activity acting as a key driver of osteoporosis. A potent cathepsin-K inhibitor called Odanacatib® (Merck) has recently been approved by the FDA for the treatment of osteoporosis. Interestingly, cathepsin-K has also

been shown to facilitate TLR9 signalling in response to pathogen DNA. In a TLR9-dependent autoimmune encephalomyelitis model, cathepsin-K deficient mice have reduced disease severity because of a failure of dendritic cells to produce IL-23 and IL-6, which are critical for Th17 cell development, a major pathogenic cell type in this particular model (Asagiri et al., 2008). Of particular note is a recent study, which demonstrated that cathepsin-K is highly overexpressed in psoriatic patients and promotes skin inflammation in a TPA-treated keratin-5-Stat3 model of psoriasis (Hirai et al., 2013). Furthermore, inhibition of cathepsin-K using a chemical inhibitor (NC-2300) significantly ameliorated psoriasis-like lesions in these mice. In light of these findings, it is tempting to speculate that cathepsin-K activation of IL-36β, in addition to cathepsin-G, may also contribute to skin inflammation and development of psoriasis.

While we have focused on IL-36 activation by neutrophil proteases, proteolytic regulation during diverse modes of cell death may represent an important mechanism which modulates the inflammatory potential of these cytokines. IL-33 inactivation by apoptotic caspases is one example of how IL-1 family members are regulated during apoptosis. Another is the translocation of IL-1α to the nucleus during apoptosis where it binds to chromatin, therefore limiting its extracellular release. It remains to be demonstrated whether IL-36 cytokines are regulated by apoptotic caspases. During the course of this work we explored effects of caspase-3 on IL-36. However, we only assessed activation, thus it remains to be formally demonstrated whether full-length IL-36 is inactivated by caspases. Furthermore, we have only explored necrosis as a mechanism by which IL-36 can gain access into the extracellular space. However, another interesting avenue of investigation is the fate of IL-36 proteins during other necrotic scenarios, such as necroptosis or pyroptosis. In the case of pyroptosis, excessive caspase-1 activation drives this form of cell death, in conjunction with release of active IL-1β. Of note, we did not see any activation of IL-36 cytokines with recombinant caspase-1.

The findings in this thesis have contributed towards a clearer picture that is

emerging regarding the proteolytic regulation of the IL-1 cytokine family, especially as conserved substrates for neutrophil proteases.

6.5 Role of neutrophils and IL-36 in inflammatory skin conditions and the potential for therapeutic intervention

The neutrophil granule proteases, cathepsin-G, elastase and proteinase-3, belong to a large family of serine proteases that play a major function in the immune and inflammatory response (Pham, 2006). During the course of this thesis we have focused on the capacity of neutrophil proteases to cleave and activate members of the IL-36 family. These findings raise the possibility that by targeting neutrophil proteases, this may provide some therapeutic benefit for patients with skin inflammatory conditions. As we have discussed previously, IL-36 has been strongly implicated a key driver of inflammation associated with psoriasis. Given the apical nature of IL-36 cytokines in driving inflammatory cascades, it is likely that by blocking IL-36 signalling in patients much of the associated inflammation will be reduced or eliminated entirely. Therefore, therapies that target IL-36 signalling, using anti-IL-36R blocking antibodies for example, will more than likely be entering clinical trials in the very near future. Over the past few years there has been a breakthrough in the treatment of psoriasis, especially with the use of anti-cytokine biologics. Leading this new generation of therapies are the anti-IL-17 based therapies (e.g. brodalumab, ixekizumab, secukinumab), which have been shown to be well tolerated in patients and have demonstrated remarkable efficacy, and in some cases resulting in complete clearance of psoriasis (Chiricozzi & Krueger, 2013). However, most patients who have psoriasis, in particular mild to moderate forms, will not benefit from these expensive and systemic cytokine-based therapies, as their use will be reserved for only the most severe psoriasis cases, such as GPP, which represent less than 5% of psoriasis patients (Crow, 2012). Therefore, cheaper and less invasive therapies, with fewer side effects, are needed.

Targeting neutrophil proteases, particularly with chemical or peptide based drugs, for the treatment of psoriasis is an attractive approach both in terms of

reducing cost but also routes of administration as they can be delivered either orally or topically, whereas biologics must be injected. Dampening down of neutrophil protease activity has been tested for a number of severe inflammatory conditions such as CF, however these are only moderately successful for a number of reasons, including inability to target multiple proteases simultaneously and failure to inhibit with similar efficiency. For example, α-1-protease inhibitor (α1-PI) therapy has been used for the treatment of CF and has been shown to significantly reduce the levels of elastase activity. However, owing to its large molecular weight α1-PI has impaired access to tissue microenviroments, in particular where activated neutrophils deposit proteases in close contact with tissue of the extracellular matrix (Korkmaz et al., 2010). Therefore, an ideal neutrophil protease inhibitor would be small (<500 kDa), inhibit multiple proteases at once with high efficiency, and would be highly stable and resist proteolysis and oxidation.

Neutrophil protease inhibitors have not yet been considered for treatment of psoriasis, yet a remarkable recent study has demonstrated that targeted depletion of neutrophils from a patient with GPP, led to a dramatic reduction in disease severity, suggesting that in principle targeting neutrophils and/or their proteases may yield benefits for psoriasis patients in general (Ikeda et al., 2013). Owing to the discovery that neutrophil proteases activate IL-36, coupled with the well established pathological role of neutrophil proteases in other inflammatory conditions, it seems reasonable to think that by targeting cathepsin-G and elastase some therapeutic benefit may be seen in patients, not just in psoriasis, but with any inflammatory condition characterised by excessive neutrophil protease activity. During the course of this thesis we have developed a panel of novel small molecular weight peptides that are potent inhibitors of cathepsin-G and elastase *in vitro*. Future experiments with the peptides described here will explore their therapeutic potential *in vivo* using appropriate mouse models of inflammatory diseases. An obvious concern when targeting neutrophil proteases as a therapy is the potential negative consequences in terms of immune suppression and risk of infection. In effect, for a successful therapy you want just

the right amount of inhibition to restore the system to its normal level of activity. The use of reversible inhibitors is one way to achieve this. We developed peptides with and without CMK modifications. Without the CMK modification, much higher concentrations of the peptide were required to achieve to suppression (~10-fold). Achieving such concentrations may be a challenge in patients, however in conditions such as psoriasis, topical application to a psoriatic lesion will allow for the efficient and direct delivery of the therapy to where it is needed. A recent example of an effective peptide-based neutrophil protease inhibitor is Gly-Phe-diazomethlyketone, which targets DPPI, the enzyme that activates elastase, cathepsin-G and proteinase 3 zymogens (Methot et al., 2008). Using this DPPI inhibitor, the authors found a dramatic reduction in the accumulation of neutrophils at an inflammatory site (Methot et al., 2008). Neutrophils derived from DPPI deficient mice display normal chemotaxis towards IL-8 and FMLP *in vitro* and *in vivo*, however these neutrophils fail to accumulate in response to inflammatory stimuli (Adkison et al., 2002; Akk et al., 2012). Furthermore, neutrophils derived form cathepsin-G/elastase double deficient mice also displayed a similar defect in accumulation *in vivo* (Adkison et al., 2002). This raises the interesting question of what role DPPI, cathepsin-G and elastase play in driving the accumulation of neutrophils to a site of infection or injury. A very exciting possibility is that neutrophil proteases, through proteolysis of key cytokines such as IL-1 family members, mediate an amplification of inflammation, promoting additional waves of further neutrophil recruitment into a site of damage or injury. Therefore, the use of small peptide-based strategies may, in time, become a viable method of selectively inhibiting neutrophil proteases in multiple inflammatory diseases.

6.6 Conclusion

The goal of this of thesis has been to expand our knowledge of how cell death is interpreted by the immune system through focusing on the inflammatory activities and proteolytic regulation of two distinct cytokine families.

First, we have shown that the cytokine, TRAIL, previously implicated as a

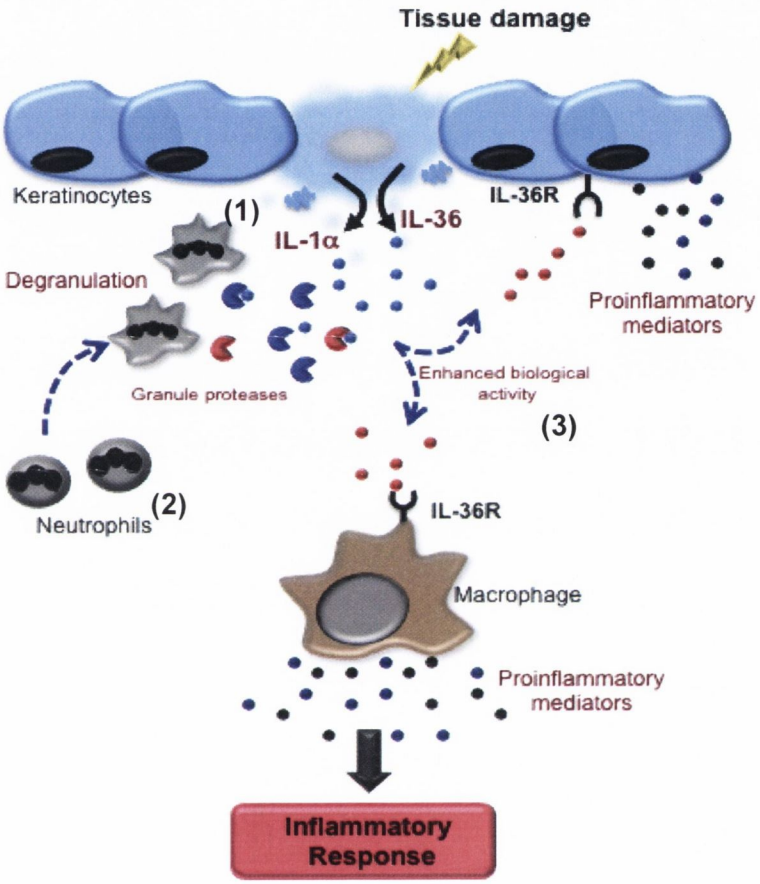


Figure 6.1 Model of IL-36 activation
IL-1α and IL-36 cytokines are released from damaged keratinocytes **(1)**. IL-1α promotes neutrophils recruitment and macrophages activation. Activated neutrophils degranulate and release granule proteases, cathepsin-G and elastase, which in turn activate IL-36 cytokines to release their biological activity **(2)**. Activated IL-36 cytokines further amplified the proinflammatory response by activating local epitheial cells as well as macrophages to promote release of proinflammatory mediators **(3)**.

pro-apoptotic molecule, also has an important function as a stimulator of inflammatory cytokine production, a subset of which recruits macrophages and neutrophils during apoptosis. Second, we discovered that neutrophil serine proteases activate IL-36 cytokines. During necrotic cell death, IL-36 activation by neutrophil proteases represents a novel mechanism to release the potent biological activity of these cytokines (**Fig. 6.1**). In addition, due to the role that IL-36 cytokines play in skin inflammatory diseases, targeted inhibition of their activating proteases may lead to the development of highly effective novel therapies.

References

References

A

Adkison, A.M., Raptis, S.Z., Kelley, D.G., Pham, C.T.N. Dipeptidyl peptidase I activates neutrophil-derived serine proteases and regulates the development of acute experimental arthritis. *J. Clin. Invest.* **109**, 363-371 (2002)

Afonina IS, Cullen SP, Martin SJ. Cytotoxic and non-cytotoxic roles of the CTL/NK protease granzyme B. *Immunol Rev.* **235**, 105-16 (2010)

Afonina, IS., Tynan, G., Logue, SE., Cullen, SP., Bots, Michael., Luthi, A., Reeves, EP., McElvaney NG., Medema, JP., Lavelle, EC, Martin, SJ. Granzyme B-Dependent Proteolysis acts as a switch to enhance the pro-inflammatory activity of IL-1α. *Mol. Cell* **44**, 265-278 (2011)

Akk, A.M., Simmon, P.M., Chan, H.W., Agapov, E.A., et al. Dipeptidyl peptidase I-dependent neutrophil recruitment modulates the inflammatory response to sendai virus infection. *J. Immunol.* **180**, 3535-3542 (2008)

Aksentijevich, I., Masters, S.L., et al. An autoinflammatory disease with deficiency of the interleukin-1-receptor antagonist. *NEJM* **360**, 2426-2437 (2009)

Altemeier, W.A., Zhu, X., Berrington, W.R., Harlan, J.M., and Liles, W.C. Fas (CD95) induces macrophage proinflammatory chemokine production via a MyD88-dependent, caspase-independent pathway. *J. Leukoc. Biol.* **82**, 721-718 (2007)

Ali, S., Nguyen, D.Q., Falk, W., Martin, M.U. Caspase 3 inactivates biologically active full-length interleukin-33 as a classical cytokine but does not prohibit nuclear translocation. *Biochem Biophys Res Commun.* **391**,1512-6 (2010)

Auron, P.E., Webb, A.C., Rosenwasser, L.J., Mucci, S.F., Rich, A., Wolff, S.M., Dinarello, C.A. Nucleotide sequence of human monocyte interleukin 1 precursor cDNA. *Proc. Natl. Acad. Sci. USA* **81**, 7907-7911 (1984)

B

Barnhart, B.C., Legembre, P., Pietras, E., Bubici, C., Franzoso, G., Peter M.E. CD95 ligand induces motility and invasiveness of apoptosis-resistant tumor cells. *EMBO J.* **23**, 3175-3185 (2004)

Bardoel, B.W., Kenny, E.F., Sollberger, G., Zychlinsky, A. The balancing act of neutrophils. *Cell Host & Microbes* **15**, 526-533 (2014)

Berg, D., Stuhmer, T., et al. Oligomerized tumor necrosis factor-related apoptosis inducing ligand strongly induces cell death in myeloma cells, but also activates proinflammatory signalling pathways. *FEBS J.* **276**, 6912-6927 (2009)

Bergsbaken, T., Fink, S.L., Cookson, B.T. Pyroptosis: host cell death and inflammation. *Nat Rev Microbiol.* **7**, 99-109. (2009)

Birge RB, Ucker DS. Innate apoptotic immunity: the calming touch of death. *Cell Death Differ.* **15**, 1096-102 (2008)

Blanton, R.A., Kupper, T.S., McDougall, J.K., Dower, S. Regulation of interleukin 1 and its receptor in human keratinocytes. *Proc. Natl. Acad. Sci. USA* **86**, 1273-1277 (1989)

Blanton, R. A., Kupper, T. S., McDougall, J. K. and Dower, S. Regulation of interleukin-1 and its receptor in human keratinocytes. *Proc.Nat. Acad. Sci. USA* **86**, 1273-1277 (1989)

Blumberg, H., Dinh, H., Trueblood, E.S., Pretorius, J., Kugler, D., Weng, N., Kanaly, S.T., Towne, J.E., Willis, C.R., Keuchle, M.K., Sims, J.E., Peschon, J.J. Opposing activities of two novel members of the IL-1 ligand family regulate skin inflammation. *J. Exp. Med.* **204**, 2603-14 (2007)

Blumberg, H., Dinh, H., Dean, C. Jr., Trueblood, E.S., Bailey, K., Shows, D., Bhangavathula, N., Aslam, M.N., Varani, J., Towne, J.E., Sims, J.E. IL-1RL2 and its ligands contribute to the cytokine network in psoriasis. *J. Immuno.* **185**, 4354-62 (2010)

Bonilla, WV., Frohlich, A., Senn, K., Kallert, S. et al. The alarmin Interleukin-33 drives protective antiviral $CD8^+$ T-Cell responses. *Science* **335**, 984- (2012)

Bournazou, I., Pound, J.D., Duffin, R., Bournazos, S., Melville, L.A., Brown, S.B., Rossi, A.G., Gregory, C.D. Apoptotic human cells inhibit migration of granulocytes via release of lactoferrin. *J. Clin. Invest.* **119**, 20-32 (2009)

Bossaller, L. et al. Cutting edge: Fas (CD95) mediates noncanonical IL-1β and IL-18 maturation via caspase-8 in a RIP3-independent manner. *J. Immunol.* **189**, 5508-5512 (2012)

Brennan, F.M., McInnes, I.B. Evidence that cytokines play a role in rheumatoid arthritis. *J Clin. Invest.* **118**, 3537-3545 (2008)

Brinkmann, V., Reichard, U., Goosmann, C., Fauler, B., Uhlemann, Y., Weiss, D.S., Weinrauch, Y., Zychlinsky, A. Neutrophil extracellular traps kill bacteria. *Science* **303**, 1532-5 (2004)

C

Cayrol, C., and Girard, J.P. The IL-1-like cytokine IL-33 is inactivated after maturation by caspase-1. *Proc. Natl. Acad. Sci. USA* **106**, 9021-6 (2009)

Casares, N., et al. Caspase-dependent immunogenicity of doxorubicin-induced tumour cell death. *J. Exp. Med.* **202**, 1691-1701 (2006)

Chou, A.H., et al. Enhanced proliferation and increased IFN-gamma production in T cells by signal transduced through TNF-related apoptosis-inducing ligand. J. Immun. **167**, 1347-1352 (2001)

Chekeni, F.B., Elliott, M.R., Sandilos, J.K., Walk, S.F., Kinchen, J.M., Lazarowski, E.R., Armstrong, A.J., Penuela, S., Laird, D.W., Salvesen, G.S., Isakson, B.E., Bayliss, D.A., Ravichandran, K.S. Pannexin 1 channels mediate 'find-me' signal release and membrane permeability during apoptosis. *Nature* **467**, 863-7 (2010)

Chen, L., Park, S.M., Tumanov, A.V., Hau, A., Sawada, K., Feig, C., Turner, J.R., Fu, Y.X., Romero, I.L., Lengyel, E., and Peter, M.E. CD95 promotes tumour growth. *Nature* **465**, 492-496 (2010)

Chen, C.J., Kono, H., Golenbock, D., Reed, G., Akira, S., Rock, K.L. Identification of a key pathway required for the sterile inflammatory response triggered by dying cells. *Nat Med.* **13**, 851-6 (2007)

Chen, Y., Corriden, R., et al. ATP Release Guides Neutrophil Chemotaxis via P2Y2 and A3 Receptors. *Science* **314**, 1792-1795 (2006)

Choi, C., Xu, X., Oh, J.W., Lee, S.J., Gillespie, G.Y., Park, H., Jo, H., and Benveniste, E.N. Fas-induced expression of chemokines in human glioma cells: involvement of extracellular signal-regulated kinase 1/2 and p38 mitogen-activated protein kinase. *Cancer Res.* **61**, 3084-3091 (2001)

Cohen, P. The TLR and IL-1 signalling network at a glance. *J Cell Sci.* **127**, 1-8 (2014)

Cohen, I., Rider, P., et al. Differential release of chromatin-bound IL-1α discriminates between necrotic and apoptotic cell death by their ability to induce sterile inflammation. *Proc. Natl. Acad. Sci. USA* **107**, 2574-9 (2010)

Cullen, S.P., Martin, S.J. Mechanisms of granule-dependent killing. *Cell Death Differ.* **15**, 251-62 (2008)

Cullen, S.P., Afonina, I.S., Donadini, R., Lüthi, A.U., Medema, J.P., Bird, P.I., Martin, S.J. Nucleophosmin is cleaved and inactivated by the cytotoxic granule protease granzyme M during natural killer cell-mediated killing. *J Biol. Chem.* **284**, 5137-47 (2009)

Cullen, S.P., Adrain, C., Lüthi, A.U., Duriez, P.J., Martin, S.J. Human and murine granzyme B exhibit divergent substrate preferences. *J, Cell Biol.* **176**, 435-44 (2007)

Cullen, S.P., Adrain, C., Lüthi, A.U., Duriez, P.J., Martin, S.J. Human and murine granzyme B exhibit divergent substrate preferences. *J, Cell Biol.* **176**, 435-44 (2007)

Cullen, S.P., Henry, C.M., Kearney, C.J., Logue, S.E., Feoktistova, M., Tynan, G.A., Lavelle, E.C., Leverkus, M., Martin, S.J. Fas/CD95-induced chemokines can serve as "find-me" signals for apoptotic cells. *Mol. Cell* **49**, 1034-1048 (2013)

Cullen, S.P., Martin, S.J. Diverse Activators of The NALP3 Inflammasome Promote IL-1b Secretion by Triggering Necrosis *Cell.* In revision (2014)

D

Debets, R., Timans, J. C., Homey, B., Zurawski, S., Sana, T. R., Lo, S., Wagner, J., Edwards, G., Clifford, T., Menon, S., Bazan, J. F., and Kastelein, R. A. Two novel IL-1 family members, IL-1δ and IL-1ε, functions as an antagonist and agonist of NF-kB activation through the orphan IL-1 receptor-related protein 2. *J. Immunol.* **167**, 1440–1446 (2001)

Dinarello, C.A., Simon, A., van der Meer, J.W. Treating inflammation by blocking interleukin-1 in a broad spectrum of diseases. Na*t Rev Drug Discov.* **11**, 633-52 (2012)

Dinarello, C.A. Immunological and inflammatory functions of the interleukin-1 family. *Ann. Rev. Immunol.* **27**, 519-550 (2009)

Dix, M.M., Simon, G.M., Cravatt, B.F. Global mapping of the topography and magnitude of proteolytic events in apoptosis. *Cell* **134**, 679-91 (2008)

Dynek, J.N., Goncharov, T., Dueber, E.C., Fedorova, A.V., Izrael-Tomasevic, A, Phu, L., Helgason, E., Fairbrother, W.J., Deshayes, K., Kirkpatrick, D.S., and Vucic, D. c-IAP1 and UbcH5 promote K11-linked polyubiquitination of RIP1 in TNF signalling. *EMBO J.* **29**, 4198-4209 (2010)

E

Ehrhadt, H., Fulda, S., Schmid, I., et al. TRAIL induced survival and proliferation in cancer cells resistant towards TRAIL-induced apoptosis mediated by NF-kB. *Oncogene* **22**, 3842-3852 (2003)

Eller, M.S., Yaar, M., Ostrom, K., Karkness, D.D., Gilchrest, B.A. A role for interleukin-1 in epidermal differentiation: regulation by expression of functional versus decoy receptors. *J. Cell. Sci.* **108**, 2741-2746 (1995)

Elliott, M.R., Chekeni, F.B., Trampont, P.C., Lazarowski, E.R., Kadl, A., Walk, S.F., Park, D., Woodson, R.I., Ostankovich, M., Sharma, P., Lysiak, J.J., Harden, T.K., Leitinger, N., Ravichandran, K.S. Nucleotides released by apoptotic cells act as a find-me signal to promote phagocytic clearance. *Nature* **461**, 282-6 (2009)

Enari, M., Sakahira, H., Yokoyama, H., Okawa, K., Iwamatsu, A., Nagata, S. A caspase-activated DNase that degrades DNA during apoptosis, and its inhibitor ICAD. *Nature* **391**, 43-50 (1998)

F

Falschehner, C., Emmerich, C.H., Gerlich, B., Walzcak H. TRAIL signalling: Decisions between life and death. *Intl. J. Bio. Cell. Signl.* **39**, 1462-1475 (2007)

Farley, S.M., Dotson, A.D., Purdy, D.E., Sundholm, A.J., Schneider, P., Magun, B.E., Iordanov, M.S. Fas ligand elicits a caspase-independent proinflammatory response in human keratinocytes: implications for dermatitis. *J. Invest. Dermatol.* **126**, 2438-2451(2006)

Fadok, V.A., Bratton, D.L., Konowal, A., Freed, P.W., Westcott, J.Y., Henson, P.M. Macrophages that have ingested apoptotic cells in vitro inhibit proinflammatory cytokine production through autocrine/paracrine mechanisms involving TGF-beta, PGE2, and PAF. *J Clin Invest.* **101**, 890-8 (1998)

Farooq, M., Nakai, H., Fujimoto, A., Fujikawa, H., Matsuyama, A., Kariya, N., Aizawa, A., Fujiwara, H., Ito, M., Shimomura, Y. Mutation analysis of the *IL36RN* gene in 14 Japanese patients with generalized pustular psoriasis. *Hum. Mutat.* **34**, 176-183 (2013)

Feoktistova, M., Gererick, P., et al. Leverkus, M. cIAPs block ripoptosome formation, a RIPK1/casapse-8 containing intracellular cell death complex differentially regulated by cFLIP isoforms. *Mol. Cell* **43**, 449-463 (2011)

Fusenig, N.E. Epithelial-mesenchymal interactions regulate keratinocyte growth and differentiation *in vitro*. In: Leigh I, Lane B, Watt

F: eds. *The keratinocyte handbook*, Cambridge University Press 71-94 (1994)

Frey, S., Derer, A., Messbacher, M.E., Baeten, D.L., Bugattia, S., Montecucco, C., Schett, G., Hueber, A.J. The novel cytokine interleukin-36a is expressed in psoriasis and rheumatoid arthritis synovium. *Ann Rheum. Dis.* **72**,1569-1574 (2013)

Frank, O., Nestle, M.D., Daniel, H., Kaplan, M.D., Barker, M.D. Psoriasis. *N. Engl. J. Med.* **361**, 496-508 (2009)

G

Garlanda, C., Dinarello, C.A., Mantovani, A. The interleukin-1 family: back to the future. *Immunity* **39**, 1003-1018 (2013)

Geffner, J.R., Fontan, P.A, Sordelli, D.O., Isturiz, M.A. Neutrophil Erythrotoxicity induced by phorbol myristate. *Jour. Leuk. Biol.* **49**, 352-359 (1991)

Gabrilovich, D.I., Nagaraj, S. Myleoid-derived suppressor cells as regulators of the immune system *Nat. Rev. Immunol.* **9**, 162-174 (2009)

Gottlieb, A.B. Psoriasis: emerging therapeutic strategies. *Nat. Rev. Drug Discov.* **4**, 19-34 (2005)

Green, D.R., and Kroemer, G. The pathophysiology of mitochondrial cell death. *Science* **305**, 626-9 (2004)

Gregory, C.D., Pound, J.D. Cell death in the neighbourhood: direct microenvironmental effects of apoptosis in normal and neoplastic tissues. *J. Pathol.* 223, 177-94 (2011)

Gross O, Yazdi AS, Thomas CJ, Masin M, Heinz LX, Guarda G, Quadroni M, Drexler SK, Tschopp J. Inflammasome activators induce interleukin-1α secretion via distinct pathways with differential requirement for the protease function of caspase-1. *Immunity* **36**, 388-400 (2012)

Grivennikov, S.I., Greten, F.R., Karin, M. Immunity, inflammation and cancer. *Cell* **140**, 883-899 (2010)

Gudbjartsson, D.F., Bjornsdottir, U.S., Halapi, E., et al. Sequence variants affecting eosinophil numbers associate with asthma and myocardial infarction. *Nat. Genet.* **41**, 342–347 (2009)

Gude, D.R., Alvarez, S.E., Paugh, S.W., Mitra, P., Yu J, Griffiths R, Barbour SE, Milstien S, Spiegel S. Apoptosis induces expression of sphingosine kinase 1 to release sphingosine-1-phosphate as a "come-and-get-me" signal. *FASEB J.* **22**, 2629-38 (2008)

H

Haas, T.L., Emmerich, C.H., Gerlach, B., Schmukle, A.C., Cordier, S.M., Rieser, E., Feltham, R., Vince, J., Warnken, U., Wenger, T., Koschny, R., Komander, D., Silke J., and Walczak, H. Recruitment of the linear ubiquitin chain assembly complex stabilizes the TNF-R1 signalling complex and is required for TNF-mediated gene induction. *Mol. Cell* **36**, 831-844 (2009)

Hadji, A., Ceppi, P., Murmann, A.E., Brockway, S., et al. Peter, M.E. Death induced by CD95 or CD95 ligand elimination. *Cell Reports.* **7**, 208-222 (2014)

Hameed, A.G., Arnold, N.D., Chamberlain, J., et al. Inhibition of tumor necrosis factor-related apoptosis-inducing ligand (TRAIL) reverses experimental pulmonary hytertension. *J. Exp. Med.* **209**, 1919-1935 (2012)

Hanahan, D., Weinberg, R.A. Hallmarks of cancer: the next generation. *Cell* **144**, 646-674 (2011)

Hahn, I., Klaus, A., Janze, A.K., Steinwede, K., Ding, N., Bohling, J., Brumshagen, C., Serrano, H., Gauthier, F., Paton, J.C., Welte, T., Maus, U.A. Cathepsin G and neutrophil elastase play critical and nonredundant roles in lung-protective immunity against Streptococcus pneumoniae in mice. *Infect. Immun.l* **12**, 4893-901 (2011)

Hazuda, D.J., Strickler, J., Kueppers, F., Simon, P.L., Young, P.R. Processing of precursor interleukin 1 beta and inflammatory disease. *J. Biol. Chem.* **265**, 6318-22 (1990)

Hazuda, D,J., Strickler, J., Simon, P., Young, P.R. Structure-function mapping of interleukin 1 precursors. Cleavage leads to a conformational change in the mature protein. *J. Biol. Chen.* **266**, 7081-7086 (1991)

Heusel, JW., Wesselschmidt, R.L., Shresta, S., Russell, J.H., Ley, T.J. Cytotoxic lymphocytes require granzyme B for the rapid induction of DNA fragmentation and apoptosis in allogeneic target cells. *Cell* **76**, 977-8 (1994)

Henry, C.M, Hollville, E., Martin, S.J. Measuring apoptosis by microscopy and flow cytometry. *Methods* **61**, 90-7. (2013)

Henson, P.M., Bratton, D.L. Antiinflammatory effects of apoptotic cells. *J. Clin. Invest.* **123**, 2773-2774 (2013)

Hill, M.M., Adrian, C., Duriez, P.J., Creagh, E.M., Martin, S.J. Analysis of the composition, assembly kinetics and activity of native Apaf-1 apoptosomes. *EMBO J* **23**, 2134-2145 (2004)

Hwei-Fang, T., et al. Induction of costimulation of human CD4 T cells by Tumor necrosis factor-related apoptosis-inducing ligand. *Arthritis and Rheumatism* **50**, 629-639 (2004)

I

Idzko, M., Hammad, H., van Nimwegen, M., Kool, M., Willart, M.A., Muskens, F., Hoogsteden, H.C., Luttmann, W., Ferrari, D., Di Virgilio, F., Virchow, J.C. Jr., Lambrecht, B.N. Extracellular ATP triggers and maintains asthmatic airway inflammation by activating dendritic cells. *Nat. Medicine* **13**, 913-9, (2007)

Ishii, K.J., Suzuki, K., Coban, C., Takeshita, F., Itoh, Y., Matoba, H., Kohn, L.D., Klinman, D.M. Genomic DNA released by dying cells induce the maturation of APCs. *J. Immunol.* **167**, 2602-7 (2001)

Isfort, K., Ebert, F., Bornhorst, J., et al. Real-time imaging reveals that $P2Y_2$ and $P2Y_{12}$ receptor agonists are not chemoattractants and macrophage chemotaxis to complement C5a is phosphatidylinositol 3-kinas (PI3K)- and p38 mitogen-activated protein kinase (MAPK)-independent. *J. Bio. Chem.* **286**, 44776- (2011)

Ikeda, S., Takahashi, H., Suga, Y., Eto, H., Okuma, K., Takahashi, K., Kanbara, T., Seishima, M., Morita, A., Imai, Y., Kanekura, T. Therapeutic depletion of myeloid lineage leukocytes in patients with generalized pustular psoriasis indicates a major role for neutrophils in the pathogenesis of psoriasis. *J Am Acad Dermatol* **4**, 609-617 (2013)

J

Jacobson, M.D., Weil, M., Raff, M.C. Programmed cell death in animal development. *Cell* **88**, 347-54 (1997).

Jesus, A.A., Goldbach-Mansky, R. IL-1 Blockade in Autoinflammtory syndromes *Annu. Rev. Med.* **65**, 223-44 (2014)

Jin, Z., El-Deiry, W.S. Distinct signalling pathways in TRAIL-versus Tumor Necrosis Factor-induced apoptosis. *Mol. Cell. Biol.* **26**, 8136-8148 (2006)

Johnston, A., Xing, X., Guzman, A.M., Riblett, M., Loyd, C.M., Ward, N.L., Wohn, C., Prens, E.P., Wang, F., Maier, L.E., Kang, S., Voorhees, J.J., Elder, J.T., Gudjonsson J.E. IL-1F5, -F6, -F8, -F9: a novel family signaling system that is active in psoriasis and promotes keratinocyte antimicrobial peptide expression. *J. Immunol.* **186**, 2613-22 (2011)

Johnston, A., Fritz, Y., Dawes, S.M., Diaconu, D., et al. Keratinocyte overexpression of IL-17C promotes psoriasiform skin inflammation. *J. Immunol.* **190**, 345-355 (2013)

Ju, G., Labriola-Tompkins, E., Campen, C.A., et al. Conversion of the interleukin 1 receptor antagonist into an agonist by site-specific mutagenesis. *Proc. Natl. Acad. Sci. USA* **88**, 2658-2662 (1992)

K

Kägi, D., Ledermann, B., Bürki, K., Seiler, P., Odermatt, B., Olsen, K.J., Podack, E.R., Zinkernagel, R.M., Hengartner, H. Cytotoxicity mediated by T cells and natural killer cells is greatly impaired in perforin-deficient mice. *Nature* **369**, 31-7 (1994)

Karin, M. NF-kB as a critical link between inflammation and cancer. *Cold Spring Harbour Perspectives in Biology* **1** (2009)

Kavuri, S.M., Geserick, P., Berg, D., et al. Cellular FLICE-inhibitory protein (cFLIP) isoforms block CD95 and TRAIL death receptor-induced gene induction irrespective of processing of caspase-8 or cFLIP in the death receptor complex. *J. Biol. Chem.* **286**, 16631-16646 (2011)

Kazama, H., Ricci, J.E., Herndon, J.M., Hoppe, G., Green, D.R., Ferguson, T.A. Induction of immunological tolerance by apoptotic cells requires caspase-dependent oxidation of high-mobility group box-1 protein. *Immunity* **29**, 21-32 (2008)

Kaser, A., et al. B lymphocyt-derived IL-16 attracts dendritic cells and Th cells. *J. Immuno.* **165**, 2474-2480 (2000)

Kerr, J.F., Wyllie, A.H., Currie, A.R. Apoptosis: a basic biological phenomenon with wide-ranging implications in tissue kinetics. *Br. J. Cancer* **26**, 239-57 (1972)

Kelly, J.M., Waterhouse, N.J., Cretney, E., Browne, K.A., Ellis, S., Trapani, J.A., Smyth, M.J. Granzyme M mediates a novel form of perforin-dependent cell death. *J Biol Chem.* **279**, 22236-42 (2004)

Kono, H., and Rock, K.L. How dying cells alert the immune system to danger. *Nat. Rev. Immunol.* **8**, 279-89 (2008)

Kleber, S., Sancho-Martinez, I., Wiestler, B., Beisel, A., et al. Yes and PI3K bind CD95 to signal invasion of glioblastoma. *Cancer Cell* **13**, 235-248. (2008)

Korkmaz, B., Marshall, S.H., Jenne, D.J., Gauthier, F. Neutrophil elastase, proteinase 3, and cathepsin G as therapeutic targets in human diseases. *Pharma. Revs.* **62**, 726-759 (2010)

L

Lauber, K., Bohn, E., Kröber, S.M., Xiao, Y.J., Blumenthal, S.G., Lindemann, RK, et al. Apoptotic cells induce migration of phagocytes via caspase-3-mediated release of a lipid attraction signal. *Cell* **113**, 717-30 (2003)

Latz, E., Xiao, T.S., Stutz, A. Activation and regulation of the inflammasomes. *Nat Rev Immunol.* **13**, 397-41 (2013)

Lamkanfi, M., Dixit, V.M. Mechanisms and functions of inflammasomes. *Cell.* **5,**1013-22 (2014)

Lefrancais, E., Cayrol, C. Mechanisms of IL-33 processing and secretion: differences and similarities between IL-1 family members. *Eur. Cytokine Netw.* **23**, 120-127 (2012)

Li, P., Nijhawan, D., Budihardjo, I., Srinivasula, S.M., Ahmad, M., Alnemri, E.S., Wang, X. Cytochrome c and dATP-dependent formation of Apaf-1/caspase-9 complex initiates an apoptotic protease cascade. *Cell* **91**, 479-89 (1997)

Liu, X., Kim, C.N., Yang, J., Jemmerson, R., Wang, X. (1996). Induction of apoptotic program in cell-free extracts: requirement for dATP and cytochrome c. Cell *86*, 147-57.

Lowes, M.A., Bowcock, A.M., Kruger, J.G.. Pathogenesis and therapy of psoriasis *Nature.* **445**, 866-873 (2007)

Lowes, M.A., Russell, C.B., Martin, D.A., Towne, J.E., Krueger, J.G. The IL-23/T17 pathogenic axis in psoriasis is amplified by keratinocyte responses.*Trends Immunol.* **34**, 174-81 (2013)

Lucas, M., Stuart, L.M., Zhang, A., Hodivala-Dilke, K., Febbraio, M., Silverstein, R., Savill, J., Lacy-Hulbert, A. Requirements for apoptotic cell contact in regulation of macrophage responses. *J. Immunol.* **177**, 4047-54 (2006)

Lucas, M., Stuart, L.M., Savill, J., Lacy-Hulbert, A. Apoptotic cells and innate immune stimuli combine to regulate macrophage cytokine secretion. *J. Immunol.* **171**, 2610-5 (2003)

Lüthi, A.U., Cullen, S.P., McNeela, E.A., Duriez, P.J., Afonina, I.S., Sheridan, C., Brumatti, G., Taylor, R.C., Kersse, K., Vandenabeele, P.,

Lavelle, E.C., Martin, S.J. Suppression of interleukin-33 bioactivity through proteolysis by apoptotic caspases. *Immunity* **31**, 84-98 (2009)

Lüthi, A.U., and Martin, S.J. The CASBAH: a searchable database of caspase substrates. *Cell Death Differ.* **14**, 641-50 (2007)

Lukens, J.R., Voge,l P., Johnson, G.R., Kelliher, M.A., Iwakura, Y., Lamkanfi, M., Kanneganti, T.D. RIP1-driven autoinflammation targets IL-1α independently of inflammasomes and RIP3. *Nature* **498**, 224-7 (2013)

Lukens, J.R., Gross, J.M., Kanneganti, T.D. IL-1 family cytokines trigger sterile inflammatory disease. *Front Immunol.* **3**, 315 (2012)

M

Maas-Szabowski, N., Shimotoyodome, A., Fusenig, N.E. Keratinocyte growth regulation in fibroblast cocultures via double paracrine mechanism. *J. Invest. Dermatol.* **112**, 1843-1853 (1999)

Maas-Szabowski, N., Stark, H.J., Fusenig, N.E. Keratinocyte growth regulation in defined organotypic cultures through IL-1-induced keratinocyte growth factor expression in resting fibroblasts. *J. Invest. Dermatol.* **114**, 1075-1084 (2000)

Marichal, T., Ohata, K., Bedoret, D., Mesnil, C., Sabatel, C., Kobiyama, K., Lekeux, P., Coban, C., Akira, S., Ishii, K.J., Bureau, F., Desmet, C.J. DNA released from dying host cells meditates aluminum adjuvant activity. *Nat. Medicine* **17**, 996-1002 (2011)

Martin, S.J., Reutelingsperger, C.P., McGahon, A.J., Rader, J.A., van Schie, R.C., LaFace, D.M., Green, D.R. Early redistribution of plasma membrane phosphatidylserine is a general feature of apoptosis regardless of the initiating stimulus: inhibition by overexpression of Bcl-2 and Abl. *J. Exp. Med.* **182**, 1545-56 (1995).

Matzinger, P. Tolerance, danger, and the extended family. *Annu. Rev. Immunol.* **12**, 991-1045 (1994)

Martin, S.J., Henry, C.M., Cullen, S.P. A perspective on mammalian caspases as positive and negative regulators of inflammation. *Mol. Cell.* **46**, 387-97 (2012)

Martin, S.J., Lennon, S.V., Bonham, A.M., Cotter, T.G. Induction of apoptosis (programmed cell death) in human leukemic HL-60 cells by inhibition of RNA or protein synthesis. *J Immunol.* **145**, 1859-67 (1990)

Martin, S.J., Green, D.R. Protease activation during apoptosis: death by a thousand cuts? *Cell* **82**, 349-52 (1995)

Martin, S.J., Amarante-Mendes, G.P., Shi, L., Chuang, T.H., Casiano, C.A., O'Brien, G.A., Fitzgerald, P., Tan, E.M., Bokoch, G.M., Greenberg, A.H., Green, D.R. The cytotoxic cell protease granzyme B initiates apoptosis in a cell-free system by proteolytic processing and activation of the ICE/CED-3 family protease, CPP32, via a novel two-step mechanism. *EMBO J.* **15**, 2407-16 (1996)

Martin, S.J., Henry, C.M., Cullen, S.P. A perspective on Mammalian Caspases as Positive and Negative Regulators of Inflammation. *Mol. Cell 46*, 387-397 (2012)

Martin, U., Scholler, J., Gurgel. J., Renshaw, B., Sims, J.E, Gabel, C.A. Externalization of the leaderless cytokine IL-1F6 in response to lipopolysaccharide/ATP activation of transduced bone marrow derived macrophages. *J. Immunol.* **183**, 4021-30 (2009)

Marrakchi, S., Guigue, P., Renshaw, B.R., Puel, A., Pei, X.Y., Fraitag, S., Zribi, J., Bal, E., Cluzeau, C., Chrabieh, M., Towne, J.E., et al. Interleukin-36-receptor antagonist deficiency and generalized pustular psoriasis. *N. Engl. J. Med.* **365**, 620-8 (2011)

Martinvalet, D., Zhu, P., Lieberman, J. Granzyme A induces caspase-independent mitochondrial damage, a required first step for apoptosis. *Immunity* **22**, 355-70 (2005)

March, C.J., Mosley, B., Larsen, A., Cerretti, D.P., et al. Cloning, sequence and expression of two distinct human interleukin-1 complementary DNAs. *Nature* **315**, 641-647 (1985)

Mantovani, A., Allavena, A., Sica, F., Balkwill, F. Cancer-related inflammation *Nature* **454**, 436-444 (2008)

McGuire, M.J., Lipsky, P.E., Thiele, D.L. Generation of active myeloid and lymphoid granule serine proteases requires processing by the granule thiol protease dipeptidyl peptidase I. *J Biol Chem.* **268**, 2458-67 (1993)

Metz, M., Piliponsky, A.M., Chen, C.C., et al. Mast cells can enhance resistance to snake and honeybee venoms. *Science* **313**, 526–530 (2006)

Moffatt, M.F., Gut, I.G., Demenais, F., Strachan, D.P., Bouzigon, E., Heath, S., von Mutius, E. Farrall, M., Lathrop, M., Cookson, W.O. GABRIEL Consortium. A large-scale, consortium-based genomewide association study of asthma. *N. Engl. J. Med.* **363**, 1211–1221 (2010)

Murdoch, C., Muthana, S.B., Coffelt, C.E., Lewis, C.E. The role of myeloid cells in the promotion of tumour angiogenesis *Nat. Rev. Cancer* **8**, 618-631 (2008)

Murphy, M., Kerr, P., Grant-Kels, J.M. The histopathologic spectrum of psoriasis. *Clin Dermatol.* **6**, 524-528 (2007)

Mizutani, H., Black, R. and Kupper, T. Post-translation modifications of IL-1 differ markedly in keratinocytes and monocytes: implications for epidermal biology. *J. Invest. Dermatol.* **92**, 483 (1989)

O

Omoto, Y., Yamanaka, K., Tokime, K., Kitano, S., Kakeda, M., Akeda, T., Kurokawa, I., Gabazza, E.C., Tsutsui, H., Katayama, N., Yamanishi, K., Nakanishi, K., Mizutani, H. Granzyme B is a novel interleukin-18 converting enzyme. *J Dermatol Sci.* **59**, 129-35 (2010)

Obeid M[a]., et al. Calreticulin exposure dictates the immunogenicity of cancer cell death. *Nat. Med.* **13**, 54-61 (2006)

Obeid M[b]., et al. Calreticulin exposure is required for the immunogenicity of gamma-irradiation and UVC light-induced apoptosis. *Cell Death Diff.* **14**, 1848 (2007)

Ohno, T., Morita, H., Arae, K., Matsumoto, K., Nakae, S. Interleukin-33 in allergy. *Allergy.* **67**, 1203-14 (2012)

Onoufriadis, A., Simpson, M.A., Pink, A.E., DiMeglio, P., Smith, C.H., Pullabhatla, V., Knight, J., Spain, S.L., Nestle, F.O., Burden, A.D., Capon, F., Trembath, R.C., et al. Mutations in IL36RN/IL1F5 are associated with the severe episodic inflammatory skin disease known as generalized pustular psoriasis. *Am. J. Hum. Genet.* **89**, 432–437 (2011)

O'Reilly, L.A., Tin, L., et al. Strasser, A. Membrane-bound fas ligand only is essential for fas-induced apoptosis *Nature* **461**, 659-663. (2009)

P

Patel, V.A., Longacre, A., Hsiao, K., Fan, H., Meng, F., Mitchell, J.E., Rauch, J., Ucker, D.S., Levine, J.S. Apoptotic cells, at all stages of the death process, trigger characteristic signalling events that are divergent from and dominant over those triggered by necrotic cells: Implications for the delayed clearance model of autoimmunity. *J. Biol. Chem.* **281**, 4663-70 (2006)

Park, D.R., Thomsen, A.R., Frevert, C.W., Pham, U., Skerrett, S.J., Kiener, P.A., and Liles, W.C. Fas (CD95) induces proinflammatory cytokine responses by human monocytes and monocyte-derived macrophages. *J. Immunol.* **170**, 6209-6216 (2003)

Pardo, J., Bosque, A., Brehm, R., Wallich, R., Naval, J., Müllbacher, A., Anel, A., Simon, M.M. Apoptotic pathways are selectively activated by granzyme A and/or granzyme B in CTL-mediated target cell lysis. *J Cell Biol.* **167**, 457-68 (2004)

Préfontaine, D., Lajoie-Kadoch, S., Foley, S., Audusseau, S., Olivenstein, R., Halayko, A.J., Lemière, C., Martin, J.G., Hamid, Q. Increased expression of IL-33 in severe asthma: evidence of expression by airway smooth muscle cells. *J. Immunol.* **183**, 5094–5103 (2009)

Pasparakis, M., Haase, I., Nestle, F.O. Mechanisms regulating skin immunity and inflammation. *Nat. Rev. Immunol.* **14**, 289-301 (2014)

Pylayeva-Gupta, Y., Eun Lee, K., et al. Oncogenic Kras-induced GM-CSF production promotes the development of pancreatic neoplasia. *Cancer Cell* **21**, 836-847 (2012)

R

Ravichandran, K.S. Beginnings of a good apoptotic Meal: The find-me and eat me signalling pathways. *Immunity* **35**, 445-455 (2011)

Ramirez-Carrozzi, V., Sambandam, A., Luis, E., Lin, Z., Jeet, S., *et al.* IL-17C regulates the innate immune function of epithelial cells in an autocrine manner. *Nat. Immunol.* **12**, 1159-1166 (2011)

Rescigno, M., Piguet, V., Valzasina, B., Lens, S., Zubler, R., French, L., Kindler, V., Tschopp, J., and Ricciardi-Castagnoli, P. Fas engagement induces the maturation of dendritic cells (DCs), the release of interleukin (IL)-1beta, and the production of interferon gamma in the absence of IL-12 during DC-T cell cognate interaction: a new role for Fas ligand in inflammatory responses. *J. Exp. Med.* **192**, 1661-1668 (2000)

Ricci, J.E., Muñoz-Pinedo, C., Fitzgerald, P., Bailly-Maitre, B., Perkins, G.A., Yadava, N., Scheffler, I.E., Ellisman, M.H., Green, D.R. Disruption of mitochondrial function during apoptosis is mediated by caspase cleavage of the p75 subunit of complex I of the electron transport chain. *Cell* **117**, 773-86 (2004)

S

Scaffidi, P., Misteli, T., Bianchi, M.E. Release of chromatin protein HMGB1 by necrotic cells triggers inflammation. *Nature* **418**, 191-5 (2002)

Sprick, M.R., Weigand, M.A., Rieser, E., Rauch, CT., Juo, P., Krammer P.H., Walczak, H. FADD/MORT1 and Caspase-8 are recruited to TRAIL Receptors 1 and 2 and are essential for apoptosis mediated by TRAIL Receptor 2. *Immunity* **12**, 599-609 (2000)

Sprick, MR., Rieser, E. et al. Caspase-10 is recruited to and activated at the native TRAIL and CD95 death-inducing signalling complexes in a FADD-dependent manner but can not functionally substitute caspase-8. *EMBO J.* **21**, 4520-4530 (2002)

Shimizu, M., Yoshimoto, T., Sato, M., Morimoto, J., Matsuzawa, A., and Takeda, Y. Roles of CXC chemokines and macrophages in the recruitment of inflammatory cells and tumor rejection induced by Fas/Apo-1 (CD95) ligand-expressing tumor. *Int. J. Cancer* **114**, 926-935 (2005)

Salvesen, G.Y., and Dixit, V.M. Caspase activation: The induced-proximity model. *Proc. Natl. Acad. Sci. USA* **96**, 10964-10967 (1999)

Segawa, K., Suzuki, J., Nagata, S. Constitutive exposure of phosphatidylserine on viable cells. *Proc. Natl. Acad. Sci. USA* **108**, 19246-51 (2011)

Schmitz, J., Owyang, A., Oldham, E., Song, Y., Murphy, E., McClanahan, T.K., Zurawski, G., Moshrefi, M., Qin, J., Li, X., Gorman, D.M., Bazan, J.F., Kastelein, R.A. IL-33, an interleukin-1-like cytokine that signals via the IL-1 receptor-related protein ST2 and induces T helper type 2-associated cytokines. *Immunity* **23**, 479-90 (2005)

Stuart, L.M., Lucas, M., Simpson, C., Lamb, J., Savill, J., Lacy-Hulbert, A. Inhibitory effects of apoptotic cell ingestion upon endotoxin-driven myeloid dendritic cell maturation. *J. Immunol.* **168**, 1627-35 (2002)

Stefan, C., Jansen, S., Bollen, M. Modulation of purinergic signalling by NPP-type ectophosphoiesterases. *Purinergic Signalling* **2**, 361-370 (2006)

Sharif-Askari, E., Alam, A., Rheaume, E., Beresford, P.J., Scotto, C., Sharma, K. et al. Direct cleavage of the human DNA fragmentation factor-45 by granzyme B induces caspase-activated DNase release and DNA fragmentation. *EMBO J.* **20**, 3101-3113 (2001)

Smyth, M.J., Thia, K.Y., Street, S.E., MacGregor, D., Godfrey, D.I., Trapani, J.A. Perforin-mediated cytotoxicity is critical for surveillance of spontaneous lymphoma. *J Exp Med.* **192**, 755-760 (2000)

Schroder, K., Tschopp, J. The inflammasomes. *Cell* **140**, 821-32. (2010)

Schonthaler, HB., Guinea-Viniegra, J., Wculek, SK., Ruppen, I., Ximénez-Embún, P., Guío-Carrión, A., Navarro, R., Hogg, N., Ashman, K., Wagner, E.F. S100A8-S100A9 protein complex mediates

psoriasis by regulating the expression of complement factor C3. *Immunity*. **39**,1171-81 (2013)

Serhan, C.N., Savill, J. Resolution of inflammation: the beginning programs the end. *Nat. Immunol.* **6**, 1191-1197 (2005)

Steinwede, K,. Heken, S., Bohling, J., Maus, R., et al. TNF-related apoptosis-inducing ligand (TRAIL) exerts therapeutic efficacy for the treatment of pneumococcal pneumonia in mice. *J. Exp. Med.* **209**, 1937-1952 (2012)

Steinwede, K., Maus, R., Bohling, J., Voedisch, S., Braun, A., Ochs, M., Schmiedl, A., Langer, F., Gauthier, F., Roes, J., Welte, T., Bange, F.C., Niederweis, M., Buhling, F., Maus, U.A. Cathepsin G and neutrophil elastase contribute to lung-protective immunity against mycobacterial infections in mice. *J. Immunol.* **199**, 4476-87 (2012)

Sims, J.E., Smith, D.E., The IL-1 family: regulators of immunity. *Nat. Rev. Immunol.* **2**, 89-102 (2010)

T

Taylor, R.C., Cullen, S.P., Martin, S.J. Apoptosis: controlled demolition at the cellular level. *Nat. Rev. Mol. Cell Biol.* **9**, 231-41 (2008)

Taylor, P.R., Roy, S., Leal, S.M Jr., Sun, Y., Howell, S.J., Cobb, B.A., Li, X., Pearlman, E. Activation of neutrophils by autocrine IL-17A-IL-17RC interactions during fungal infection is regulated by IL-6, IL-23, RORγt and dectin-2. *Nat Immunol.* (2014) **2**,143-51 (2014)

Tenev, T., Bianchi, K., et al. Meier, P. The ripoptosome, a signaling platform that assembles in response to genotoxic stress and loss of IAPs. *Mol Cell* **43**, 432-348 (2011)

Telfer, N.R., Chalmers, R.J., Whale, K., Colman, G. The role of streptococcal infection in the initiation of guttate psoriasis. *Arch Dermatol.* **128**, 39-42 (1992)

Thomas, D.A., Du, C., Xu, M., Wang, X., Ley, T.J. DFF45/ICAD can be directly processed by granzyme B during the induction of apoptosis. *Immunity* **12**, 621-632 (2000)

Truman, L.A., Ford, C.A., Pasikowska, M., Pound, J.D., Wilkinson, S.J., Dumitriu, I.E., Melville, L., Melrose, L.A., Ogden, C.A., Nibbs, R., Graham, G., Combadiere, C., Gregory, C.D. CXCL1/fractalkine is released from apoptotic lymphocytes to stimulate macrophage chemotaxis. *Blood* **112**, 5026-36. (2008)

Thornberry, N.A., et al. A novel heterodimeric cysteine protease is required for interleukin-1b processing in monocytes. *Nature* **356**, 768-774 (1992)

Towne, J.E., Garka, K.E., Renshaw, B.R., Virca, G.D., Sims, J.E. Interleukin (IL)-1F6, IL-1F8, and IL-1F9 signal through IL-1Rrp2 and IL-1RAcP to activate the pathway leading to NF-kappaB and MAPKs. *J. Biol. Chem.* **279**, 13677-88 (2004)

Towne, J.E., Sims, J.E. IL-36 in psoriasis. *Curr. Opin. Pharmacol.* **4**, 486-90 (2012)

Tortola, L., Rosenwald, E., Abel, B., Blumberg, H., Schafer, M., Coyle, A.J., Renauld, J.C., Werner, S., Kisielow, J., Kofp, M. Psoriasiform dermatitis is driven by IL-36-mediated DC-keratinocyte crosstalk. *J Clin. Invest.* **122**, 3965-76 (2012)

V

Varfolomeev, E., Blankenship, J.W., Wayson, S.M., Fedorova, A.V., Kayagaki, N., Garg, P., Zobel, K., Dynek, J.N., Elliott, L.O., Wallweber, H.J., Flygare, J.A., Fairbrother, W.J., Deshayes, K., Dixit, V.M., and Vucic, D. IAP antagonists induce autoubiquitination of c-IAPs, NF-kappaB activation, and TNFalpha-dependent apoptosis. *Cell* **131**, 669-681 (2007)

Valdimarsson, H., Baker, B.S., Jonsdottir, I., Powles, A., Fry, L. Psoriasis: a T-cell-mediated autoimmune disease induced by streptococcal superantigens? *Immunol Today* 16, 145-9 (1995)

Varfolomeev, E., Maecker, H., Sharp, D., Lawerance, D., Renz, M., Vucic, D., Ashkenazi, A. Molecular determinants of kinase pathway activation by Apo2 ligand/Tumor necrosis factor-related apoptosis inducing ligand. *J. Cell Biol.* **280**, 40599-40608 (2005)

Vince, J.E., Wong, W.W., Khan, N., Feltham, R., Chau, D., Ahmed, A.U., Benetatos, C.A., Chunduru, S.K., Condon, S.M., McKinlay, M., Brink, R., Leverkus, M., Tergaonkar, V., Schneider P., Callus, B.A., Koentgen, F., Vaux, D.L., and Silke, J. IAP antagonists target cIAP1 to induce TNFalpha-dependent apoptosis. *Cell* **13**, 682-693 (2007)

Voll, R.E., Herrmann, M., Roth, E.A., Stach, C., Kalden, J.R., Girkontaite, I. Immunosuppressive effects of apoptotic cells. *Nature* **390**, 350-1 (1997)

Vigne, S., Palmer, G., Lammacchia, C., Martin, P., Talabot-Ayer, D., Rodriguez, E., Ronchi, F., Sallusto, F., Dinh, H., Sims, J.E., Gabay, C. IL-36R ligands are potent regulators of dendritic and T-cells. *Blood* **118**, 5813-23 (2011)

Vigne, S., Palmer, G., Martin, P., Lammacchia, C., Strebel, D., Rodriguez, E., Olleros, M.L., Vesin, D., Garcia, I., Ronchi, F., Sallusto,

F., Sims, J.E., Gabay, C. IL-36 signaling amplifies Th1 responses by enhancing proliferation and Th1 polarization of naive CD4+ T cells. *Blood* **120**, 3478-87 (2012)

W

Wallach, D., Kang, T.B., Kovalenko, A. Concepts of tissue injury and cell death in inflammation: a historical perspective. *Nat. Rev. Immunol.* **14**, 51-59 (2014)

Weckmann, M., Collison, A., et al. Critical link between TRAIL and CCL20 for the activation of the Th2 cells and the expression of allergic airway disease. *Nat Med.* **13,** 1308-1315 (2007)

Wessendorf, J.H., Garfinkel, S., Zhan, X., Brown, S., Maciag, T. Identification of a nuclear localization sequence within the structure of the human interleukin-1 alpha precursor. *J. Biol. Chem.* **268**, 22100-22104 (1993)

Werman, A., Werman-Venkert, R., et al., The precursor form of IL-1a is an intracrine proinflammatory activator of transcription. *Proc. Natl. Acad. Sci. USA* **101**, 2434-2439 (2004)

Weiss, G., Shemer, A., Trau, H. The Koebner phenomenon: review of the literature. *JEADV*. **16**, 241-248 (2002)

Whyte, H.J., Baughman, R.D. Acute guttate psoriasis and streptococcal infection. *Arch Dermatol.* **89**, 350-356 (1964)

Wiley, S.R., Schooley, K., Smolak, P.J., et al. Identification and characterization of a new member of the TNF family that induces apoptosis. *Immunity* **3**, 673-682 (1995)

Wu JK, Siller G, Strutton G. Psoriasis induced by topical imiquimod. Aust, *J. Dermatol.* **45**, 47-50 (2004)

Wiedow, O., Wiese, F., Streit, V., Kalm, C., Christophers, E. Lesional elastase activity in psoriasis, contact dermatitis, and atopoc dermatitis. *J. Invest. Dermatol.* **99**, 306-9 (1992)

Y

Yegutkin, G.G. Nucleotide- and nucleoside-converting ectoenzymes: Importent modulators of purinergic signalling cascade. *Bio. BioPhy. Acta.* **1783**, 673-694 (2008).

Youle, R.J., Strasser, A. The BCL-2 protein family: opposing activities that mediate cell death. *Nat. Rev. Mol. Cell Biol.* **9**, 47-59. (2008)

Z

Zheng, Y., Humphry, M., Maguire, J.J., Bennett, M.R., Clarke, M.C. Intracellular Interleukin-1 receptor 2 binding prevents cleavage and activity of interleukin-1a, controlling necrosis-induced sterile inflammation. *Immunity* 38, 285-295 (2013)

Appendices

APPENDIX I

Table A.1 Genes common among 3 microarray data sets (IL-36 8h vs. IL-36 24h vs. TNF 8 h)

IL17C
CCL20
IL8
beta-defensin 2
GM-CSF
IL36G
CXCL1
IL6
TNF
CXCL3
MMP9
CXCL2
ICAM1
CXCL5
MMP10
IL1R2
IL23A
SPRR2C
SPRR2E
STAT5A
IRAK2
IL13RA2
C3
IL7R
LCE3A
CCL27
HBEGF
IL24
IL1A

Table A.2 Genes common among 2 microarray data sets (IL-36 8h vs. IL-36 24h)

GCSF
CFB
VNN1
CXCL6
SPRR2B
SPRR2A
SPRR2F
S100A12
S100A7
S100A9

Table A.3 Genes common among 2 microarray data sets (IL-36 8h vs. TNF 8 h)

PTX3
SOD2
TNFAIP3
SPRR2D
IL1RN
TNIP1
IL32

Table A.4 Genes common among 2 microarray data sets (IL-36 24h vs. TNF 8 h)

LTB
C1R
P100
SERPINB2
IL1B LTB
C1R
SERPINB2
IL1B

Table A.5 Genes distinct in each dataset (IL-36 8h)

IL-27 beta
GPP2
IGFL1
NCF2
PDZK1IP1
IGFBP3
ELAFIN
G0S2
p100
MMP1
PI3
beta-defensin 103
CEACAM1
TRAIL
CYP4F22
FLG
PADI3
EPHA4
WNT2B
ID3
SPINK5

Table A.6 Genes distinct in each dataset (IL-36 24h)

IL20
SAA2
GDF15
DDIT3
SPRR2G
IL33
SLC17A9
FOXA2
PLAU
LCE2D
VEGFA
ELF3
LCE3D
C1S
IL36RN
C1QTNF1
S100P
CNFN
LCE3E
KPRP
KLF8

JAK3
FGF2
LCE3C

Table A.7 Genes distinct in each dataset (TNF 8h)

CXCL10
ZP4
CXCL11
C15orf48
RELB
STRA6
PRDM1
HCAR3
IL15
SAA1
ROBO4
ADAM8
LRRC4
SERPINB1
TGFA
IL6ST
GLIPR2
RNF207
STYK1
IKZF2
ANKS1B
DCLK1
C10orf140
RDH12
SOX6

APPENDIX II

Table B.1 Upregulated genes in primary keratinocytes after IL-36 stimulations for 24 h

Fold	Gene name	Description
69.433014	CSF3	Homo sapiens colony stimulating factor 3 (granulocyte) (CSF3), transcript variant 1, mRNA [NM_000759]
51.760067	CSF3	Homo sapiens colony stimulating factor 3 (granulocyte) (CSF3), transcript variant 1, mRNA [NM_000759]
40.823593	CCL20	Homo sapiens chemokine (C-C motif) ligand 20 (CCL20), transcript variant 1, mRNA [NM_004591]
38.880642	DEFB4A	Homo sapiens defensin, beta 4A (DEFB4A), mRNA [NM_004942] -beta defensin-2 (protein)
31.843754	SPAG17	Homo sapiens sperm associated antigen 17 (SPAG17), mRNA [NM_206996]
29.184593	XLOC_012171	BROAD Institute lincRNA (XLOC_012171), lincRNA [TCONS_00025895]
23.35521	CSF2	Homo sapiens colony stimulating factor 2 (granulocyte-macrophage) (CSF2), mRNA [NM_000758]
21.988441	IL8	Homo sapiens interleukin 8 (IL8), mRNA [NM_000584]
20.697691	XLOC_013743	BROAD Institute lincRNA (XLOC_013743), lincRNA [TCONS_00028388]
18.262558	TRIM63	Homo sapiens tripartite motif containing 63 (TRIM63), mRNA [NM_032588]
16.528027	C10orf10	Homo sapiens chromosome 10 open reading frame 10 (C10orf10), mRNA [NM_007021]
16.34225	C15orf48	Homo sapiens chromosome 15 open reading frame 48 (C15orf48), transcript variant 2, mRNA [NM_032413]
14.976621	CFB	Homo sapiens complement factor B (CFB), mRNA [NM_001710]
13.771075	IL20	Homo sapiens interleukin 20 (IL20), mRNA [NM_018724]
13.76288	VNN1	Homo sapiens vanin 1 (VNN1), mRNA [NM_004666]
13.731143	SAA2	Homo sapiens serum amyloid A2 (SAA2), transcript variant 1, mRNA [NM_030754]
13.260761	GDF15	Homo sapiens growth differentiation factor 15 (GDF15), mRNA [NM_004864]
13.137954	DDIT3	Homo sapiens DNA-damage-inducible transcript 3 (DDIT3), transcript variant 5, mRNA [NM_004083]
12.606268	IL17C	Homo sapiens interleukin 17C (IL17C), mRNA [NM_013278]
11.600558	XLOC_009826	BROAD Institute lincRNA (XLOC_009826), lincRNA [TCONS_00020509]
11.379206	BIRC3	Homo sapiens baculoviral IAP repeat containing 3 (BIRC3), transcript variant 1, mRNA [NM_001165]
10.94114	IL23A	Homo sapiens interleukin 23, alpha subunit p19 (IL23A), mRNA [NM_016584]
10.690276	IRAK2	Homo sapiens interleukin-1 receptor-associated kinase 2 (IRAK2), mRNA [NM_001570]
10.209315	C3	Homo sapiens complement component 3 (C3), mRNA [NM_000064]
9.495374	HSD11B1	Homo sapiens hydroxysteroid (11-beta) dehydrogenase 1 (HSD11B1), transcript variant 2, mRNA [NM_181755]
9.1202755	CD200	Homo sapiens CD200 molecule (CD200), transcript variant 2, mRNA [NM_001004196]
9.101638	ZP4	Homo sapiens zona pellucida glycoprotein 4 (ZP4), mRNA [NM_021186]
9.035993	CXCL3	Homo sapiens chemokine (C-X-C motif) ligand 3 (CXCL3), mRNA [NM_002090]
9.017041	IL36G	Homo sapiens interleukin 36, gamma (IL36G), mRNA [NM_019618]
8.854294		
8.803818	CXCL1	Homo sapiens chemokine (C-X-C motif) ligand 1 (melanoma growth stimulating activity, alpha) (CXCL1), mRNA [NM_001511]
8.734587	ZPLD1	Homo sapiens zona pellucida-like domain containing 1 (ZPLD1), mRNA [NM_175056]
8.720672	ICAM1	Homo sapiens intercellular adhesion molecule 1 (ICAM1), mRNA [NM_000201]
8.620493		
8.604077	CXCL1	Homo sapiens chemokine (C-X-C motif) ligand 1 (melanoma growth stimulating activity, alpha) (CXCL1), mRNA [NM_001511]
8.459235	MMP9	Homo sapiens matrix metallopeptidase 9 (gelatinase B, 92kDa gelatinase, 92kDa type IV collagenase) (MMP9), mRNA [NM_004994]
8.367012	HSPA5	Homo sapiens heat shock 70kDa protein 5 (glucose-regulated protein, 78kDa) (HSPA5), mRNA [NM_005347]
8.3178215	SAA1	Homo sapiens serum amyloid A1 (SAA1), transcript variant 1, mRNA [NM_000331]
8.191223	LOC100507410	Homo sapiens uncharacterized LOC100507410 (LOC100507410), transcript variant 1, non-coding RNA [NR_040018]
8.16783	SPRR2B	Homo sapiens small proline-rich protein 2B (SPRR2B), mRNA [NM_001017418]
8.124735	CXCL2	Homo sapiens chemokine (C-X-C motif) ligand 2 (CXCL2), mRNA [NM_002089]
8.102803	HSD17B2	Homo sapiens hydroxysteroid (17-beta) dehydrogenase 2 (HSD17B2), mRNA [NM_002153]
8.087323	XLOC_I2_0158(	BROAD Institute lincRNA (XLOC_I2_015800), lincRNA [TCONS_I2_00030845]
7.9605412	CXCL2	Homo sapiens chemokine (C-X-C motif) ligand 2 (CXCL2), mRNA [NM_002089]

7.776843	HBEGF	Homo sapiens heparin-binding EGF-like growth factor (HBEGF), mRNA [NM_001945]
7.6685796	ERO1LB	Homo sapiens ERO1-like beta (S. cerevisiae) (ERO1LB), mRNA [NM_019891]
7.6007347	SPRR2G	Homo sapiens small proline-rich protein 2G (SPRR2G), mRNA [NM_001014291]
7.3526845	IL33	Homo sapiens interleukin 33 (IL33), transcript variant 1, mRNA [NM_033439]
7.3103323	MAL	Homo sapiens mal, T-cell differentiation protein (MAL), transcript variant a, mRNA [NM_002371]
7.0721674	BIN2	Homo sapiens bridging integrator 2 (BIN2), mRNA [NM_016293]
7.002684	HERPUD1	Homo sapiens homocysteine-inducible, endoplasmic reticulum stress-inducible, ubiquitin-like domain member 1 (HERPUD1), transcript variant 1, mRNA [NM_014685]
6.995055	INHBA	Homo sapiens inhibin, beta A (INHBA), mRNA [NM_002192]
6.9926744	TNF	Homo sapiens tumor necrosis factor (TNF), mRNA [NM_000594]
6.8046994	LOC100130331	Homo sapiens POTE ankyrin domain family, member F pseudogene (LOC100130331), non-coding RNA [NR_027247]
6.778828	PLAT	Homo sapiens plasminogen activator, tissue (PLAT), transcript variant 1, mRNA [NM_000930]
6.704366	Q29HP5	Q29HP5_DROPS (Q29HP5) GA14742-PA (Fragment), partial (9%) [THC2614488]
6.6746635	S100A12	Homo sapiens S100 calcium binding protein A12 (S100A12), mRNA [NM_005621]
6.6273284	S100A7	Homo sapiens S100 calcium binding protein A7 (S100A7), mRNA [NM_002963]
6.5584235	EBI3	Homo sapiens Epstein-Barr virus induced 3 (EBI3), mRNA [NM_005755] IL-27B subunit
6.53614	ZBTB20	Homo sapiens zinc finger and BTB domain containing 20 (ZBTB20), transcript variant 2, mRNA [NM_015642]
6.4258595	APOBEC3A	Homo sapiens apolipoprotein B mRNA editing enzyme, catalytic polypeptide-like 3A (APOBEC3A), transcript variant 1, mRNA [NM_145699]
6.2368503	DEFB103B	Homo sapiens defensin, beta 103B (DEFB103B), mRNA [NM_018661]
6.1417527	PDZK1IP1	Homo sapiens PDZK1 interacting protein 1 (PDZK1IP1), mRNA [NM_005764]
6.0443163	TM4SF19	Homo sapiens transmembrane 4 L six family member 19 (TM4SF19), transcript variant 1, mRNA [NM_138461]
5.956803	S100A12	Homo sapiens S100 calcium binding protein A12 (S100A12), mRNA [NM_005621]
5.891213	CXCL6	Homo sapiens chemokine (C-X-C motif) ligand 6 (granulocyte chemotactic protein 2) (CXCL6), mRNA [NM_002993]
5.6514606	HSP90B3P	Homo sapiens heat shock protein 90kDa beta (Grp94), member 3, pseudogene (HSP90B3P), non-coding RNA [NR_003130]
5.6511436	HSP90B1	Homo sapiens heat shock protein 90kDa beta (Grp94), member 1 (HSP90B1), mRNA [NM_003299]
5.5709887	LOC282980	Homo sapiens uncharacterized LOC282980 (LOC282980), non-coding RNA [NR_040253]
5.2285357	C5orf41	Homo sapiens chromosome 5 open reading frame 41 (C5orf41), transcript variant 1, mRNA [NM_153607]
5.205643	CDH15	Homo sapiens cadherin 15, type 1, M-cadherin (myotubule) (CDH15), mRNA [NM_004933]
5.09709	LCE3A	Homo sapiens late cornified envelope 3A (LCE3A), mRNA [NM_178431]
5.0935235	SLC17A9	Homo sapiens solute carrier family 17, member 9 (SLC17A9), mRNA [NM_022082]
5.066864	HSD17B7	hydroxysteroid (17-beta) dehydrogenase 7 [Source:HGNC Symbol;Acc:5215] [ENST00000367915]
5.0124826	FOXA2	Homo sapiens forkhead box A2 (FOXA2), transcript variant 1, mRNA [NM_021784]
4.973112	TNFAIP3	Homo sapiens tumor necrosis factor, alpha-induced protein 3 (TNFAIP3), mRNA [NM_006290]
4.9654317	SLC6A14	Homo sapiens solute carrier family 6 (amino acid transporter), member 14 (SLC6A14), mRNA [NM_007231]
4.832312	C9orf30-TMEFF	Homo sapiens C9orf30-TMEFF1 readthrough (C9orf30-TMEFF1), mRNA [NM_001198812]
4.823201	PLAU	Homo sapiens plasminogen activator, urokinase (PLAU), transcript variant 2, mRNA [NM_001145031]
4.801179	PTGS2	Homo sapiens prostaglandin-endoperoxide synthase 2 (prostaglandin G/H synthase and cyclooxygenase) (PTGS2), mRNA [NM_000963] COX-2
4.776519	PDIA4	Homo sapiens protein disulfide isomerase family A, member 4 (PDIA4), mRNA [NM_004911]
4.567659	MANF	Homo sapiens mesencephalic astrocyte-derived neurotrophic factor (MANF), mRNA [NM_006010]
4.564704	SPRR2A	Homo sapiens small proline-rich protein 2A (SPRR2A), mRNA [NM_005988]
4.5474405	HSP90B1	Homo sapiens heat shock protein 90kDa beta (Grp94), member 1 (HSP90B1), mRNA [NM_003299]
4.5244412	IL7R	Homo sapiens interleukin 7 receptor (IL7R), mRNA [NM_002185]
4.488422	SPRR2E	Homo sapiens small proline-rich protein 2E (SPRR2E), mRNA [NM_001024209]
4.379859	XLOC_009869	BROAD Institute lincRNA (XLOC_009869), lincRNA [TCONS_00021206]
4.3612504	LTB	Homo sapiens lymphotoxin beta (TNF superfamily, member 3) (LTB), transcript variant 1, mRNA [NM_002341]
4.3541923	S100A9	Homo sapiens S100 calcium binding protein A9 (S100A9), mRNA [NM_002965]
4.3519993	XLOC_007966	BROAD Institute lincRNA (XLOC_007966), lincRNA [TCONS_00017158]
4.3113766	SPRR2A	Homo sapiens small proline-rich protein 2A (SPRR2A), mRNA [NM_005988]
4.2790117	DNAJB9	Homo sapiens DnaJ (Hsp40) homolog, subfamily B, member 9 (DNAJB9), mRNA [NM_012328]
4.1901636	C14orf49	Homo sapiens chromosome 14 open reading frame 49 (C14orf49), mRNA [NM_152592]
4.1779623	SPRR2C	Homo sapiens small proline-rich protein 2C (pseudogene) (SPRR2C), non-coding RNA [NR_003062]

4.175999	SPRR2F	Homo sapiens small proline-rich protein 2F (SPRR2F), mRNA [NM_001014450]
4.1480713	CHST6	Homo sapiens carbohydrate (N-acetylglucosamine 6-O) sulfotransferase 6 (CHST6), mRNA [NM_021615]
4.1326447	ADAMTS4	Homo sapiens ADAM metallopeptidase with thrombospondin type 1 motif, 4 (ADAMTS4), mRNA [NM_005099]
4.131739	PLAU	Homo sapiens plasminogen activator, urokinase (PLAU), transcript variant 1, mRNA [NM_002658]
4.101029	SLC39A2	Homo sapiens solute carrier family 39 (zinc transporter), member 2 (SLC39A2), transcript variant 1, mRNA [NM_014579]
4.096435	C3	Homo sapiens complement component 3 (C3), mRNA [NM_000064]
4.091649	IL24	Homo sapiens interleukin 24 (IL24), transcript variant 3, mRNA [NM_001185156]
4.0819373	ZNF165	Homo sapiens zinc finger protein 165 (ZNF165), mRNA [NM_003447]
3.9998243	AGR2	Homo sapiens anterior gradient homolog 2 (Xenopus laevis) (AGR2), mRNA [NM_006408]
3.9731362	CRELD1	Homo sapiens cysteine-rich with EGF-like domains 1 (CRELD1), transcript variant 2, mRNA [NM_015513]
3.972158	CEACAM6	Homo sapiens carcinoembryonic antigen-related cell adhesion molecule 6 (non-specific cross reacting antigen) (CEACAM6), mRNA [NM_002483]
3.9639387	RELB	Homo sapiens v-rel reticuloendotheliosis viral oncogene homolog B (RELB), mRNA [NM_006509]
3.9486969	G0S2	Homo sapiens G0/G1switch 2 (G0S2), mRNA [NM_015714]
3.9125137	SPRR2D	Homo sapiens small proline-rich protein 2D (SPRR2D), mRNA [NM_006945]
3.911955	IL4I1	Homo sapiens interleukin 4 induced 1 (IL4I1), transcript variant 2, mRNA [NM_172374]
3.8268902	TMEM125	Homo sapiens transmembrane protein 125 (TMEM125), mRNA [NM_144626]
3.7989657	DNAJC3-AS1	PREDICTED: Homo sapiens DNAJC3 antisense RNA 1 (non-protein coding) (DNAJC3-AS1), miscRNA [XR_109147]
3.7907703	CXCL5	Homo sapiens chemokine (C-X-C motif) ligand 5 (CXCL5), mRNA [NM_002994]
3.7777674	ANXA6	Homo sapiens annexin A6 (ANXA6), transcript variant 1, mRNA [NM_001155]
3.7752984	LCE2D	Homo sapiens late cornified envelope 2D (LCE2D), mRNA [NM_178430]
3.7563047	VEGFA	Homo sapiens vascular endothelial growth factor A (VEGFA), transcript variant 6, mRNA [NM_001025370]
3.7526937	XLOC_008100	UI-E-EJ0-aiq-m-17-0-UI.r1 UI-E-EJ0 Homo sapiens cDNA clone UI-E-EJ0-aiq-m-17-0-UI 5', mRNA sequence [BM723547]
3.7433336	WIPI1	Homo sapiens WD repeat domain, phosphoinositide interacting 1 (WIPI1), mRNA [NM_017983]
3.7066054	FA2H	Homo sapiens fatty acid 2-hydroxylase (FA2H), mRNA [NM_024306]
3.697084	STAT5A	Homo sapiens signal transducer and activator of transcription 5A (STAT5A), mRNA [NM_003152]
3.6759412	SLFN11	Homo sapiens schlafen family member 11 (SLFN11), transcript variant 1, mRNA [NM_001104587]
3.6081522	BST2	bone marrow stromal cell antigen 2 [Source:HGNC Symbol;Acc:1119] [ENST00000252593]
3.6044452	TNFAIP2	Homo sapiens tumor necrosis factor, alpha-induced protein 2 (TNFAIP2), mRNA [NM_006291]
3.5928674	C1R	Homo sapiens complement component 1, r subcomponent (C1R), mRNA [NM_001733]
3.5797102	C1R	Homo sapiens complement component 1, r subcomponent (C1R), mRNA [NM_001733]
3.5714023	IL1A	Homo sapiens interleukin 1, alpha (IL1A), mRNA [NM_000575]
3.5457125	ELF3	Homo sapiens E74-like factor 3 (ets domain transcription factor, epithelial-specific) (ELF3), transcript variant 1, mRNA [NM_004433]
3.5307097	LOC645431	Homo sapiens uncharacterized LOC645431 (LOC645431), non-coding RNA [NR_024334]
3.530615	IGFL1	Homo sapiens IGF-like family member 1 (IGFL1), mRNA [NM_198541]
3.5238976	NFKBIA	Homo sapiens nuclear factor of kappa light polypeptide gene enhancer in B-cells inhibitor, alpha (NFKBIA), mRNA [NM_020529]
3.516241	XLOC_I2_0091	BROAD Institute lincRNA (XLOC_I2_009182), lincRNA [TCONS_I2_00017188]
3.4827483	LCE3D	Homo sapiens late cornified envelope 3D (LCE3D), mRNA [NM_032563]
3.4782722	ANKRD56	Homo sapiens ankyrin repeat domain 56 (ANKRD56), mRNA [NM_001029870]
3.424185	PI3	Homo sapiens peptidase inhibitor 3, skin-derived (PI3), mRNA [NM_002638]
3.409569	XLOC_005633	ig67d02.y1 HR85 islet Homo sapiens cDNA 5', mRNA sequence [BM352801]
3.4047909	POU2F2	Homo sapiens POU class 2 homeobox 2 (POU2F2), transcript variant 3, mRNA [NM_001207026]
3.3791223	C1S	Homo sapiens complement component 1, s subcomponent (C1S), transcript variant 2, mRNA [NM_001734]
3.356883	KYNU	Homo sapiens kynureninase (KYNU), transcript variant 2, mRNA [NM_001032998]
3.3561497	SDF2L1	Homo sapiens stromal cell-derived factor 2-like 1 (SDF2L1), mRNA [NM_022044]
3.3184495	C12orf76	Homo sapiens chromosome 12 open reading frame 76 (C12orf76), mRNA [NM_207435]
3.3097785	MYZAP	Homo sapiens myocardial zonula adherens protein (MYZAP), transcript variant 1, mRNA [NM_001018100]
3.303456	PTX3	Homo sapiens pentraxin 3, long (PTX3), mRNA [NM_002852]
3.3015218	TRIM47	Homo sapiens tripartite motif containing 47 (TRIM47), mRNA [NM_033452]
3.2941937	TCP11L2	Homo sapiens t-complex 11 (mouse)-like 2 (TCP11L2), mRNA [NM_152772]
3.2897513	BAMBI	Homo sapiens BMP and activin membrane-bound inhibitor homolog (Xenopus laevis) (BAMBI), mRNA [NM_012342]

3.289262	PRSS22	Homo sapiens protease, serine, 22 (PRSS22), mRNA [NM_022119]
3.287536	TM4SF19	Homo sapiens transmembrane 4 L six family member 19 (TM4SF19), transcript variant 1, mRNA [NM_138461]
3.2730165	EREG	Homo sapiens epiregulin (EREG), mRNA [NM_001432]
3.2464726	CRELD1	Homo sapiens cysteine-rich with EGF-like domains 1 (CRELD1), transcript variant 1, mRNA [NM_001031717]
3.2444592		UI-H-FH1-bfk-h-04-0-UI.s1 NCI_CGAP_FH1 Homo sapiens cDNA clone UI-H-FH1-bfk-h-04-0-UI 3', mRNA sequence [BU618747]
3.2365463	BST2	Homo sapiens bone marrow stromal cell antigen 2 (BST2), mRNA [NM_004335]
3.2296154	LOC100507165	PREDICTED: Homo sapiens hypothetical LOC100507165 (LOC100507165), miscRNA [XR_110530]
3.2259817	IL36RN	Homo sapiens interleukin 36 receptor antagonist (IL36RN), transcript variant 1, mRNA [NM_012275]
3.2197673	LCP1	Homo sapiens lymphocyte cytosolic protein 1 (L-plastin) (LCP1), mRNA [NM_002298]
3.2128575	NRCAM	Homo sapiens neuronal cell adhesion molecule (NRCAM), transcript variant 1, mRNA [NM_001037132]
3.1948323	IFI27	Homo sapiens interferon, alpha-inducible protein 27 (IFI27), transcript variant 2, mRNA [NM_005532]
3.1890678		UI-H-FH1-bfk-h-04-0-UI.s1 NCI_CGAP_FH1 Homo sapiens cDNA clone UI-H-FH1-bfk-h-04-0-UI 3', mRNA sequence [BU618747]
3.1668882	FOXQ1	Homo sapiens forkhead box Q1 (FOXQ1), mRNA [NM_033260]
3.1429155	RN5-8S1	Homo sapiens RNA, 5.8S ribosomal 1 (RN5-8S1), ribosomal RNA [NR_003285]
3.1348345	MYZAP	Homo sapiens myocardial zonula adherens protein (MYZAP), transcript variant 1, mRNA [NM_001018100]
3.1264005	CRCT1	Homo sapiens cysteine-rich C-terminal 1 (CRCT1), mRNA [NM_019060]
3.111231	NDRG2	Homo sapiens NDRG family member 2 (NDRG2), transcript variant 1, mRNA [NM_201535]
3.0981865	CALB1	Homo sapiens calbindin 1, 28kDa (CALB1), mRNA [NM_004929]
3.0980656	ZC3H12A	Homo sapiens zinc finger CCCH-type containing 12A (ZC3H12A), mRNA [NM_025079]
3.0961103		Homo sapiens cDNA clone IMAGE:40134159. [BC127811]
3.093814	APOBEC3G	Homo sapiens apolipoprotein B mRNA editing enzyme, catalytic polypeptide-like 3G (APOBEC3G), mRNA [NM_021822]
3.086952		glycogenin 2 pseudogene 1 [Source:HGNC Symbol;Acc:4701] [ENST00000382965]
3.0777607	XLOC_I2_0146(	BROAD Institute lincRNA (XLOC_I2_014602), lincRNA [TCONS_I2_00028340]
3.0744328	UBE2H	Homo sapiens ubiquitin-conjugating enzyme E2H (UBE2H), transcript variant 1, mRNA [NM_003344]
3.0714164	FICD	Homo sapiens FIC domain containing (FICD), mRNA [NM_007076]
3.0676627	B3GALT4	Homo sapiens UDP-Gal:betaGlcNAc beta 1,3-galactosyltransferase, polypeptide 4 (B3GALT4), mRNA [NM_003782]
3.0670593	AGPAT4-IT1	Homo sapiens AGPAT4 intronic transcript 1 (non-protein coding) (AGPAT4-IT1), non-coding RNA [NR_024277]
3.0566711	BIK	Homo sapiens BCL2-interacting killer (apoptosis-inducing) (BIK), mRNA [NM_001197]
3.0527558	XLOC_I2_0091:	full-length cDNA clone CS0DI053YO09 of Placenta Cot 25-normalized of Homo sapiens (human) [CR614803]
3.0527053	SPRR2D	Homo sapiens small proline-rich protein 2D (SPRR2D), mRNA [NM_006945]
3.0241356	DNAJC3-AS1	PREDICTED: Homo sapiens DNAJC3 antisense RNA 1 (non-protein coding) (DNAJC3-AS1), miscRNA [XR_109147]
3.0045614	TNFRSF10C	Homo sapiens tumor necrosis factor receptor superfamily, member 10c, decoy without an intracellular domain (TNFRSF10C), mRNA [NM_003841]
3.004313	LOC100286793	Homo sapiens uncharacterized LOC100286793 (LOC100286793), non-coding RNA [NR_027469]
2.9889772	DOK7	Homo sapiens docking protein 7 (DOK7), transcript variant 1, mRNA [NM_173660]
2.9850104	LOC152225	Homo sapiens uncharacterized LOC152225 (LOC152225), non-coding RNA [NR_026934]
2.9782557	LOC100506544	PREDICTED: Homo sapiens hypothetical LOC100506544 (LOC100506544), miscRNA [XR_109720]
2.9692929	LOC645638	Homo sapiens WDNM1-like pseudogene (LOC645638), non-coding RNA [NR_030732]
2.9666374	IL1R2	Homo sapiens interleukin 1 receptor, type II (IL1R2), transcript variant 1, mRNA [NM_004633]
2.9662118	NFKB2	Homo sapiens nuclear factor of kappa light polypeptide gene enhancer in B-cells 2 (p49/p100) (NFKB2), transcript variant 3, mRNA [NM_001077493]
2.9564447	MCTP1	Homo sapiens multiple C2 domains, transmembrane 1 (MCTP1), transcript variant L, mRNA [NM_024717]
2.9523883	IL24	Homo sapiens interleukin 24 (IL24), transcript variant 3, mRNA [NM_001185156]
2.9454944	COL4A4	Homo sapiens collagen, type IV, alpha 4 (COL4A4), mRNA [NM_000092]
2.9430752	HLA-B	major histocompatibility complex, class I, B [Source:HGNC Symbol;Acc:4932] [ENST00000466304]
2.942795	PRDM1	Homo sapiens PR domain containing 1, with ZNF domain (PRDM1), transcript variant 1, mRNA [NM_001198]
2.936699		
2.9354684	MMP10	Homo sapiens matrix metallopeptidase 10 (stromelysin 2) (MMP10), mRNA [NM_002425]
2.93116	SERPINB2	Homo sapiens serpin peptidase inhibitor, clade B (ovalbumin), member 2 (SERPINB2), transcript variant 2, mRNA [NM_002575]
2.9293044	PPP1R3B	Homo sapiens protein phosphatase 1, regulatory subunit 3B (PPP1R3B), transcript variant 1, mRNA [NM_001201329]
2.926407	PPP1R15A	Homo sapiens protein phosphatase 1, regulatory subunit 15A (PPP1R15A), mRNA [NM_014330]
2.9179425	CCDC149	Homo sapiens coiled-coil domain containing 149 (CCDC149), transcript variant 1, mRNA [NM_173463]

2.917354	TNFRSF6B	Homo sapiens tumor necrosis factor receptor superfamily, member 6b, decoy (TNFRSF6B), mRNA [NM_003823]
2.9173446	ANKK1	Homo sapiens ankyrin repeat and kinase domain containing 1 (ANKK1), mRNA [NM_178510]
2.9140604	ADAM8	Homo sapiens ADAM metallopeptidase domain 8 (ADAM8), transcript variant 1, mRNA [NM_001109]
2.9079123	YPEL2	Homo sapiens yippee-like 2 (Drosophila) (YPEL2), mRNA [NM_001005404]
2.904725	CLIP2	Homo sapiens CAP-GLY domain containing linker protein 2 (CLIP2), transcript variant 1, mRNA [NM_003388]
2.9010484	PIM1	Homo sapiens pim-1 oncogene (PIM1), transcript variant 1, mRNA [NM_002648]
2.8983746	GLIS2	Homo sapiens GLIS family zinc finger 2 (GLIS2), mRNA [NM_032575]
2.8975546	C1QTNF1	Homo sapiens C1q and tumor necrosis factor related protein 1 (C1QTNF1), mRNA [NM_198594]
2.8891335	RPS6KA5	Homo sapiens ribosomal protein S6 kinase, 90kDa, polypeptide 5 (RPS6KA5), transcript variant 1, mRNA [NM_004755]
2.888907	IL6	Homo sapiens interleukin 6 (interferon, beta 2) (IL6), mRNA [NM_000600]
2.8862443	DNASE1	Homo sapiens deoxyribonuclease I (DNASE1), mRNA [NM_005223]
2.8702517	TMEM45B	Homo sapiens transmembrane protein 45B (TMEM45B), mRNA [NM_138788]
2.867881	VEGFA	Homo sapiens vascular endothelial growth factor A (VEGFA), transcript variant 1, mRNA [NM_001025366]
2.8621435	C11orf96	Homo sapiens chromosome 11 open reading frame 96 (C11orf96), mRNA [NM_001145033]
2.8604932	NDRG2	Homo sapiens NDRG family member 2 (NDRG2), transcript variant 1, mRNA [NM_201535]
2.8498769	CCDC149	Homo sapiens coiled-coil domain containing 149 (CCDC149), transcript variant 1, mRNA [NM_173463]
2.8392866	KLHL24	Homo sapiens kelch-like 24 (Drosophila) (KLHL24), mRNA [NM_017644]
2.8330977	TNIP1	Homo sapiens TNFAIP3 interacting protein 1 (TNIP1), transcript variant 5, mRNA [NM_006058]
2.8297548	PRDM1	Homo sapiens PR domain containing 1, with ZNF domain (PRDM1), transcript variant 1, mRNA [NM_001198]
2.8250413	LOC100507165	PREDICTED: Homo sapiens hypothetical LOC100507165 (LOC100507165), miscRNA [XR_110530]
2.8248909	MYZAP	Homo sapiens myocardial zonula adherens protein (MYZAP), transcript variant 1, mRNA [NM_001018100]
2.8206022	LOC100505697	PREDICTED: Homo sapiens hypothetical LOC100505697 (LOC100505697), miscRNA [XR_108646]
2.8205183	PRDM8	Homo sapiens PR domain containing 8 (PRDM8), transcript variant 1, mRNA [NM_020226]
2.8172443	SLC7A11	Homo sapiens solute carrier family 7 (anionic amino acid transporter light chain, xc- system), member 11 (SLC7A11), mRNA [NM_014331]
2.8128824	TNFRSF6B	Homo sapiens tumor necrosis factor receptor superfamily, member 6b, decoy (TNFRSF6B), mRNA [NM_003823]
2.8084214	SQSTM1	Homo sapiens sequestosome 1 (SQSTM1), transcript variant 1, mRNA [NM_003900]
2.7984495	FAM100B	Homo sapiens family with sequence similarity 100, member B (FAM100B), mRNA [NM_182565]
2.7935157	LOC100652730	PREDICTED: Homo sapiens hypothetical LOC100652730 (LOC100652730), miscRNA [XR_132670]
2.7888873	PDE4DIP	Homo sapiens phosphodiesterase 4D interacting protein (PDE4DIP), transcript variant 5, mRNA [NM_001002811]
2.7873704	CLIP3	Homo sapiens CAP-GLY domain containing linker protein 3 (CLIP3), transcript variant 2, mRNA [NM_015526]
2.7832875	RNASE7	Homo sapiens ribonuclease, RNase A family, 7 (RNASE7), mRNA [NM_032572]
2.7803867	IL1B	Homo sapiens interleukin 1, beta (IL1B), mRNA [NM_000576]
2.7596788	NFKBIZ	Homo sapiens nuclear factor of kappa light polypeptide gene enhancer in B-cells inhibitor, zeta (NFKBIZ), transcript variant 1, mRNA [NM_031419]
2.754685	CEACAM7	Homo sapiens carcinoembryonic antigen-related cell adhesion molecule 7 (CEACAM7), mRNA [NM_006890]
2.749902	PNRC1	Homo sapiens proline-rich nuclear receptor coactivator 1 (PNRC1), mRNA [NM_006813]
2.7483337	GAB2	Homo sapiens GRB2-associated binding protein 2 (GAB2), transcript variant 2, mRNA [NM_012296]
2.7332218	NUCB2	Homo sapiens nucleobindin 2 (NUCB2), mRNA [NM_005013]
2.7317822	ABCG1	Homo sapiens ATP-binding cassette, sub-family G (WHITE), member 1 (ABCG1), transcript variant 5, mRNA [NM_207627]
2.7311213	C12orf70	Homo sapiens chromosome 12 open reading frame 70 (C12orf70), mRNA [NM_001145010]
2.7237384	KRT24	Homo sapiens keratin 24 (KRT24), mRNA [NM_019016]
2.7216218	RHCG	Homo sapiens Rh family, C glycoprotein (RHCG), mRNA [NM_016321]
2.718733	LARP1B	Homo sapiens La ribonucleoprotein domain family, member 1B (LARP1B), transcript variant 1, mRNA [NM_018078]
2.7172642	FGF2	Homo sapiens fibroblast growth factor 2 (basic) (FGF2), mRNA [NM_002006]
2.6935291	KCNG1	potassium voltage-gated channel, subfamily G, member 1 [Source:HGNC Symbol;Acc:6248] [ENST00000396017]
2.6881645	C20orf195	Homo sapiens chromosome 20 open reading frame 195 (C20orf195), mRNA [NM_024059]
2.687644	SLC22A15	Homo sapiens solute carrier family 22, member 15 (SLC22A15), mRNA [NM_018420]
2.6835501		Uncharacterized protein [Source:UniProtKB/TrEMBL;Acc:F5H305] [ENST00000538264]
2.6771326	LCE3B	Homo sapiens late cornified envelope 3B (LCE3B), mRNA [NM_178433]
2.6743202	SOD2	Homo sapiens superoxide dismutase 2, mitochondrial (SOD2), nuclear gene encoding mitochondrial protein, transcript variant 2, mRNA [NM_001024465]
2.6655645	C4orf34	Homo sapiens chromosome 4 open reading frame 34 (C4orf34), mRNA [NM_174921]

2.6541955	PION	Homo sapiens pigeon homolog (Drosophila) (PION), mRNA [NM_017439]
2.6534553	NUPR1	Homo sapiens nuclear protein, transcriptional regulator, 1 (NUPR1), transcript variant 1, mRNA [NM_001042483]
2.650235	FLYWCH1	Homo sapiens FLYWCH-type zinc finger 1 (FLYWCH1), transcript variant 2, mRNA [NM_020912]
2.649501	LOC100507053	Homo sapiens uncharacterized LOC100507053 (LOC100507053), non-coding RNA [NR_037884]
2.6436238	XLOC_l2_0014	BROAD Institute lincRNA (XLOC_l2_001496), lincRNA [TCONS_l2_00002904]
2.6256723	HOPX	Homo sapiens HOP homeobox (HOPX), transcript variant 2, mRNA [NM_139211]
2.6203837	ZSWIM4	Homo sapiens zinc finger, SWIM-type containing 4 (ZSWIM4), mRNA [NM_023072]
2.6186435	LOC645638	Homo sapiens WDNM1-like pseudogene (LOC645638), non-coding RNA [NR_030732]
2.6165984	CRELD2	Homo sapiens cysteine-rich with EGF-like domains 2 (CRELD2), transcript variant 2, mRNA [NM_024324]
2.6113057	LYPD5	Homo sapiens LY6/PLAUR domain containing 5 (LYPD5), transcript variant B, mRNA [NM_182573]
2.6103513	CLIP4	Homo sapiens CAP-GLY domain containing linker protein family, member 4 (CLIP4), mRNA [NM_024692]
2.608635	XLOC_002830	Q7NI46_GLOVI (Q7NI46) Cytochrome c550, partial (8%) [THC2717131]
2.6071281	SYNPO	synaptopodin [Source:HGNC Symbol;Acc:30672] [ENST00000394243]
2.6011488	APOBEC3B	Homo sapiens apolipoprotein B mRNA editing enzyme, catalytic polypeptide-like 3B (APOBEC3B), mRNA [NM_004900]
2.5766144	XLOC_012701	BROAD Institute lincRNA (XLOC_012701), lincRNA [TCONS_00026194]
2.560265	SLC22A18AS	Homo sapiens solute carrier family 22 (organic cation transporter), member 18 antisense (SLC22A18AS), mRNA [NM_007105]
2.5537195	C3orf67	Homo sapiens chromosome 3 open reading frame 67 (C3orf67), mRNA [NM_198463]
2.552452	NDRG4	Homo sapiens NDRG family member 4 (NDRG4), transcript variant 3, mRNA [NM_022910]
2.5427015	S100P	Homo sapiens S100 calcium binding protein P (S100P), mRNA [NM_005980]
2.53535	KREMEN2	Homo sapiens kringle containing transmembrane protein 2 (KREMEN2), transcript variant 4, mRNA [NM_172229]
2.53371	LOC388242	Homo sapiens coiled-coil domain containing 101 pseudogene (LOC388242), non-coding RNA [NR_002556]
2.5085833	IL13RA2	Homo sapiens interleukin 13 receptor, alpha 2 (IL13RA2), mRNA [NM_000640]
2.5057127	NRCAM	Homo sapiens neuronal cell adhesion molecule (NRCAM), transcript variant 4, mRNA [NM_001193582]
2.5052657	CNFN	Homo sapiens cornifelin (CNFN), mRNA [NM_032488]
2.5003684	ADM2	Homo sapiens adrenomedullin 2 (ADM2), mRNA [NM_024866]
2.4988036	SYNPO	Homo sapiens synaptopodin (SYNPO), transcript variant 1, mRNA [NM_007286]
2.4901154	PPBP	Homo sapiens pro-platelet basic protein (chemokine (C-X-C motif) ligand 7) (PPBP), mRNA [NM_002704]
2.4852183	INSIG1	Homo sapiens insulin induced gene 1 (INSIG1), transcript variant 1, mRNA [NM_005542]
2.4796932	BCL3	Homo sapiens B-cell CLL/lymphoma 3 (BCL3), mRNA [NM_005178]
2.4765298	LOC100293962	PREDICTED: Homo sapiens hypothetical LOC100293962 (LOC100293962), miscRNA [XR_110349]
2.4764366	RNF222	Homo sapiens ring finger protein 222 (RNF222), mRNA [NM_001146684]
2.4757917	HYOU1	Homo sapiens hypoxia up-regulated 1 (HYOU1), transcript variant 1, mRNA [NM_006389]
2.4594114	CALR	Homo sapiens calreticulin (CALR), mRNA [NM_004343]
2.4457476	FUT3	Homo sapiens fucosyltransferase 3 (galactoside 3(4)-L-fucosyltransferase, Lewis blood group) (FUT3), transcript variant 1, mRNA [NM_000149]
2.4435692	DHRS9	Homo sapiens dehydrogenase/reductase (SDR family) member 9 (DHRS9), transcript variant 1, mRNA [NM_005771]
2.4377322	XLOC_009810	BROAD Institute lincRNA (XLOC_009810), lincRNA [TCONS_00020478]
2.4349024	KRT23	Homo sapiens keratin 23 (histone deacetylase inducible) (KRT23), mRNA [NM_015515]
2.4265985	GALNT5	Homo sapiens UDP-N-acetyl-alpha-D-galactosamine:polypeptide N-acetylgalactosaminyltransferase 5 (GalNAc-T5) (GALNT5), mRNA [NM_014568]
2.4261076	KIAA1217	Homo sapiens cDNA FLJ43687 fis, clone TBAES2002197. [AK125675]
2.4218864	GIT2	Homo sapiens G protein-coupled receptor kinase interacting ArfGAP 2 (GIT2), transcript variant 4, mRNA [NM_139201]
2.4134417	EXOC7	Homo sapiens exocyst complex component 7, mRNA (cDNA clone IMAGE:4093432), with apparent retained intron. [BC029432]
2.4115431	SEL1L	Homo sapiens sel-1 suppressor of lin-12-like (C. elegans) (SEL1L), transcript variant 1, mRNA [NM_005065]
2.4097137	GFPT1	Homo sapiens glutamine--fructose-6-phosphate transaminase 1 (GFPT1), transcript variant 1, mRNA [NM_001244710]
2.4074306	LYST	Homo sapiens lysosomal trafficking regulator (LYST), mRNA [NM_000081]
2.4054422	C11orf68	Homo sapiens chromosome 11 open reading frame 68 (C11orf68), transcript variant 2, mRNA [NM_031450]
2.4038558	DNAJB5	Homo sapiens DnaJ (Hsp40) homolog, subfamily B, member 5 (DNAJB5), transcript variant 3, mRNA [NM_012266]
2.4035368	DOC2A	Homo sapiens double C2-like domains, alpha (DOC2A), mRNA [NM_003586]
2.3967156	CDK2AP2	Homo sapiens cyclin-dependent kinase 2 associated protein 2 (CDK2AP2), mRNA [NM_005851]
2.3961535	SLC9A7P1	Homo sapiens solute carrier family 9 (sodium/hydrogen exchanger), member 7 pseudogene 1 (SLC9A7P1), non-coding RNA [NR_033801]
2.3959887	LCE3E	Homo sapiens late cornified envelope 3E (LCE3E), mRNA [NM_178435]

2.39416	NCF2	Homo sapiens neutrophil cytosolic factor 2 (NCF2), transcript variant 1, mRNA [NM_000433]
2.3941348	XLOC_I2_0146(	BROAD Institute lincRNA (XLOC_I2_014602), lincRNA [TCONS_I2_00028340]
2.3882675	LOC100652850	PREDICTED: Homo sapiens hypothetical LOC100652850 (LOC100652850), miscRNA [XR_132554]
2.385744	DNAJC3	Homo sapiens DnaJ (Hsp40) homolog, subfamily C, member 3 (DNAJC3), mRNA [NM_006260]
2.3803551	RPS29	Homo sapiens ribosomal protein S29 (RPS29), transcript variant 2, mRNA [NM_001030001]
2.3796535	FBXL16	Homo sapiens F-box and leucine-rich repeat protein 16 (FBXL16), mRNA [NM_153350]
2.3746862	ITGA5	Homo sapiens integrin, alpha 5 (fibronectin receptor, alpha polypeptide) (ITGA5), mRNA [NM_002205]
2.3736417	XLOC_I2_01187	BROAD Institute lincRNA (XLOC_I2_011873), lincRNA [TCONS_I2_00022662]
2.3655052	TNFSF12	Homo sapiens tumor necrosis factor (ligand) superfamily, member 12 (TNFSF12), transcript variant 1, mRNA [NM_003809]
2.3622222	SRGAP2	Homo sapiens SLIT-ROBO Rho GTPase activating protein 2 (SRGAP2), transcript variant 2, mRNA [NM_001042758]
2.3610046	EMILIN2	Homo sapiens elastin microfibril interfacer 2 (EMILIN2), mRNA [NM_032048]
2.3608594	CCDC149	Homo sapiens coiled-coil domain containing 149 (CCDC149), transcript variant 1, mRNA [NM_173463]
2.3601325	DUSP5	Homo sapiens dual specificity phosphatase 5 (DUSP5), mRNA [NM_004419]
2.3589547		
2.353063	MNX1	Homo sapiens motor neuron and pancreas homeobox 1 (MNX1), transcript variant 1, mRNA [NM_005515]
2.351948	MAFF	Homo sapiens v-maf musculoaponeurotic fibrosarcoma oncogene homolog F (avian) (MAFF), transcript variant 1, mRNA [NM_012323]
2.3463547	KPRP	Homo sapiens keratinocyte proline-rich protein (KPRP), mRNA [NM_001025231]
2.3416443	XLOC_014399	BROAD Institute lincRNA (XLOC_014399), lincRNA [TCONS_00029924]
2.3372169	FUT8	Homo sapiens fucosyltransferase 8 (alpha (1,6) fucosyltransferase) (FUT8), transcript variant 1, mRNA [NM_178155]
2.3371487	JHDM1D	Homo sapiens jumonji C domain containing histone demethylase 1 homolog D (S. cerevisiae) (JHDM1D), mRNA [NM_030647]
2.3275144	UPP1	uridine phosphorylase 1 [Source:HGNC Symbol;Acc:12576] [ENST00000457596]
2.3206272	HLA-B	Homo sapiens major histocompatibility complex, class I, B (HLA-B), mRNA [NM_005514]
2.3190384	H1F0	Homo sapiens H1 histone family, member 0 (H1F0), mRNA [NM_005318]
2.31881	PELI1	Homo sapiens pellino homolog 1 (Drosophila) (PELI1), mRNA [NM_020651]
2.3124063	DUSP5P	Homo sapiens dual specificity phosphatase 5 pseudogene (DUSP5P), non-coding RNA [NR_002834]
2.3104866		
2.30493	C17orf100	Homo sapiens chromosome 17 open reading frame 100 (C17orf100), mRNA [NM_001105520]
2.3032553	QPRT	Homo sapiens quinolinate phosphoribosyltransferase (QPRT), mRNA [NM_014298]
2.3008144	B3GNT3	Homo sapiens UDP-GlcNAc:betaGal beta-1,3-N-acetylglucosaminyltransferase 3 (B3GNT3), mRNA [NM_014256]
2.3007581	ACSS2	Homo sapiens acyl-CoA synthetase short-chain family member 2 (ACSS2), transcript variant 1, mRNA [NM_018677]
2.297319	OBSCN	obscurin, cytoskeletal calmodulin and titin-interacting RhoGEF [Source:HGNC Symbol;Acc:15719] [ENST00000366706]
2.2954276	TMEM105	Homo sapiens transmembrane protein 105 (TMEM105), mRNA [NM_178520]
2.2909217	LOC100129931	Homo sapiens uncharacterized LOC100129931 (LOC100129931), non-coding RNA [NR_033828]
2.2813427		
2.2807224	MAPK10	Homo sapiens mitogen-activated protein kinase 10 (MAPK10), transcript variant 3, mRNA [NM_138980]
2.2779884	RHBDL2	Homo sapiens rhomboid, veinlet-like 2 (Drosophila) (RHBDL2), mRNA [NM_017821]
2.2773077	NCCRP1	Homo sapiens non-specific cytotoxic cell receptor protein 1 homolog (zebrafish) (NCCRP1), mRNA [NM_001001414]
2.2748373	TEP1	Homo sapiens telomerase-associated protein 1 (TEP1), mRNA [NM_007110]
2.2633872	PLEKHF1	Homo sapiens pleckstrin homology domain containing, family F (with FYVE domain) member 1 (PLEKHF1), mRNA [NM_024310]
2.2627327	FAM110C	Homo sapiens family with sequence similarity 110, member C (FAM110C), mRNA [NM_001077710]
2.2587996	CYP27A1	Homo sapiens cytochrome P450, family 27, subfamily A, polypeptide 1 (CYP27A1), nuclear gene encoding mitochondrial protein, mRNA [NM_000784]
2.2575247	MPZL2	Homo sapiens myelin protein zero-like 2 (MPZL2), transcript variant 2, mRNA [NM_144765]
2.2496054	SLC16A3	Homo sapiens solute carrier family 16, member 3 (monocarboxylic acid transporter 4) (SLC16A3), transcript variant 2, mRNA [NM_001042422]
2.2486079	XLOC_I2_01162	RST34200 Athersys RAGE Library Homo sapiens cDNA, mRNA sequence [BG214557]
2.2444959	FASN	Homo sapiens fatty acid synthase (FASN), mRNA [NM_004104]
2.2393858	SH3RF2	Homo sapiens protein phosphatase 1, regulatory subunit 39 (PPP1R39), mRNA [NM_152550]
2.2330058	SEC24D	Homo sapiens SEC24 family, member D (S. cerevisiae) (SEC24D), mRNA [NM_014822]
2.2321978	PLA2G4C	Homo sapiens phospholipase A2, group IVC (cytosolic, calcium-independent) (PLA2G4C), transcript variant 1, mRNA [NM_003706]
2.2311158	KLK12	Homo sapiens kallikrein-related peptidase 12 (KLK12), transcript variant 2, mRNA [NM_145894]
2.229312	LOC100507165	PREDICTED: Homo sapiens hypothetical LOC100507165 (LOC100507165), miscRNA [XR_110530]

2.2242687	XLOC_I2_0082(	Q46HA9_PROMT (Q46HA9) Uncharacterized conserved membrane protein, partial (7%) [THC2607024]
2.2214258	KLF8	Homo sapiens Kruppel-like factor 8 (KLF8), transcript variant 1, mRNA [NM_007250]
2.220324	NFKBIE	Homo sapiens nuclear factor of kappa light polypeptide gene enhancer in B-cells inhibitor, epsilon (NFKBIE), mRNA [NM_004556]
2.2187467	CCL27	Homo sapiens chemokine (C-C motif) ligand 27 (CCL27), mRNA [NM_006664]
2.2161977	OGT	Homo sapiens O-linked N-acetylglucosamine (GlcNAc) transferase (UDP-N-acetylglucosamine:polypeptide-N-acetylglucosaminyl transferase) (OGT), transcript variant 1, [NM_181672]
2.2112706	PNLIPRP3	Homo sapiens pancreatic lipase-related protein 3 (PNLIPRP3), mRNA [NM_001011709]
2.210642	JAK3	Homo sapiens Janus kinase 3 (JAK3), mRNA [NM_000215]
2.2096193	EHF	Homo sapiens ets homologous factor (EHF), transcript variant 2, mRNA [NM_012153]
2.2089696	FBXL20	Homo sapiens F-box and leucine-rich repeat protein 20 (FBXL20), transcript variant 1, mRNA [NM_032875]
2.2057812	RUNX2	Homo sapiens runt-related transcription factor 2 (RUNX2), transcript variant 3, mRNA [NM_004348]
2.1999376	XLOC_I2_0024(	BROAD Institute lincRNA (XLOC_I2_002469), lincRNA [TCONS_I2_00004769]
2.1993735	PVRL4	Homo sapiens poliovirus receptor-related 4 (PVRL4), mRNA [NM_030916]
2.1982164	SPRR3	Homo sapiens small proline-rich protein 3 (SPRR3), transcript variant 1, mRNA [NM_005416]
2.1980035	ADAMTS6	Homo sapiens ADAM metallopeptidase with thrombospondin type 1 motif, 6 (ADAMTS6), mRNA [NM_197941]
2.1968539	VASN	Homo sapiens vasorin (VASN), mRNA [NM_138440]
2.1911368	EIF4A2	Homo sapiens eukaryotic translation initiation factor 4A2 (EIF4A2), mRNA [NM_001967]
2.1908803	MSMO1	Homo sapiens methylsterol monooxygenase 1 (MSMO1), transcript variant 1, mRNA [NM_006745]
2.190514	KIF13B	Homo sapiens kinesin family member 13B (KIF13B), mRNA [NM_015254]
2.1884465	AEBP1	Homo sapiens AE binding protein 1 (AEBP1), mRNA [NM_001129]
2.1867683	HMSD	Homo sapiens histocompatibility (minor) serpin domain containing (HMSD), mRNA [NM_001123366]
2.1858788	CPAMD8	Homo sapiens C3 and PZP-like, alpha-2-macroglobulin domain containing 8 (CPAMD8), mRNA [NM_015692]
2.1794095	UTY	Homo sapiens ubiquitously transcribed tetratricopeptide repeat gene, Y-linked (UTY), transcript variant 3, mRNA [NM_007125]
2.1789317	C1orf54	Homo sapiens chromosome 1 open reading frame 54 (C1orf54), mRNA [NM_024579]
2.1765823	ZC3H6	Homo sapiens zinc finger CCCH-type containing 6 (ZC3H6), mRNA [NM_198581]
2.1751685	SELK	Homo sapiens selenoprotein K (SELK), mRNA [NM_021237]
2.174714	FGF2	Homo sapiens fibroblast growth factor 2 (basic) (FGF2), mRNA [NM_002006]
2.1739883	TRIB3	Homo sapiens tribbles homolog 3 (Drosophila) (TRIB3), mRNA [NM_021158]
2.1716053	MSI2	Homo sapiens musashi homolog 2 (Drosophila) (MSI2), transcript variant 1, mRNA [NM_138962]
2.162892		UI-H-FH1-bfk-h-04-0-UI.s1 NCI_CGAP_FH1 Homo sapiens cDNA clone UI-H-FH1-bfk-h-04-0-UI 3', mRNA sequence [BU618747]
2.1601145	XLOC_014399	PREDICTED: Homo sapiens hypothetical LOC100506737 (LOC100506737), miscRNA [XR_109732]
2.1537867	LCE3C	Homo sapiens late cornified envelope 3C (LCE3C), mRNA [NM_178434]
2.1503918	HOXA11-AS1	Homo sapiens HOXA11 antisense RNA 1 (non-protein coding) (HOXA11-AS1), antisense RNA [NR_002795]
2.1474364	LOC100134237	Homo sapiens cDNA FLJ46594 fis, clone THYMU3045692. [AK128451]
2.1459308	MALAT1	Homo sapiens metastasis associated lung adenocarcinoma transcript 1 (non-protein coding) (MALAT1), non-coding RNA [NR_002819]
2.143376		MPP8_HUMAN (Q99549) M-phase phosphoprotein 8, partial (48%) [THC2494281]
2.139148	CEBPB	Homo sapiens CCAAT/enhancer binding protein (C/EBP), beta (CEBPB), mRNA [NM_005194]
2.138762	TRIM8	Homo sapiens tripartite motif containing 8 (TRIM8), mRNA [NM_030912]
2.1383176	LOC100127983	Homo sapiens uncharacterized protein LOC100127983 (LOC100127983), mRNA [NM_001190972]
2.137911	MDM2	Homo sapiens Mdm2 p53 binding protein homolog (mouse) (MDM2), transcript variant MDM2, mRNA [NM_002392]
2.1327674	SAT1	Homo sapiens spermidine/spermine N1-acetyltransferase 1 (SAT1), transcript variant 1, mRNA [NM_002970]
2.132535	WDR33	Homo sapiens WD repeat domain 33 (WDR33), transcript variant 2, mRNA [NM_001006622]
2.127674	CCDC102A	Homo sapiens coiled-coil domain containing 102A (CCDC102A), mRNA [NM_033212]
2.1266282	SEL1L	Homo sapiens sel-1 suppressor of lin-12-like (C. elegans) (SEL1L), transcript variant 1, mRNA [NM_005065]
2.1265178	RHBDL2	Homo sapiens rhomboid, veinlet-like 2 (Drosophila) (RHBDL2), mRNA [NM_017821]
2.1253674	XLOC_I2_00918	BROAD Institute lincRNA (XLOC_I2_009182), lincRNA [TCONS_I2_00017189]
2.1248386	PDE9A	Homo sapiens phosphodiesterase 9A (PDE9A), transcript variant 1, mRNA [NM_002606]
2.1228821	ABL2	Homo sapiens v-abl Abelson murine leukemia viral oncogene homolog 2 (ABL2), transcript variant b, mRNA [NM_007314]
2.1224275	SERPINB1	Homo sapiens serpin peptidase inhibitor, clade B (ovalbumin), member 1 (SERPINB1), mRNA [NM_030666]
2.1222746	GJB4	Homo sapiens gap junction protein, beta 4, 30.3kDa (GJB4), mRNA [NM_153212]
2.1212018	FUT6	Homo sapiens fucosyltransferase 6 (alpha (1,3) fucosyltransferase) (FUT6), transcript variant 1, mRNA [NM_000150]

2.1189594	MICALCL	Homo sapiens MICAL C-terminal like (MICALCL), mRNA [NM_032867]
2.114384	KIF3C	Homo sapiens kinesin family member 3C (KIF3C), mRNA [NM_002254]
2.1139019	COL8A1	Homo sapiens collagen, type VIII, alpha 1 (COL8A1), transcript variant 1, mRNA [NM_001850]
2.1119535	CTH	Homo sapiens cystathionase (cystathionine gamma-lyase) (CTH), transcript variant 1, mRNA [NM_001902]
2.1038778	AKT3	Homo sapiens v-akt murine thymoma viral oncogene homolog 3 (protein kinase B, gamma) (AKT3), transcript variant 1, mRNA [NM_005465]
2.103866	ZNF449	Homo sapiens zinc finger protein 449 (ZNF449), mRNA [NM_152695]
2.1033683	RAB26	Homo sapiens RAB26, member RAS oncogene family (RAB26), mRNA [NM_014353]
2.1019366	AASS	Homo sapiens aminoadipate-semialdehyde synthase (AASS), nuclear gene encoding mitochondrial protein, mRNA [NM_005763]
2.0990818	RTTN	Homo sapiens rotatin (RTTN), mRNA [NM_173630]
2.0979457	NACAD	Homo sapiens NAC alpha domain containing (NACAD), mRNA [NM_001146334]
2.0977516	KLF7	Homo sapiens Kruppel-like factor 7 (ubiquitous) (KLF7), mRNA [NM_003709]
2.0967035	UTRN	Homo sapiens utrophin (UTRN), mRNA [NM_007124]
2.093583	MCTP1	Homo sapiens multiple C2 domains, transmembrane 1 (MCTP1), transcript variant L, mRNA [NM_024717]
2.0899584	ITGA1	Homo sapiens integrin, alpha 1 (ITGA1), mRNA [NM_181501]
2.0898776	GABARAPL1	Homo sapiens GABA(A) receptor-associated protein like 1 (GABARAPL1), mRNA [NM_031412]
2.0885394	XLOC_l2_0015	PREDICTED: Homo sapiens hypothetical LOC100505562 (LOC100505562), miscRNA [XR_109022]
2.087627	HLA-B	Homo sapiens major histocompatibility complex, class I, B (HLA-B), mRNA [NM_005514]
2.0861385	DDIT4L	Homo sapiens DNA-damage-inducible transcript 4-like (DDIT4L), mRNA [NM_145244]
2.081587	GCH1	Homo sapiens GTP cyclohydrolase 1 (GCH1), transcript variant 4, mRNA [NM_001024071]
2.0808854	XLOC_003123	BROAD Institute lincRNA (XLOC_003123), lincRNA [TCONS_00005774]
2.077091	HSPA13	Homo sapiens heat shock protein 70kDa family, member 13 (HSPA13), mRNA [NM_006948]
2.0764897	ZEB1-AS1	Homo sapiens ZEB1 antisense RNA 1 (non-protein coding) (ZEB1-AS1), non-coding RNA [NR_024284]
2.0706382	ARNTL	Homo sapiens aryl hydrocarbon receptor nuclear translocator-like (ARNTL), transcript variant 3, mRNA [NM_001030273]
2.0640335	RHBDL2	Homo sapiens rhomboid, veinlet-like 2 (Drosophila) (RHBDL2), mRNA [NM_017821]
2.063009	SLC2A14	solute carrier family 2 (facilitated glucose transporter), member 14 [Source:HGNC Symbol;Acc:18301] [ENST00000431042]
2.0611587	CCNG2	Homo sapiens cyclin G2 (CCNG2), mRNA [NM_004354]
2.060404	ADAMTS6	Homo sapiens ADAM metallopeptidase with thrombospondin type 1 motif, 6 (ADAMTS6), mRNA [NM_197941]
2.060289	C17orf39	Homo sapiens chromosome 17 open reading frame 39 (C17orf39), mRNA [NM_024052]
2.0598068	IFI6	Homo sapiens interferon, alpha-inducible protein 6 (IFI6), transcript variant 3, mRNA [NM_022873]
2.0597034	GKN1	Homo sapiens gastrokine 1 (GKN1), mRNA [NM_019617]
2.0596926	MAP1B	Homo sapiens microtubule-associated protein 1B (MAP1B), mRNA [NM_005909]
2.0545197	FGD6	Homo sapiens FYVE, RhoGEF and PH domain containing 6 (FGD6), mRNA [NM_018351]
2.0522203	GRB10	Homo sapiens growth factor receptor-bound protein 10 (GRB10), transcript variant 4, mRNA [NM_001001555]
2.051838	IFFO1	Homo sapiens intermediate filament family orphan 1 (IFFO1), transcript variant 4, mRNA [NM_001039670]
2.0489388	MGC23284	Homo sapiens uncharacterized LOC197187 (MGC23284), transcript variant 1, non-coding RNA [NR_024402]
2.0467985	TTC39A	Homo sapiens tetratricopeptide repeat domain 39A (TTC39A), transcript variant 2, mRNA [NM_001080494]
2.0444171	SLC9A7	Homo sapiens solute carrier family 9 (sodium/hydrogen exchanger), member 7 (SLC9A7), mRNA [NM_032591]
2.0433269	CLIP4	Homo sapiens CAP-GLY domain containing linker protein family, member 4 (CLIP4), mRNA [NM_024692]
2.0404937	PRSS16	Homo sapiens protease, serine, 16 (thymus) (PRSS16), mRNA [NM_005865]
2.0404074	MURC	Homo sapiens muscle-related coiled-coil protein (MURC), mRNA [NM_001018116]
2.0344694	ATM	ataxia telangiectasia mutated [Source:HGNC Symbol;Acc:795] [ENST00000389511]
2.0319304	MID2	Homo sapiens midline 2 (MID2), transcript variant 1, mRNA [NM_012216]
2.0312362	XLOC_l2_0135	RST11549 Athersys RAGE Library Homo sapiens cDNA, mRNA sequence [BG192435]
2.0301776		Homo sapiens mRNA similar to collagen, type XVII, alpha 1 (cDNA clone IMAGE:5431129). [BC044628]
2.0295677	DDIT4L	Homo sapiens DNA-damage-inducible transcript 4-like, mRNA (cDNA clone MGC:9960 IMAGE:3877854), complete cds. [BC013592]
2.028834	XLOC_008282	BROAD Institute lincRNA (XLOC_008282), lincRNA [TCONS_00017630]
2.0240412	ANG	Homo sapiens angiogenin, ribonuclease, RNase A family, 5 (ANG), transcript variant 1, mRNA [NM_001145]
2.0234191	STARD4	Homo sapiens StAR-related lipid transfer (START) domain containing 4 (STARD4), mRNA [NM_139164]
2.0218427	KRTDAP	Homo sapiens keratinocyte differentiation-associated protein (KRTDAP), transcript variant 1, mRNA [NM_207392]
2.0151033	MRGPRX4	Homo sapiens MAS-related GPR, member X4 (MRGPRX4), mRNA [NM_054032]

2.013423	XBP1	Homo sapiens X-box binding protein 1 (XBP1), transcript variant 1, mRNA [NM_005080]
2.0123	LAYN	Homo sapiens layilin (LAYN), mRNA [NM_178834]
2.0112958	DNAJB11	Homo sapiens DnaJ (Hsp40) homolog, subfamily B, member 11 (DNAJB11), mRNA [NM_016306]
2.009952	GPR172B	Homo sapiens G protein-coupled receptor 172B (GPR172B), transcript variant 2, mRNA [NM_017986]
2.0065563	SAT1	Homo sapiens spermidine/spermine N1-acetyltransferase 1 (SAT1), transcript variant 1, mRNA [NM_002970]
2.0063586	FEZ1	Homo sapiens fasciculation and elongation protein zeta 1 (zygin I) (FEZ1), transcript variant 1, mRNA [NM_005103]
2.0043676	UAP1L1	Homo sapiens UDP-N-acteylglucosamine pyrophosphorylase 1-like 1 (UAP1L1), mRNA [NM_207309]
2.0034113	LINC00246A	Homo sapiens long intergenic non-protein coding RNA 246A (LINC00246A), non-coding RNA [NR_026595]
2.001337	CLCN6	Homo sapiens chloride channel 6 (CLCN6), transcript variant CIC-6a, mRNA [NM_001286]

APPENDIX II

Table B.2 Downregulated genes in primary keratinocytes after IL-36 stimulations for 24 h

Fold	Gene name	Description
-8.191788	TNNT3	Homo sapiens troponin T type 3 (skeletal, fast) (TNNT3), transcript variant 1, mRNA [NM_006757]
-6.8947883	XLOC_l2_0152	BROAD Institute lincRNA (XLOC_l2_015213), lincRNA [TCONS_l2_00029348]
-6.137759	IFIT1	Homo sapiens interferon-induced protein with tetratricopeptide repeats 1 (IFIT1), transcript variant 2, mRNA [NM_001548]
-6.0330105	HYMAI	Homo sapiens hydatidiform mole associated and imprinted (non-protein coding) (HYMAI), non-coding RNA [NR_002768]
-5.5801773	SPATA13	Homo sapiens spermatogenesis associated 13 (SPATA13), transcript variant 1, mRNA [NM_001166271]
-5.4950542	PALMD	Homo sapiens palmdelphin (PALMD), mRNA [NM_017734]
-5.410405	TXNIP	Homo sapiens thioredoxin interacting protein (TXNIP), mRNA [NM_006472]
-5.3707027	XLOC_011482	BROAD Institute lincRNA (XLOC_011482), lincRNA [TCONS_00023278]
-5.217255	SNX22	Homo sapiens sorting nexin 22 (SNX22), mRNA [NM_024798]
-5.1811795		
-5.00303		
-4.8557553	C21orf71	Homo sapiens chromosome 21 open reading frame 71 (C21orf71), non-coding RNA [NR_024092]
-4.8274083	LPPR5	Homo sapiens lipid phosphate phosphatase-related protein type 5 (LPPR5), transcript variant 1, mRNA [NM_001037317]
-4.717105	LOC100506895	Homo sapiens uncharacterized LOC100506895 (LOC100506895), non-coding RNA [NR_038276]
-4.7055974	CMPK2	Homo sapiens cytidine monophosphate (UMP-CMP) kinase 2, mitochondrial (CMPK2), nuclear gene encoding mitochondrial protein, mRNA [NM_207315]
-4.6945524	IFIT3	Homo sapiens interferon-induced protein with tetratricopeptide repeats 3 (IFIT3), transcript variant 1, mRNA [NM_001549]
-4.565911	DPP4	Homo sapiens dipeptidyl-peptidase 4 (DPP4), mRNA [NM_001935]
-4.5468516	CTSC	Homo sapiens cathepsin C (CTSC), transcript variant 2, mRNA [NM_148170]
-4.4568377	XLOC_013542	BROAD Institute lincRNA (XLOC_013542), lincRNA [TCONS_00028183]
-4.4563923	BMP6	Homo sapiens bone morphogenetic protein 6 (BMP6), mRNA [NM_001718]
-4.3981786	RPL27A	Homo sapiens ribosomal protein L27a (RPL27A), mRNA [NM_000990]
-4.259488	OASL	Homo sapiens 2'-5'-oligoadenylate synthetase-like (OASL), transcript variant 1, mRNA [NM_003733]
-4.185221	NALCN	Homo sapiens sodium leak channel, non-selective (NALCN), mRNA [NM_052867]
-4.1595645	XLOC_l2_0070	AGENCOURT_6797022 NIH_MGC_85 Homo sapiens cDNA clone IMAGE:5787713 5', mRNA sequence [BQ049787]
-4.149437	MPP4	Homo sapiens membrane protein, palmitoylated 4 (MAGUK p55 subfamily member 4) (MPP4), mRNA [NM_033066]
-4.1024175	MT1G	Homo sapiens metallothionein 1G (MT1G), mRNA [NM_005950]
-4.0154357		D86966 Start codon is not identified similarto human ZFY protein. {Homo sapiens} (exp=-1; wgp=0; cg=0), partial (3%) [THC2652081]
-4.010152		
-3.9694479	C1orf51	Homo sapiens chromosome 1 open reading frame 51 (C1orf51), mRNA [NM_144697]
-3.939485	LCLAT1	lysocardiolipin acyltransferase 1 [Source:HGNC Symbol;Acc:26756] [ENST00000319406]
-3.9371805	FECH	Homo sapiens ferrochelatase (FECH), nuclear gene encoding mitochondrial protein, transcript variant 1, mRNA [NM_001012515]
-3.878685	SLITRK5	Homo sapiens SLIT and NTRK-like family, member 5 (SLITRK5), mRNA [NM_015567]
-3.843521	HIST1H1A	Homo sapiens histone cluster 1, H1a (HIST1H1A), mRNA [NM_005325]
-3.8093967	C1QTNF9B-AS	Homo sapiens C1QTNF9B antisense RNA 1 (non-protein coding) (C1QTNF9B-AS1), transcript variant 1, mRNA [NM_001014442]
-3.7906632	AFG3L1P	Homo sapiens AFG3 ATPase family gene 3-like 1 (S. cerevisiae), pseudogene (AFG3L1P), transcript variant 3, non-coding RNA [NR_003228]
-3.7845924	LOC100652761	PREDICTED: Homo sapiens hypothetical LOC100652761 (LOC100652761), miscRNA [XR_132756]
-3.7741382	EPHA4	Homo sapiens EPH receptor A4 (EPHA4), mRNA [NM_004438]
-3.7716055	MT1H	Homo sapiens metallothionein 1H (MT1H), mRNA [NM_005951]
-3.750955		
-3.721235	CASC2	Homo sapiens cancer susceptibility candidate 2 (non-protein coding) (CASC2), transcript variant 1, non-coding RNA [NR_026939]
-3.7182229	LOC100505683	PREDICTED: Homo sapiens hypothetical LOC100505683 (LOC100505683), miscRNA [XR_109654]
-3.714969	C10orf140	Homo sapiens chromosome 10 open reading frame 140 (C10orf140), mRNA [NM_207371]
-3.7009816	SNORA30	Homo sapiens small nucleolar RNA, H/ACA box 30 (SNORA30), small nucleolar RNA [NR_002966]
-3.6792233	HSPA2	Homo sapiens heat shock 70kDa protein 2 (HSPA2), mRNA [NM_021979]

-3.6702075	LOC100507431	Homo sapiens cDNA clone IMAGE:4838987. [BC031979]
-3.634269	PRR22	Homo sapiens proline rich 22 (PRR22), mRNA [NM_001134316]
-3.609055	WDR33	Homo sapiens WD repeat domain 33 (WDR33), transcript variant 1, mRNA [NM_018383]
-3.5751438	TNNI2	Homo sapiens troponin I type 2 (skeletal, fast) (TNNI2), transcript variant 1, mRNA [NM_003282]
-3.5750303	CD244	Homo sapiens CD244 molecule, natural killer cell receptor 2B4 (CD244), transcript variant 2, mRNA [NM_001166663]
-3.554521	DOK3	Homo sapiens docking protein 3 (DOK3), transcript variant 1, mRNA [NM_024872]
-3.5539641	LPHN2	Homo sapiens latrophilin 2 (LPHN2), mRNA [NM_012302]
-3.5242286	FLJ45684	Homo sapiens cDNA FLJ45684 fis, clone FCBBF3005160. [AK127589]
-3.505555	CYP24A1	Homo sapiens cytochrome P450, family 24, subfamily A, polypeptide 1 (CYP24A1), nuclear gene encoding mitochondrial protein, transcript variant 1, mRNA [NM_000782]
-3.4832041	PER2	Homo sapiens period homolog 2 (Drosophila) (PER2), mRNA [NM_022817]
-3.4566667	CHRNA10	Homo sapiens cholinergic receptor, nicotinic, alpha 10 (CHRNA10), mRNA [NM_020402]
-3.4539316	CPA4	Homo sapiens carboxypeptidase A4 (CPA4), transcript variant 1, mRNA [NM_016352]
-3.433503	RPP30	Homo sapiens ribonuclease P/MRP 30kDa subunit (RPP30), transcript variant 1, mRNA [NM_001104546]
-3.4230292	APBA2	Homo sapiens amyloid beta (A4) precursor protein-binding, family A, member 2 (APBA2), transcript variant 1, mRNA [NM_005503]
-3.3976424	LFNG	Homo sapiens LFNG O-fucosylpeptide 3-beta-N-acetylglucosaminyltransferase (LFNG), transcript variant 1, mRNA [NM_001040167]
-3.3921576	LOC100131864	Homo sapiens cDNA FLJ36900 fis, clone BRACE2001954. [AK094219]
-3.3711917	XLOC_000605	BROAD Institute lincRNA (XLOC_000605), lincRNA [TCONS_00001323]
-3.3107708	SRSF6	Homo sapiens serine/arginine-rich splicing factor 6 (SRSF6), transcript variant 1, mRNA [NM_006275]
-3.307153	ZBTB24	Homo sapiens zinc finger and BTB domain containing 24 (ZBTB24), transcript variant 2, mRNA [NM_001164313]
-3.2843494	LOC729178	Homo sapiens cDNA clone IMAGE:5266307. [BC035182]
-3.2778351	LOC100505899	PREDICTED: Homo sapiens hypothetical LOC100505899 (LOC100505899), miscRNA [XR_109386]
-3.2540226	TEF	Homo sapiens thyrotrophic embryonic factor (TEF), transcript variant 1, mRNA [NM_003216]
-3.2490134	DDX58	Homo sapiens DEAD (Asp-Glu-Ala-Asp) box polypeptide 58 (DDX58), mRNA [NM_014314]
-3.2293186	HR	Homo sapiens hairless homolog (mouse) (HR), transcript variant 1, mRNA [NM_005144]
-3.2238522	USP41	ubiquitin specific peptidase 41 [Source:HGNC Symbol;Acc:20070] [ENST00000454608]
-3.217279		
-3.1571562	TIMP3	Homo sapiens TIMP metallopeptidase inhibitor 3 (TIMP3), mRNA [NM_000362]
-3.1434276	AQP6	Homo sapiens aquaporin 6, kidney specific (AQP6), mRNA [NM_001652]
-3.0852077	THEM4	Homo sapiens thioesterase superfamily member 4 (THEM4), mRNA [NM_053055]
-3.0650153	ID3	Homo sapiens inhibitor of DNA binding 3, dominant negative helix-loop-helix protein (ID3), mRNA [NM_002167]
-3.061606	LRFN1	Homo sapiens leucine rich repeat and fibronectin type III domain containing 1 (LRFN1), mRNA [NM_020862]
-3.0346048	CELSR1	Homo sapiens cadherin, EGF LAG seven-pass G-type receptor 1 (flamingo homolog, Drosophila) (CELSR1), mRNA [NM_014246]
-3.0332801	FRA10AC1	Homo sapiens fragile site, folic acid type, rare, fra(10)(q23.3) or fra(10)(q24.2) candidate 1 (FRA10AC1), mRNA [NM_145246]
-3.031495	MCPH1	Homo sapiens cDNA FLJ13884 fis, clone THYRO1001534. [AK023946]
-3.0014646	DOK3	Homo sapiens docking protein 3 (DOK3), transcript variant 2, mRNA [NM_001144875]
-2.9840713	ERP27	Homo sapiens endoplasmic reticulum protein 27 (ERP27), mRNA [NM_152321]
-2.9597208	TFRC	Homo sapiens transferrin receptor (p90, CD71) (TFRC), transcript variant 1, mRNA [NM_003234]
-2.9559927	NPPA-AS1	Homo sapiens NPPA antisense RNA 1 (non-protein coding) (NPPA-AS1), antisense RNA [NR_037806]
-2.9434779	XLOC_003221	BROAD Institute lincRNA (XLOC_003221), lincRNA [TCONS_00007239]
-2.923617	LOC145694	PREDICTED: Homo sapiens hypothetical LOC145694 (LOC145694), miscRNA [XR_109210]
-2.9225986	XLOC_l2_0068	PREDICTED: Homo sapiens hypothetical LOC100653267 (LOC100653267), miscRNA [XR_133194]
-2.910697	USP18	Homo sapiens ubiquitin specific peptidase 18 (USP18), mRNA [NM_017414]
-2.909085	TGFBR3	Homo sapiens transforming growth factor, beta receptor III (TGFBR3), transcript variant 1, mRNA [NM_003243]
-2.9041348	CCNE2	Homo sapiens cyclin E2 (CCNE2), mRNA [NM_057749]
-2.8913038	LOC100507431	PREDICTED: Homo sapiens hypothetical LOC100507431 (LOC100507431), miscRNA [XR_132807]
-2.8842769	SYT8	Homo sapiens synaptotagmin VIII (SYT8), mRNA [NM_138567]
-2.8645616	RIOK2	Homo sapiens RIO kinase 2 (yeast) (RIOK2), transcript variant 2, mRNA [NM_001159749]
-2.862065	ANKS1B	Homo sapiens ankyrin repeat and sterile alpha motif domain containing 1B (ANKS1B), transcript variant 1, mRNA [NM_152788]
-2.8538952	HIST1H2BE	Homo sapiens histone cluster 1, H2be (HIST1H2BE), mRNA [NM_003523]
-2.8508623	IFIT5	Homo sapiens interferon-induced protein with tetratricopeptide repeats 5 (IFIT5), mRNA [NM_012420]

-2.8464859	CC2D1B	Homo sapiens coiled-coil and C2 domain containing 1B (CC2D1B), mRNA [NM_032449]
-2.8316326	GFOD1	Homo sapiens glucose-fructose oxidoreductase domain containing 1 (GFOD1), transcript variant 4, mRNA [NM_001242629]
-2.8315043	PSMD9	Homo sapiens proteasome (prosome, macropain) 26S subunit, non-ATPase, 9 (PSMD9), mRNA [NM_002813]
-2.8310673	TNIK	Homo sapiens TRAF2 and NCK interacting kinase (TNIK), transcript variant 9, non-coding RNA [NR_027767]
-2.823377	C9orf43	Homo sapiens chromosome 9 open reading frame 43 (C9orf43), mRNA [NM_152786]
-2.814867	DDX58	Homo sapiens DEAD (Asp-Glu-Ala-Asp) box polypeptide 58 (DDX58), mRNA [NM_014314]
-2.800187	HIST1H4L	Homo sapiens histone cluster 1, H4l (HIST1H4L), mRNA [NM_003546]
-2.791831	LSM3	LSM3 homolog, U6 small nuclear RNA associated (S. cerevisiae) [Source:HGNC Symbol;Acc:17874] [ENST00000306024]
-2.7869945	METTL1	Homo sapiens methyltransferase like 1 (METTL1), transcript variant 1, mRNA [NM_005371]
-2.779488	TGFB2	Homo sapiens transforming growth factor, beta 2 (TGFB2), transcript variant 2, mRNA [NM_003238]
-2.77338	XAF1	Homo sapiens XIAP associated factor 1 (XAF1), transcript variant 1, mRNA [NM_017523]
-2.7697287	C1QTNF9B-AS	Homo sapiens C1QTNF9B antisense RNA 1 (non-protein coding) (C1QTNF9B-AS1), transcript variant 2, mRNA [NM_001135816]
-2.7662907	HMGB3	Homo sapiens high mobility group box 3 (HMGB3), mRNA [NM_005342]
-2.765582	ANKH	Homo sapiens ankylosis, progressive homolog (mouse) (ANKH), mRNA [NM_054027]
-2.7613328	TMOD1	Homo sapiens tropomodulin 1 (TMOD1), transcript variant 1, mRNA [NM_003275]
-2.7612474	TXNL4B	Homo sapiens thioredoxin-like 4B (TXNL4B), transcript variant 1, mRNA [NM_017853]
-2.7571151	C9orf100	Homo sapiens chromosome 9 open reading frame 100 (C9orf100), mRNA [NM_032818]
-2.7468715	MAT2A	Homo sapiens methionine adenosyltransferase II, alpha (MAT2A), mRNA [NM_005911]
-2.7437937	SNHG9	Homo sapiens small nucleolar RNA host gene 9 (non-protein coding) (SNHG9), non-coding RNA [NR_003142]
-2.7431018	SFXN2	Homo sapiens sideroflexin 2 (SFXN2), mRNA [NM_178858]
-2.7322047		histone cluster 1, H4c [Source:HGNC Symbol;Acc:4787] [ENST00000377803]
-2.7291722		
-2.7159157	SNORD50B	Homo sapiens small nucleolar RNA, C/D box 50B (SNORD50B), small nucleolar RNA [NR_003044]
-2.711811	HIST1H3B	Homo sapiens histone cluster 1, H3b (HIST1H3B), mRNA [NM_003537]
-2.6871324	LOC100129148	Homo sapiens uncharacterized LOC100129148 (LOC100129148), non-coding RNA [NR_033999]
-2.6752698	RASL11A	Homo sapiens RAS-like, family 11, member A (RASL11A), mRNA [NM_206827]
-2.6697862	KRT33B	Homo sapiens keratin 33B (KRT33B), mRNA [NM_002279]
-2.6652448	MGC45800	Homo sapiens uncharacterized LOC90768 (MGC45800), non-coding RNA [NR_027107]
-2.6612492	PNPT1	Homo sapiens polyribonucleotide nucleotidyltransferase 1 (PNPT1), mRNA [NM_033109]
-2.6582363	SNORD56B	Homo sapiens small nucleolar RNA, C/D box 56B (SNORD56B), small nuclear RNA [NR_001276]
-2.653671	RBM15B	Homo sapiens RNA binding motif protein 15B (RBM15B), mRNA [NM_013286]
-2.6450038	METTL1	Homo sapiens methyltransferase like 1 (METTL1), transcript variant 1, mRNA [NM_005371]
-2.6428664	RPL23AP7	Homo sapiens ribosomal protein L23a pseudogene 7 (RPL23AP7), transcript variant 4, non-coding RNA [NR_024530]
-2.634312	XLOC_013308	BROAD Institute lincRNA (XLOC_013308), lincRNA [TCONS_00027310]
-2.633799	LOC100128881	Homo sapiens uncharacterized LOC100128881 (LOC100128881), non-coding RNA [NR_036480]
-2.6309383	HIST1H2BF	Homo sapiens histone cluster 1, H2bf (HIST1H2BF), mRNA [NM_003522]
-2.6299403	C9orf116	Homo sapiens chromosome 9 open reading frame 116 (C9orf116), transcript variant 1, mRNA [NM_001048265]
-2.6271574	IFIT2	Homo sapiens interferon-induced protein with tetratricopeptide repeats 2 (IFIT2), mRNA [NM_001547]
-2.624239	HSPA8	heat shock 70kDa protein 8 [Source:HGNC Symbol;Acc:5241] [ENST00000532091]
-2.620538	CD3EAP	Homo sapiens CD3e molecule, epsilon associated protein (CD3EAP), mRNA [NM_012099]
-2.6191223	NR1D2	Homo sapiens nuclear receptor subfamily 1, group D, member 2 (NR1D2), transcript variant 1, mRNA [NM_005126]
-2.6036906	HIST2H3A	Homo sapiens histone cluster 2, H3a (HIST2H3A), mRNA [NM_001005464]
-2.5976443	XLOC_004229	BROAD Institute lincRNA (XLOC_004229), lincRNA [TCONS_00008716]
-2.5968874	HSPA8	Homo sapiens heat shock 70kDa protein 8 (HSPA8), transcript variant 2, mRNA [NM_153201]
-2.5966256	EEPD1	Homo sapiens endonuclease/exonuclease/phosphatase family domain containing 1 (EEPD1), mRNA [NM_030636]
-2.5963001	VGLL3	Homo sapiens vestigial like 3 (Drosophila) (VGLL3), mRNA [NM_016206]
-2.595648	CCNF	Homo sapiens cyclin F (CCNF), mRNA [NM_001761]
-2.5935016	NKD1	Homo sapiens naked cuticle homolog 1 (Drosophila) (NKD1), mRNA [NM_033119]
-2.5928442	PNPT1	Homo sapiens polyribonucleotide nucleotidyltransferase 1 (PNPT1), mRNA [NM_033109]
-2.5906026	PNN	Homo sapiens pinin, desmosome associated protein (PNN), mRNA [NM_002687]

-2.56704	CDON	Homo sapiens Cdon homolog (mouse) (CDON), transcript variant 2, mRNA [NM_016952]
-2.5662506	EME2	Homo sapiens mRNA for FLJ00151 protein. [AK074080]
-2.5613172	HIST1H4D	Homo sapiens histone cluster 1, H4d (HIST1H4D), mRNA [NM_003539]
-2.561273	NCKAP5	Homo sapiens NCK-associated protein 5 (NCKAP5), transcript variant 2, mRNA [NM_207481]
-2.5607517	CCK	Homo sapiens cholecystokinin (CCK), transcript variant 1, mRNA [NM_000729]
-2.5584896	HIST1H1B	Homo sapiens histone cluster 1, H1b (HIST1H1B), mRNA [NM_005322]
-2.5551329	RPL23AP7	Homo sapiens ribosomal protein L23a pseudogene 7 (RPL23AP7), transcript variant 4, non-coding RNA [NR_024530]
-2.5545352	HIST1H2AI	Homo sapiens histone cluster 1, H2ai (HIST1H2AI), mRNA [NM_003509]
-2.5528529	HIST1H2AL	Homo sapiens histone cluster 1, H2al (HIST1H2AL), mRNA [NM_003511]
-2.5412939	STXBP6	Homo sapiens syntaxin binding protein 6 (amisyn) (STXBP6), mRNA [NM_014178]
-2.5386035	SNORA62	Homo sapiens small nucleolar RNA, H/ACA box 62 (SNORA62), small nucleolar RNA [NR_002324]
-2.533813	FBP1	Homo sapiens fructose-1,6-bisphosphatase 1 (FBP1), transcript variant 1, mRNA [NM_000507]
-2.5321076	MLPH	Homo sapiens melanophilin (MLPH), transcript variant 1, mRNA [NM_024101]
-2.5273702	PYCRL	Homo sapiens pyrroline-5-carboxylate reductase-like (PYCRL), mRNA [NM_023078]
-2.5268958	SP110	Homo sapiens SP110 nuclear body protein (SP110), transcript variant b, mRNA [NM_004510]
-2.5216637	SF3B4	Homo sapiens splicing factor 3b, subunit 4, 49kDa (SF3B4), mRNA [NM_005850]
-2.5216603	CES4A	Homo sapiens carboxylesterase 4A (CES4A), transcript variant 1, mRNA [NM_173815]
-2.5166104	ZNFX1	Homo sapiens zinc finger, NFX1-type containing 1 (ZNFX1), mRNA [NM_021035]
-2.508737	FAM75D3	Homo sapiens family with sequence similarity 75, member D3 (FAM75D3), mRNA [NM_207416]
-2.508139	SRSF2	Homo sapiens serine/arginine-rich splicing factor 2 (SRSF2), transcript variant 1, mRNA [NM_003016]
-2.5060291	MX2	Homo sapiens myxovirus (influenza virus) resistance 2 (mouse) (MX2), mRNA [NM_002463]
-2.4981232	NR1D2	Homo sapiens nuclear receptor subfamily 1, group D, member 2 (NR1D2), transcript variant 1, mRNA [NM_005126]
-2.4906802	ELOVL6	ELOVL fatty acid elongase 6 [Source:HGNC Symbol;Acc:15829] [ENST00000394607]
-2.485233	SERPINE1	Homo sapiens serpin peptidase inhibitor, clade E (nexin, plasminogen activator inhibitor type 1), member 1 (SERPINE1), transcript variant 1, mRNA [NM_000602]
-2.482478	USF1	Homo sapiens upstream transcription factor 1 (USF1), transcript variant 1, mRNA [NM_007122]
-2.475862	LOC100127904	Homo sapiens cDNA clone IMAGE:30403562, partial cds. [BC065739]
-2.4738867	MRVI1	Homo sapiens murine retrovirus integration site 1 homolog (MRVI1), transcript variant 2, mRNA [NM_130385]
-2.4712029	LOC100652883	PREDICTED: Homo sapiens arachidonate 15-lipoxygenase-like (LOC100652883), mRNA [XM_003403469]
-2.4711726	DGCR8	Homo sapiens DiGeorge syndrome critical region gene 8 (DGCR8), transcript variant 1, mRNA [NM_022720]
-2.4699967	OSR2	Homo sapiens odd-skipped related 2 (Drosophila) (OSR2), transcript variant 2, mRNA [NM_053001]
-2.469246	SYTL2	Homo sapiens synaptotagmin-like 2 (SYTL2), transcript variant c, mRNA [NM_206927]
-2.468921	Q8WNA4	Q8WNA4_DAUMA (Q8WNA4) Luteinizing hormone beta subunit (Fragment), partial (10%) [THC2605385]
-2.4616773	MMRN2	multimerin 2 [Source:HGNC Symbol;Acc:19888] [ENST00000474994]
-2.452254	PYCRL	Homo sapiens pyrroline-5-carboxylate reductase-like (PYCRL), mRNA [NM_023078]
-2.4494958	RRP15	Homo sapiens ribosomal RNA processing 15 homolog (S. cerevisiae) (RRP15), mRNA [NM_016052]
-2.4481091	FBXO5	Homo sapiens F-box protein 5 (FBXO5), transcript variant 2, mRNA [NM_001142522]
-2.4471934	TMEM201	Homo sapiens transmembrane protein 201 (TMEM201), transcript variant 2, mRNA [NM_001010866]
-2.4433699		
-2.4431841	LOC100653304	PREDICTED: Homo sapiens putative uncharacterized protein C12orf63-like (LOC100653304), mRNA [XM_003403651]
-2.4264894	USP37	Homo sapiens ubiquitin specific peptidase 37 (USP37), mRNA [NM_020935]
-2.4230256	XLOC_009147	Q9A772_CAUCR (Q9A772) Heptosyltransferase family protein, partial (5%) [THC2608613]
-2.4221306	SPEF1	Homo sapiens sperm flagellar 1 (SPEF1), mRNA [NM_015417]
-2.418668	C1orf21	Homo sapiens chromosome 1 open reading frame 21 (C1orf21), mRNA [NM_030806]
-2.4172888	ACADSB	Homo sapiens acyl-CoA dehydrogenase, short/branched chain (ACADSB), nuclear gene encoding mitochondrial protein, mRNA [NM_001609]
-2.4166791	ZNF367	Homo sapiens zinc finger protein 367 (ZNF367), mRNA [NM_153695]
-2.4161146	SOX11	Homo sapiens SRY (sex determining region Y)-box 11 (SOX11), mRNA [NM_003108]
-2.4141262		zinc finger protein 451 [Source:HGNC Symbol;Acc:21091] [ENST00000370708]
-2.411108	E2F2	Homo sapiens E2F transcription factor 2 (E2F2), mRNA [NM_004091]
-2.4062016	GUSBP1	Homo sapiens glucuronidase, beta pseudogene 1 (GUSBP1), transcript variant 2, non-coding RNA [NR_027027]
-2.4049206	HIST1H2AM	Homo sapiens histone cluster 1, H2am (HIST1H2AM), mRNA [NM_003514]

-2.402904	XLOC_005143	BROAD Institute lincRNA (XLOC_005143), lincRNA [TCONS_00011660]
-2.4012814	CXorf56	Homo sapiens chromosome X open reading frame 56 (CXorf56), transcript variant 1, mRNA [NM_022101]
-2.3996358	FAM111B	Homo sapiens family with sequence similarity 111, member B (FAM111B), transcript variant 1, mRNA [NM_198947]
-2.393371		
-2.393145	XLOC_003739	BROAD Institute lincRNA (XLOC_003739), lincRNA [TCONS_00008906]
-2.389818	ZNF559	Homo sapiens zinc finger protein 559 (ZNF559), transcript variant 2, mRNA [NM_032497]
-2.3885388	FUS	Homo sapiens fused in sarcoma (FUS), transcript variant 1, mRNA [NM_004960]
-2.3882606	SERHL2	Homo sapiens serine hydrolase-like 2 (SERHL2), mRNA [NM_014509]
-2.3874385	LOC92249	Homo sapiens uncharacterized LOC92249 (LOC92249), non-coding RNA [NR_015353]
-2.386476	KDM4C	Homo sapiens cDNA clone IMAGE:6165770, partial cds. [BC053678]
-2.375495	NCOA5	Homo sapiens nuclear receptor coactivator 5 (NCOA5), mRNA [NM_020967]
-2.374275	TIA1	Homo sapiens TIA1 cytotoxic granule-associated RNA binding protein (TIA1), transcript variant 2, mRNA [NM_022173]
-2.3711326	EGLN3	Homo sapiens egl nine homolog 3 (C. elegans) (EGLN3), mRNA [NM_022073]
-2.3696685	RPS6KL1	Homo sapiens ribosomal protein S6 kinase-like 1 (RPS6KL1), mRNA [NM_031464]
-2.3684955	C19orf51	Homo sapiens chromosome 19 open reading frame 51 (C19orf51), mRNA [NM_178837]
-2.3656085	MT1X	Homo sapiens metallothionein 1X (MT1X), mRNA [NM_005952]
-2.35842	ARL3	Homo sapiens ADP-ribosylation factor-like 3 (ARL3), mRNA [NM_004311]
-2.3508189	ADAM32	Homo sapiens ADAM metallopeptidase domain 32 (ADAM32), mRNA [NM_145004]
-2.3507605	CDNF	Homo sapiens cerebral dopamine neurotrophic factor (CDNF), mRNA [NM_001029954]
-2.3504374	HIST1H3F	Homo sapiens histone cluster 1, H3f (HIST1H3F), mRNA [NM_021018]
-2.3499029	NDUFC2	Homo sapiens NADH dehydrogenase (ubiquinone) 1, subcomplex unknown, 2, 14.5kDa (NDUFC2), nuclear gene encoding mitochondrial protein, transcript variant 1, mRNA [NM_004549]
-2.3492002	LOC339290	Homo sapiens uncharacterized LOC339290 (LOC339290), non-coding RNA [NR_015389]
-2.3350918	ATP6V0E2	Homo sapiens ATPase, H+ transporting V0 subunit e2 (ATP6V0E2), transcript variant 1, mRNA [NM_145230]
-2.3305757	LOC730961	Homo sapiens cDNA clone IMAGE:4826905. [BC034282]
-2.3296108	RSPH1	Homo sapiens radial spoke head 1 homolog (Chlamydomonas) (RSPH1), mRNA [NM_080860]
-2.3283129	TTLL11	Homo sapiens tubulin tyrosine ligase-like family, member 11 (TTLL11), transcript variant 2, mRNA [NM_194252]
-2.3266644	CHP2	Homo sapiens calcineurin B homologous protein 2 (CHP2), mRNA [NM_022097]
-2.3221157		Homo sapiens cDNA clone IMAGE:3453690, partial cds. [BC000817]
-2.3214862	VAPB	Homo sapiens VAMP (vesicle-associated membrane protein)-associated protein B and C (VAPB), transcript variant 1, mRNA [NM_004738]
-2.3152552		mucin 3A, cell surface associated [Source:HGNC Symbol;Acc:7513] [ENST00000319509]
-2.3104079	SNORD22	Homo sapiens small nucleolar RNA, C/D box 22 (SNORD22), small nucleolar RNA [NR_000008]
-2.3092222	GPAM	Homo sapiens glycerol-3-phosphate acyltransferase, mitochondrial (GPAM), nuclear gene encoding mitochondrial protein, transcript variant 2, mRNA [NM_020918]
-2.3075962	TP53TG5	Homo sapiens TP53 target 5 (TP53TG5), mRNA [NM_014477]
-2.3067286	ZNF43	Homo sapiens zinc finger protein 43 (ZNF43), mRNA [NM_003423]
-2.3039854	PIGW	Homo sapiens phosphatidylinositol glycan anchor biosynthesis, class W (PIGW), mRNA [NM_178517]
-2.30338	KBTBD11	Homo sapiens kelch repeat and BTB (POZ) domain containing 11 (KBTBD11), mRNA [NM_014867]
-2.301645	DIEXF	Homo sapiens digestive organ expansion factor homolog (zebrafish) (DIEXF), mRNA [NM_014388]
-2.2864714	HIST1H4L	Homo sapiens histone cluster 1, H4l (HIST1H4L), mRNA [NM_003546]
-2.2850466	RFT1	Homo sapiens RFT1 homolog (S. cerevisiae) (RFT1), mRNA [NM_052859]
-2.2830513	LOC100506473	PREDICTED: Homo sapiens hypothetical LOC100506473 (LOC100506473), miscRNA [XR_109933]
-2.2728133	LOC389634	Homo sapiens uncharacterized LOC389634 (LOC389634), non-coding RNA [NR_024420]
-2.271901	MX1	Homo sapiens myxovirus (influenza virus) resistance 1, interferon-inducible protein p78 (mouse) (MX1), transcript variant 2, mRNA [NM_002462]
-2.271345	STAG3	Homo sapiens stromal antigen 3 (STAG3), mRNA [NM_012447]
-2.27103	PNPLA4	Homo sapiens patatin-like phospholipase domain containing 4 (PNPLA4), transcript variant 1, mRNA [NM_004650]
-2.2705054	NCOA5	Homo sapiens nuclear receptor coactivator 5 (NCOA5), mRNA [NM_020967]
-2.2665637	LOC100009676	Homo sapiens uncharacterized LOC100009676 (LOC100009676), non-coding RNA [NR_024407]
-2.2648592	SUB1	Homo sapiens SUB1 homolog (S. cerevisiae) (SUB1), mRNA [NM_006713]
-2.264735	SNORA48	Homo sapiens small nucleolar RNA, H/ACA box 48 (SNORA48), small nucleolar RNA [NR_002918]
-2.264411		EP400 N-terminal like [Source:HGNC Symbol;Acc:26602] [ENST00000443539]
-2.257873	ROR1	receptor tyrosine kinase-like orphan receptor 1 [Source:HGNC Symbol;Acc:10256] [ENST00000371079]

-2.250974	FEN1	Homo sapiens flap structure-specific endonuclease 1 (FEN1), mRNA [NM_004111]
-2.2508543	GPR19	Homo sapiens G protein-coupled receptor 19 (GPR19), mRNA [NM_006143]
-2.25071	LOC100506469	Homo sapiens uncharacterized LOC100506469 (LOC100506469), non-coding RNA [NR_038396]
-2.2504227	NDNF	Homo sapiens neuron-derived neurotrophic factor (NDNF), mRNA [NM_024574]
-2.2502434	TRIM21	Homo sapiens tripartite motif containing 21 (TRIM21), mRNA [NM_003141]
-2.2402506	CCNE2	Homo sapiens cyclin E2 (CCNE2), mRNA [NM_057749]
-2.2348304	LOC100125556	Homo sapiens family with sequence similarity 86, member A pseudogene (LOC100125556), transcript variant 1, non-coding RNA [NR_024251]
-2.233112	HIST1H4E	Homo sapiens histone cluster 1, H4e (HIST1H4E), mRNA [NM_003545]
-2.233056	GLYCTK	Homo sapiens glycerate kinase (GLYCTK), transcript variant 1, mRNA [NM_145262]
-2.2321322	POLR3H	Homo sapiens polymerase (RNA) III (DNA directed) polypeptide H (22.9kD) (POLR3H), transcript variant 1, mRNA [NM_138338]
-2.2309787	MED31	Homo sapiens mediator complex subunit 31 (MED31), mRNA [NM_016060]
-2.2291934	C17orf69	Homo sapiens chromosome 17 open reading frame 69 (C17orf69), transcript variant 2, non-coding RNA [NR_026906]
-2.2255845	NCDN	Homo sapiens neurochondrin (NCDN), transcript variant 3, mRNA [NM_014284]
-2.2244065	SRSF2	Homo sapiens serine/arginine-rich splicing factor 2 (SRSF2), transcript variant 1, mRNA [NM_003016]
-2.2183619	FAM123B	Homo sapiens family with sequence similarity 123B (FAM123B), mRNA [NM_152424]
-2.2100217	VKORC1	Homo sapiens cDNA FLJ43630 fis, clone SPLEN2030479. [AK125618]
-2.209786	HIST1H4A	Homo sapiens histone cluster 1, H4a (HIST1H4A), mRNA [NM_003538]
-2.2095318	ACOX2	Homo sapiens acyl-CoA oxidase 2, branched chain (ACOX2), mRNA [NM_003500]
-2.2063544	HIST1H4C	Homo sapiens histone cluster 1, H4c (HIST1H4C), mRNA [NM_003542]
-2.204204	HIST1H4B	Homo sapiens histone cluster 1, H4b (HIST1H4B), mRNA [NM_003544]
-2.2039652		PREDICTED: Homo sapiens hypothetical LOC100507253 (LOC100507253), miscRNA [XR_110118]
-2.2037382		DA209974 BRAWH2 Homo sapiens cDNA clone BRAWH2017942 5', mRNA sequence [DA209974]
-2.1982427	CALM1	Homo sapiens calmodulin 1 (phosphorylase kinase, delta) (CALM1), transcript variant 1, mRNA [NM_006888]
-2.194618	LOC153577	Homo sapiens cDNA FLJ30091 fis, clone BNGH41000017. [AK054653]
-2.1937237	PGBD1	Homo sapiens piggyBac transposable element derived 1 (PGBD1), transcript variant 2, mRNA [NM_032507]
-2.1932511	ASF1B	Homo sapiens ASF1 anti-silencing function 1 homolog B (S. cerevisiae) (ASF1B), mRNA [NM_018154]
-2.1928828	ASF1A	Homo sapiens ASF1 anti-silencing function 1 homolog A (S. cerevisiae) (ASF1A), mRNA [NM_014034]
-2.1928275	RPP30	Homo sapiens ribonuclease P/MRP 30kDa subunit (RPP30), transcript variant 2, mRNA [NM_006413]
-2.1898737	OK/SW-CL.58	Homo sapiens mRNA for OK/SW-CL.58, complete cds. [AB064667]
-2.1885023	ZWINT	Homo sapiens ZW10 interactor (ZWINT), transcript variant 2, mRNA [NM_032997]
-2.1882007	U2SURP	Homo sapiens U2 snRNP-associated SURP domain containing (U2SURP), mRNA [NM_001080415]
-2.1874783	AFG3L1P	Homo sapiens AFG3 ATPase family gene 3-like 1 (S. cerevisiae), pseudogene (AFG3L1P), transcript variant 1, non-coding RNA [NR_003226]
-2.1863043	SRSF8	Homo sapiens serine/arginine-rich splicing factor 8 (SRSF8), mRNA [NM_032102]
-2.180026	EPHX1	Homo sapiens epoxide hydrolase 1, microsomal (xenobiotic) (EPHX1), transcript variant 1, mRNA [NM_000120]
-2.1777105	PMEPA1	Homo sapiens prostate transmembrane protein, androgen induced 1 (PMEPA1), transcript variant 1, mRNA [NM_020182]
-2.176817	ALPL	Homo sapiens alkaline phosphatase, liver/bone/kidney (ALPL), transcript variant 1, mRNA [NM_000478]
-2.1764715	ANAPC2	Homo sapiens anaphase promoting complex subunit 2 (ANAPC2), mRNA [NM_013366]
-2.1762817	ZNF296	Homo sapiens zinc finger protein 296 (ZNF296), mRNA [NM_145288]
-2.1751146	P2RY1	Homo sapiens purinergic receptor P2Y, G-protein coupled, 1 (P2RY1), mRNA [NM_002563]
-2.1741953	CHCHD7	Homo sapiens coiled-coil-helix-coiled-coil-helix domain containing 7 (CHCHD7), transcript variant 1, mRNA [NM_001011667]
-2.1723485	XLOC_I2_00399	BROAD Institute lincRNA (XLOC_I2_003992), lincRNA [TCONS_I2_00007209]
-2.1719902	HIST1H4H	Homo sapiens histone cluster 1, H4h (HIST1H4H), mRNA [NM_003543]
-2.1700184	HIST1H4D	Homo sapiens histone cluster 1, H4d (HIST1H4D), mRNA [NM_003539]
-2.169347	RIBC2	Homo sapiens RIB43A domain with coiled-coils 2 (RIBC2), mRNA [NM_015653]
-2.1637073	LOC100133311	Homo sapiens uncharacterized LOC100133311 (LOC100133311), transcript variant 1, non-coding RNA [NR_038831]
-2.1632748	SDPR	Homo sapiens serum deprivation response (SDPR), mRNA [NM_004657]
-2.1632068	PCM1	Homo sapiens pericentriolar material 1 (PCM1), mRNA [NM_006197]
-2.162213	FAM46B	Homo sapiens family with sequence similarity 46, member B (FAM46B), mRNA [NM_052943]
-2.1592622	SKP2	Homo sapiens S-phase kinase-associated protein 2 (p45) (SKP2), transcript variant 2, mRNA [NM_032637]
-2.157389	AGFG1	Homo sapiens ArfGAP with FG repeats 1 (AGFG1), transcript variant 1, mRNA [NM_001135187]

-2.15533	LOC100287482	Homo sapiens uncharacterized protein LOC100287482 (LOC100287482), mRNA [NM_001195243]
-2.1528473	HSPA1A	Homo sapiens heat shock 70kDa protein 1A (HSPA1A), mRNA [NM_005345]
-2.14991	SCML2	Homo sapiens sex comb on midleg-like 2 (Drosophila) (SCML2), transcript variant 1, mRNA [NM_006089]
-2.1463315	XLOC_l2_0035	PREDICTED: Homo sapiens zinc finger protein 891 (ZNF891), miscRNA [XR_110103]
-2.1439087	XLOC_l2_0053	Q8WUU7_HUMAN (Q8WUU7) MGC70863 protein, complete [THC2476569]
-2.1430743	TCF19	Homo sapiens transcription factor 19 (TCF19), transcript variant 1, mRNA [NM_007109]
-2.141375	SCG5	Homo sapiens secretogranin V (7B2 protein) (SCG5), transcript variant 2, mRNA [NM_003020]
-2.1408994	HIST1H2AG	Homo sapiens histone cluster 1, H2ag (HIST1H2AG), mRNA [NM_021064]
-2.136826	GINS1	Homo sapiens GINS complex subunit 1 (Psf1 homolog) (GINS1), mRNA [NM_021067]
-2.133488	S1PR1	Homo sapiens sphingosine-1-phosphate receptor 1 (S1PR1), mRNA [NM_001400]
-2.1323037	NUP98	Homo sapiens nucleoporin 98kDa (NUP98), transcript variant 3, mRNA [NM_005387]
-2.1317441	FAM86C2P	Homo sapiens family with sequence similarity 86, member C2, pseudogene (FAM86C2P), non-coding RNA [NR_024249]
-2.131721	TAOK2	Homo sapiens TAO kinase 2 (TAOK2), transcript variant 2, mRNA [NM_004783]
-2.126858	NASP	Homo sapiens nuclear autoantigenic sperm protein (histone-binding) (NASP), transcript variant 2, mRNA [NM_002482]
-2.1257849	FZD1	Homo sapiens frizzled family receptor 1 (FZD1), mRNA [NM_003505]
-2.1229594	PDAP1	Homo sapiens PDGFA associated protein 1 (PDAP1), mRNA [NM_014891]
-2.1189663	C1orf116	Homo sapiens chromosome 1 open reading frame 116 (C1orf116), transcript variant 1, mRNA [NM_023938]
-2.118773	GALK1	Homo sapiens galactokinase 1 (GALK1), mRNA [NM_000154]
-2.1185434		
-2.1155324	PPAN-P2RY11	Homo sapiens PPAN-P2RY11 readthrough (PPAN-P2RY11), transcript variant 2, mRNA [NM_001198690]
-2.114073	C1orf86	Homo sapiens cDNA FLJ30256 fis, clone BRACE2002458. [AK054818]
-2.1137846	CCDC137	Homo sapiens coiled-coil domain containing 137 (CCDC137), mRNA [NM_199287]
-2.1136637	TMPO	Homo sapiens thymopoietin (TMPO), transcript variant 1, mRNA [NM_003276]
-2.1111498	OR52A1	Homo sapiens olfactory receptor, family 52, subfamily A, member 1 (OR52A1), mRNA [NM_012375]
-2.110915	SEMA5A	Homo sapiens sema domain, seven thrombospondin repeats (type 1 and type 1-like), transmembrane domain (TM) and short cytoplasmic domain, (semaphorin) 5A (SEMA5A), mRNA [NM_003966]
-2.1099901	TNS1	Homo sapiens tensin 1 (TNS1), mRNA [NM_022648]
-2.1083002	RSPH1	Homo sapiens radial spoke head 1 homolog (Chlamydomonas) (RSPH1), mRNA [NM_080860]
-2.1066556	ATRIP	Homo sapiens ATR interacting protein (ATRIP), transcript variant 2, mRNA [NM_032166]
-2.1022825	LOC730755	Homo sapiens keratin associated protein 2-4-like (LOC730755), mRNA [NM_001165252]
-2.101535	FAM86A	Homo sapiens family with sequence similarity 86, member A (FAM86A), transcript variant 1, mRNA [NM_201400]
-2.1013637	LOC254128	Homo sapiens uncharacterized LOC254128 (LOC254128), transcript variant 3, non-coding RNA [NR_037857]
-2.1002977	TCF4	Homo sapiens transcription factor 4 (TCF4), transcript variant 2, mRNA [NM_003199]
-2.0998056	DLEU2L	Homo sapiens deleted in lymphocytic leukemia 2-like (DLEU2L), non-coding RNA [NR_002771]
-2.0981967	XLOC_l2_0067	BROAD Institute lincRNA (XLOC_l2_006718), lincRNA [TCONS_l2_00012515]
-2.0976877		
-2.0931003	HR	Homo sapiens hairless homolog (mouse) (HR), transcript variant 1, mRNA [NM_005144]
-2.092163	DSC1	Homo sapiens desmocollin 1 (DSC1), transcript variant Dsc1b, mRNA [NM_004948]
-2.0916646	LOC100507433	Homo sapiens uncharacterized LOC100507433 (LOC100507433), transcript variant 1, non-coding RNA [NR_038247]
-2.090873	C1orf52	Homo sapiens chromosome 1 open reading frame 52 (C1orf52), transcript variant 1, mRNA [NM_198077]
-2.0907784	CYB5D1	Homo sapiens cytochrome b5 domain containing 1 (CYB5D1), mRNA [NM_144607]
-2.0905151	IGLL1	Homo sapiens immunoglobulin lambda-like polypeptide 1 (IGLL1), transcript variant 1, mRNA [NM_020070]
-2.089901	SCAF11	SR-related CTD-associated factor 11 [Source:HGNC Symbol;Acc:10784] [ENST00000395453]
-2.0877082	MAP6D1	Homo sapiens MAP6 domain containing 1 (MAP6D1), mRNA [NM_024871]
-2.086957	LOC100506649	Homo sapiens uncharacterized LOC100506649 (LOC100506649), non-coding RNA [NR_038924]
-2.0848866	ZWINT	Homo sapiens ZW10 interactor (ZWINT), transcript variant 2, mRNA [NM_032997]
-2.0840483	PPHLN1	Homo sapiens periphilin 1 (PPHLN1), transcript variant 1, mRNA [NM_016488]
-2.0833697	GPR180	Homo sapiens G protein-coupled receptor 180 (GPR180), mRNA [NM_180989]
-2.0822492	SERTAD4	Homo sapiens SERTA domain containing 4 (SERTAD4), mRNA [NM_019605]
-2.081277	TXLNG2P	Homo sapiens taxilin gamma 2, pseudogene (TXLNG2P), transcript variant 2, non-coding RNA [NR_045129]
-2.0786788	HSPA1B	Homo sapiens heat shock 70kDa protein 1B (HSPA1B), mRNA [NM_005346]

-2.0784006	USP7	Homo sapiens ubiquitin specific peptidase 7 (herpes virus-associated) (USP7), mRNA [NM_003470]
-2.07673	DLX1	Homo sapiens distal-less homeobox 1 (DLX1), transcript variant 1, mRNA [NM_178120]
-2.0706902	LOC100652760	PREDICTED: Homo sapiens hypothetical LOC100652760 (LOC100652760), miscRNA [XR_132680]
-2.07063	GLMN	Homo sapiens glomulin, FKBP associated protein (GLMN), mRNA [NM_053274]
-2.0628238	RNASET2	Homo sapiens ribonuclease T2 (RNASET2), mRNA [NM_003730]
-2.0605464		
-2.0589752	DCLRE1B	Homo sapiens DNA cross-link repair 1B (DCLRE1B), mRNA [NM_022836]
-2.0581872	ZNF544	Homo sapiens zinc finger protein 544 (ZNF544), mRNA [NM_014480]
-2.0559313	NXF1	Homo sapiens nuclear RNA export factor 1 (NXF1), transcript variant 1, mRNA [NM_006362]
-2.0546677	DLEU1	Homo sapiens deleted in lymphocytic leukemia 1 (non-protein coding) (DLEU1), non-coding RNA [NR_002605]
-2.0515733	PLD6	Homo sapiens phospholipase D family, member 6 (PLD6), mRNA [NM_178836]
-2.0507314	RPP30	Homo sapiens ribonuclease P/MRP 30kDa subunit (RPP30), transcript variant 1, mRNA [NM_001104546]
-2.050421	FAR1	Homo sapiens fatty acyl CoA reductase 1 (FAR1), mRNA [NM_032228]
-2.0473518	TP53RK	Homo sapiens TP53 regulating kinase (TP53RK), mRNA [NM_033550]
-2.0419214	C11orf87	Homo sapiens chromosome 11 open reading frame 87 (C11orf87), mRNA [NM_207645]
-2.0406811	WDR73	Homo sapiens WD repeat domain 73 (WDR73), mRNA [NM_032856]
-2.0382032	MEPCE	Homo sapiens methylphosphate capping enzyme (MEPCE), transcript variant 1, mRNA [NM_019606]
-2.0377722	HIST1H2AE	Homo sapiens histone cluster 1, H2ae (HIST1H2AE), mRNA [NM_021052]
-2.0371425	TARSL2	Homo sapiens threonyl-tRNA synthetase-like 2 (TARSL2), mRNA [NM_152334]
-2.0370646	LOC100133315	Homo sapiens transient receptor potential cation channel, subfamily C, member 2-like (LOC100133315), non-coding RNA [NR_029192]
-2.0353732	SFRP1	Homo sapiens secreted frizzled-related protein 1 (SFRP1), mRNA [NM_003012]
-2.034741		
-2.0346763	XLOC_I2_0066(	BROAD Institute lincRNA (XLOC_I2_006665), lincRNA [TCONS_I2_00012420]
-2.033698	RFT1	Homo sapiens RFT1 homolog (S. cerevisiae) (RFT1), mRNA [NM_052859]
-2.0324745	PEX3	Homo sapiens peroxisomal biogenesis factor 3 (PEX3), mRNA [NM_003630]
-2.0295773	PTGES	Homo sapiens prostaglandin E synthase (PTGES), mRNA [NM_004878]
-2.0277078	FAM78A	Homo sapiens family with sequence similarity 78, member A (FAM78A), mRNA [NM_033387]
-2.0254807	ABCC4	Homo sapiens ATP-binding cassette, sub-family C (CFTR/MRP), member 4 (ABCC4), transcript variant 1, mRNA [NM_005845]
-2.0212667	LOC284408	Homo sapiens uncharacterized LOC284408 (LOC284408), transcript variant 1, non-coding RNA [NR_040027]
-2.0207458	FBXW12	Homo sapiens F-box and WD repeat domain containing 12 (FBXW12), transcript variant 1, mRNA [NM_207102]
-2.02056	NSFL1C	Homo sapiens NSFL1 (p97) cofactor (p47) (NSFL1C), transcript variant 1, mRNA [NM_016143]
-2.0201674	RNASET2	Homo sapiens ribonuclease T2 (RNASET2), mRNA [NM_003730]
-2.0195925	PRR19	Homo sapiens proline rich 19 (PRR19), mRNA [NM_199285]
-2.0189927	PRR15L	Homo sapiens proline rich 15-like (PRR15L), mRNA [NM_024320]
-2.0152965	C20orf134	Homo sapiens chromosome 20 open reading frame 134 (C20orf134), mRNA [NM_001024675]
-2.013403	MAPRE2	Homo sapiens microtubule-associated protein, RP/EB family, member 2 (MAPRE2), transcript variant 1, mRNA [NM_014268]
-2.0119035	DIDO1	Homo sapiens death inducer-obliterator 1 (DIDO1), transcript variant 4, mRNA [NM_033081]
-2.0111322	TOE1	Homo sapiens target of EGR1, member 1 (nuclear) (TOE1), mRNA [NM_025077]
-2.0053396	WDR3	Homo sapiens WD repeat domain 3 (WDR3), mRNA [NM_006784]
-2.0025287	SLFN12	Homo sapiens schlafen family member 12 (SLFN12), mRNA [NM_018042]
-2.001738	ING3	Homo sapiens inhibitor of growth family, member 3 (ING3), transcript variant 3, mRNA [NM_198267]
-2.0015	XYLT1	Homo sapiens xylosyltransferase I (XYLT1), mRNA [NM_022166]
-2.0011783	CC2D2A	Homo sapiens coiled-coil and C2 domain containing 2A (CC2D2A), transcript variant 2, mRNA [NM_020785]

Table B.3 **Upregulated genes in primary keratinocytes after IL-36 stimulations for 8 h**

Fold	Gene name	Description
63.263947	CSF3	Homo sapiens colony stimulating factor 3 (granulocyte) (CSF3), transcript variant 1, mRNA [NM_000759]
49.11069	IL17C	Homo sapiens interleukin 17C (IL17C), mRNA [NM_013278]
45.855167	CSF3	Homo sapiens colony stimulating factor 3 (granulocyte) (CSF3), transcript variant 1, mRNA [NM_000759]
44.31563	ROS1	c-ros oncogene 1 , receptor tyrosine kinase [Source:HGNC Symbol;Acc:10261] [ENST00000403284]
33.154594	TNFAIP2	Homo sapiens tumor necrosis factor, alpha-induced protein 2 (TNFAIP2), mRNA [NM_006291]
31.011215	CCL20	Homo sapiens chemokine (C-C motif) ligand 20 (CCL20), transcript variant 1, mRNA [NM_004591]
26.424435	IL8	Homo sapiens interleukin 8 (IL8), mRNA [NM_000584]
25.602303	CFB	Homo sapiens complement factor B (CFB), mRNA [NM_001710]
24.747133	DEFB4A	Homo sapiens defensin, beta 4A (DEFB4A), mRNA [NM_004942]
23.39492	CSF2	Homo sapiens colony stimulating factor 2 (granulocyte-macrophage) (CSF2), mRNA [NM_000758]
22.315847	C15orf48	Homo sapiens chromosome 15 open reading frame 48 (C15orf48), transcript variant 2, mRNA [NM_032413]
18.645624	OLR1	Homo sapiens oxidized low density lipoprotein (lectin-like) receptor 1 (OLR1), transcript variant 1, mRNA [NM_002543]
16.742622	TNFAIP6	Homo sapiens tumor necrosis factor, alpha-induced protein 6 (TNFAIP6), mRNA [NM_007115]
14.789509	IL36G	Homo sapiens interleukin 36, gamma (IL36G), mRNA [NM_019618]
13.946556	XLOC_007852	BROAD Institute lincRNA (XLOC_007852), lincRNA [TCONS_00015880]
13.209056	CXCL1	Homo sapiens chemokine (C-X-C motif) ligand 1 (melanoma growth stimulating activity, alpha) (CXCL1), mRNA [NM_001511]
12.91094	IL6	Homo sapiens interleukin 6 (interferon, beta 2) (IL6), mRNA [NM_000600]
12.864111	TNF	Homo sapiens tumor necrosis factor (TNF), mRNA [NM_000594]
12.714474	SLC44A4	Homo sapiens solute carrier family 44, member 4 (SLC44A4), transcript variant 1, mRNA [NM_025257]
12.534851	CXCL3	Homo sapiens chemokine (C-X-C motif) ligand 3 (CXCL3), mRNA [NM_002090]
12.029445	CXCL1	Homo sapiens chemokine (C-X-C motif) ligand 1 (melanoma growth stimulating activity, alpha) (CXCL1), mRNA [NM_001511]
11.732647	LOC440896	Homo sapiens uncharacterized LOC440896 (LOC440896), non-coding RNA [NR_015361]
11.391068	EBI3	Homo sapiens Epstein-Barr virus induced 3 (EBI3), mRNA [NM_005755]
11.255576	MMP9	Homo sapiens matrix metallopeptidase 9 (gelatinase B, 92kDa gelatinase, 92kDa type IV collagenase) (MMP9), mRNA [NM_004994]
11.206088	CXCL2	Homo sapiens chemokine (C-X-C motif) ligand 2 (CXCL2), mRNA [NM_002089]
11.149268	CXCL2	Homo sapiens chemokine (C-X-C motif) ligand 2 (CXCL2), mRNA [NM_002089]
10.120449	XLOC_I2_011805	BROAD Institute lincRNA (XLOC_I2_011805), lincRNA [TCONS_I2_00023572]
9.90666	VNN1	Homo sapiens vanin 1 (VNN1), mRNA [NM_004666]
9.463602	LOC100507410	Homo sapiens uncharacterized LOC100507410 (LOC100507410), transcript variant 1, non-coding RNA [NR_040018]
9.022297	SGPP2	sphingosine-1-phosphate phosphatase 2 [Source:HGNC Symbol;Acc:19953] [ENST00000321276]
8.648464	ICAM1	Homo sapiens intercellular adhesion molecule 1 (ICAM1), mRNA [NM_000201]
8.279761	APOBEC3A	Homo sapiens apolipoprotein B mRNA editing enzyme, catalytic polypeptide-like 3A (APOBEC3A), transcript variant 1, mRNA [NM_145699]
8.112992	SAA2	Homo sapiens serum amyloid A2 (SAA2), transcript variant 1, mRNA [NM_030754]
8.039274	MRGPRX3	Homo sapiens MAS-related GPR, member X3 (MRGPRX3), mRNA [NM_054031]
7.976473	CXCL6	Homo sapiens chemokine (C-X-C motif) ligand 6 (granulocyte chemotactic protein 2) (CXCL6), mRNA [NM_002993]
7.654762	CXCL5	Homo sapiens chemokine (C-X-C motif) ligand 5 (CXCL5), mRNA [NM_002994]
7.606027	MMP10	Homo sapiens matrix metallopeptidase 10 (stromelysin 2) (MMP10), mRNA [NM_002425]
7.462407	IL1R2	Homo sapiens interleukin 1 receptor, type II (IL1R2), transcript variant 1, mRNA [NM_004633]
7.433632	IL23A	Homo sapiens interleukin 23, alpha subunit p19 (IL23A), mRNA [NM_016584]
7.1825104	PTX3	Homo sapiens pentraxin 3, long (PTX3), mRNA [NM_002852]
7.1460867	XLOC_I2_015800	BROAD Institute lincRNA (XLOC_I2_015800), lincRNA [TCONS_I2_00030845]
7.0355535	ZP4	Homo sapiens zona pellucida glycoprotein 4 (ZP4), mRNA [NM_021186]
6.8754315	IGFL1	Homo sapiens IGF-like family member 1 (IGFL1), mRNA [NM_198541]
6.8667517	MRGPRX4	Homo sapiens MAS-related GPR, member X4 (MRGPRX4), mRNA [NM_054032]

6.4496436	SGPP2	Homo sapiens sphingosine-1-phosphate phosphatase 2 (SGPP2), mRNA [NM_152386]
6.4387383	SPRR2B	Homo sapiens small proline-rich protein 2B (SPRR2B), mRNA [NM_001017418]
6.278748	CES1	Homo sapiens carboxylesterase 1 (CES1), transcript variant 1, mRNA [NM_001025195]
6.022716	LTB	Homo sapiens lymphotoxin beta (TNF superfamily, member 3) (LTB), transcript variant 1, mRNA [NM_002341]
6.0204306	SPRR2C	Homo sapiens small proline-rich protein 2C (pseudogene) (SPRR2C), non-coding RNA [NR_003062]
5.920706	XLOC_l2_015752	PREDICTED: Homo sapiens uncharacterized protein CXorf49-like (LOC100129291), miscRNA [XR_132685]
5.8816657	SPRR2A	Homo sapiens small proline-rich protein 2A (SPRR2A), mRNA [NM_005988]
5.749561	NCF2	Homo sapiens neutrophil cytosolic factor 2 (NCF2), transcript variant 1, mRNA [NM_000433]
5.7319303	SERPINA3	Homo sapiens serpin peptidase inhibitor, clade A (alpha-1 antiproteinase, antitrypsin), member 3 (SERPINA3), mRNA [NM_001085]
5.710781	ZNF287	Homo sapiens zinc finger protein 287 (ZNF287), mRNA [NM_020653]
5.6963973	SPRR2E	Homo sapiens small proline-rich protein 2E (SPRR2E), mRNA [NM_001024209]
5.672083	AQP9	Homo sapiens aquaporin 9 (AQP9), mRNA [NM_020980]
5.672049	SPRR2A	Homo sapiens small proline-rich protein 2A (SPRR2A), mRNA [NM_005988]
5.6391087	SPRR2F	Homo sapiens small proline-rich protein 2F (SPRR2F), mRNA [NM_001014450]
5.5922966	STAT5A	Homo sapiens signal transducer and activator of transcription 5A (STAT5A), mRNA [NM_003152]
5.591199	SLC6A14	Homo sapiens solute carrier family 6 (amino acid transporter), member 14 (SLC6A14), mRNA [NM_007231]
5.5726776	SPRR2D	Homo sapiens small proline-rich protein 2D (SPRR2D), mRNA [NM_006945]
5.5505967	SOD2	Homo sapiens superoxide dismutase 2, mitochondrial (SOD2), nuclear gene encoding mitochondrial protein, transcript variant 2, mRNA [NM_001024465]
5.51842		Q6BEA3_RAT (Q6BEA3) WDNM1 homolog, partial (33%) [THC2682885]
5.3314323	ZC3H12A	Homo sapiens zinc finger CCCH-type containing 12A (ZC3H12A), mRNA [NM_025079]
5.2784348	PLAT	Homo sapiens plasminogen activator, tissue (PLAT), transcript variant 1, mRNA [NM_000930]
5.2504177	NFKBIZ	Homo sapiens nuclear factor of kappa light polypeptide gene enhancer in B-cells inhibitor, zeta (NFKBIZ), transcript variant 1, mRNA [NM_031419]
5.190099	LOC645638	Homo sapiens WDNM1-like pseudogene (LOC645638), non-coding RNA [NR_030732]
5.133421	TNFAIP3	Homo sapiens tumor necrosis factor, alpha-induced protein 3 (TNFAIP3), mRNA [NM_006290]
5.0584807	CTHRC1	Homo sapiens collagen triple helix repeat containing 1 (CTHRC1), mRNA [NM_138455]
5.050288	IRAK2	Homo sapiens interleukin-1 receptor-associated kinase 2 (IRAK2), mRNA [NM_001570]
5.020446	BIRC3	Homo sapiens baculoviral IAP repeat containing 3 (BIRC3), transcript variant 1, mRNA [NM_001165]
5.006757	CFHR3	Homo sapiens complement factor H-related 3 (CFHR3), transcript variant 1, mRNA [NM_021023]
4.7368937	NTN1	Homo sapiens netrin 1 (NTN1), mRNA [NM_004822]
4.734892	ESM1	Homo sapiens endothelial cell-specific molecule 1 (ESM1), transcript variant 1, mRNA [NM_007036]
4.657242	PDZK1IP1	Homo sapiens PDZK1 interacting protein 1 (PDZK1IP1), mRNA [NM_005764]
4.629907	SPRR2G	Homo sapiens small proline-rich protein 2G (SPRR2G), mRNA [NM_001014291]
4.4680963	IGFBP3	Homo sapiens insulin-like growth factor binding protein 3 (IGFBP3), transcript variant 1, mRNA [NM_001013398]
4.3502564	S100A12	Homo sapiens S100 calcium binding protein A12 (S100A12), mRNA [NM_005621]
4.2607527	INHBA	Homo sapiens inhibin, beta A (INHBA), mRNA [NM_002192]
4.139629	LOC100506328	Q1YA75_STAAU (Q1YA75) ABC transporter related, partial (5%) [THC2632354]
4.1200795	IL13RA2	Homo sapiens interleukin 13 receptor, alpha 2 (IL13RA2), mRNA [NM_000640]
4.0758653	S100A12	Homo sapiens S100 calcium binding protein A12 (S100A12), mRNA [NM_005621]
3.9722354	NFKBIA	Homo sapiens nuclear factor of kappa light polypeptide gene enhancer in B-cells inhibitor, alpha (NFKBIA), mRNA [NM_020529]
3.9606123	SPRR2D	Homo sapiens small proline-rich protein 2D (SPRR2D), mRNA [NM_006945]
3.8934114	C3	Homo sapiens complement component 3 (C3), mRNA [NM_000064]
3.8814108	LOC100506328	Homo sapiens cDNA FLJ31315 fis, clone LIVER1000303. [AK055877]
3.802795	ANKK1	Homo sapiens ankyrin repeat and kinase domain containing 1 (ANKK1), mRNA [NM_178510]
3.7083652	RELB	Homo sapiens v-rel reticuloendotheliosis viral oncogene homolog B (RELB), mRNA [NM_006509]
3.7049508	C9orf30-TMEFF1	Homo sapiens C9orf30-TMEFF1 readthrough (C9orf30-TMEFF1), mRNA [NM_001198812]
3.6826954	GPR68	Homo sapiens G protein-coupled receptor 68 (GPR68), transcript variant 2, mRNA [NM_003485]
3.4077225	IL4I1	Homo sapiens interleukin 4 induced 1 (IL4I1), transcript variant 2, mRNA [NM_172374]
3.385502	WISP2	Homo sapiens WNT1 inducible signaling pathway protein 2 (WISP2), mRNA [NM_003881]
3.3800528	IL1RN	Homo sapiens interleukin 1 receptor antagonist (IL1RN), transcript variant 4, mRNA [NM_173843]
3.3292277	STRA6	Homo sapiens stimulated by retinoic acid gene 6 homolog (mouse) (STRA6), transcript variant 8, mRNA [NM_001199042]

3.3240402	SAA1	Homo sapiens serum amyloid A1 (SAA1), transcript variant 1, mRNA [NM_000331]
3.3190649	IL7R	Homo sapiens interleukin 7 receptor (IL7R), mRNA [NM_002185]
3.2363849	APOBEC3B	Homo sapiens apolipoprotein B mRNA editing enzyme, catalytic polypeptide-like 3B (APOBEC3B), mRNA [NM_004900]
3.1987216	S100A7	Homo sapiens S100 calcium binding protein A7 (S100A7), mRNA [NM_002963]
3.1771522	C1QTNF1	Homo sapiens C1q and tumor necrosis factor related protein 1 (C1QTNF1), mRNA [NM_198594]
3.164308	TNIP1	Homo sapiens TNFAIP3 interacting protein 1 (TNIP1), transcript variant 5, mRNA [NM_006058]
3.1474497	IL1RN	Homo sapiens interleukin 1 receptor antagonist (IL1RN), transcript variant 4, mRNA [NM_173843]
3.1375163	AKR1C4	Homo sapiens aldo-keto reductase family 1, member C4 (AKR1C4), mRNA [NM_001818]
3.1087248	LOC282980	Homo sapiens uncharacterized LOC282980 (LOC282980), non-coding RNA [NR_040253]
3.068482	ELF3	Homo sapiens E74-like factor 3 (ets domain transcription factor, epithelial-specific) (ELF3), transcript variant 1, mRNA [NM_004433]
3.0335026	ALDH1A3	Homo sapiens aldehyde dehydrogenase 1 family, member A3 (ALDH1A3), mRNA [NM_000693]
3.0184317	LCE3A	Homo sapiens late cornified envelope 3A (LCE3A), mRNA [NM_178431]
2.9463649	XLOC_l2_007456	BROAD Institute lincRNA (XLOC_l2_007456), lincRNA [TCONS_l2_00013854]
2.9340193	CCL27	Homo sapiens chemokine (C-C motif) ligand 27 (CCL27), mRNA [NM_006664]
2.8810813	G0S2	Homo sapiens G0/G1switch 2 (G0S2), mRNA [NM_015714]
2.8608053	NFKB2	Homo sapiens nuclear factor of kappa light polypeptide gene enhancer in B-cells 2 (p49/p100) (NFKB2), transcript variant 3, mRNA [NM_001077493]
2.7979558	PRDM1	Homo sapiens PR domain containing 1, with ZNF domain (PRDM1), transcript variant 1, mRNA [NM_001198]
2.766084	PGLYRP4	Homo sapiens peptidoglycan recognition protein 4 (PGLYRP4), mRNA [NM_020393]
2.73197	LOC100130331	Homo sapiens POTE ankyrin domain family, member F pseudogene (LOC100130331), non-coding RNA [NR_027247]
2.6793172	RHCG	Homo sapiens Rh family, C glycoprotein (RHCG), mRNA [NM_016321]
2.6389349	MMP1	Homo sapiens matrix metallopeptidase 1 (interstitial collagenase) (MMP1), transcript variant 1, mRNA [NM_002421]
2.6289616	KRT34	Homo sapiens keratin 34 (KRT34), mRNA [NM_021013]
2.5978057	XLOC_003917	BROAD Institute lincRNA (XLOC_003917), lincRNA [TCONS_00008455]
2.510461	GLIPR2	Homo sapiens GLI pathogenesis-related 2 (GLIPR2), mRNA [NM_022343]
2.4771323	TNC	Homo sapiens tenascin C (TNC), mRNA [NM_002160]
2.4657829	PLAU	Homo sapiens plasminogen activator, urokinase (PLAU), transcript variant 2, mRNA [NM_001145031]
2.4577343	PI3	Homo sapiens peptidase inhibitor 3, skin-derived (PI3), mRNA [NM_002638]
2.4374082	S100A9	Homo sapiens S100 calcium binding protein A9 (S100A9), mRNA [NM_002965]
2.4275002	HBEGF	Homo sapiens heparin-binding EGF-like growth factor (HBEGF), mRNA [NM_001945]
2.4132621	SERPINB1	Homo sapiens serpin peptidase inhibitor, clade B (ovalbumin), member 1 (SERPINB1), mRNA [NM_030666]
2.3679178	HCAR3	Homo sapiens hydroxycarboxylic acid receptor 3 (HCAR3), mRNA [NM_006018]
2.3650486	SERPINB2	Homo sapiens serpin peptidase inhibitor, clade B (ovalbumin), member 2 (SERPINB2), transcript variant 2, mRNA [NM_002575]
2.3625822	MAP3K8	Homo sapiens mitogen-activated protein kinase kinase kinase 8 (MAP3K8), transcript variant 1, mRNA [NM_005204]
2.3540993	FUT2	Homo sapiens fucosyltransferase 2 (secretor status included) (FUT2), transcript variant 1, mRNA [NM_000511]
2.3496451	PLAU	Homo sapiens plasminogen activator, urokinase (PLAU), transcript variant 1, mRNA [NM_002658]
2.3444786	HAS2	Homo sapiens hyaluronan synthase 2 (HAS2), mRNA [NM_005328]
2.3182514	GLIPR2	Homo sapiens GLI pathogenesis-related 2 (GLIPR2), mRNA [NM_022343]
2.3179886	LOC152225	Homo sapiens uncharacterized LOC152225 (LOC152225), non-coding RNA [NR_026934]
2.3154647	AKR1CL1	Homo sapiens aldo-keto reductase family 1, member C-like 1 (AKR1CL1), non-coding RNA [NR_027916]
2.3045177	IRF1	Homo sapiens interferon regulatory factor 1 (IRF1), mRNA [NM_002198]
2.293556	XLOC_003917	BROAD Institute lincRNA (XLOC_003917), lincRNA [TCONS_00009035]
2.2914116	CD70	Homo sapiens CD70 molecule (CD70), mRNA [NM_001252]
2.2527678	IL24	Homo sapiens interleukin 24 (IL24), transcript variant 3, mRNA [NM_001185156]
2.2518134	XLOC_l2_003293	
2.2285113	DEFB103B	Homo sapiens defensin, beta 103B (DEFB103B), mRNA [NM_018661]
2.2242286	TNFSF10	Homo sapiens tumor necrosis factor (ligand) superfamily, member 10 (TNFSF10), transcript variant 1, mRNA [NM_003810]
2.2137582	PTPRK	Homo sapiens protein tyrosine phosphatase, receptor type, K (PTPRK), transcript variant 2, mRNA [NM_002844]
2.2003071	BIK	Homo sapiens BCL2-interacting killer (apoptosis-inducing) (BIK), mRNA [NM_001197]
2.1838214	BATF3	Homo sapiens basic leucine zipper transcription factor, ATF-like 3 (BATF3), mRNA [NM_018664]
2.18375	MURC	Homo sapiens muscle-related coiled-coil protein (MURC), mRNA [NM_001018116]

2.1826077	TMEM158	Homo sapiens transmembrane protein 158 (gene/pseudogene) (TMEM158), mRNA [NM_015444]
2.16861	IL32	Homo sapiens interleukin 32 (IL32), transcript variant 1, mRNA [NM_001012631]
2.1683908	CEACAM1	Homo sapiens carcinoembryonic antigen-related cell adhesion molecule 1 (biliary glycoprotein) (CEACAM1), transcript variant 1, mRNA [NM_001712]
2.1461678	AKR1C1	Homo sapiens aldo-keto reductase family 1, member C1 (AKR1C1), mRNA [NM_001353]
2.134137	KAL1	Homo sapiens Kallmann syndrome 1 sequence (KAL1), mRNA [NM_000216]
2.128932	LMO2	Homo sapiens LIM domain only 2 (rhombotin-like 1) (LMO2), transcript variant 1, mRNA [NM_005574]
2.126451	ZSWIM4	Homo sapiens zinc finger, SWIM-type containing 4 (ZSWIM4), mRNA [NM_023072]
2.084181	ELOVL7	Homo sapiens ELOVL fatty acid elongase 7 (ELOVL7), transcript variant 1, mRNA [NM_024930]
2.083856	TRIM47	Homo sapiens tripartite motif containing 47 (TRIM47), mRNA [NM_033452]
2.0739424	SERPINB9	Homo sapiens serpin peptidase inhibitor, clade B (ovalbumin), member 9 (SERPINB9), mRNA [NM_004155]
2.0694013	TMPRSS11D	Homo sapiens transmembrane protease, serine 11D (TMPRSS11D), mRNA [NM_004262]
2.0663571	SDCBP2	Homo sapiens syndecan binding protein (syntenin) 2 (SDCBP2), transcript variant 1, mRNA [NM_080489]
2.0625482	TMEM106A	Homo sapiens transmembrane protein 106A (TMEM106A), mRNA [NM_145041]
2.0587165	TNFSF10	Homo sapiens tumor necrosis factor (ligand) superfamily, member 10 (TNFSF10), transcript variant 1, mRNA [NM_003810]
2.0494006	FUT3	Homo sapiens fucosyltransferase 3 (galactoside 3(4)-L-fucosyltransferase, Lewis blood group) (FUT3), transcript variant 1, mRNA [NM_000149]
2.0492787	IL1A	Homo sapiens interleukin 1, alpha (IL1A), mRNA [NM_000575]
2.048859	BMP6	Homo sapiens bone morphogenetic protein 6 (BMP6), mRNA [NM_001718]
2.044478	SOCS3	Homo sapiens suppressor of cytokine signaling 3 (SOCS3), mRNA [NM_003955]
2.043223	SPOCD1	Homo sapiens SPOC domain containing 1 (SPOCD1), mRNA [NM_144569]
2.0357366	AKR1C3	Homo sapiens aldo-keto reductase family 1, member C3 (3-alpha hydroxysteroid dehydrogenase, type II) (AKR1C3), mRNA [NM_003739]
2.0153258	IL6ST	Homo sapiens interleukin 6 signal transducer (gp130, oncostatin M receptor) (IL6ST), transcript variant 1, mRNA [NM_002184]

Table B.4 Downregulated genes in primary keratinocytes after IL-36 stimulations for 8 h

Fold	Gene name	Description
-5.68193	GCET2	Homo sapiens germinal center expressed transcript 2 (GCET2), transcript variant 3, mRNA [NM_001190259]
-4.974732	CYP4F22	Homo sapiens cytochrome P450, family 4, subfamily F, polypeptide 22 (CYP4F22), mRNA [NM_173483]
-4.447021	XLOC_007350	BROAD Institute lincRNA (XLOC_007350), lincRNA [TCONS_00015669]
-4.351619	PITPNM3	Homo sapiens PITPNM family member 3 (PITPNM3), transcript variant 1, mRNA [NM_031220]
-4.2436614	RDH12	Homo sapiens retinol dehydrogenase 12 (all-trans/9-cis/11-cis) (RDH12), mRNA [NM_152443]
-4.112106	NUDT16P1	Homo sapiens nudix (nucleoside diphosphate linked moiety X)-type motif 16 pseudogene 1 (NUDT16P1), transcript v
-3.802311	GPR75	Homo sapiens G protein-coupled receptor 75 (GPR75), mRNA [NM_006794]
-3.678668		
-3.359215	FLG	Homo sapiens filaggrin (FLG), mRNA [NM_002016]
-3.245788	PADI3	Homo sapiens peptidyl arginine deiminase, type III (PADI3), mRNA [NM_016233]
-3.0842044	HYDIN	Homo sapiens hydrocephalus inducing homolog (mouse), mRNA (cDNA clone IMAGE:4837075), partial cds. [BC028
-3.0013008	EPHA4	Homo sapiens EPH receptor A4 (EPHA4), mRNA [NM_004438]
-2.8100295	PALMD	Homo sapiens palmdelphin (PALMD), mRNA [NM_017734]
-2.807833	MGP	Homo sapiens matrix Gla protein (MGP), transcript variant 1, mRNA [NM_001190839]
-2.7847157	WNT2B	Homo sapiens wingless-type MMTV integration site family, member 2B (WNT2B), transcript variant WNT-2B1, mRNA
-2.7711902	TRIM66	Homo sapiens tripartite motif containing 66 (TRIM66), mRNA [NM_014818]
-2.749652	PLA2G3	Homo sapiens phospholipase A2, group III (PLA2G3), mRNA [NM_015715]
-2.6998932	TMEM63C	Homo sapiens transmembrane protein 63C (TMEM63C), mRNA [NM_020431]
-2.6770618	MT1H	Homo sapiens metallothionein 1H (MT1H), mRNA [NM_005951]
-2.610567	NCKAP5	Homo sapiens NCK-associated protein 5 (NCKAP5), transcript variant 1, mRNA [NM_207363]
-2.6097836	ID3	Homo sapiens inhibitor of DNA binding 3, dominant negative helix-loop-helix protein (ID3), mRNA [NM_002167]
-2.5954165	XLOC_011989	BROAD Institute lincRNA (XLOC_011989), lincRNA [TCONS_00025039]
-2.579851	SPINK5	Homo sapiens serine peptidase inhibitor, Kazal type 5 (SPINK5), transcript variant 1, mRNA [NM_001127698]
-2.5341752	C10orf129	Homo sapiens chromosome 10 open reading frame 129 (C10orf129), mRNA [NM_207321]
-2.4894655	ODZ3	Homo sapiens odz, odd Oz/ten-m homolog 3 (Drosophila) (ODZ3), mRNA [NM_001080477]
-2.474841	C16orf86	Homo sapiens chromosome 16 open reading frame 86 (C16orf86), mRNA [NM_001012984]
-2.4634354	DNM1	dynamin 1 [Source:HGNC Symbol;Acc:2972] [ENST00000393589]
-2.4441888	PHYHIP	Homo sapiens phytanoyl-CoA 2-hydroxylase interacting protein (PHYHIP), transcript variant 2, mRNA [NM_014759]
-2.3930876	XLOC_I2_0079(	BROAD Institute lincRNA (XLOC_I2_007964), lincRNA [TCONS_I2_00015761]
-2.3300235	RAB44	BROAD Institute lincRNA (XLOC_I2_012524), lincRNA [TCONS_I2_00024199]
-2.3256462	PPIL6	Homo sapiens peptidylprolyl isomerase (cyclophilin)-like 6 (PPIL6), transcript variant 1, mRNA [NM_173672]
-2.3074453	METTL7A	Homo sapiens methyltransferase like 7A (METTL7A), mRNA [NM_014033]
-2.3025618		
-2.2988906	LOC100288842	Homo sapiens UDP-GlcNAc:betaGal beta-1,3-N-acetylglucosaminyltransferase 5 pseudogene (LOC100288842), nor
-2.2922843	LOC400684	Homo sapiens hypothetical gene supported by BC000922, mRNA (cDNA clone IMAGE:3447073), partial cds. [BC00(
-2.2912223	TNNI2	Homo sapiens troponin I type 2 (skeletal, fast) (TNNI2), transcript variant 1, mRNA [NM_003282]
-2.2882867	RFPL1-AS1	Homo sapiens RFPL1 antisense RNA 1 (non-protein coding) (RFPL1-AS1), antisense RNA [NR_002727]
-2.2869287	TGFBR3	Homo sapiens transforming growth factor, beta receptor III (TGFBR3), transcript variant 1, mRNA [NM_003243]
-2.2819138	SDS	Homo sapiens serine dehydratase (SDS), mRNA [NM_006843]
-2.2779574	LOC641510	Homo sapiens, mRNA (cDNA clone IMAGE:4713722). [BC030809]
-2.275472	AMOT	Homo sapiens angiomotin (AMOT), transcript variant 2, mRNA [NM_133265]
-2.275169	XLOC_012895	BROAD Institute lincRNA (XLOC_012895), lincRNA [TCONS_00026578]
-2.2381182	MGC14436	Homo sapiens uncharacterized LOC84983 (MGC14436), transcript variant 1, non-coding RNA [NR_026661]
-2.2330797	PRODH	Homo sapiens proline dehydrogenase (oxidase) 1 (PRODH), nuclear gene encoding mitochondrial protein, transcript

-2.2325985	SPTLC3	Homo sapiens serine palmitoyltransferase, long chain base subunit 3 (SPTLC3), mRNA [NM_018327]
-2.2298868		full-length cDNA clone CS0DD005YE10 of Neuroblastoma Cot 50-normalized of Homo sapiens (human) [CR607463]
-2.2264311	XLOC_l2_0108	BROAD Institute lincRNA (XLOC_l2_010863), lincRNA [TCONS_l2_00020791]
-2.2216558	MPV17L	Homo sapiens MPV17 mitochondrial membrane protein-like (MPV17L), nuclear gene encoding mitochondrial protein,
-2.2082322	XLOC_014172	BROAD Institute lincRNA (XLOC_014172), lincRNA [TCONS_00029776]
-2.149379	PREX2	Homo sapiens phosphatidylinositol-3,4,5-trisphosphate-dependent Rac exchange factor 2 (PREX2), transcript varian
-2.1481981	HSD17B6	Homo sapiens hydroxysteroid (17-beta) dehydrogenase 6 homolog (mouse) (HSD17B6), mRNA [NM_003725]
-2.1468444	XLOC_001748	BROAD Institute lincRNA (XLOC_001748), lincRNA [TCONS_00003935]
-2.127694	XLOC_l2_0140	BROAD Institute lincRNA (XLOC_l2_014050), lincRNA [TCONS_l2_00026968]
-2.1197636	SLC13A5	Homo sapiens solute carrier family 13 (sodium-dependent citrate transporter), member 5 (SLC13A5), transcript varia
-2.10794	RIMS2	Homo sapiens regulating synaptic membrane exocytosis 2 (RIMS2), transcript variant 2, mRNA [NM_014677]
-2.106508	XLOC_l2_0071	BROAD Institute lincRNA (XLOC_l2_007135), lincRNA [TCONS_l2_00013243]
-2.0948617	GRAMD2	Homo sapiens GRAM domain containing 2 (GRAMD2), mRNA [NM_001012642]
-2.0767918	XLOC_l2_0001	UI-E-EJ1-ajb-m-22-0-UI.r1 UI-E-EJ1 Homo sapiens cDNA clone UI-E-EJ1-ajb-m-22-0-UI 5', mRNA sequence [BM93(
-2.075652	LOC643770	Homo sapiens uncharacterized LOC643770 (LOC643770), non-coding RNA [NR_038383]
-2.0513952	XLOC_011183	17000600026802 GRN_PREHEP Homo sapiens cDNA 5', mRNA sequence [CN388809]
-2.0508778	TP53TG5	Homo sapiens TP53 target 5 (TP53TG5), mRNA [NM_014477]
-2.0396845	XLOC_l2_0000	RST7083 Athersys RAGE Library Homo sapiens cDNA, mRNA sequence [BG188075]
-2.035384	LOC100652739	Homo sapiens uncharacterized LOC100652739 (LOC100652739), transcript variant 1, non-coding RNA [NR_045126
-2.0351808	NAT8L	Homo sapiens N-acetyltransferase 8-like (GCN5-related, putative) (NAT8L), mRNA [NM_178557]
-2.0186477	ARID4A	Homo sapiens AT rich interactive domain 4A (RBP1-like) (ARID4A), transcript variant 1, mRNA [NM_002892]
-2.0156596	UGT1A6	Homo sapiens UDP glucuronosyltransferase 1 family, polypeptide A6 (UGT1A6), transcript variant 1, mRNA [NM_001
-2.0118935	CPA4	Homo sapiens carboxypeptidase A4 (CPA4), transcript variant 1, mRNA [NM_016352]
-2.0038733	FIGN	Homo sapiens fidgetin (FIGN), mRNA [NM_018086]
-2.0033212	THBS4	BROAD Institute lincRNA (XLOC_l2_011649), lincRNA [TCONS_l2_00022386]
-2.0024903	C11orf70	Homo sapiens chromosome 11 open reading frame 70 (C11orf70), transcript variant 2, mRNA [NM_001195005]
-2.0013735	LOC100506778	PREDICTED: Homo sapiens hypothetical LOC100506778 (LOC100506778), miscRNA [XR_110850]
-2.0010843	WBSCR22	PREDICTED: Homo sapiens hypothetical LOC100505484 (LOC100505484), miscRNA [XR_108831]